## *Aspects of the taphonomy of the Cambrian Explosion in North Greenland*

STRANG, KATIE,MARGARET


# Aspects of the taphonomy of the Cambrian Explosion in North Greenland

**Katie Margaret Strang**

**This thesis is submitted in partial fulfillment of the requirements for the Degree of Doctor of Philosophy at Durham University**

**Department of Earth Sciences**
**Durham University**

**I declare that this thesis, which I submit for the degree of Doctor of Philosophy at Durham University, is my own work and not substantially the same as any which has been previously submitted at this or any other University.**

**Katie Margaret Strang**

**Durham University**

***This thesis is dedicated to my Mum, Dad, Brother and Granny. Anne Strang, Robert Strang, John Strang and Margaret Mitchell; I would never have made it this far without your support. Thank you!***

# Abstract

**Aspects of the taphonomy of the Cambrian Explosion in North Greenland**

**Katie Margaret Strang**
**Doctor of Philosophy**
**Department of Earth Sciences**
**Durham University**

This thesis describes and elucidates the taphonomic pathways responsible for the exceptional preservation of some of the most common elements of the Sirius Passet Lagerstätte (early Cambrian), North Greenland. Investigative techniques including cathodoluminescence, are tested first on silicified molluscs from the Oligocene of Antigua, associated with a volcanic source; described in chapter 2. By describing the depositional environment of the Sirius Passet biota in detail and using a combination of analytical techniques such as SEM, EDAX, SEM-CL and elemental mapping two published papers address a number of the key research questions surrounding the unique taphonomic pathways in the Sirius Passet biota and their broader significance in understanding Cambrian ecosystems. The papers are included in the form of chapters 3 and 4 and the published versions included in the appendices. A unique, mat-dominated, tissue specific taphonomic pathway is proposed, more akin to the Proterozoic than the typical Burgess Shale Type (BST) preservation seen elsewhere in the Cambrian. This together with mouldic preservation indicates a range of taphonomic styles concomitant with the range of new biotas at the dawn of the Cambrian Explosion.

## Acknowledgements

Firstly, a massive thank you to David Harper and Howard Armstrong for everything you have done and for your continued support and guidance along the way, it wouldn't have been possible with out you!

Thank you to all the staff and students from Durham University Earth Science Department who I have known during my time here. I can't possibly name you all but every single one of you deserves a huge thanks. In particular, I would like to send a huge wave of gratitude to Bob Jamieson, Cat Hirst, Samantha Clark, Gillian Foulger, Janice Oakes and João Trabucho-Alexandre for their amazing support and encouragement during the last 4 years.

To all the technical staff who have been involved in some way or another, Leon Bowen, Budhika Mendis, Ian Chaplin to name a few, you guys are superstars.

To everyone who I have spoken to or interacted with at conferences and seminars; you all contributed to this thesis in some way. Whether it be a discussion over a beer or a grilling after a talk, you are all a never-ending source of useful knowledge and inspiration.

My deepest gratitude goes out to Alistair McGowan. If it weren't for you I wouldn't be where I am today. You have shown nothing but support, patience and encouragement since my undergraduate days and I more than owe you a dram or ten! Tapadh leibh! Alba gu bràth.

Thank you to all my family and friends who have put up with my endless conversations about rocks, or my moaning when I am stressed. You all have the patience of saints. To my Granny Margaret, 96 years young, thank you for believing in me and showing me what I was capable of. Also, sending a very special thanks to my best friend Marnie-Jane Liddle (and Holden!). Thank you for keeping me sane over the last few months. I am eternally grateful to you. And there will always be special thanks for my 'Burnmouth Crew', Ruth, JG and Thomas, Tha gaol agam ort.

And finally, thank you to my wee Brother and oldest friend, John Strang. Thank you for listening to me, and thank you for all the help and advice you have given to me over the years.

*Detailed acknowledgements of funding sources and resource providers are included in each relevant Appendix. This project was funded by a (NERC) Natural Environmental Research Council studentship (RF050232) to Katie Margaret Strang.*

## Table of Contents

**Abstract** ..... iv

**Acknowledgements** ..... v

**List of figures** ..... viii

**List of tables** ..... ix

**Chapter 1. Introduction** ..... 1

**1.1 The Cambrian Explosion** ..... 2

The Ediacaran-Cambrian boundary ..... 2

The early history of the Metazoa ..... 3

What caused the Cambrian Explosion? ..... 6

**1.2 Exceptional Preservation** ..... 10

1.2.1 Taphonomic bias ..... 10

1.2.2 The Cambrian Substrate Revolution ..... 11

1.2.3 Taphonomic filters ..... 12

1.2.3 The role of experiments in taphonomy ..... 13

**1.3 Overview of Cambrian Lagerstätten** ..... 15

1.3.1 The Burgess Shale ..... 17

1.3.2 Chengjiang ..... 20

1.3.3 Emu Bay Shale ..... 22

**1.4 The Sirius Passet** ..... 24

1.4.1 Overview of the Sirius Passet ..... 24

1.4.2 Depositional environment ..... 26

1.4.3 Previous work on the taphonomy of the SP ..... 33

**1.5 Research Questions** ..... 36

1.5.1 Aims ..... 36

1.5.2 Summary of work done ..... 37

**1.6 Methods** ..... 38

1.6.1 Fieldwork ..... 38

1.6.2 Polished thin sections ..... 38

1.6.3 Thin section scans ..... 38

1.6.4 Petrology ..... 38

1.6.5 SEM ..... 39

1.6.6 SEM CL ..... 39

1.6.7 CL in Palaeontology ..... 40

1.6.8 XRD ..... 41

1.6.9 High-resolution photographs of hand specimens ..... 42

**1.7 References** ..... 43

**Chapter 2: Silicification of low-magnesium mollusc shells from the Upper Oligocene of Antigua, Lesser Antilles – a case study on Cathodoluminescence as a tool in Palaeontology** ..... 54

**2.1 Abstract** ..... 55

**2.2 Introduction** ..... 56

**2.3 Geological Setting** ..... 59

2.3.1 Locality 1. Hughes Point ..... 59

2.3.2 Locality 2. Half Moon Bay ..... 59

**2.4 Results** ..... 62

2.4.1 Locality 1: Hughes Point ..... 62

2.4.2 Locality 2: Half Moon Bay ..... 65

**2.5 Conclusion** ..... 66

**2.6 References** ..... 67

**Chapter 3. The Sirius Passet Lagerstätte: Silica death masking opens the window on the earliest matground community of the Cambrian Explosion – A detailed study on the taphonomy of trilobite *Buenellus higginsi*..... 69**
**3.1 Abstract..... 70**
**3.2 Introduction..... 72**
**3.3 Results..... 75**
**3.4 Discussion..... 84**
**3.5 Conclusions..... 93**
**3.6 References..... 94**

**Chapter 4. Minerals in the gut: Scoping a Cambrian digestive system – A detailed study on the three-dimensionally preserved guts of *Campanamuta mantonae*..... 98**
**4.1 Abstract..... 99**
**4.2 Introduction..... 100**
**4.3 Specimens..... 102**
**4.4 Results..... 104**
**4.5 Discussion..... 107**
**4.6 Taphonomic pathway..... 111**
**4.7 Gut morphology and ecological implications..... 112**
**4.8 Conclusions..... 114**
**4.9 References..... 115**

**Chapter 5. Conclusions..... 118**
**5.1 Summary..... 119**
**5.2 Overview of key findings addressing the research questions..... 122**
**5.3 Summary of palaeobiological implications..... 127**
**5.4 Future work..... 129**
**5.5 References..... 130**

**Appendix I: Silicification of low-magnesium mollusc shells from the Upper Oligocene of Antigua, Lesser Antilles..... 132**

**Appendix II. The Sirius Passet Lagerstatte: Silica death masking opens the window on the earliest matground community of the Cambrian explosion..... 153**

**Appendix III. Minerals in the gut: scoping a Cambrian digestive system..174**

## List of figures

Figure 1.1: Showing distribution of major landmasses during the Early-Mid Cambrian and the location of major Lagerstätten. 9
Figure 1.2: Geological map showing the present day locality of the Sirius Passet Lagerstätte 24
Figure 1.3: Image showing the present day field locality of the SP 25
Figure 1.4: Graphic log of the Buen Formation at Sirius Passet based on thin section analysis and interpretation.. 29
Figure 1.5: Thin section and SEM photomicrographs of the "spotted" facies. 30
Figure 1.6: Thin section and SEM photomicrographs of the silt-rich facies.. 31
Figure 1.7: Block diagram illustrating the depositional environment at Sirius Passet during the Early Cambrian (modified after Plint, 2014) 32
Figure 2.1: Outline map of Antigua showing the principal geological subdivisions and the city of Saint John's. 58
Figure 2.2: Measured section in the lower part of the cliff at Hughes Point (Locality 1) 60
Figure 2.3: A measured section of the northeast point of Half Moon Bay (Locality 2) 61
Figure 2.4: Elemental maps of specimens from both localities. 63
Figure 2.5: SEM and CL images of specimens from Hughes Point and Half Moon Bay. 64
Figure 2.6: CL-SEM spectrum of quartz 66
Figure 3.1: A. Sirius Passet locality map, lithostratigraphy. B, Cambrian palaeogeography. 72
Figure 3.2: High resolution photographs and SEM images. 76
Figure 3.3: XRD plot of 2θ against intensity from sample 0.06 which is the 'spotted' facies. 77
Figure 3.4: XRD plot of 2θ against intensity for sample 4.56, the silt-rich facies. 77
Figure 3.5: Thin section photomicrographs; SEM and BSE images showing the different facies types. 78
Figure 3.6: A, elemental maps, SEM, BSE SEM and SEM-CL images of trilobite *Buenellus*. 83
Figure 3.7: Block diagram illustrating the depositional environment at Sirius Passet during the Early Cambrian (modified after Plint 2014). 86
Figure 3.8: Chemical pathways leading to the precipitation of silica and the reconstructed taphonomy of Buenellus. 92
Figure 4.1: Diagram shows the main features, appendages and internal anatomy of *Campanamuta mantonae*. 102
Figure 4.2: SEM and BSE images of the phosphate contained in the gut of *C. mantonae.* 104
Figure 4.3: SEM, BSE and SEM-CL images of the silicified muscle tissue.. 106
Figure 4.4: Schematic model shows the preferred taphonomic pathway of non-mineralizing *C. mantonae* compared with that of mineralizing *Buenellus*.. 111

## List of tables

Table 2.1: EDS data for specimen from Hughes Point (Locality 1). ..... 62
Table 2.2 EDS data for specimen from Half Moon Bay (Locality 2) ..... 65
Table 3.1: Bulk-rock chemistry (in wt. %) of the low-carbonate Burgess Shale metamudstones (Walcott Quarry, Raymond Quarry and Tuzoia Beds extracted from Powell 2003) compared with the bulk-rock chemistry of SP. ..... 80
Table 3.2: Results from EDAX (sample 4.56) silt-rich facies ..... 80
Table 3.3: EDAX spectra from sample 1.12 m from the spotted facies ..... 81
Table 3.4: EDAX spectra data from the mat material (taken from a cross section through an epirelief cast of Buenellus) ..... 81
Table 4.1: EDAX data for phosphatized regions in sample SP0511. ..... 105
Table 4.2: EDAX data for silicified regions in sample SP0511.. ..... 106

# Chapter 1. Introduction

## 1.1 The Cambrian Explosion

The Cambrian Explosion represents a significant and important interval in Earth's History. It marks an increase in the diversification of complex animal body plans and the expansion of marine ecosystems. This expansion of the roots of the animal phylogenetic tree and rapid development of morphological complexity was one of the most significant evens in the geological record and coincided with a variety of biotic and abiotic global changes (Briggs et al., 1992; Erwin, 2007; Schiffbauer et al., 2016). The fossil record is strongly biased towards the preservation of organisms that possessed shelly (biomineralised) skeletons; with exceptional preservation of soft-bodied organisms being relatively rare in comparison. The fossil record of the Cambrian is in stark contrast with that of the Precambrian world, where, in comparison, the fossil record is somewhat devoid of animal fossils (Marshall, 2006).

### The Ediacaran-Cambrian boundary

The Ediacaran-Cambrian boundary Global Standard Stratotype Section and Point (GSSP) has been established at the base of the *Treptichnus pedum* Zone at Fortune Head, Newfoundland (Narbonne et al., 1987; Brasier et al., 1994; Landing, 1994) but more recent work has moved the base of the zone to slightly below the GSSP (Gehling et al., 2001; Buatois et al., 2013) dating the beginning of the Cambrian at around 541 million years ago (MA) in the now exposed Fortunian Stage of the Terreneuvian Series, 541 – 530 MA (Landing, 1994; Erwin et al., 2011). The appearance of ichnospecies *T. pedum* represents the "agronomic revolution" or Cambrian Substrate revolution (Bottjer et al., 2000; Narbonne, 2005; Bottjer, 2010) where we see a switch from the Ediacaran age trace fossils which are horizontal, simple and exhibit feeding strategies related to exploitation of microbial "matgrounds" to those in the Early Cambrian which show a an increase in diversity with the onset of vertical bioturbation and the disappearance of a "matground" ecology (Seilacher et al., 2005). Thus, the Cambrian expansion of infaunal bioturbation was one of the most profound changes of environment caused by organisms in the history of life on Earth and

subsequently this ichnological diversification is used to help define the base of the Phanerozoic (Geyer and Landing, 2016; Mcilroy and Brasier, 2016; Herringshaw et al., 2017).

The Ediacaran biota marks the first appearance of large, architecturally complex organisms in Earth's history (Narbonne, 2005; Laflamme et al., 2013; Boag et al., 2016), consisting of various metazoan stem lineages in addition to extinct eukaryotic clades (Laflamme et al., 2013). Although the very earliest skeletal fossils occur in the late Precambrian, it is not until the Early Cambrian that most elements associated with bilaterian animals such as plates, spines and shells are found (Erwin et al., 2011). They reveal sizeable variations in morphology and phylogeny and are collectively referred to as small shelly fauna (SFF).

## The early history of the Metazoa

The early history of the Metazoa remains controversial as to whether it originated as part of a "Cambrian Explosion" or as the result of an extended "phylogenetic fuse". The earliest palaeontological evidence for metazoans appears in rocks of Vendian age (Valentine et al., 1999). These are simple, slightly curved meandering furrows, which suggest the presence of bilaterian worms. These traces become more diverse and complex later in the Neoproterozoic (Crimes, 1992; Valentine et al., 1999). As you reach the Ediacaran – Cambrian boundary, the Ediacara biota disappear from the fossil record and are replaced by more familiar Cambrian and Palaeozoic metazoan groups. Although metazoans are present in the Ediacaran, their ecological contribution is dwarfed by Ediacaran-type clades of uncertain phylogenetic affinities, and these Ediacaran type morphologies are non-existent in younger rocks (Laflamme et al., 2013). There is a high degree of variability in the overall morphology of Ediacaran biota, indicating that these organisms likely represent an assortment of clades, including extinct lineages as well as potentially stem- and crown-group animals (Laflamme et al., 2013).

Molecular evidence has also been used to predict the origins of the metazoan crown-groups using housekeeping genes, which consistently indicate that Metazoa originated somewhere between 850 and 650 Ma in the Tonian or

Cryogenian intervals, before diversifying through the Cryogenian and the Ediacaran (Peterson and Butterfield, 2005; Erwin et al., 2011; dos Reis et al., 2015). However, the appearance of extant phyla and classes occurs within the Cambrian. It is suggested that this evidence can distinguish two inter-related events. Therefore the origin of high level crown-groups, as suggested by molecular evidence, it temporally distant from the increase in diversity and expanding food webs which we see in the fossil record, i.e. the Cambrian Explosion *sensu stricto* (Valentine et al., 1999; Smith and Harper, 2013). The oldest fossil evidence of a lineage will typically reflect the time at which a population of organisms possessing a diagnostic set of characters has become geographically widespread and ecologically stable enough for individuals to be preserved through taphonomic processes and appear in the geological record as fossils (Cunningham et al., 2017). On the other hand, dates given by molecular clock studies represent the time when the lineage became genetically isolated and are therefore inevitably earlier (Benton and Donoghue, 2007; Cunningham et al., 2017).

"Molecular clock" studies use genetic distance to infer time since separation of lineages to try and locate the origin of the metazoans. Previous estimates of metazoan divergence from molecular clock results places the origin from the shallow Ediacaran to the very deep Mesoproterozoic (Peterson et al., 2008). This then causes difficulty in ascertaining whether these deep times are true, and if the so called Cambrian explosion is actually just a result of preservational bias? The early molecular clock studies assumed a strict clock, based on poorly justified single calibration points that failed to accommodate phylogenetic and dating uncertainty (Cunningham et al., 2017), which infers a constant rate of molecular evolution across every lineage, such as the early study by (Runnegar, 1982). Runnegar's studies assume that α and β haemoglobins have been evolving at a statistically constant rate, therefore by calculating the percentage differences in sequences of both invertebrate and vertebrate globins he places the initial radiation of the metazoans at 900-1000 million years ago (Runnegar, 1982) and these divergence dates were consistently too old to correlate with fossil evidence.

More recent studies have shown that rates of evolution are not always constant between lineages (Bromham, 2006; Bromham, 2009). To get around this problem, researchers began applying clock methods which exclude rate-variable sequences and select 'well-behaved' clock-like genes, such as the study by (Wang et al., 1999). Wang et al (1999) analysed a larger number of genes, compared to previous studies, among well-represented animal phyla, and among plants, animals and fungi. The results show that divergences among chordates, arthropods and nematodes average at about 993±46 Ma (Wang et al., 1999). This is still around 400 million years before the fossil record records evidence of the first metazoans, raising the question of whether the Cambrian Explosion is indeed an explosion, or is it just the result of preservation, interpretation or collecting bias in the Cambrian?

Most modern divergence time analyses have been undertaken using a framework of Bayesian inference as it is capable of integrating much of the uncertainty associated with divergence time estimation such as the relationships between fossil evidence and clade age, rate variation among lineages (the relaxed clock), branch length estimation, tree topology, and parameters such as data partitioning (dos Reis et al., 2015). Molecular clock studies rely on calibration to establish evolutionary rates throughout the phylogenetic tree and fossils are the most commonly used form of calibration and are widely acknowledged as being underestimates of the true divergence times between two lineages. However, it also has to be accepted that if fossils are gross underestimates this can lead to substantial miscalculations in divergence times (Blair and Hedges, 2005). Differing results among studies are likely due to previous molecular clock dating methods having suffered from limited data and biases in methodologies (dos Reis et al., 2012; dos Reis et al., 2015) and essentially all have failed to take into account the large uncertainties associated with the fossil record of early animals, thus leading to inconsistent estimates. By using an unprecedented amount of molecular data, in parallel with reflecting disparate and controversial interpretations of the metazoan fossil record, to obtain Bayesian estimates of metazoan divergence times, these relaxed clock methods (Erwin et al., 2011) have suggested a divergence of bilaterian phyla at

about 100 million years before the Cambrian, where the first certain crown-bilaterian fossils occur (dos Reis et al., 2015). This consistency in dates, estimating divergence one hundred million years before the oldest documented animal fossils, throws up uncertainty on how complete the fossil record actually is and whether the Cambrian Explosion is an artifact of fossilization and the real 'explosion' of biological diversity is rooted in the Precambrian, and to what extent methodology is preventing molecular clock methods from answering the question of early animal evolution (Cunningham et al., 2017).

## What caused the Cambrian Explosion?

Over the last decade there has been around thirty differing hypotheses put forward to try and explain this fascinating Cambrian 'Explosion' (Smith and Harper, 2013) and although the record of early metazoan evolution is increasingly well understood, the underlying cause of this major biotic event is still widely debated. Global redox changes such as the rapid rise or fall in atmospheric and ocean oxygen levels have been suggested (Li et al., 2017). For example isotope data (molybdenum) has demonstrated that the areal extent of oxygenated bottom waters increased in-line with the rapid rise of metazoan diversity and modern-like oxygen levels characterized the ocean at ~521 Ma (Chen et al., 2015). Also Fe-S-C-Al-trace element data from early Cambrian sections in South China was studied and results suggest a low sulphate and highly redox-heterogeneous ocean (Jin et al., 2016) indicating that the "Cambrian Explosion" in South China may have been a consequence of locally improved oxygenation of the surface layer, as opposed to improved oxygenation of the global ocean (Jin et al., 2016). This is inconsistent with changes in ocean chemistry being a result of the effect of early animals, and increased oxygen levels have even been proposed as a possible feedback mechanism whereby increased levels of oxygen would have a stimulating effect on established ecologies, which in turn would impart more oxygen to the ocean surface layer (Knoll, 1999; Budd, 2008).

This hypothesis of a feedback loop was also suggested in another study where it was demonstrated that increased bioturbation, as in the early Cambrian,

systematically triggers a net decrease in the global oxygen reservoir and also reduces the steady-state marine phosphate levels (Boyle et al., 2014). This effect is balanced by the decline in iron-absorbed phosphate burial that stems from a decrease in oxygen. Thus, the introduction of oxygen sensitive bioturbation is sufficient enough to trigger a negative feedback loop; the intensity of bioturbation is thus limited by the oxygen decrease it initially causes and ultimately bioturbation helped to regulate early oxygen and phosphorus cycles in the Cambrian oceans (Boyle et al., 2014). Another study using statistical analysis of ~4700 published iron speciation measurements from fine grained clastic rocks to test hypotheses of global redox change in Precambrian/Cambrian oceans found that the geochemical data does not show a statistically significant change in oxygen content through this boundary and these oceans were predominantly anoxic and ferruginous (Sperling et al., 2016).

The late Proterozoic Snowball Earth was first proposed in 1992 and it is now widely believed that the surface of the earth was completely frozen at least twice in the Marinoan and Sturtian from 1000 to 545 Ma (Kirschvink, 1992; Maruyama and Santosh, 2008). During these periods of extreme glaciation where continental glaciers reached to sea level in the low equatorial latitudes (Hoffman and Schrag, 2002) and it is postulated that the glaciation continued over millions of years until such time where there was sufficient levels of volumes of volcanically derived $CO_2$ accumulated in the atmosphere to counteract the icehouse climate; kick-starting the positive feedback which began to thaw the Earth (Hoffman et al., 1998; Hoffman and Schrag, 2002; Maruyama and Santosh, 2008). Many cases have been put forward to establish a link between the Snowball Earth and the Cambrian Explosion (e.g. Hoffman et al., 1998; Peterson et al., 2005; McCall, 2006) however a problem exists between timing of Snowball Earth which is constrained as 770-635 MA with two inter-glacial warming periods, and the fossil evidence for the Cambrian Explosion which places it between 520-488 Ma, thus denoting a time gap between these two events; does this imply that there is no relationship at all between these events? Another interesting puzzle is that some molecular clock studies place the origin of metazoans during this Snowball Earth period (dos Reis et al., 2015), inferring

that the internal conditions for the Cambrian Explosion were in place earlier on, whereas the external conditions remained too adverse for metazoan evolution.

As well as the above external controls a number of hypotheses have been put forward suggesting internal controls based on evolutionary, ecological or genomic break through to explain the observed increases in diversity across the Precambrian – Cambrian transition (Sperling et al., 2013). The evolution of macrophagy, which resulted in the evolution of larger body sizes, and subsequently skeletons, in response to increased benthic predation pressures, is proposed as a like cause of the Cambrian Explosion (Peterson et al., 2005). This predation pressure also stemmed the evolution of mesozooplankton, which irreversibly linked the pelagos to the benthos food webs and established the Phanerozoic ocean (Peterson et al., 2005). Another hypothesis is based on the unique and rapid coevolution that accompanied the early Ediacaran introduction of eumetazoans, succeeded by their early Cambrian expansion into the pelagic system (Butterfield, 2007; Butterfield, 2011). By reinventing the rules of macroecology by expanding into multi-trophic food webs, exhibiting larger body sizes, ecological succession etc. (Butterfield, 2011; Sperling et al., 2013). Both the Precambrian and Cambrian biospheres were integrally stable, however the former was derived from principally static physical environments whereas the Cambrian saw induced diversity and dynamic ecosystem engineering with the creation of new infaunal environments for macrobiotic and microbiotic organisms alike (Butterfield, 2011; Herringshaw et al., 2017). Other internal factors such as ecological hypotheses focusing on predation and the rise of carnivory suggest that this rise would have set off an evolutionary arms race, leading to a surge of new complex body types and morphological innovation due to changing selection pressures involving the increasingly complex food webs (Marshall, 2006). Consistent with this hypothesis, the origin of carnivory itself appears to be temporally correlated with the Precambrian-Cambrian transition and this hypothesis has been linked back to the idea of increased oxygenation as a driver for rapid evolution, consequently carnivory is a metabolically expensive feeding strategy and may have been driven as a consequence of increased oxygenation (Marshall, 2006; Erwin et al., 2011)

It has been proposed that around 540 – 480 Ma the Early Cambrian world underwent a significant sea level rise, in turn flooding continental margins and thus creating more habitable zones in the shallow continental shelves: and the landmasses were concentrated along low latitudes (Fig. 1). This also resulted in an increase in weathering of exposed basement rock. There is evidence for enhanced chemical sedimentation, indicative of increased ocean alkalinity and greater chemical weathering (Peters and Gaines, 2012; Smith and Harper, 2013). This great event that triggered the creation of new shallow marine habitats, shows a link between abiotic and biotic factors (Smith and Harper, 2013). The majority of these hypotheses have been presented as individual processes, primarily responsible for the causal modes of the radiation. It is likely that each of these hypotheses is intrinsically linked and there is not one single mechanism which is solely responsible for this event (Smith and Harper, 2013).

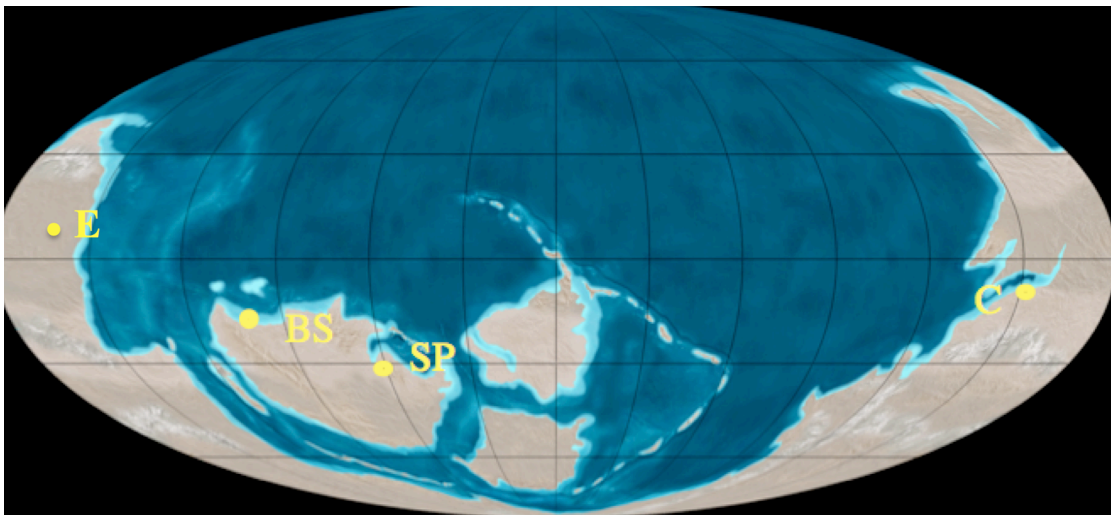


**Figure 1.1: Showing distribution of major landmasses during the Early-Mid Cambrian and the location of major Lagerstätten, BS – Burgess Shale, SP – Sirius Passet, C – Chengjiang, E – Emu Bay. Modified after Torsvik and Cocks (2013).**

## 1.2 Exceptional Preservation

After an organism dies it is normally destroyed by scavengers and various decay processes, and its component parts essentially get recycled into the surrounding environment, meaning that there is no record of the vast majority of organisms which have lived on Earth. However, under certain conditions, some organisms are fossilized and thus recorded in the fossil record. The occurrence of such fossils is critical in enabling us to gain insight into the evolution of life throughout geological time. The study of these processes, which affect the organisms after death, and up to its discovery as a fossil, is called taphonomy.

### 1.2.1 Taphonomic bias

These taphonomic processes have undoubtedly exerted a widespread bias to the fossil record and likely every fossil biota has been subjected to taphonomic bias. In normal marine near-shore communities soft bodied fauna make up around two thirds of the total species and individuals however the preservation of such fauna is relatively rare (Allison, 1988b), therefore the occurrence of exceptional preservation of fossilized soft parts is a profound example of preservational bias (Allison and Bottjer, 2011). However, there is evidence in the fossil record of biotas which do preserve soft tissues (e.g. Butterfield, 1995) so it would be erroneous to presume that exceptional preservation of soft-tissues had been subjected to minimal taphonomic bias.

The Cambrian Explosion marks the interval when virtually all present day bilaterian body plans evolved and therefore, the study of these deposits offers unique insight into the evolution of early life, allowing for reconstruction of extinct fauna that make up the stem lineages of major extant clades (Allison, 1988a; Butterfield, 2003; Sansom et al., 2010). Preservation of soft-bodied fossil biota localities, known as Konservat-Lagerstätten (Seilacher, 1970; Seilacher et al., 1985), preserve traces of normally unstable non-mineralizing tissues and these sites are not evenly distributed through geological time, and these exceptional faunas appear to be over-represented in the Cambrian and Jurassic (Allison and Briggs, 1993). The temporal concentrations of these deposits

correspond to particular sedimentary environments, and spatially the controls of their distribution may have been operating on a global scale (Allison, 1988b; Allison and Briggs, 1993; Allison and Bottjer, 2011).

### 1.2.2 The Cambrian Substrate Revolution

The reduction in the number of exceptionally preserved faunas after the Cambrian has been attributed to the evolution and diversification of deep bioturbators and the Cambrian Substrate Revolution (Allison and Briggs, 1993; Bottjer et al., 2000; Bottjer, 2010). As benthic metazoans increased the depth and intensity of bioturbation they in turn succeeded microbes as the dominant biological influence on seafloor conditions, moving away from the "matgrounds" which prevailed in the Ediacaran to the Early Cambrian seafloors (Hagadorn and Bottjer, 1997; Gehling, 1999; Bottjer, 2010) and subsequently making available to other biota a variety of previously inaccessible and unexploited resources and ecological niches (Bottjer et al., 2000; Bottjer, 2010).

Diminutive ichnofaunas directly associated with weakly or non-biomineralised taxa have been recorded in Cambrian Lagerstätten worldwide and are characterized as being millimeters to micrometers in diameter, relatively simple and non-branching in terms of morphology, show scarce penetration and exhibit part-counterpart type preservation (Zhang et al., 2007; Mángano, 2011; Mángano et al., 2012). The absence of biogenic reworking of sediment by burrowing taxa along with the presence of microbial mats has been put forward as a mechanism for the development of firm substrates at the sediment-water interface at the Ediacaran-Cambrian transition (McIlroy and Logan, 1999; Seilacher, 1999; Jensen et al., 2005; Mángano et al., 2012). This combination of processes would have resulted in unique taphonomic conditions for the exceptional preservation of carbonaceous matter and these tiny biogenic ichnofaunas that are characteristic of Cambrian Lagerstätten (Mángano et al., 2012). The taphonomic bias which stems from greater preservation under reduced bioturbation levels in the Cambrian is a captivating example of how evolving biological processes can directly influence taphonomic processes, adding to the complexity of inducing bias throughout geological time.

### 1.2.3 Taphonomic filters

Decay of organisms, before they are subject to fossilization and preserved in the fossil record, can lead to complex difficulties when comparing these taxa to extant organisms when trying to compare the shared characters, or synamorphies, on which evolutionary study ultimately rests (Sansom et al., 2010). For example, the placement of fossils in the appropriate stem or extant clades is dependent upon the absence (or possession) or certain characters, therefore a fossil missing certain key characters may be placed on a certain stem based on the morphological features identified in the fossil. However, if care is not taken to distinguish whether these morphological features are true to the original organism and haven't been lost due to taphonomic filters leading to its preservation, it may be considered as being 'less evolved' than it actually is. Inability to differentiate between the causes of character absence can lead to flawed evolutionary assumptions (Sansom et al., 2010).

Hence, a persistent problem with regards to the fossil record is that not all organisms are preserved completely intact; events such as predation, combined with complex taphonomic processes, can result in exceptional preservation, which does not provide an accurate duplicate of the original organism's in-vivo anatomy. Unlike the skeletons of vertebrates; soft tissues can be distorted and altered by processes of decay and digenesis that are the same processes, which are ultimately, key to their fossilization (Sansom et al., 2010; Sansom, 2014). In terms of taphonomic processes, two main pathways are the leading mechanisms of preservation; organic preservation and authigenic microbially mediated preservation (Gehling, 1999; Briggs, 2003; Sansom, 2014). Organic preservation occurs when decay is inhibited to allow the organism's original biomolecules to be preserved, such as nucleic acids, proteins, carbohydrates, lipids, and resistant biopolymers etc. (Briggs et al., 2000; Briggs, 2003) and this kind of preservation can be enhanced depending on the subsequent diagenesis (Butterfield, 2003; Powell, 2003; Page et al., 2008). This leads on to the role of experimental taphonomy: biomolecules are transformed during the fossilization process and this transformation can be investigated experimentally.

### 1.2.3 The role of experiments in taphonomy

The role of experiments in investigating taphonomy and exceptional preservation are based on two main premises: that some of the key processes involved in the preservation of soft-tissue take place on a measurable laboratory timescale and that the complex processes involved in taphonomy can be simplified to allow individual aspect to be determined (Sansom, 2014; Briggs and Mcmahon, 2016). The digenetic processes involved in the fossilization of organisms most likely operate over geological timescales spanning millions of years, however the initial taphonomic filters of decay, degradation and disarticulation likely take place over timescales spanning days, weeks or months because if tissues do not survive these initial processes there will be nothing left to be fossilised (Briggs, 2003; Briggs and Mcmahon, 2016). Organic preservation requires the retardation of decay therefore experimental procedures can be used to investigate the factors that influence and affect rates of soft-tissue decomposition, and anaerobic conditions along with rapid burial are regularly cited as fundamental conditions for organic preservation and have been tested through experimental processes (Allison, 1988b; Briggs and Kear, 1993a; Sansom, 2014). Information lost through decay is a major problem in determining the phylogenetic position of soft-bodied organisms and this loss of information, or characters, can challenge any interpretation based on cladistic analysis (Sansom et al., 2010; Sansom et al., 2011).

Microbially mediated mineralisation is the second pathway and authigenic mineralization relies on almost immediate action by microbes which work to actively decay structures in an organism to leave a characteristic chemical signature, though means of phosphatisation, silicification, pyritisation etc. (Gehling, 1999; Briggs, 2003; Darroch et al., 2012; Sansom, 2014). This mechanism of preservation has successfully been demonstrated in a laboratory setting, where mineralisation was induced on a measurable laboratory timescale (Briggs and Kear, 1993b; Briggs and Kear, 1994; Sagemann et al., 1999; Darroch et al., 2012). These experiments allow identification of the conditions necessary for mineralisation and allow insight into the specific mechanisms involved

(Briggs and McMahon, 2016). The chemical microenvironments favorable to soft-tissue preservation were successfully characterized by Sagemann et al., (1999) and they demonstrated that the growth of authigenic minerals in association with decaying organic matter is a rapid process that is intrinsically linked with bacterial activity; oxygen was depleted, pH increased and sulphide accumulated around the decaying tissue which created steep chemical gradients and anaerobic decay (Sagemann et al., 1999).

Essentially, to make sense of exceptional preservation we need to understand the taphonomic processes that lead to their preservation and how they may have been altered through these processes. The resulting information that can be inferred from a fossil has essentially been passed through taphonomic filters (i.e. death, decay, burial, diagenesis), and these filters need to be unravelled to allow us to understand the palaeobiological implications of the fossilised organism. Taphonomic bias is influenced by diverse biological, physical and geochemical processes, which are ultimately dependent upon the depositional environment (Allison and Bottjer, 2011).

## 1.3 Overview of Cambrian Lagerstätten

Our knowledge and understanding of the Cambrian Explosion is unsurprisingly biased towards mineralizing organisms, due to their skeletal remains being robust enough to lead to preservation (Butterfield, 2003). This bias is revealed in sites of exceptional preservation, such as the Burgess Shale and Chengjiang, where the large majority of taxa and individuals were soft-bodied (non-biomineralising) (Butterfield, 2003). Corresponding with the radiation of skeletal fossils there is also evidence in the fossil record for the diversification of trace fossils (Conway Morris, 2006), and although examination of trace fossils only leads to speculation of the animal that left the traces, it is apparent that soft-bodied organisms made the majority of these. Since the record shows an increase in biomineralising organisms but also an increase in traces made by soft-bodied animals; it suggests that the Cambrian Explosion was not just an artifact of this increase in biomineralisation. And as previously discussed, the Proterozoic-Cambrian transition hosts a rich record of non-biomineralising fossils from sites known as Lagerstätten.

There are over 50 known Burgess Shale-type (BST) deposits, which occur worldwide over multiple palaeocontinents and are primarily restricted to Early and Middle Cambrian strata (Gaines, 2014). The importance of these deposits is widely accepted, however there is still a degree of controversy surrounding the exact mode of preservation in these localities. BST preservation resulted from a combination of pathways and specific conditions which operated at a local and global scale (Gaines, 2014). These combined influences operated to drastically slow microbial decay by sulphate reduction during early burial, thus resulting in incomplete decomposition and preservation of soft-bodies (Gaines et al., 2012; Gaines, 2014). Anoxia in bottom waters is accepted as a prerequisite for BST preservation but this alone cannot be responsible for exceptional preservation (Briggs, 2003; Gaines, 2014) since anaerobic decay of labile tissues due to sulphate reduction may occur as rapidly as aerobic decomposition of the tissue. Therefore, anoxia is ineffective as a long-term conservation pathway in the

preservation of soft tissues, however studies has shown that decay-induced mineralisation can occur rapidly, so even a small reduction in the rate of decay may lead to improved chances of preservation (Allison, 1988b; Petrovich, 2001). Conventionally low oxygen levels and rapid burial of organisms are considered to be the essential driving factors in the preservation of soft-bodied fossils and the formation of Konservat-Lagerstätten, however these are only a starting point in promoting early diagenetic mineralisation, with the latter being the most efficient way in preventing information and character loss through decay (Petrovich, 2001; Gaines et al., 2012; Gaines, 2014).

Several hypotheses for BST preservation have been put forward but none have adequately explained their temporal and spatial distribution. Without these Lagerstätten, our only window into the origin of animal phyla would be the fossil record of mineralised parts and because biomineralisation has developed numerous times across different animal lineages (Murdock and Donoghue, 2011) most of their early history would be missing from the fossil record. Therefore, this soft-bodied fossil record provides us with a window into early evolution of the major animal groups. The next section will outline the three most famous Cambrian Lagerstätten and discuss the different taphonomic pathways that have been proposed in each to provide a picture of both the similarities and contrasts between each.

### 1.3.1 The Burgess Shale

The Burgess Shale of British Columbia is an iconic example of a Cambrian fossil Lagerstätte of extraordinary quality, diversity and evolutionary significance (Butterfield, 1990) and arguably the most famous of Cambrian Lagerstätten. Burgess Shale-type preservation (BST) is usually recognized as carbonaceous compressions in marine shales where soft-bodied features are preserved (Butterfield, 2003; Broce and Schiffbauer, 2017). The fossils of the Burgess Shale notably retain the outline of three-dimensional features via the process of kerogenization, whereby organic tissues are converted to a more stable form of carbon, a consequence of rapid collapse due to the degradation of supporting cellular tissues (Butterfield, 2003; Broce and Schiffbauer, 2017). These are sometimes associated with aluminosilicates, which may have replicated decay-prone tissues prior to decomposition (Orr, 1998).

The "Phyllopod Bed" (PB) is an informal rock unit within the Walcott Quarry Member of the Burgess Shale Formation. It is the most fossiliferous of beds within the formation and contains classic Burgess Shale fauna (Fletcher and Collins, 1998; Gabbott et al., 2008) and was discovered by Walcott in 1909. Since the discovery of the PB, subsequent excavations have extended the unit to 5m below Walcott's original quarry floor and laterally to the top of the Wash Limestone (Gabbott et al., 2008). This newly exposed stratigraphic section is about 7m thick and is referred to as the "Greater Phyllopod Bed". The fauna of the GPB is represented by ~158 genera, mostly monospecific and non-biomineralising, representing 17 major taxonomic groups (Caron and Jackson, 2008). Understanding the mode of exceptional preservation is key to our understanding the palaeoecological and evolutionary processes occurring at this time (Conway Morris, 1989; Caron and Jackson, 2008).

Mineral- specific diagenesis by suppressing the normal microbial decay based processes (Butterfield, 1990; Butterfield, 1995; Gaines et al., 2012) or by a secondary enhancement of the recalcitrance of labile substrates (e.g., Petrovich,

2001) are both considered as an essential criterion in BST preservation. There have been attempts to constrain these models, such as experimental decay studies on lobster eggs, which have shown that sedimentary particles will attach to lobster eggs in the presence of bacteria (as opposed to authigenic precipitation) (Martin et al., 2004) and those by Briggs and Kear (1994) where they studied the decay of the shrimp *Crangon*, and the prawn *Palaemon*, both of which are not fully biomineralised, with the main experimental controls being the availability of oxygen at the beginning of decay and whether the system was open of closed to diffusion. They showed that pH is influenced by the open or closed nature of the system and pH decreases most in a closed system, inhibiting the precipitation of calcium carbonate in favour or calcium phosphate (Briggs and Kear, 1994). This study was looking at decay in a sediment-free system and was subsequently adapted by Wilson and Butterfield (1994) to investigate the effect of the mineralogy of sediment on the decay and early diagenesis of the marine invertebrates *Nereis virens* (polychaete annelids) and *Crangon crangon* (crustacean arthropods) (Wilson and Butterfield, 2014). This showed a lack of correlation between sediment grain size and morphological preservation, suggesting that permeability of sediment was not a primary factor in the preservation of carbonaceous films and that initial sediment sealing may be an essential criterion for fossilization by early diagenetic mineralization (Wilson and Butterfield, 2014).

Therefore, in light of the decay experiments, changes in ocean chemistry and clay mineralogy of the sediment are probable significant factors in the opening and closing of the BST preservation taphonomic window. During the early Paleozoic oceanic pH is estimated to have been at the Phanerozoic minimum which is coincident with the interval of heightened BST preservation (Arvidson et al., 2013) along with low global oceanic sulphate concentrations and low-oxygen bottom water conditions at the BST sites, causing reduced oxidant availability (Gaines et al., 2012). Experiments have also shown that elevated kaolinite may have also been a controlling factor but this is problematic to constrain in BST settings due to the significant metamorphic overprint in the rocks of the Burgess Shale (Powell, 2003) and a better understanding of the metamorphic history of

the fossil rich beds is required to unravel the puzzle of the early Cambrian taphonomic window (Powell, 2003; Forchielli et al., 2014).

### 1.3.2 Chengjiang

The Chengjiang Lagerstätte was first discovered in 1984 by Hou Xianguang in the Yunnan Province, China. It represents one of the oldest Cambrian Lagerstätten dated at around 525 Ma (Gabbott et al., 2004; Zhang et al., 2007). There are strong similarities with the Burgess Shale fauna, with the biota being dominated by arthropods and sponges and the rest composed of a variety of taxa including; lobopodians, annelids and brachiopods. The Chengjiang Lagerstätte also contains an occurrence of trace fossils, however unlike the Burgess Shale where the trace fossils are preserved in beds isolated from those bearing soft-bodied preservation (Allison and Brett, 1995), the traces in Chengjiang occur alongside the fossils and are particularly associated with soft carapaces or skeletons (Zhang et al., 2007). Despite this there are strong similarities between Chengjiang and the Burgess Shale and many species from the two sites are closely related.

The Chengjiang biota is widely accepted to be a typical BST deposit, influenced by post diagenetic alteration and weathering which led to alterations in clay and iron minerals (i.e. pyrite later pseudomorphed by iron oxides) (Gabbott et al., 2004; Forchielli et al., 2014). Many of the fossils from the classic Chengjiang sections are heavily weathered and light gray to yellowish or brown in color, with EDX analysis confirming the presence of aluminosilicates on the fossil surfaces and surrounding matrix (Zhu et al., 2005). Many of the weathered specimens also appear to be covered with a thin pale brown mineral film; composed of Fe- rich aluminosilicates (Zhu et al., 2005). The pathway for the precipitation of pyrite is that decaying carcasses may have acted as a local substrate for Fe- and Sulphate reducing bacteria, due to the clay-rich sediment being depleted in organic carbon (Gabbott et al., 2004; Forchielli et al., 2014). The differing morphology of pyrite which shows both framboidal and euhedral habits is explained as being a consequence of differing decay rates which in turn would influence the supply of $H_2S$; framboidal habits would occur due to rapidly decaying tissues, quickly supplying $H_2S$, producing many pyrite nuclei. Larger

euhedral pyrite would form where more recalcitrant tissues would initiate a slower $H_2S$ production allowing for crystal growth operating on fewer nuclei.

Non-weathered specimens have been found to retain dark films consisting of organic carbon, pyrite, apatite and Fe-rich clay minerals on their surface (in particular gut traces of priapulid worms *Maotianshania* and *Palaeoscolex*) with the presence of carbon being tissue specific and occurring in places such as the alimentary canals (Gabbott et al., 2004; Zhu et al., 2005; Forchielli et al., 2012). It has been argued by Zhu et al., (2005) that early diagenetic mineralization such as phosphatisation and pyritisation played a key role in the preservation of nonmineralised organisms of BST deposits, however this has also been disputed that the conservation of organic tissues is the primary mechanism in the preservation of non-biomineralised fossils since this requires suppression of the processes and filters which lead to the decomposition and loss of character information in organic remains in the marine realm (Gaines et al., 2008).

### 1.3.3 Emu Bay Shale

The Emu Bay Shale (EBS) is a lower Cambrian (Series 2, Stage 4) BST fauna, and is by far the richest of these known in the southern hemisphere. Some have argued that although it contains a biota that are taxonomically similar to other Cambrian BST deposits (see Briggs and Nedin, 1997; Paterson et al., 2016) the EBS differs from current understanding of typical BST deposits and their accompanying taphonomic pathways (Gaines et al., 2008; Gaines et al., 2012) and resulted in is being unequivocally ruled out from the global list of more that 50 known BST deposits (Gaines, 2014).

The EBS fossils display a range of taphonomic pathways and are characteristically preserved as two-dimensional compression fossils, made up of both carbonaceous and mineralized films (McKirdy et al., 2011). Soft tissues are preserved through a variety of processes such as preservation in phosphate or pyrite, and in some cases they preserve a level of detail that is somewhat absent from most other Cambrian Konservat-Lagerstätten (McKirdy et al., 2011; Paterson et al., 2016). The EBS contains the oldest recorded phosphatised muscle tissues of the geological record; preserved muscle tissues have been documented in the Sirius Passet but these are preserved in silica (Strang et al., 2016a).

Most studies on the taphonomy of the EBS fossils have been concentrated around the diagenetic aspects, particularly on early diagenetic mineralisation of soft-tissues (Gaines, 2014; Paterson et al., 2016) and late stage diagenetic mineralization whereby pink to white fibrous calcite replicates fossils such as the phosphatisation of labile tissues (Briggs and Nedin, 1997), gut tracts (see García-Bellido et al., 2009; Edgecombe et al., 2011; Paterson et al., 2012) but is also present in recalcitrant extracellular cuticle such as in the preservation of non-trilobite arthropod eyes which show fine detail of the visual surfaces (Lee et al., 2011). Full understanding of the taphonomy is also hindered by extensive surface weathering at the EBS locality (similar to that seen in Chengjiang (Forchielli et al., 2014)).

Certain taxonomic groups that are commonly represented in other Cambrian BST biotas are either very scarce in the EBS or are completely absent (e.g. echinoderms) and unraveling whether this is due to taphonomically controlled filters (rather than biogeographical or environmental controls) remains an important challenge in the EBS (Paterson et al., 2016). The depositional environment of the EBS is interpreted to have been deposited in an isolated, anoxic depression in the seafloor with evidence of syndepositional slumping implying a nearshore setting (Gehling et al., 2011; Paterson et al., 2016). The combination of this nearshore setting and the diversity if preservational modes discussed (i.e. 3D relief of soft-bodied taxa and the range of early diagenetic mineralization of both labile and recalcitrant tissues) is the reason that it has been proposed that the EBS doesn't sit well with the other typical BST deposits (Gaines, 2014) and more work needs to be done to conclude whether the taphonomic filters such as extensive surface weathering and post-preservation alteration, along with tissue specific controls are the main factor in influencing the appearance and composition of the EBS.

## 1.4 The Sirius Passet

### 1.4.1 Overview of the Sirius Passet

The Sirius Passet Lagerstätten of Peary Land, North Greenland occurs in marine mudstones (Buen Formation) (Fig. 1.3). The Buen Formation crops out across a large part of the Franklinian Basin (Higgins et al., 1991) (Fig. 1.2). These marine mudstones were originally interpreted to have been deposited in a slope environment along the eroded scarp of a pre-existing carbonate platform (Peel and Ineson, 2011) that represents the subsidence and subsequent regression of the eroded scarp (Budd and Peel, 1998). The mud-dominated siliciclastics of the Buen Formation record the transgression and on-lap of a degraded carbonate platform in the Early Cambrian (Peel and Ineson, 2011) and was a storm dominated shelf environment. This is indicative of rapid burial, which has been postulated as a major factor in the environmental setting of the Burgess Shale. This general geological setting of the Sirius Passet is somewhat similar to that of the Burgess Shale in British Columbia.

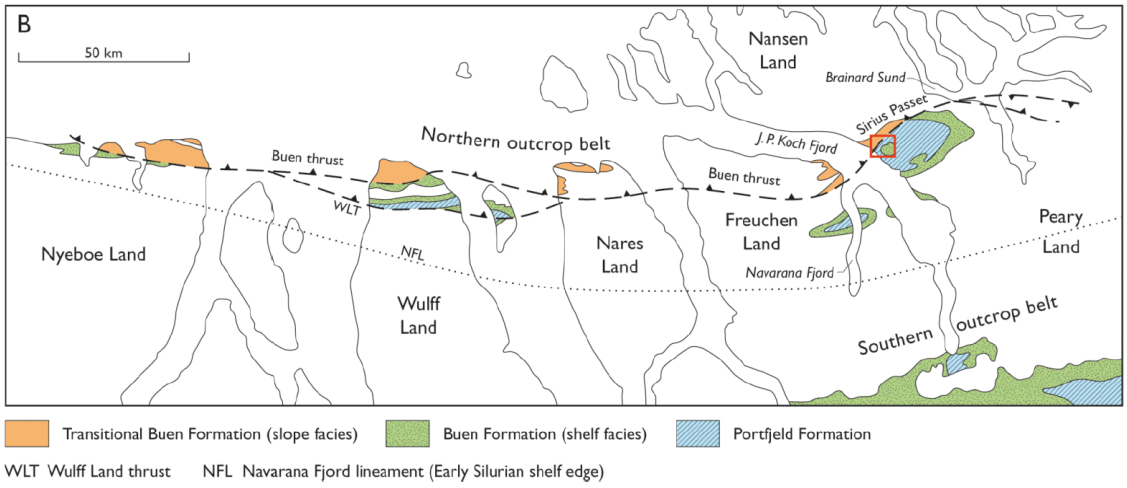


**Figure 1.2: Geological map showing the present day locality of the Sirius Passet Lagerstätte, indicated by red box. Modified from Ineson and Peel (2011)**

At the present day Sirius Passet is located at 82°47.6'N, 42°13.7'W (Fig. 1.2). It represents the oldest known exceptional preservation of soft tissues, predating both Burgess Shale and Chengjiang, and has been postulated to fall within the

spectrum of Burgess Shale-Type preservation (Budd, 2011). Since its discovery in 1984 there have been subsequent expeditions, which have collected over 8000 specimens (belonging to ~40 described species). Later expeditions in 2009 and 2011 assembled new collections including in situ material from outcrops (Vinther et al., 2011; Mángano et al., 2012). The taxonomy of Sirius Passet has been widely studied. For instance, it contains the oldest Lower Cambrian trilobites known from North Greenland (*Buenellus higginsi*) (Morris and Peel, 2008) along with sponges, worms, halkieriids, lobopods and non-trilobite bivalve arthropods (Williams et al., 1996). Bioturbation is evident throughout the majority of the Buen Formation, indicated by mottling, but is not present in the Lagerstätte interval (Stein et al., 2013). Lamination in these beds is strongly developed (3-10 mm scale).

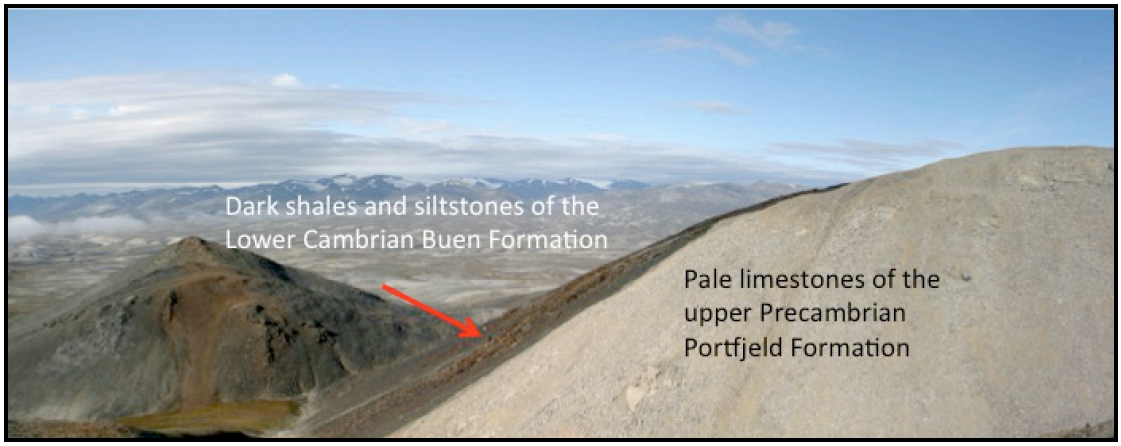


**Figure 1.3: Image showing the present day field locality of the SP. The relationship of the dark shales of the Buen Formation to the limestones of the Portfjeld Formation is highlighted with the red arrow. (Courtesy of David Harper.)**

### 1.4.2 Depositional environment

The formation at Sirius Passet includes two end member lithofacies and their distribution can be seen in Fig. 1.4; a 'spotted' (Fig. 1.5) and a silt-rich (Fig. 1.6) facies (Strang et al., 2016b). Despite greenschist facies metamorphism, the primary sedimentary fabric remains preserved. The "spotted facies" is characterized by concentrated chlorite-mica aggregates, which are apparent as face-face aligned crystallites, and are distributed throughout the section in discontinuous wavy beds (Fig. 1.5A-B). The beds of the silt-rich facies are characterised by normal and reverse grading and show irregular contacts and scouring at the base of normal graded beds (Fig. 1.6A). Lamination in this facies is typically of single grain thickness layers of quartz (Fig. 1.6B). There is also some evidence of low angle cross lamination picked out by these single grain layer laminations (Fig. 1.6C) and both facies contain abundant chloritoid porphyroblasts, indicative of greenschist facies metamorphism. (Fig.1.5D; Fig. 1.6D). A number of lines of evidence indicate the facies described are not distal turbidites such as seen in the BS: a) laminations seen in thin sections are not ordered, b) fluctuations occur between finer grained and courser grained layers, c) bioclasts are present within the layers, i.e. 'floating'.

Acritarchs and olenelloid trilobites have been recovered from the informal member of the Buen Formation, the "Transitional" Buen, in Peary Land, and they broadly constrain the stratigraphical position of the lower Buen Formation to Cambrian Stage 3 (Babcock and Peel, 2007). Acritarchs are indicative of the *Heliosphaeridium dissimilare–Skiagia ciliosa* Biozone and perhaps the *Volkovia dentifera–Liepaina plana* Biozone as used in the Eastern European Platform and Baltoscandinavia (Moczydłowska and Vidal, 1986; Vidal and Peel, 1993). The biozones correlate approximately with the *Holmia* and *Protolenus* trilobite biozones [*sensu* (Geyer and Shergold, 2000)] indicative of Cambrian Series 2 (Babcock, 2005).

The *Holmia* Biozone correlates to the upper part of Cambrian Stage 3 and the lower part of Stage 4 and the *Protolenus* Biozone correlates to Stage 4 as

presently conceived (Babcock and Peel, 2007). The occurrence of the olenelloid trilobites *Olenellus hyperboreus* and *O. svalbardensis* in the upper Buen Formation indicates the *Olenellus* Biozone of Laurentian usage (Blaker and Peel, 1997). The *Olenellus* Biozone belongs to the provisional Stage 4 of the Cambrian (Babcock, 2005). Its base is historically regarded as the base of the Dyeran Stage of Laurentian usage (Palmer, 2011) and correlates approximately with the onset of the Mingxinsi Carbon Isotope Excursion [MICE: (Zhu et al., 2006)].

*Buenellus higginsi* is the most common macrofossil in the "Transitional" Buen at Sirius Passet and provides a biostratigraphical age. This species is included within the family Nevadiidae and its presence is indicative of the *Nevadella* Biozone as used in Laurentia (Blaker, 1988; Blaker and Peel, 1997). This biozone correlates to the middle part of provisional Stage 3 (the lowest stage of the provisional Series 2) (Babcock et al., 2005). Historically, the *Nevadella* Biozone has been assigned to the upper part of the Montezuman Stage as used in Laurentia (Palmer, 2011). Sirius Passet has been correlated with the Chengjiang and Guanshan Lagerstätten from South China, which are temporally related to the Cambrian Arthropod Radiation (CARE) isotopic excursion (Zhu et al., 2006). Within biostratigraphical uncertainty the "Transitional" Buen is older than the Buen Formation *s.s.* in southern Peary Land.

The presence of a diverse invertebrate benthos in Cambrian Konservat-Lagerstätten indicates the overlying water column was oxic with a sharp redox boundary at the sediment-water interface. Bioturbation is surficial and typically only occurs in association with generally large arthropod carcasses (Mángano et al., 2012). Cyanobacteria are photoautotrophic and oxygenic microorganisms and could have produced the oxygenated conditions at the seafloor. However, in extant cyanobacterial mats, sulphate reduction of the biomass can produce hydrogen sulphide ($H_2S$) emissions above the mat surface, particularly at night (Jørgensen, 1979). Periodic high levels of $H_2S$ could have been a major factor impeding the settlement of benthonic organisms on the seafloor. Either the mat dwelling fauna was ephemeral and able to escape $H_2S$ emissions or had adapted a resistance to $H_2S$ toxicity. Occasional massive sulphide expulsion from the

decaying mats might have led to mass mortalities of the mat dwelling community [cf. Weeks et al., 2002].

It appears that normal marine carbonaceous shales in the Cambrian were limited to shallow-water regions with turbulent circulation (Raiswell and Berner, 1986). Negative $d^{13}C$ values commonly associated with Cambrian black shale deposition indicate either: (1) export production was low due to the removal of phosphorous into deep-water brines and nitrate by expansion of nitrate-reducing bacteria in association with an expanded oxygen minimum zone (Brasier, 1992), or (2) extensive fractionation by sulphate reducing or methanogenic bacteria (Murray et al., 1989) The latter is supported by widespread positive $d^{34}S$ during black shale deposition and relatively low C/S, which are both indicative of a major expansion of the sulphate-reducing biotope (Raiswell and Berner, 1986)

It is proposed that the arthropod-lobopodian fauna that characterizes the Sirius Passet inhabited a warm, muddy, matground habitat close to or just below storm wave base, but within the photic zone. Primary productivity was mainly by benthic cyanobacteria. Contemporary shallow subtidal to intertidal carbonate environments had a distinct shelly fauna including archaeocyathans, halkieriids, tommotiids, hyoliths, molluscs, rare trilobites, and a variety of other small shelly fossils of unknown affinity [examples cited in (Mount and Signer, 1985)]. The rapid appearance in the geological record and ecological stability of the "Burgess Shale-type assemblages," over some 10 million years, suggest that rather than being long-lived holdovers, successively displaced from the shallow water (Mount and Signer, 1985; Conway Morris, 2008), these animals were members of new Bambachian megaguilds (groups of organisms with mutually similar adaptive strategies), highly specialised and adapted to the dynamic and unstable nature of the tropical, muddy lower shoreface and shelf (Fig. 1.7). The discovery of large suspension feeders such as anomalocarid *Tamisiocaris borealis* from the Sirius Passet suggests a well-developed pelagic biota which is supported by high primary productivity and abundant mesozooplankton

supports this theory because small prey can only be exploited by larger animals if they existed in significant densities (Vinther et al., 2014).

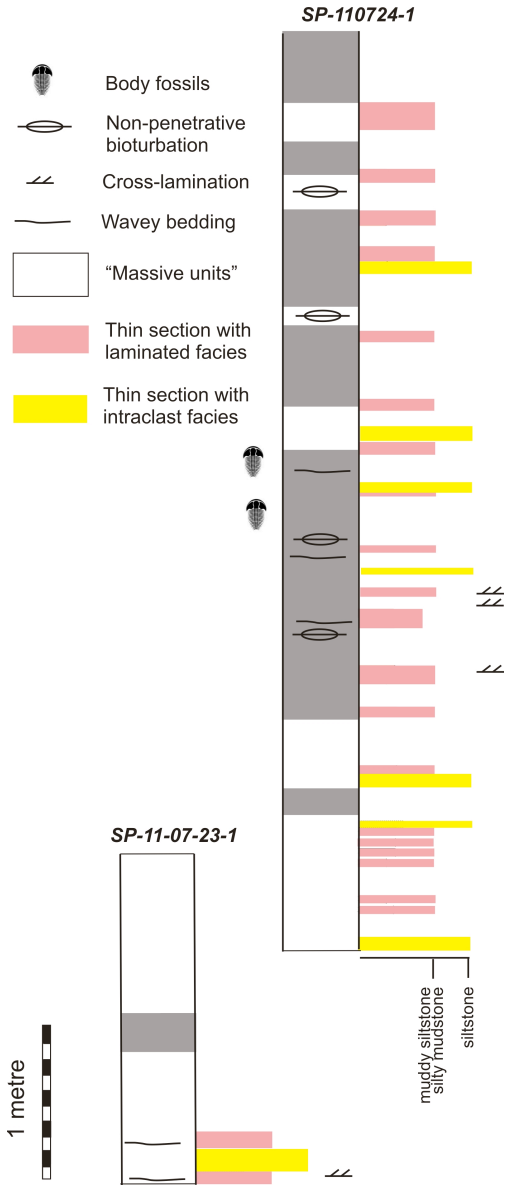


**Figure 1.4: Graphic log of the Buen Formation at Sirius Passet based on thin section analysis and interpretation. Drawn with the aid of field notes/logs and labeled samples collected by Professor David Harper in 2009 and 2011. Samples were sectioned according to height from the base of the log to create graphic log. The main Lagerstätte interval is represented by trilobite (body fossil) symbols. Pink bars indicate thin sections showing laminated facies. Yellow bars are thin sections with "spotted" facies.**

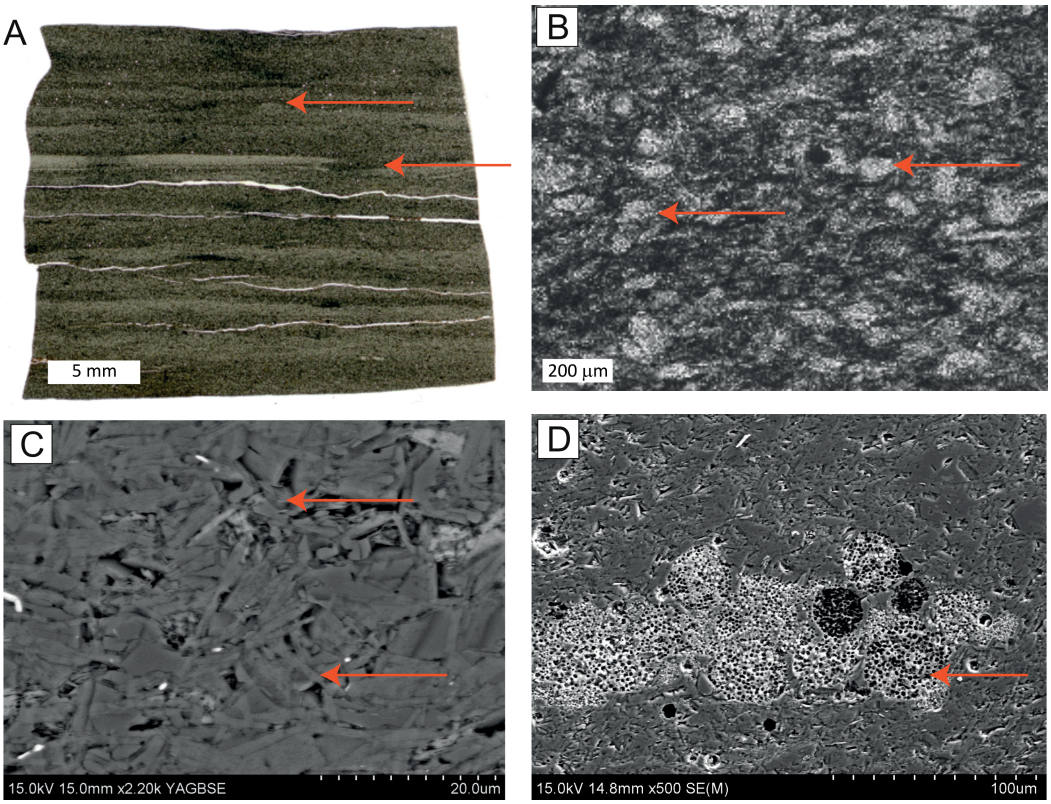


**Figure 1.5: Thin section and SEM photomicrographs of the "spotted" facies. A. High resolution scan of a thin section showing the concentration of chlorite-mica aggregates into discontinuous wavy beds (3.4m from base of log). Indicated by red arrows. B. Photomicrograph in plane-polarized light showing chlorite-mica aggregates of varying sizes (1.12 m above base of log). Light areas/patches; examples indicated by red arrows. C. SEM-backscatter (BSE) image showing face-to-face alignment of crystallites making chlorite-mica aggregates (5.5 m from base of log). Indicated by red arrows. D. BSE photomicrograph of silicified microbial mat fragment in a matrix of predominantly chlorite-mica aggregates (5.5 m above base of log). Indicated by red arrows.**

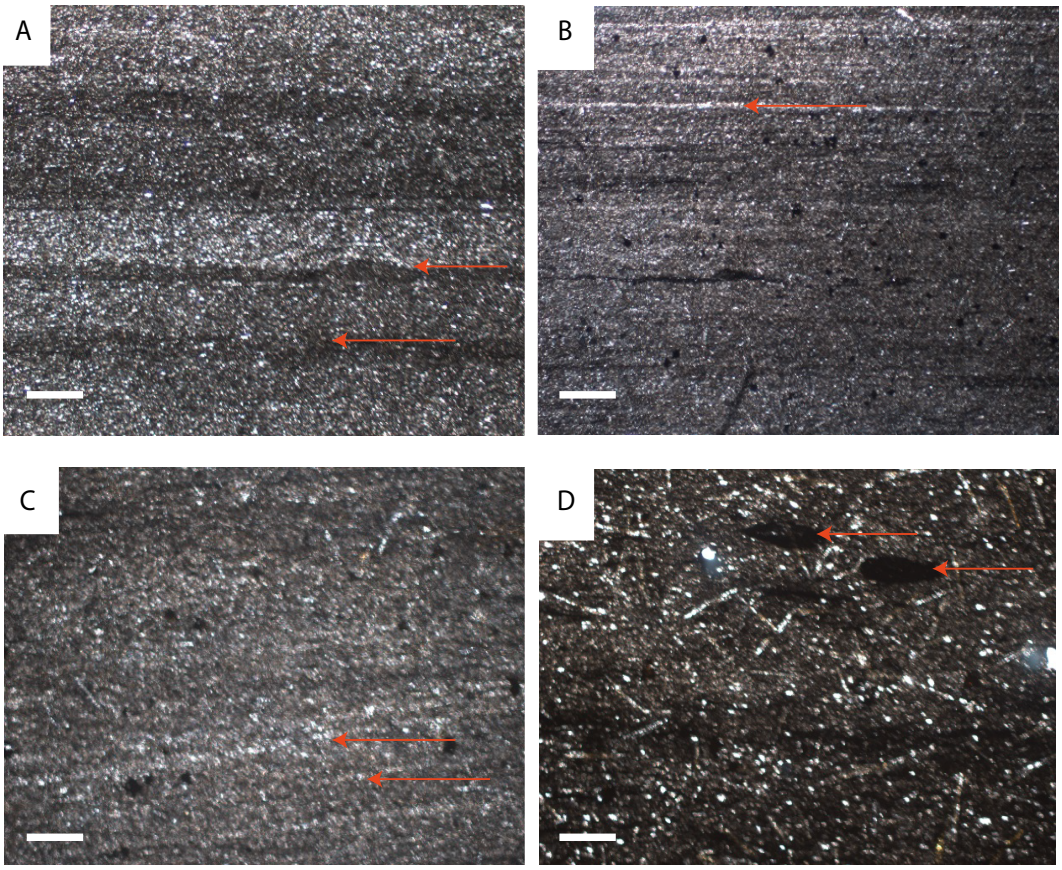


**Figure 1.6: Thin section and SEM photomicrographs of the silt-rich facies. A. Photomicrograph in plane polarized light showing normal (and reverse?) grading. Sharp, irregular contacts indicate scouring at the base of normal graded beds, indicated by red arrows (0.76 m above base of log). Scale bar is 1mm. B. Photomicrograph in plane-polarized light showing lamination picked out by single grain thickness layers of detrital quartz, indicated by red arrows (4.56 m up from base of log). Scale bar is 5mm. C. Photomicrograph in plane polarized light showing low angle cross lamination picked out by single grain thickness layers of detrital quartz, example indicated by arrows (4.77 m above base of log). Scale bar 5mm. D. Photomicrograph in plane-polarized light showing elliptical outsized floating grains of dark mudstone within a matrix of phyllosilicates, quartz, and chloritoid porphyroblasts, examples indicated by red arrows (3.31 m above the base of log). Scale bar is 5mm.**

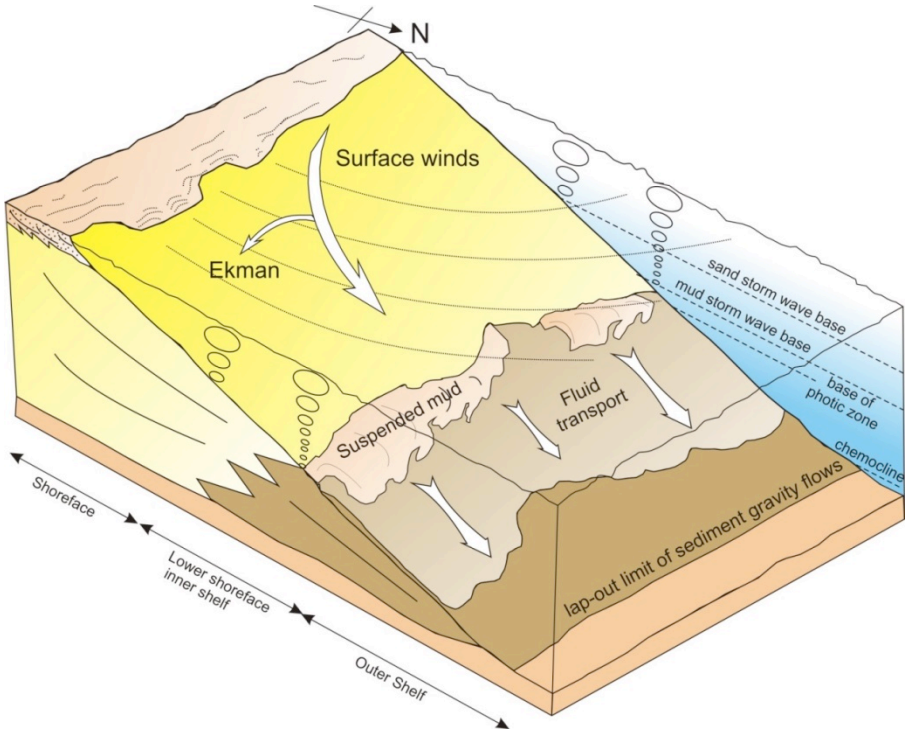


**Figure 1.7: Block diagram illustrating the depositional environment at Sirius Passet during the Early Cambrian (modified after Plint, 2014)**

### 1.4.3 Previous work on the taphonomy of the SP

Preservation in the Sirius Passet varies, with three main types of preservation present; moulds, films and silicified guts. The combination of these structures is similar to those seen in the Burgess Shale, and Butterfield (2003) discussed that despite the alteration due to weathering and metamorphism, the Sirius Passet fossils are likely to have undergone the same taphonomic pathway as Burgess Shale and therefore can be characterised as BST preservation.

Although the Sirius Passet Lagerstätte may not match the species richness of the Burgess Shale or Chengjiang biotas, is has still yielded an impressive variety of organisms which show exceptional preservation (Conway Morris et al., 1987; Peel et al., 1992; Morris and Peel, 2008). Particular focus of previous studies has been on the exceptionally preserved trilobites (Budd, 1995; Blaker and Peel, 1997; Babcock and Peel, 2007; Stein et al., 2013), halkieriids (Morris and Peel, 1990; Conway Morris and Peel, 1995), sponges (Rigby, 1986; Botting et al., 2015; Botting and Peel, 2016) and non-trilobite arthropods such as *Kerymachela kierkegaardi*, which shares characters with biramous arthropods and two famous burgess Shale problematica, *Opabinia* and *Anomalocaris* (Budd, 1993; Budd, 1997). Other arthropods include *Amisiocaris borealis* which possesses an elongated appendage with possibly anomalocaridid affinities, however differs from the frontal appendage of *Anomalocaris* in that segment boundaries are absent and ventral spines are relatively long and spineless (Daley and Peel, 2010). It is suggested that these differences may be caused by taphonomic filters, however the morphology of the described specimen does indicate it was unlikely that this appendage was originally segmented or sclerotized (Daley and Peel, 2010). In the descriptions of other Sirius Passet arthropods (Budd, 1993; Budd, 1995; Budd, 1997; Budd and Peel, 1998; Budd, 1999; Budd, 2011; Peel 2017) reference is made to the taphonomic history of the SP and the bias and filters present in the Sirius Passet to explain missing characters or appendages, and early mineralization has been cited as a leading factor in the preservation of internal structures (e.g. *Kerygmachela kierkegaardi* where circularly arranged musculature is preserved (Budd, 1993)).

Early post-mortem mineralisation has also been proposed as the preservational method for the three-dimensional preservation of the digestive tract in some SP arthropods (Budd 2011; Peel 2017a). Most of these three-dimensional traces show good preservation of the digestive tract and axial area but appendages become unclear distally (Budd, 2011). Endogenous bacteria have been suggested as a mechanism for mediated phosphatisation within the digestive system (Butterfield 2002; Butler et al., 2015; Zacaï et al., 2016; Strang et al., 2016a; Peel 2017b) but it is also possible that phosphorous and calcium were present in the animal's digestive tract during life.

Vetulicolians have also been described from the SP and are preserved as reflective films, this differs from the preservation of vetulicolians from Chengjiang, which show significant relief (Shu et al., 2009; Vinther et al., 2011). These differences in preservation are likely a function of differing taphonomic pathways because soft-bodied taxa and moulted trilobites are also preserved with slight to moderate relief in the SP (Budd, 2011; Vinther et al., 2011) whereas mineralizing taxa such as trilobites (i.e. *Buenellus*) exhibit significant relief (Strang et al., 2016b). In the SP some limb traces of non-mineralizing organisms are preserved with slight to moderate relief as depressions in exoskeletons, however, evidence in some rare specimens show that these depressions in the exoskeleton overlie the limb, therefore the naive interpretation of robustness of these limbs during decay and compaction can be ruled out (Budd, 2011). Consequently, it has been inferred that taxa that preserve relief in the SP cannot be used as evidence of early mineralization, for example, like the *Leanchoilia* guts common in the Burgess Shale (Butterfield, 2002; Butterfield, 2003; Budd, 2011).

Previous work on the taphonomy of arthropod *Campanamuta mantonae* was initially discussed by Budd (2011). The most prominent preservational feature of this soft-bodied arthropod is the silicified muscle tissue, which is mostly restricted to the axial region of the animal, which in many specimens has preserved rather more relief along the axis than in the more abaxial regions;

Budd (2011) suggests a possible mechanism of silicification by chemical bonding of silica (Leo and Barghoorn, 1976) however a more in-depth taphonomic description and alternative silicification model is proposed by Strang et al. (2016a).

Along with body fossils, trace fossils have also been reported in most BST Cambrian deposits including the Burgess Shale (Allison and Brett, 1995; Powell, 2003; Mángano, 2011), Chengjiang (Zhang et al., 2007) and the Sirius Passet (Babcock and Peel, 2007; Peel, 2010; Mángano et al., 2012). In the SP large non-biomineralised arthropod carapaces are commonly associated with trace fossils such as interconnected burrow systems (Mángano et al., 2012). Taphonomic controls are likely responsible for the association of these structures with carapaces but ecological controls would also have played a significant role (Mángano et al., 2012). Morphological evidence in interconnected burrow systems suggests re-use of these structures and suggests grazing on bacteria (Mángano et al, 2012), which is also supported by evidence of microbial mat fragments associated with the trilobite *Buenellus* described by Strang et al., (2016b) and it is likely that sulphur bacteria were abundant in Cambrian sediments (Mángano et al., 2012; Strang et al., 2016b).

Overall previous research on the Sirius Passet has mainly been focused around systematic descriptions of the SP biota as cited above, and arguably very little research has been done on the taphonomy of the Sirius Passet, which is the main purpose of this PhD.

## 1.5 Research Questions

### 1.5.1 Aims

The key questions to be answered in this thesis are outlined below and will be addressed by way of two chapters (which are included in the appendices in their published form) and a synthesis chapter; in addition a largely methodological paper (accepted for publication in the Caribbean Journal of Earth Sciences) proofs the use of the techniques (elemental mapping, SEM and cathodoluminescence) applied to the Sirius Passet material, on a more recent and less complex environmental setting, the Oligocene rocks of the Caribbean island of Antigua.

1. Explore the use of cathodoluminescence as a tool in palaeontology and its role in understanding the mechanism of silicification as a primary taphonomic pathway in fossil preservation. Can this methodology be applied to the silicified material from the Sirius Pass (SP)?

2. Elucidate the taphonomic pathways of common taxa in the SP, making comparisons with a range of better-known Cambrian Lagerstätten including the Burgess Shale and Chengjiang. In particular, investigate the role of silicification in the preservation of Cambrian arthropods, with reference to the trilobite *Buenellus*. Examine the association of common SP arthropods with 'matground' communities, more akin to the Ediacaran, and look at their role in taphonomy. Does the Sirius Passet show Burgess Shale-Type preservation or is it a unique taphonomic pathway?

3. Another common preservational style in the SP (and other Cambrian Lagerstätten) is the presence of three-dimensionally preserved gut tracts. Investigate and explain the presence of both phosphate and silica in the preserved guts of SP arthropods. Explore what this can reveal about the feeding

habits of the organisms and how this can expand on our understanding of Cambrian food webs.

### 1.5.2 Summary of work done

**Chapter 2:** Katie Strang designed the experiment and carried out the SEM work, participated in data analysis and writing of the manuscript. David Harper and Stephen Donovan were involved with fieldwork, revising and editing the article.

**Chapter 3:** All three authors designed the project. Katie Strang carried out the SEM, XRD and petrology work, participated in data analysis and writing of the manuscript. Howard Armstrong was involved with analysis and revising the article. David Harper assisted with revising and editing the article.

**Chapter 4:** All three authors designed the project. Katie Strang carried out the SEM work, participated in data analysis and writing of the manuscript. Howard Armstrong was involved with data analysis and revising the article. David Harper assisted with revising and editing the article.

## 1.6 Methods

### 1.6.1 Fieldwork

Samples used in this study were collected during expeditions led by Professor David Harper in the summers of 2009 and 2011, each taken from a specific height on a measured sedimentary log. Fieldwork was sponsored by The Danish Council for Independent Research, The Agouron Institute and the Carlsberg Foundation.

### 1.6.2 Polished thin sections

Thin (25 μm) double polished thin sections were cut perpendicular to bedding from each marked interval on the sedimentary log. These sections were made by Ian Chaplin, in Durham University Department of Earth Sciences. Thin sections made through fossil material were first set in non-luminescing resin to avoid breakage of the sample.

### 1.6.3 Thin section scans

Thin sections were scanned using a flat bed scanner in refractive light mode to give the best quality image. These images were then analysed in image viewing software such as imageJ to identify areas of interest for further investigation.

### 1.6.4 Petrology

All thin sections were analysed using a Leica polarizing microscope in Durham University. Thin sections were categorised according to mineralogy, grain size and sedimentary features. Two end member lithofacies are recognised; a 'spotted' and a silt-rich facies (Strang et al., 2016b). All thin sections were photographed using a Leica camera attached to the microscope.

### 1.6.5 SEM

Samples were imaged and analyzed for composition using optical microscopy and Scanning Electron microscopy. Thin (25 μm) double polished thin sections, cut perpendicular to bedding, provided petrographic and textural data. Prior to SEM imaging all samples were coated with ~20 nm Carbon. SEM imaging and analysis was carried out using the **Hitachi SU-70 FEG SEM** in Durham University using secondary electron and backscattered electron detectors at 15 kV. Both primary and secondary backscatter techniques were used to produce general images prior to elemental mapping (SEM-EDAX) and SEM-CL analysis. EDAX was carried out using the backscatter detector and the same voltage settings used for imaging. For point analysis a Cobalt standard was run before analysis to confirm quantative results. This was done by using the QUANT software and running the standard several times to ensure maximum accuracy. (100 ± 5%).

### 1.6.6 SEM CL

Cathodoluminescence was carried out using an SEM-CL mirror type detector based in the University of Durham, Department of Physics (Gatan Mono-CL cathodoluminescence). The machine was set to the low magnification position with a 10Kv voltage to allow the site of interest to be determined. The working distance was set to 20mm and then adjusted as necessary to allow focusing of the sample. The first results are obtained using the panchromatic mode (clear filter) with mirror A at position P. Working distance is then set to 16.2 – 16.7 mm and CL luminosities collected. Each colour filter was then inserted one by one. (red > 600nm, green > 480 – 580nm and blue <480 nm). Various studies have been carried out which show that Quartz grains display a variety of

luminescence intensity dependent on their provenance and the standards used were adapted from (Seyedolali et al., 1997). CL intensity is dependent on the density of intrinsic and extrinsic defects within the band gap of the mineral. These defects are usually structural imperfections in the quartz crystal due to vacancies within the crystal lattice. These include point defects, translations, radiation damage, shock damage, melt inclusions, and fluid inclusions (Frelinger et al., 2014). These types of defects can provide information of the conditions during mineralization and subsequent post-mineralization events such as deformation and metamorphism (Frelinger et al., 2014). Once results were obtained they were then compared to other quartz CL provenance data in the literature to identify the luminosities.

### 1.6.7 CL in Palaeontology

Cathodoluminescence (CL) is a widely used tool in sedimentary petrology, however it is relatively new in palaeontology. To our knowledge previous applications have concentrated on shells with a calcitic composition (e.g. (Barbin and Gaspard, 1995; Gorzelak and Zamora, 2013) rather than those which are silicified. We used combined data from the literature to study the microstructures in the silica grains of the Antiguan silicified molluscs, to determine the likely source of the silica.

### 1.6.8 XRD

X-ray diffraction can be used to identify mineral phases within a sample. X-rays are diffracted off the atoms in distinct patterns as determined by Bragg's Law:

$2d\sin\theta = n\lambda$.

Where d is the spacing between diffracting planes, θ is the incident angle, n is an integer and λ is the wavelength of the beam. These patterns are unique to a mineral phase and therefore mineral phase can be identified by analyzing these patterns.

Bulk mineralogy was checked using XRD of the <2m clay fraction following the standard procedures outlined by Moore and Reynolds (1997) and advice given by João Trabucho-Alexandre. Fluorescence settings were applied to limit any backscatter caused by high content of heavy metals such as Iron. Rock samples were then gently disaggregated an agate with mortar and pestle, after being pulverized with a geological hammer to speed up the process. Efforts were made to avoid shearing the clays as this can damage the structures. The sample was then sieved to remove any larger fragments.

Since organic matter can cause background noise when reading XRD results it was removed by leaving the sample in a solution of 5% hydrogen peroxide (100ml) until reaction ceased. The sample was then transferred to a 250ml sample tube, suitable for centrifuge use. Sample was then centrifuged at 2000cpm, before pouring the clear liquid off. Clear water was then added and the sample stirred. The above steps were undertaken until the liquid was neutral and clay did not fluctuate.

*Separation of clay fraction and saturation for XRD measurements*

1. 5ml of dispersion agent was added and sample stirred well
2. Centrifuged for 84 seconds at 800rpm before siphoning off 10mm of liquid into another tube.
3. Repeat step 2 until sample is clean.

*Analysis*

Samples were then sent to Dr Manohara GV (Research Associate in the Department of Chemistry, Durham University) where they were prepared as air-dried samples in line with the procedures in (Moore and Reynolds, 1997). Samples were then analyzed in a Bruker D8 Advance Diffractometer. (CuKα radiation) counting from 2 to 60° 2θ with a 0.02° 2θ steps at 0.85 s per step. Lower angles were run than in bulk analysis in order to see low angle clay peaks. D spacing was used and data were plotted in excel to standard d spacing and matched to those present in the literature.

### 1.6.9 High-resolution photographs of hand specimens

High-resolution photographs were taken using a Canon 5od camera. Specimens were placed on a copy stand and lit from the NE to give best resolution of composition and topography.

## 1.7 References


Allison, P.A., 1988a, Konservat-Lagerstatten : Cause and Classification: Paleobiology, v. 14, no. 4, p. 331–344.

Allison, P.A., 1988b, The Role of Anoxia in the Decay and Mineralization of Proteinaceous Macro-Fossils: Paleobiology, v. 14, no. 2, p. 139–154.

Allison, P.A., and Bottjer, D.J., 2011, Taphonomy: Bias and Process Through Time, *in* Allison P.A., Bottjer D.J. (eds) Taphonomy. Aims & Scope Topics in Geobiology Book Series, vol 32. Springer, Dordrecht, p. 1–17.

Allison, P.A., and Brett, C.E., 1995, In situ benthos and paleo-oxygenation in the Middle Cambrian Burgess Shale, British Columbia, Canada: Geology, v. 23, no. 12, p. 1079-1082.

Allison, P.A., and Briggs, D.E.G., 1993, Exceptional fossil record: distribution of soft-tissue preservation through the Phanerozoic: Geology, v. 21, no. 6, p. 527–530.

Arvidson, R.S., Mackenzie, F.T., and Guidry, M.W., 2013, Geologic history of seawater: A MAGic approach to carbon chemistry and ocean ventilation: Chemical Geology, v. 362, p. 287–304.

Babcock, L.E., 2005, Interpretation of biological and environmental changes across the Neoproterozoic–Cambrian boundary: developing a refined understanding of the radiation and preservational record of early multicellular organisms: Palaeogeography, Palaeoclimatology, Palaeoecology, v. 220, no. 1–2, p. 1–5.

Babcock, L.E., and Peel, J.S., 2007, Palaeobiology, Taphonomy and Stratigraphic Significance of the Trilobite Buenellus from the Sirius Passet Biota, Cambrian of North Greenland: Memoirs of the Association of Australasian Palaeontologists, , no. 34, p. 401-418.

Babcock, L., Peng, S., Geyef, G., and Shergold, J., 2005, Changing perspectives on Cambrian chronostratigraphy and progress toward subdivision of the Cambrian System: Geosciences Journal, v. 9, no. 2, p. 101–106.

Barbin, V., and Gaspard, D., 1995, Cathodoluminescence of recentarticulate brachiopod shells. Implications for growth stages and diagenesis evaluation: Geobios, v. 28, p. 39–45.

Benton, M.J., and Donoghue, P.C.J., 2007, Paleontological evidence to date the tree of life: Molecular Biology and Evolution, v. 24, no. 1, p. 26–53.

Blair, J.E., and Hedges, S.B., 2005, Molecular clocks do not support the Cambrian explosion: Molecular Biology and Evolution, v. 22, no. 3, p. 387–390.

Blaker, M., 1988, A new genus of nevadiid trilobite from the Buen Formation (Early Cambrian) of Peary Land, central North Greenland: Grønlands Geologiske Undersøgelse Rapport, v. 137, p. 33–41.

Blaker, M.R., and Peel, J.S., 1997, Lower Cambrian trilobites from North Greenland: Meddr Grönland Geoscience, v. 35, p. 145.

Boag, T.H., Darroch, S.A.F., and Laflamme, M., 2016, Ediacaran distributions in space and time: testing assemblage concepts of earliest macroscopic body fossils: Paleobiology, v. 42, no. 4, p. 574–594.

Botting, J.P., Cárdenas, P., and Peel, J.S., 2015, A crown-group demosponge from the early Cambrian Sirius Passet Biota, North Greenland: Palaeontology, v. 58, no. 1, p. 35–43.

Botting, J.P., and Peel, J.S., 2016, Early Cambrian sponges of the Sirius Passet Biota, North Greenland: Papers in Palaeontology, v. 2, no. 4, p. 463–487.
Bottjer, D.J., 2010, The cambrian substrate revolution and early evolution of the phyla: Journal of Earth Science, v. 21, no. S1, p. 21–24.
Bottjer, D.J., Hagadorn, J.W., and Dornbos, S.Q., 2000, The Cambrian Substrate Revolution: Gsa Today, v. 10, no. 9, p. 1–32.
Boyle, R.A., Dahl, T.W., Dale, A.W., Shields-Zhou, G.A., Zhu, M., Brasier, M.D., Canfield, D.E., and Lenton, T.M., 2014, Stabilization of the coupled oxygen and phosphorus cycles by the evolution of bioturbation: Nature Geoscience, v. 7, no. 9, p. 671–676.
Brasier, M.D., 1992, Global ocean-atmosphere change across the Precambrian-Cambrian transition: v. 129, no. 2, p. 161–168.
Brasier, M.D, Cowie, J., and Taylor, M., 1994, Decision on the Precambrian-Cambrian boundary type: Episodes, v. 17, no. 1–2, p. 3–8.
Briggs, D.E.G., 2003, The role of decay and mineralization in the preservation of soft-bodied fossils: Annual Review of Earth and Planetary Sciences, v. 31, no. 1, p. 275–301.
Briggs, D.E.G., Evershed, R.P., and Lockheart, M.J., 2000, The biomolecular paleontology of continental fossils: Paleobiology, v. 26, no. 4, p. 169–193.
Briggs, D.E., Fortey, R.A., and Wills, M.A., 1992, Morphological disparity in the Cambrian: Science, v. 256, p. 1670–1673.
Briggs, D.E.G., and Kear, A.J., 1994, Decay and Mineralization of Shrimps: Palaios, v. 9, no. 5, p. 431.
Briggs, D.E.G., and Kear, A.J., 1993a, Decay and Preservation of Polychaetes: Taphonomic Thresholds in Soft-Bodied Organisms: Paleobiology, v. 19, no. 1, p. 107–135.
Briggs, D.E.G., and Kear, A.J., 1993b, Fossilization of Soft Tissue in the Laboratory: v. 259, no. 5100, p. 1439–1442.
Briggs, D.E.G., and Mcmahon, S., 2016, The role of experiments in investigating the taphonomy of exceptional preservation: Palaeontology, v. 59, no. 1, p. 1–11.
Briggs, D.E.G., and McMahon, S., 2016, The role of experiments in investigating the taphonomy of exceptional preservation: Palaeontology, v. 59, no. 1, p. 1–11.
Briggs, D.E.G., and Nedin, C., 1997, The Taphonomy and Affinities of the Problematic Fossil Myoscolex from the Lower Cambrian Emu Bay Shale of South Australia: Journal of Paleontology, v. 71, no. 1, p. 22–32.
Broce, J.S., and Schiffbauer, J.D., 2017, Taphonomic analysis of Cambrian vermiform fossils of Utah and Nevada, and implications for the chemistry of Burgess Shale-type preservation: PALAIOS, v. 32, no. 9, p.600-619.
Bromham, L., 2006, Molecular dates for the Cambrian Explosion: Is the light at the end of the tunnel an oncoming train? Palaeontologica Electronica, v. 9, p. 2004–2006.
Bromham, L., 2009, Why do species vary in their rate of molecular evolution? Biology letters, v. 5, no. 3, p. 401–404.
Buatois, L.A., Almond, J., and Germs, G.J.B., 2013, Environmental tolerance and range offset of Treptichnus pedum: Implications for the recognition of the Ediacaran-Cambrian boundary: Geology, v. 41, no. 4, p. 519–522.

Budd, G.E, 1993, A Cambrian gilled lobopod from Greenland: Nature, v. 364, no. 6439, p. 709–711.
Budd, G.E., 1999, A nektaspid arthropod from the Early Cambrian Sirius Passet fauna, with a description of retrodeformation based on functional morphology: Palaeontology, v. 42, no. 1, p. 99–122.
Budd, G.E., 2011, Campanamuta mantonae gen. et. sp. nov., an exceptionally preserved arthropod from the Sirius Passet Fauna (Buen Formation, lower Cambrian, North Greenland): Journal of Systematic Palaeontology, v. 9, no. 2, p. 217–260.
Budd, G.E., 1995, Kleptothule rasmusseni gen. et sp. nov.: an ?olenellinid-like trilobite from the Sirius Passet fauna (Buen Formation, Lower Cambrian, North Greenland): Transactions of the Royal Society of Edinburgh: Earth Sciences, v. 86, p. 1–12.
Budd, G.E., 1997, Stem group arthropods from the Lower Cambrian Sirius Passet fauna of North Greenland, *in* Arthropod Relationships. Systematics Association Special Volume Series, 55, Springer Netherlands, Dordrecht, p. 125–138.
Budd, G.E., 2008, The earliest fossil record of the animals and its significance: Philosophical Transactions of the Royal Society B: Biological Sciences, v. 363, no. 1496, p. 1425-1434.
Budd, G.E., and Peel, J.S., 1998, A new xenusiid lobopod from the early Cambrian Sirius Passet fauna of North Greenland: Palaeontology, v. 41, p. 1201–1213.
Butler, A.D., Cunningham, J.A., Budd, G.E., and Donoghue, P.C.J., 2015, Experimental taphonomy of Artemia reveals the role of endogenous microbes in mediating decay and fossilization: Philosophical Transactions of the Royal Society B: Biological Sciences, v. 282, no. 1808, p. 20150476.
Butterfield, N.J., 2011, Animals and the invention of the Phanerozoic Earth system: Trends in Ecology and Evolution, v. 26, no. 2, p. 81–87.
Butterfield, N.J., 2003, Exceptional fossil preservation and the cambrian explosion.: Integrative and comparative biology, v. 43, no. 1, p. 166–177.
Butterfield, N.J., 2002, Leanchoilia guts and the interpretation of three-dimensional structures in Burgess Shale-type fossils: Paleobiology, v. 28, no. 1, p. 155–171.
Butterfield, N.J., 2007, Macroevolution and macroecology throught deep time: Palaeontology, v. 50, p. 41–55.
Butterfield, N.J., 1990, Organic preservation of non-mineralizing organisms and the taphonomy of the Burgess Shale: Paleobiology, v. 16, no. 3, p. 272–286.
Butterfield, N.J., 1995, Secular distribution of Burgess-Shale-type preservation: Lethaia, v. 28, no. 1, p. 1–13.
Caron, J.B., and Jackson, D.A., 2008, Paleoecology of the Greater Phyllopod Bed community, Burgess Shale: Palaeogeography, Palaeoclimatology, Palaeoecology, v. 258, no. 3, p. 222–256.
Chen, X., Ling, H.-F., Vance, D., Shields-Zhou, G.A., Zhu, M., Poulton, S.W., Och, L.M., Jiang, S.-Y., Li, D., Cremonese, L., and Archer, C., 2015, Rise to modern levels of ocean oxygenation coincided with the Cambrian radiation of animals: Nature Communications, v. 6, p. 7142.
Conway Morris, S., 2006, Darwin's dilemma: the realities of the Cambrian "explosion": Philosophical transactions of the Royal Society of London. Series B, Biological sciences, v. 361, no. 1470, p. 1069–1083.

Conway Morris, S., 1989, The persistence of Burgess Shale-type faunas: implications for the evolution of deeper-water faunas: Transactions of the Royal Society of Edinburgh: Earth Sciences, v. 80, no. 3–4, p. 271–283.

Conway Morris, S., and Peel, J.S., 1995, Articulated Halkieriids from the Lower Cambrian of North Greenland and their Role in Early Protostome Evolution: Philosophical Transactions of the Royal Society B: Biological Sciences, v. 347, no. 1321, p. 305–358.

Conway Morris, S., Peel, J.S., Higgins, A.K., Soper, N.J., and Davis, N.C., 1987, A Burgess shale-like fauna from the Lower Cambrian of North Greenland: Nature, v. 326, no. 6109, p. 181–183.

Crimes, T.P., 1992, Changes in the trace fossil biota across the Proterozoic-Phanerozoic boundary: Journal of the Geological Society, v. 149, no. 4, p. 637–646.

Cunningham, J.A., Liu, A.G., Bengtson, S., and Donoghue, P.C.J., 2017, The origin of animals: Can molecular clocks and the fossil record be reconciled? BioEssays, v. 39, no. 1, p. 1–12.

Daley, A.C., and Peel, J.S., 2010, A possible anomalocaridid from the Cambrian Sirius Passet Lagerstätte, North Greenland: Journal of Paleontology, v. 84, no. 2, p. 352–355.

Darroch, S.A.F., Laflamme, M., Schiffbauer, J.D., and Briggs, D.E.G., 2012, Experimental Formation of a Microbial Death Mask: Palaios, v. 27, no. 5, p. 293–303.

Edgecombe, G.D., García-Bellido, D.C., and Paterson, J.R., 2011, A New Leanchoiliid Megacheiran Arthropod from the Lower Cambrian Emu Bay Shale, South Australia: Acta Palaeontologica Polonica, v. 56, no. 2, p. 385–400.

Erwin, D.H., 2007, Disparity: Morphological pattern and developmental context: Palaeontology, v. 50, p. 57–73.

Erwin, D.H., Laflamme, M., Tweedt, S.M., Sperling, E.A., Pisani, D., and Peterson, K.J., 2011, The Cambrian conundrum: early divergence and later ecological success in the early history of animals.: Science, v. 334, no. 6059, p. 1091–1097.

Fletcher, T.P., and Collins, D.H., 1998, The Middle Cambrian Burgess Shale and its relationship to the Stephen Formation in the southern Canadian Rocky Mountains: Canadian Journal of Earth Sciences, v. 35, no. 4, p. 413–436.

Forchielli, A., Steiner, M., Hu, S., Lüter, C., and Keupp, H., 2012, Taphonomy of the earliest Cambrian linguliform brachiopods: Acta Palaeontologica Polonica, v.59, no. 1, p. 185–207.

Forchielli, A., Steiner, M., Kasbohm, J., Hu, S., and Keupp, H., 2014, Taphonomic traits of clay-hosted early Cambrian Burgess Shale-type fossil Lagerstätten in South China: Palaeogeography, Palaeoclimatology, Palaeoecology, v. 398, p. 59–85.

Frelinger, S.N., Ledvina, M.D., Kyle, J.R., and Zhao, D., 2014, Scanning electron microscopy cathodoluminescence of quartz: Principles, techniques and applications in ore geology: Ore Geology Reviews, v. 65, no. 4, p. 840–852.

Gabbott, S.E., Xian-guang, H., Norry, M.J., and Siveter, D.J., 2004, Preservation of Early Cambrian animals of the Chengjiang biota: Geology, v. 32, no. 10, p. 901-904.

Gabbott, S.E., Zalasiewicz, J., and Collins, D., 2008, Sedimentation of the Phyllopod Bed within the Cambrian Burgess Shale Formation of British Columbia: Journal of the Geological Society, v. 165, no. 1, p. 307–318.
Gaines, R.R., 2014, Burgess shale-type preservation and its distribution in space and time: Palaeontological Society Papers, v. 20, p. 123–146.
Gaines, R.R., Briggs, D.E.G., and Yuanlong, Z., 2008, Cambrian Burgess Shale–type deposits share a common mode of fossilization: Geology, v. 36, no. 10, p. 755-758.
Gaines, R.R., Hammarlund, E.U., Hou, X., Qi, C., Gabbott, S.E., Zhao, Y., Peng, J., and Canfield, D.E., 2012, Mechanism for Burgess Shale-type preservation: Proceedings of the National Academy of Sciences of the United States of America, v. 109, no. 14, p. 5180–5184.
García-Bellido, D.C., Paterson, J.R., Edgecombe, G.D., Jago, J.B., Gehling, J.G., and Lee, M.S.Y., 2009, The bivalved arthropods isoxys and Tuzoia with soft-part preservation from the lower cambrian emu bay shale lagerstätte (Kangaroo Island, Australia): Palaeontology, v. 52, no. 6, p. 1221–1241.
Gehling, J.G., 1999, Microbial Mats in Terminal Proterozoic Siliciclastics: Ediacaran Death Masks: PALAIOS, v. 14, no. 1, p. 40-47.
Gehling, J.G., Jago, J.B., Paterson, J.R., García-Bellido, D.C., and Edgecombe, G.D., 2011, The geological context of the Lower Cambrian (Series 2) Emu Bay Shale Lagerstätte and adjacent stratigraphic units, Kangaroo Island, South Australia: Australian Journal of Earth Sciences, v. 58, no. 3, p. 243–257.
Gehling, J.G., Jensen, S., Droser, M.L., Myrow, P.M., and Narbonne, G.M., 2001, Burrowing below the basal Cambrian GSSP, Fortune Head, Newfoundland: Geological Magazine, v. 138, no. 2, p. 213–218.
Geyer, G., and Landing, E., 2016, The Precambrian–Phanerozoic and Ediacaran–Cambrian boundaries: a historical approach to a dilemma: Geological Society, London, Special Publications, v. 448.
Geyer, G., and Shergold, J., 2000, The quest for internationally recognized divisions of Cambrian time: Episodes; Journal of International Geoscience, v. 23, no. 3, p. 188–195.
Gorzelak, P., and Zamora, S., 2013, Stereom microstructures of Cambrian echinoderms revealed by cathodoluminescence (CL): Palaeontologia Electronica, v. 16, no. 3, p. 32–17.
Hagadorn, J.W., and Bottjer, D.J., 1997, Wrinkle structures: Microbially mediated sedimentary structures common in subtidal siliciclastic settings at the Proterozoic-Phanerozoic transition: Geology, v. 25, no. 11, p. 1047.
Herringshaw, L.G., Callow, R.H.T., and McIlroy, D., 2017, Engineering the Cambrian explosion: the earliest bioturbators as ecosystem engineers: Geological Society, London, Special Publications, v. 448, no. 1, p. 369–382.
Higgins, A.K., Ineson, J.R., Peel, J.S., Surlyk, F., and Sønderholm, M., 1991, The Franklinian Basin in North Greenland: Bulletin Grønlands Geologiske Undersøgelse, no. 160, p. 71–139.
Hoffman, P.F., Kaufman, A.J., Halverson, G.P., and Schrag, D.P., 1998, A Neoproterozoic Snowball Earth: Science, v. 281, no. 5381, p. 1342–1346.
Hoffman, P.F., and Schrag, D.P., 2002, The snowball Earth hypothesis: Testing the limits of global change: Terra Nova, v. 14, no. 3, p. 129–155.

Jensen, S., Droser, M.L., and Gehling, J.G., 2005, Trace fossil preservation and the early evolution of animals: Palaeogeography, Palaeoclimatology, Palaeoecology, v. 220, no. 1–2, p. 19–29.

Jin, C., Li, C., Algeo, T.J., Planavsky, N.J., Cui, H., Yang, X., Zhao, Y., Zhang, X., and Xie, S., 2016, A highly redox-heterogeneous ocean in South China during the early Cambrian (~529-514 Ma): Implications for biota-environment co-evolution: Earth and Planetary Science Letters, v. 441, p. 38–51.

Jørgensen, B., 1979, Diurnal cycle of oxygen and sulfide microgradients and microbial photosynthesis in a cyanobacterial mat sediment: Applied and Environmental Microbiology, v. 38, p. 46-58.

Kirschvink, J.L., 1992, Late Proterozoic low-latitude global glaciation: the snowball Earth: The Proterozoic Biosphere, v. 52, p. 51–52.

Knoll, A.H., 1999, Early Animal Evolution: Emerging Views from Comparative Biology and Geology: Science, v. 284, no. 5423, p. 2129–2137.

Laflamme, M., Darroch, S.A.F., Tweedt, S.M., Peterson, K.J., and Erwin, D.H., 2013, The end of the Ediacara biota: Extinction, biotic replacement, or Cheshire Cat? Gondwana Research, v. 23, no. 2, p. 558–573.

Landing, E., 1994, Precambrian-Cambrian boundary global stratotype ratified and a new perspective of Cambrian time: Geology, v. 22, no. 2, p. 179-182.

Lee, M.S.Y., Jago, J.B., García-Bellido, D.C., Edgecombe, G.D., Gehling, J.G., and Paterson, J.R., 2011, Modern optics in exceptionally preserved eyes of Early Cambrian arthropods from Australia: Nature, v. 474, no. 7353, p. 631–634.

Leo, R.F., and Barghoorn, E.S., 1976, Silicification of wood: Botanical Museum Leaflets, Harvard University, v. 25, no. 25, p. 1–47.

Li, C., Jin, C., Planavsky, N.J., Algeo, T.J., Cheng, M., Yang, X., Zhao, Y., and Xie, S., 2017, Coupled oceanic oxygenation and metazoan diversification during the early-middle Cambrian? Geology, v. 45, no. 8, p. 743–746.

Mángano, M.G., 2011, Trace-fossil assemblages in a Burgess Shale-type deposit from the Stephen Formation at Stanley Glacier, Canadian Rocky Mountains: Unraveling ecologic and evolutionary controls: Palaeontographica Canadiana, , no. 31, p. 89–108.

Mángano, M.G., Bromley, R.G., Harper, D.A.T., Nielsen, A.T., Smith, M.P., and Vinther, J., 2012, Nonbiomineralized carapaces in Cambrian seafloor landscapes (Sirius Passet, Greenland): Opening a new window into early Phanerozoic benthic ecology: Geology, v. 40, no. 6, p. 519–522.

Marshall, C.R., 2006, Explaining the Cambrian "Explosion" of animals: Annual Review of Earth and Planetary Sciences, v. 34, no. 1, p. 355–384.

Martin, D., Briggs, D.E.G., and Parkes, R.J., 2004, Experimental attachment of sediment particles to invertebrate eggs and the preservation of soft-bodied fossils: Journal of the Geological Society, v. 161, no. 5, p. 735–738.

Maruyama, S., and Santosh, M., 2008, Models on Snowball Earth and Cambrian explosion: A synopsis: Gondwana Research, v. 14, no. 1–2, p. 22–32.

McCall, G.J.H., 2006, The Vendian (Ediacaran) in the geological record: Enigmas in geology's prelude to the Cambrian explosion: Earth-Science Reviews, v. 77, no. 1–3, p. 1–229.

Mcilroy, D., and Brasier, M.D., 2016, Ichnological evidence for the Cambrian explosion in the Ediacaran to Cambrian succession of Tanafjord, Finnmark, northern Norway: Geological Society, London, Special Publications, v. 448.

McIlroy, D., and Logan, G.A., 1999, The impact of bioturbation on infaunal ecology and evolution during the Proterozoic-Cambrian transition: PALAIOS, v. 14, no. 1, p. 58–72.
McKirdy, D.M., Hall, P.A., Nedin, C., Halverson, G.P., Michaelsen, B.H., Jago, J.B., Gehling, J.G., and Jenkins, R.J.F., 2011, Paleoredox status and thermal alteration of the lower Cambrian (Series 2) Emu Bay Shale Lagerstätte, South Australia: Australian Journal of Earth Sciences, v. 58, no. 3, p. 259–272.
Moczydłowska, M., and Vidal, G., 1986, Lower Cambrian acritarch zonation in southern Scandinavia and southeastern Poland: Geologiska Föreningan i Stockholm. Förhandlingar, v. 108, no. 3, p. 201–223.
Moore, D.M., and Reynolds, R.C., 1997, X-ray diffraction and the identification and analysis of clay minerals 2nd ed.: Oxford university press.
Morris, S.C., 2008, A Redescription of a Rare Chordate, Metaspriggina walcotti Simonetta and Insom, from the Burgess Shale (Middle Cambrian), British Columbia, Canada: Journal of Paleontology, v. 82, no. 2, p. 424–430.
Morris, S.C., and Peel, J.S., 1990, Articulated halkieriids from the Lower Cambrian of north Greenland: Nature, v. 345, no. 6278, p. 802–805.
Morris, S.C., and Peel, J.S., 2008, The Earliest Annelids: Lower Cambrian Polychaetes from the Sirius Passet Lagerstätte, Peary Land, North Greenland: Acta Palaeontologica Polonica, v. 53, no. 1, p. 137–148.
Mount, J.F., and Signer, P.W., 1985, Early Cambrian innovation in shallow subtidal environments: Paleoenvironments of Early Cambrian shelly fossils: Geology, v. 13, no. 10, p. 730–733.
Murdock, D.J.E., and Donoghue, P.C.J., 2011, Evolutionary origins of animal skeletal biomineralization: Cells Tissues Organs, v. 194, no. 2-4, p. 98–102.
Murray, J.W., Jannasch, H.W., Honjo, S., Anderson, R.F., Reeburgh, W.S., Top, Z., Friederich, G.E., Codispoti, L.A., and Izdar, E., 1989, Unexpected changes in the oxic/anoxic interface in the Black Sea: Nature, v. 338, no. 6214, p. 411–413.
Narbonne, G.M., 2005, The Ediacara biota: Neoproterozoic Origin of Animals and Their Ecosystems: Annual Review of Earth and Planetary Sciences, v. 33, no. 1, p. 421–442.
Narbonne, G.M., Myrow, P.M., Landing, E., and Anderson, M.M., 1987, A candidate stratotype for the Precambrian–Cambrian boundary, Fortune Head, Burin Peninsula, southeastern Newfoundland: Canadian Journal of Earth Sciences, v. 24, no. 7, p. 1277–1293.
Orr, P.J., 1998, Cambrian Burgess Shale Animals Replicated in Clay Minerals: Science, v. 281, no. 5380, p. 1173–1175.
Page, A., Gabbott, S.E., Wilby, P.R., and Zalasiewicz, J..A., 2008, Ubiquitous Burgess Shale–style "clay templates" in low-grade metamorphic mudrocks: Geology, v. 36, no. 11, p. 855-858.
Palmer, A.R., 2011, A proposed nomenclature for stages and series for the Cambrian of Laurentia: Canadian Journal of Earth Sciences, v. 35, no. 4, p. 323–328.
Paterson, J.R., García-Bellido, D.C., and Edgecombe, G.D., 2012, New artiopodan arthropods from the early Cambrian Emu Bay Shale Konservat-Lagerstätte of South Australia: Journal of Paleontology, v. 86, no. 2, p. 340–357.

Paterson, J.R., García-Bellido, D.C., Jago, J.B., Gehling, J.G., Lee, M.S.Y., and Edgecombe, G.D., 2016, The Emu Bay Shale Konservat-Lagerstätte: a view of Cambrian life from East Gondwana: Journal of the Geological Society, v. 173, no. 1, p. 1–11.

Peel, J.S., 2010, A corset-like fossil from the Cambrian Sirius Passet Lagerstätte of North Greenland and its implications for cycloneuralian evolution: Journal of Paleontology, v. 84, no. 2, p. 332–340.

Peel, J.S., Conway Morris, S., and Ineson, J.R., 1992, A second glimpse of Early Cambrian life: New collections from Sirius Passet, North Greenland: Rapport Grønlands Geologiske Undersøgelse, v. 155, p. 48–50.

Peel, J.S., and Ineson, J.R., 2011, The extent of the Sirius Passet Lagerstätte (early Cambrian) of North Greenland: Bulletin of Geosciences, p. 535–543.

Peel, J.S., 2017a, Molaria (Euarthropoda) from the Sirius Passet Lagerstätte (Cambrian Series 2, Stage 3) of North Greenland: Bulletin of Geosciences, v. 92, no. 2, p. 133–142.

Peel, J.S., 2017b, Mineralized gutfills from the Sirius Passet Lagerstätte (Cambrian Series 2) of North Greenland: GFF, v. 139, no. 2, p. 83–91.

Peters, S.E., and Gaines, R.R., 2012, Formation of the "Great Unconformity" as a trigger for the Cambrian explosion.: Nature, v. 484, no. 7394, p. 363–366.

Peterson, K.J., and Butterfield, N.J., 2005, Origin of the Eumetazoa: Testing ecological predictions of molecular clocks against the Proterozoic fossil record: Proceedings of the National Academy of Sciences, v. 102, no. 27, p. 9547–9552.

Peterson, K.J., Cotton, J.A., Gehling, J.G., and Pisani, D., 2008, The Ediacaran emergence of bilaterians: congruence between the genetic and the geological fossil records: Philisophical Transactions of the Royal Society B, no. 363, p. 1435–1443.

Peterson, K.J., McPeek, M.A., and Evans, D.A.D., 2005, Tempo and mode of early animal evolution: inferences from rocks, Hox, and molecular clocks: Paleobiology, v. 31, no. s2, p. 36–55.

Plint, A., 2014, Mud dispersal across a Cretaceous prodelta: Storm-generated, wave-enhanced sediment gravity flows inferred from mudstone microtexture and microfacies: Sedimentology, v. 61, no. 3, p. 609–647.

Petrovich, R., 2001, Mechanisms of fossilization of the soft-bodied and lightly armored faunas of the Burgess Shale and of some other classical localities: American Journal of Science, v. 301, no. 8, p. 683–726.

Powell, W., 2003, Greenschist-facies metamorphism of the Burgess Shale and its implications for models of fossil: Canadian Journal of Earth Sciences, v. 40, p. 13–25.

Raiswell, R., and Berner, R.A., 1986, Pyrite and organic matter in Phanerozoic normal marine shales: Geochimica et Cosmochimica Acta, v. 50, no. 9, p. 1967–1976.

dos Reis, M., Inoue, J., Hasegawa, M., Asher, R.J., Donoghue, P.C.J., and Yang, Z., 2012, Phylogenomic datasets provide both precision and accuracy in estimating the timescale of placental mammal phylogeny: Proceedings of the Royal Society B: Biological Sciences, v. 279, no. 1742, p. 3491–3500.

dos Reis, M., Thawornwattana, Y., Angelis, K., Telford, M.J., Donoghue, P.C.J., and Yang, Z., 2015, Uncertainty in the Timing of Origin of Animals and the Limits

of Precision in Molecular Timescales: Current Biology, v. 25, no. 22, p. 2939–2950.
Rigby, J.K., 1986, Sponges of the Burgess Shale (Middle Cambrian), British Columbia: Palaeontographica Canadiana, v. 2, p. 1–105.
Runnegar, B., 1982, A molecular-clock date for the origin of the animal phyla: Lethaia, v. 15, no. 3, p. 199–205.
Sagemann, J., Bale, S.J., Briggs, D.E.G., and Parkes, R.J., 1999, Controls on the formation of authigenic minerals in association with decaying organic matter: An experimental approach: Geochimica et Cosmochimica Acta, v. 63, no. 7–8, p. 1083–1095.
Sansom, R.S., 2014, Experimental decay of soft tissues: Paleontological Society Papers, v. 20, p. 259–274.
Sansom, R.S., Gabbott, S.E., and Purnell, M.A., 2011, Decay of vertebrate characters in hagfish and lamprey (Cyclostomata) and the implications for the vertebrate fossil record.: Proceedingsof the Royal Society B, v. 278, no. 1709, p. 1150-1157.
Sansom, R.S., Gabbott, S.E., and Purnell, M.A., 2010, Non-random decay of chordate characters causes bias in fossil interpretation.: Nature, v. 463, no. 7282, p. 797–800.
Schiffbauer, J.D., Huntley, J.W., O'Neil, G.R., Darroch, S.A.F., Laflamme, M., and Cai, Y., 2016, The Latest Ediacaran Wormworld Fauna: Setting the Ecological Stage for the Cambrian Explosion: GSA Today, v. 26, no. 11, p. 4–11.
Seilacher, A., 1970, Begriff und Bedeutung der Fossil-Lagerstätten: Neues Jahrbuch fur Geologie und Palaontologie, Monatshefte, p. 34–39.
Seilacher, A., 1999, Biomat-related lifestyles in the Precambrian: PALAIOS, v. 14, no. 1, p. 86–93.
Seilacher, A., Buatois, L.A., and Mángano, M.G., 2005, Trace fossils in the Ediacaran-Cambrian transition: Behavioral diversification, ecological turnover and environmental shift: Palaeogeography, Palaeoclimatology, Palaeoecology, v. 227, no. 4, p. 323–356.
Seilacher, A., Reif, W.-E., and Westphal, F., 1985, Sedimentological, Ecological and Temporal Patterns of Fossil Lagerstätten: Philosophical Transactions of the Royal Society B: Biological Sciences, v. 311, no. 1148, p. 5–24.
Seyedolali, A., Krinsley, D.H., Boggs, S., Hara, P.F.O., Dypvik, H., Gordon, G., Exploration, K., and Drive, R., 1997, Provenance interpretation of quartz by scanning electron microscope – cathodoluminescence fabric analysis: Geology, v. 25, no. 9, p. 787-790.
Shu, D.-G., Conway Morris, S., Zhang, Z.-F., and Han, J., 2009, The earliest history of the deuterostomes: the importance of the Chengjiang Fossil-Lagerstätte: Proceedings of the Royal Society of London B: Biological Sciences, v. 277, no. 1679, p. 165-174.
Smith, M.P., and Harper, D.A.T., 2013, Causes of the Cambrian explosion.: Science, v. 341, no. 6152, p. 1355–1356.
Sperling, E.A., Carbone, C., Strauss, J. V., Johnston, D.T., Narbonne, G.M., and Macdonald, F.A., 2016, Oxygen, facies, and secular controls on the appearance of Cryogenian and Ediacaran body and trace fossils in the Mackenzie Mountains of northwestern Canada: Bulletin of the Geological Society of America, v. 128, no. 3–4, p. 558–575.

Sperling, E.A., Frieder, C.A., Raman, A. V., Girguis, P.R., Levin, L.A., and Knoll, A.H., 2013, Oxygen, ecology, and the Cambrian radiation of animals: Proceedings of the National Academy of Sciences, v. 110, no. 33, p. 13446–13451.

Stein, M., Budd, G.E., Peel, J.S., and Harper, D.A.T., 2013, Arthroaspis n. gen., a common element of the Sirius Passet Lagerstätte (Cambrian, North Greenland), sheds light on trilobite ancestry: BMC Evolutionary Biology, v. 13, no. 1, p. 99.

Strang, K.M., Armstrong, H.A., and Harper, D.A.T., 2016a, Minerals in the gut : scoping a Cambrian digestive system: Royal Society Open Science, v. 3, no. 11, p. 1–9.

Strang, K.M., Armstrong, H.A., Harper, D.A.T., and Trabucho-Alexandre, J.P., 2016b, The Sirius Passet Lagerstatte: Silica death masking opens the window on the earliest matground community of the Cambrian explosion: Lethaia, v. 49, no. 4, p. 631-643.

Torsvik, T.H., and Cocks, L.R.M., 2013, Gondwana from top to base in space and time: Gondwana Research, v. 24, no. 3–4, p. 999–1030.

Valentine, J.W., Jablonski, D., and Erwin, D.H., 1999, Fossils, molecules and embryos: new perspectives on the Cambrian explosion: Development, v. 126, no. 5, p. 851–859.

Vidal, G., and Peel, J.S., 1993, Acritarchs from the Lower Cambrian Buen Formation in North Greenland: Copenhagen: Geological Survey of Greenland, v. 164.

Vinther, J., Smith, M.P., and Harper, D.A.T., 2011, Vetulicolians from the Lower Cambrian Sirius Passet Lagerstätte, North Greenland, and the polarity of morphological characters in basal deuterostomes: Palaeontology, v. 54, no. 3, p. 711–719.

Vinther, J., Stein, M., Longrich, N.R., and Harper, D.A.T., 2014, A suspension-feeding anomalocarid from the Early Cambrian: Nature, v. 507, no. 7493, p. 496–499.

Wang, D.Y.-C., Kumar, S., and Hedges, S.B., 1999, Divergence time estimates for the early history of animal phyla and the origin of plants, animals and fungi: Proceedings of the Royal Society of London B: Biological Sciences, v. 266, no. 1415, p. 163-171.

Weeks, S.J., Currie, B., and Bakun, A., 2002, Massive emissions of toxic gas in the Atlantic.: Nature, v. 415, no. 6871, p. 493–494.

Williams, M., Siveter, D.J., and Peel, J.S., 1996, Isoxys (Arthropoda) from the Early Cambrian Sirius Passet Lagerstätte, North Greenland: Journal of Paleontology, v. 70, no. 6, p. 947–954.

Wilson, L.A., and Butterfield, N.J., 2014, Sediment effects on the preservation of Burgess Shale-Type compression fossils: PALAIOS, v. 29, no. 4, p. 145–154.

Zacaï, A., Vannier, J., and Lerosey-Aubril, R., 2016, Reconstructing the diet of a 505-million-year-old arthropod: Sidneyia inexpectans from the Burgess Shale fauna: Arthropod Structure and Development, v. 45, no. 2, p. 200–220.

Zhang, X., Bergström, J., Bromley, R.G., and Hou, X., 2007, Diminutive trace fossils in the Chengjiang Lagerstätte: Terra Nova, v. 19, no. 6, p. 407–412.

Zhu, M., Babcock, L., and Peng, S., 2006, Advances in Cambrian stratigraphy and paleontology: integrating correlation techniques, paleobiology, taphonomy and paleoenvironmental reconstruction: Palaeoworld, v. 15, no. 3–4, p. 217–222.

Zhu, M., Babcock, L.E., and Steiner, M., 2005, Fossilization modes in the Chengjiang Lagerstätte (Cambrian of China): testing the roles of organic preservation and diagenetic alteration in exceptional preservation: Palaeogeography, Palaeoclimatology, Palaeoecology, v. 220, no. 1–2, p. 31–46.

# Chapter 2: Silicification of low-magnesium mollusc shells from the Upper Oligocene of Antigua, Lesser Antilles – a case study on Cathodoluminescence as a tool in Palaeontology

## 2.1 Abstract

Despite its widespread application in sedimentary petrology, Cathodoluminescence remains a relatively new tool in palaeontology. As far as we are aware in previous studies it has mainly been used to look at shells of calcitic composition. In this chapter we applied the CL methodology to answer a simple hypothesis: was the silica derived from a volcanic source underlying the carbonate platform. This methodology was applied to this project to proof the use of CL on the Sirius Passet material. A version of this chapter has been accepted for publication in the Caribbean Journal of Earth Sciences (Appendix I). SEM-CL allowed us to view a variety of microstructures and textures, which aren't visible under normal SEM or optical photography. By examining these textures, such as mottling, fracturing and irregular zoning, along with data from the literature, we were able to deduce the silica source as volcanically derived. Silicified molluscs, namely the oyster *Hyotissa* and the scallop *Aequipecten*?, are commonly preserved as silica in the carbonate successions on the island of Antigua. These fossil assemblages are located within the Antigua Formation, above and adjacent to a variety of volcanic and volcaniclastic rocks, suggesting, on geological grounds, an igneous source for the silica. Energy dispersive spectroscopy (EDS) and cathodoluminescence (CL) have been applied to characterise the silicification and its conditions of formation which may have been associated with hydrothermal activity.

## 2.2 Introduction

Silicification is a relatively common mode of preservation in the fossil record. It generally occurs along thin zones within the fossil as the original calcium carbonate is dissolved and replaced by silica. The process of silicification (see Butts, 2014, for a comprehensive review) can occur through permineralization (precipitation of silica into voids), entombment (precipitation on external surfaces) and replacement (or silicification *sensu stricto*), that is, dissolution of skeletal material virtually concurrent with the precipitation of silica. The process is controlled by shell mineralogy, including the amount and location of organic matter, and the availability of silica. Thus, silicification of fossils in limestones can be considered an indication of early diagenetic conditions whereby there is a source of excess dissolved silica and the replacement mechanism is the likely one where monomers bond directly with organic material (Butts, 2014) rather than by force of crystallization (Maliva and Siever, 1998). The sources of silica can be many and various (e.g., Upchurch et al., 1980).

Cathodoluminescence (CL) is a tool for determining the nature and distribution of luminescence in quartz. These data may reflect specific conditions during the formation of quartz. Cathodoluminescence is the result of photon emission in the visible range resulting from excitation of high-energy electrons (Ségalen et al., 2008). The intensity of CL is dependent on the density of intrinsic and extrinsic defects within the band gap of the mineral. These defects are usually structural imperfections in the quartz crystal due to vacancies within the crystal lattice, and include point and planar lattice defects, radiation damage, shock damage, melt inclusions and fluid inclusions (Frelinger et al., 2015). These defects can provide information on the conditions during mineralization, and subsequent post-mineralization events such as deformation and metamorphism. The combination of scanning electron microscope (SEM) and CL data highlighting textural features allows distinction of different quartz types more easily than with conventional microscopy or colour CL analysis (Bernet and Bassett, 2005). Studies have shown that CL textures such as zoning, microcracks and deformation fractures can remain preserved in sedimentary rocks, withstanding processes such as

uplift, sediment deposition and diagenesis (Seyedolali et al., 1997; Bernet and Bassett, 2005; Götze, 2012). This has made the textures a useful tool, because comparison with published CL data of specimens from well-typified settings enables the identification of the provenance of minerals and their conditions of formation. To the best of our knowledge, previous CL studies on Recent and fossil shells have focussed only on those with a carbonate composition, to determine, for example, growth trajectories, and the luminosity of calcite has been used to decide whether a shell is modern or ancient (see, for example, Barbin and Gaspard, 1995; England et al., 2006; and references therein). The application of using CL to determine information from silicified shells is therefore a new approach.

Herein, we characterise the silica prevalent in bioclasts of the Antigua Formation (upper Oligocene) of Antigua using a number of spectroscopy techniques. The island of Antigua (Fig. 2.1) is characterised by an abundant and diverse Oligocene fossil fauna. Locally, these fossils are beautifully preserved, albeit silicified.

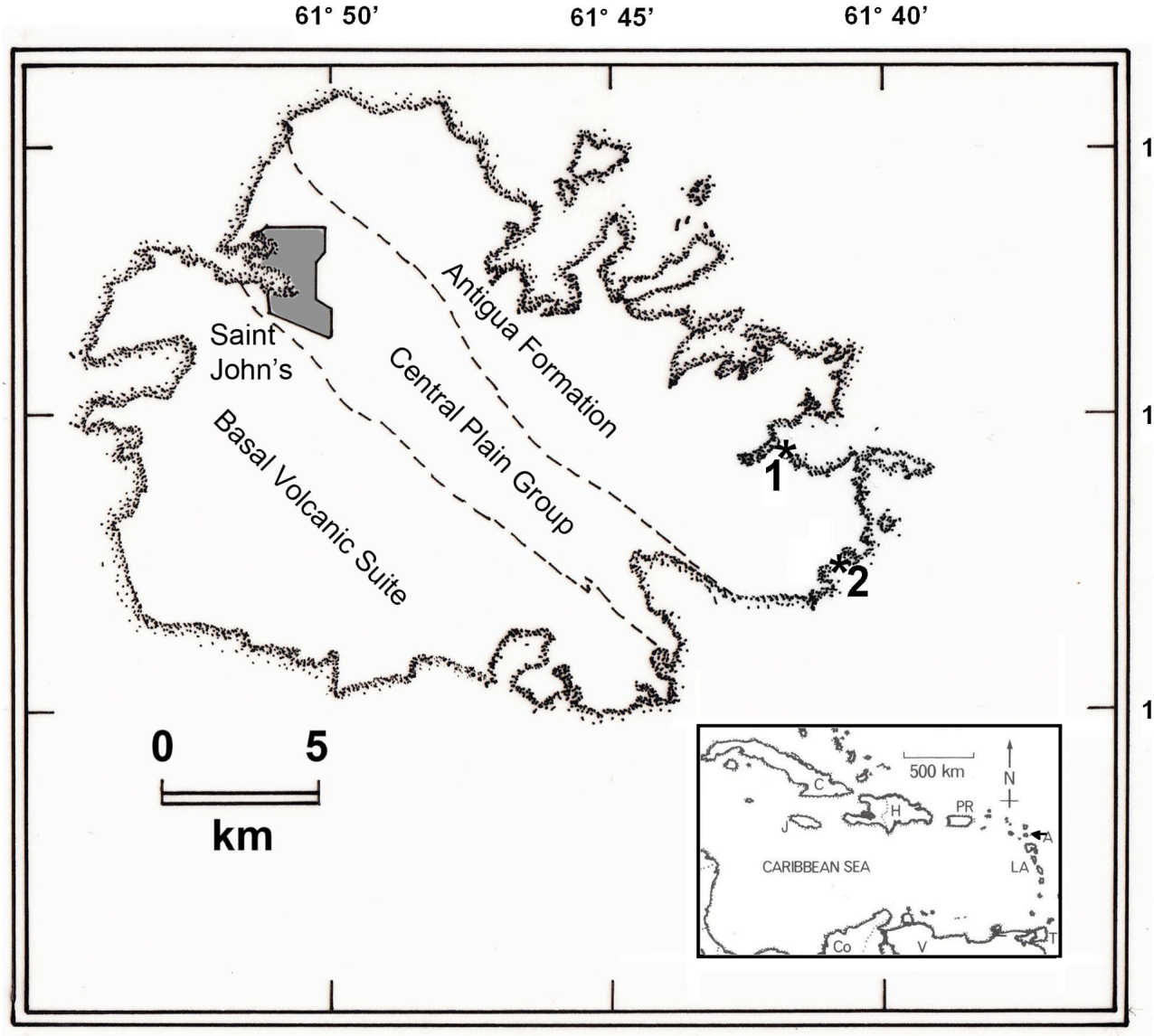


**Figure 2.1: Outline map of Antigua (redrawn and modified after Weiss, 1994, fig. 3), showing the principal geological subdivisions and the city of Saint John's. The regional dip is towards the northeast. Localities 1 (Hughes Point) and 2 (Half Moon Bay) are marked. Inset map (modified after Donovan, 2010, fig. 2) shows the position of Antigua in the Caribbean. Key (clockwise from Jamaica): J=Jamaica; C=Cuba; H=Hispaniola (Haiti+Dominican Republic); PR=Puerto Rico; A = Antigua (arrowed); LA=Lesser Antilles; T=Trinidad; V=Venezuela; Co=Colombia.**

## 2.3 Geological Setting

The Caribbean island of Antigua lies towards the northern end of the Lesser Antilles volcanic arc. It is a Limestone Caribee, an island of volcanic origin capped by carbonates (Wadge, 1994; Donovan et al., 2014a, b). As such, it is a perfect field laboratory to investigate the relationships between a volcanic arc and the evolution of its carbonate cover succession. The rock record of the entire island is late Oligocene in age (Weiss, 1994), with the exception of some minor upper Quaternary sediments. The regional dip of the strata is towards the northeast, with the oldest rocks, the Basal Volcanic Suite, cropping out and exposed in the western and southern regions of the island. The stratigraphical succession can be defined in terms of three conformable units, in ascending order: the Basal Volcanic Suite; the Central Plain Group; and the Antigua Formation. The Antigua Formation is a succession of diverse limestones with minor siliciclastic and volcaniclastic, commonly tuffaceous, horizons that are exposed in the north and east of the island (Fig. 2.1). The specimens analysed herein were collected from two localities in the Antigua Formation.

### 2.3.1 Locality 1. Hughes Point

Oysters were collected from float and *in situ* from limestone beds in the Hughes Point area on the south coast of Nonsuch Bay, parish of St. Philip, eastern Antigua (Locality 1). Large gryphaeid oysters assigned to *Hyotissa antiguensis* (Brown, 1913) are locally common both *in situ* in an extensive coastal exposure, and reworked as float in adjacent shallow water, the latter associated with common bored clasts of limestone (Donovan et al., 2014a). A measured section of part of the coastal exposure appeared in Collins and Donovan (1995, fig. 2; Figure 2.2 herein). Oysters are common and were noted in all beds identified in this illustration.

### 2.3.2 Locality 2. Half Moon Bay

Scallops, including *Aequipecten*? sp., were collected from the northeast point of Half Moon Bay, parish of Saint Philip, southeast Antigua (Locality 2). Here the section exposes

over 8 m of the Antigua Formation. These limestones have yielded a diverse fauna (Donovan et al., 2015), including calcareous algae, articulated sponges, brachiopods, crinoid columnals, asteroid marginal ossicles, echinoids, rare oysters and other benthic molluscs, including scallops. Foraminiferans from these beds include flat *Lepidocyclina canellei* Lemoine and Douville and inflated *Eulepidina* sp. cf. *E. undosa* (Cushman). A measured section was published in Donovan *et al*. (2015, fig. 3; Figure 2.3 herein).

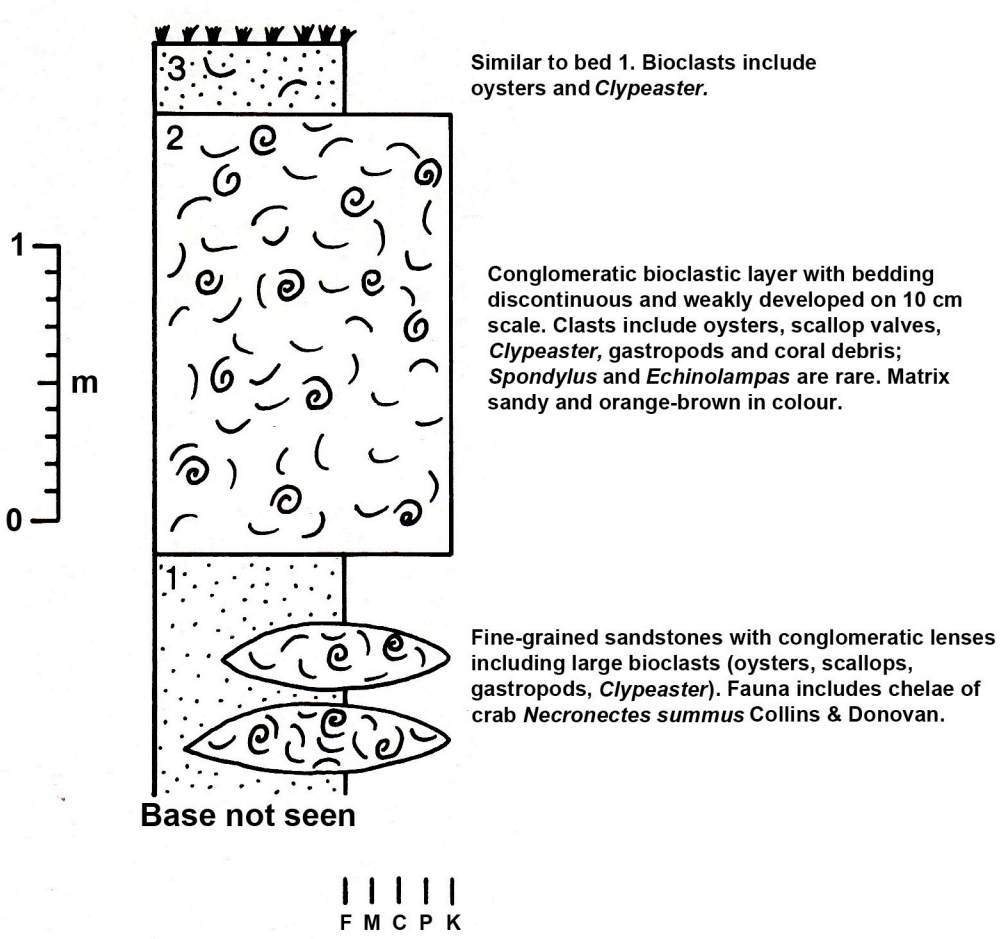


**Figure 2.2: Measured section in the lower part of the cliff at Hughes Point (Locality 1), Nonsuch Bay, Antigua Formation (modified after Collins and Donovan, 1995, fig. 2). Key: F, M, C = fine-, medium- and coarse-grained sandstone, respectively; P = pebble conglomerate; K = cobble conglomerate; all rocks are limestone.**

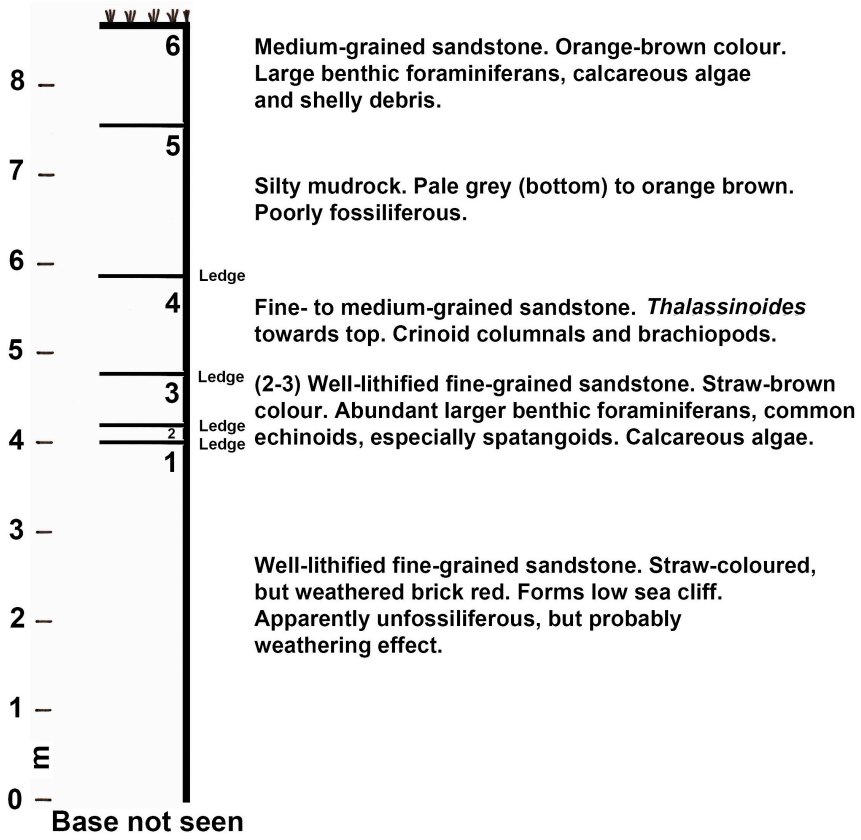


**Figure 2.3: A measured section of the northeast point of Half Moon Bay (Locality 2), parish of Saint Philip, south-east Antigua; Antigua Formation (Upper Oligocene) (after Donovan *et al.*, 2015, fig. 3). Note the section is entirely in limestone; terms such as sandstone and mudrock refer to grain size. Crinoid columnals and a brachiopod were collected from bed 4; crinoid columnals are present, but rare, higher in the section.**

## 2.4 Results

### 2.4.1 Locality 1: Hughes Point

Data using EDS show that the gryphaeid oysters are composed predominantly of silica (>80%) intermixed with calcite (Table 2.1), lacking any correspondence to the original growth lamellae or shell ultrastructure (Fig. 2.4A). Under the backscatter detector (BSE), the silica grains in the samples appear relatively uniform with no visible distinguishing features (Fig. 2.5A). The silica studied by SEM-CL shows a range of grey scale luminosities ranging from dark grey to white (white being the strongest luminescence) with the majority of grains appearing mottled in texture (Fig. 2.5B). These varying intensities highlight features in the silica such as zoning. This distinct zoning appears as varying shades of grey, with the outer rim showing almost no luminescence; however, zonation is not uniform. An emission spectrum was produced using the intensity of counts against wavelength. The emission band of this silica lies between 540 – 740 nm (Fig. 2.6), indicated neoformed silica (e.g., Aparicio and Bustillo 2012), which correlates with a possible hydrothermal source (Götze et al., 2001).

Table 2.1: EDS data for specimen from Hughes Point (Locality 1). These data (wt.100%) are normalised to 100 and are calculated using the oxide option in QUANT software.

| Spot | CaO | MgO | SiO | Total |
|---|---|---|---|---|
| 1 | 0 | 0 | 100.00 | 100.00 |
| 2 | 0 | 0 | 100.00 | 100.00 |
| 3 | 98.61 | 1.39 | 0 | 100.00 |
| 4 | 100.00 | 0.00 | 0 | 100.00 |

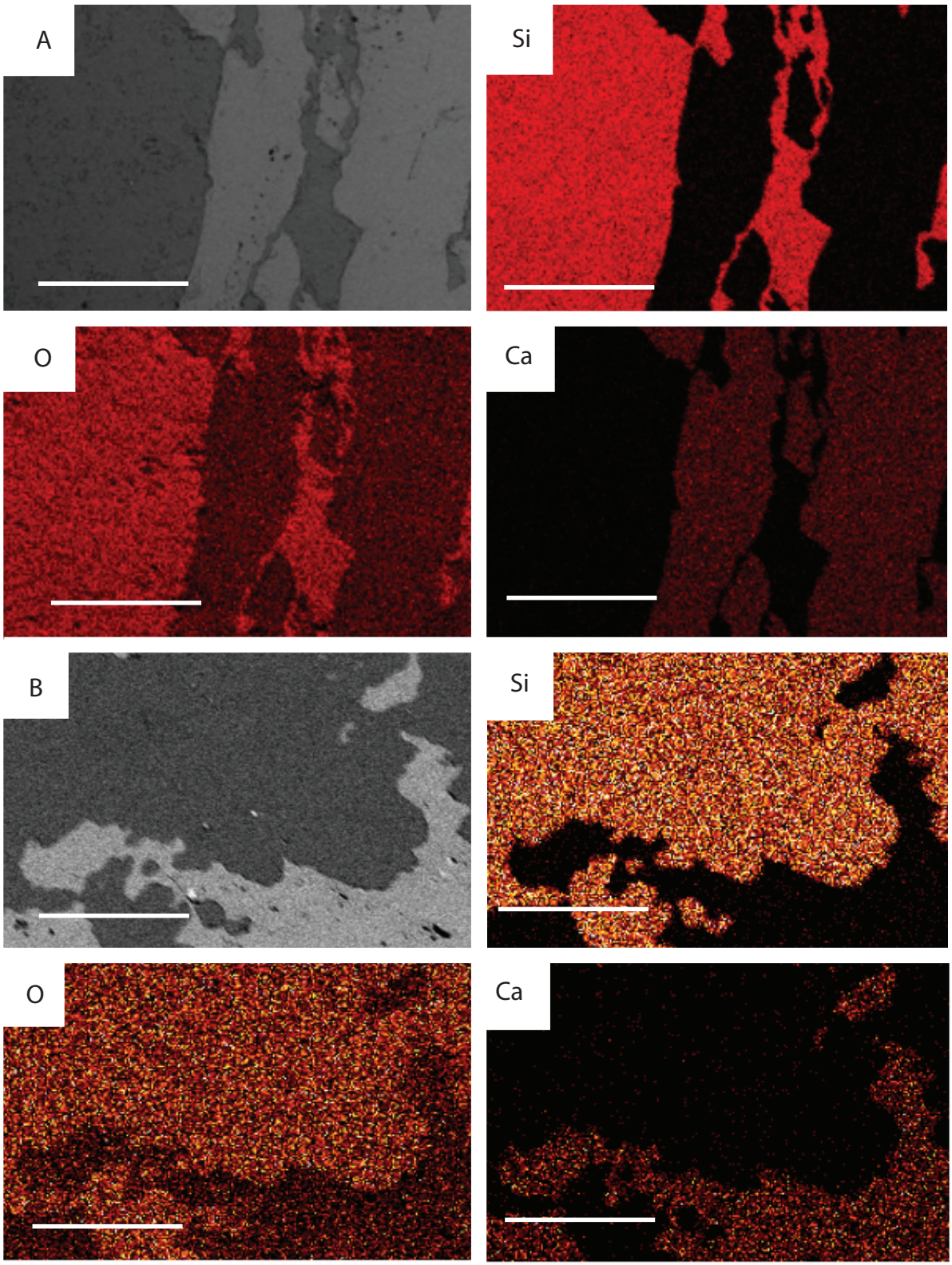


**Figure 2.4: Elemental maps of specimens from both localities. A. Elemental maps showing the distribution of Si, Ca and O of a sample from Hughes Point of the oyster *Hyotissa antiguensis*. B. Elemental maps showing the distribution of Si, Ca and O of the Half Moon Bay sample of *Aequipecten*? sp. Scale bars represent 100µm.**

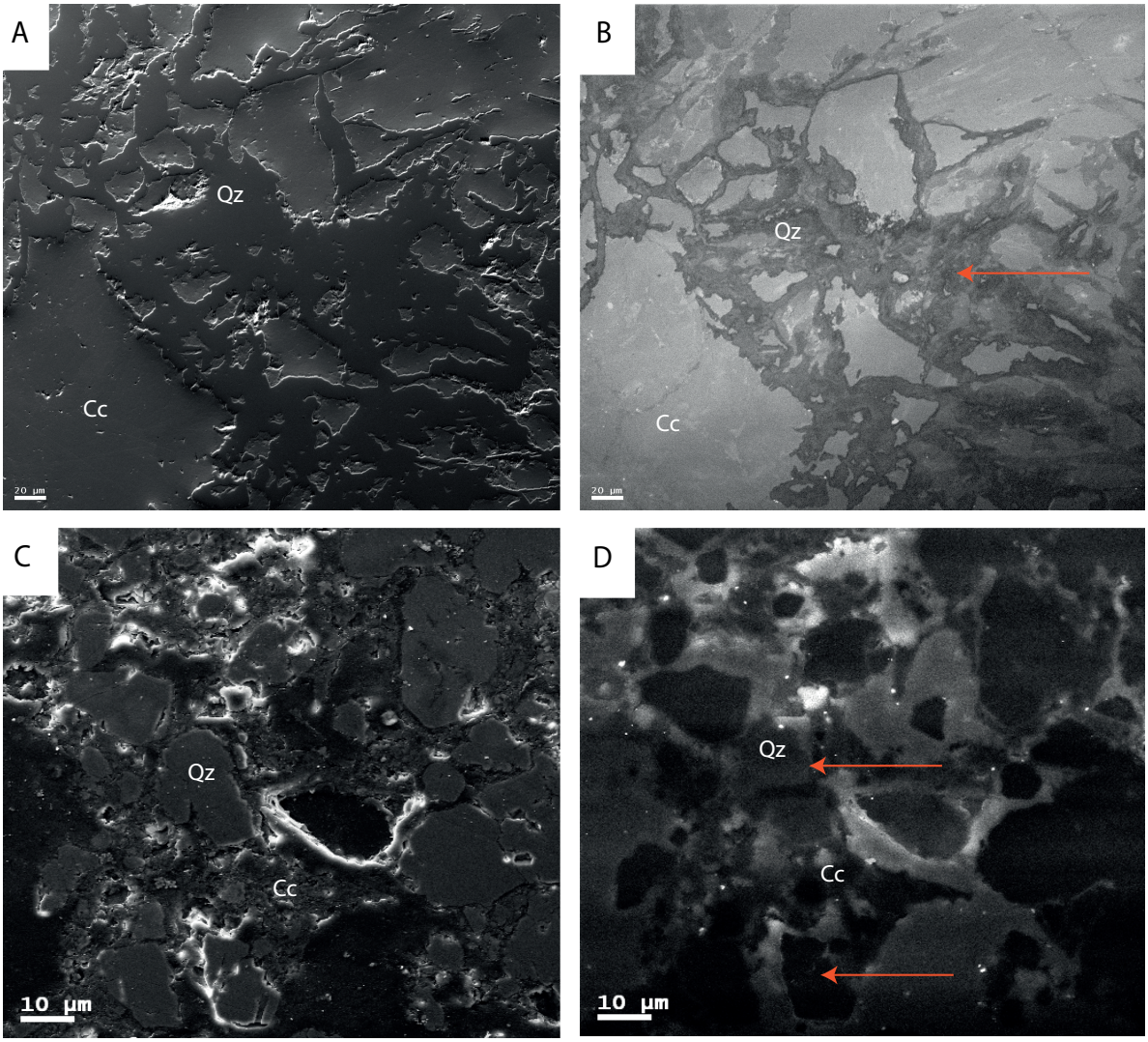


**Figure 2.5: SEM and CL images of specimens from Hughes Point and Half Moon Bay. A. SE image showing the relationship of calcite to silica zones in the oyster *Hyotissa antiguensis*. B. SEM-CL of same area and specimen as (A), showing distinct mottled texture (red arrow). C. SE image of *Aequipecten*? sp. from Half Moon Bay, showing the distribution of calcite and silica zones. D. SEM-CL of same area and specimen as (C), showing differing luminosity in silica and mottled textures (red arrows). Scale bars represent 20 µm (above) and 10 µm (below). Abbreviations: Cc – calcite; Qz – quartz.**

### 2.4.2 Locality 2: Half Moon Bay

Scallops (pectinid bivalves) from Half Moon Bay share the same composition as the oysters (Table 2.2) from Locality 1, composed of silica and calcite; this pattern, similar to that of the oysters from Hughes Point, does not conform to the original growth lines or shell ultrastructure (Fig. 2.4B). The optical BSE textures are homogenous, and there are no clear defects visible under normal SEM imaging (Fig. 2.5C). However, SEM-CL again shows a distinct mottled texture and similar irregular distribution of luminosity intensities, as at Locality 1. This irregular distribution (Fig. 2.5D) of luminosity helps distinguish neoformed silica from that of metamorphic origin (Matter and Ramseyer, 1985). There is also evidence of zoning present, with the overall texture similar to that found at Hughes Point.

Table 2.2 EDS data for specimen from Half Moon Bay (Locality 2). These data (wt.100%) are normalised to 100 and are calculated using the oxide option in QUANT software. Note – the value for MgO of 3.17 is probably an artefact.

| Spot | CaO | MgO | SiO | Total |
|---|---|---|---|---|
| 1 | 0 | 0.11 | 99.89 | 100.00 |
| 2 | 0 | 3.17 | 96.83 | 100.00 |
| 3 | 97.24 | 2.76 | 0 | 100.00 |
| 4 | 100.00 | 0 | 0 | 100.00 |

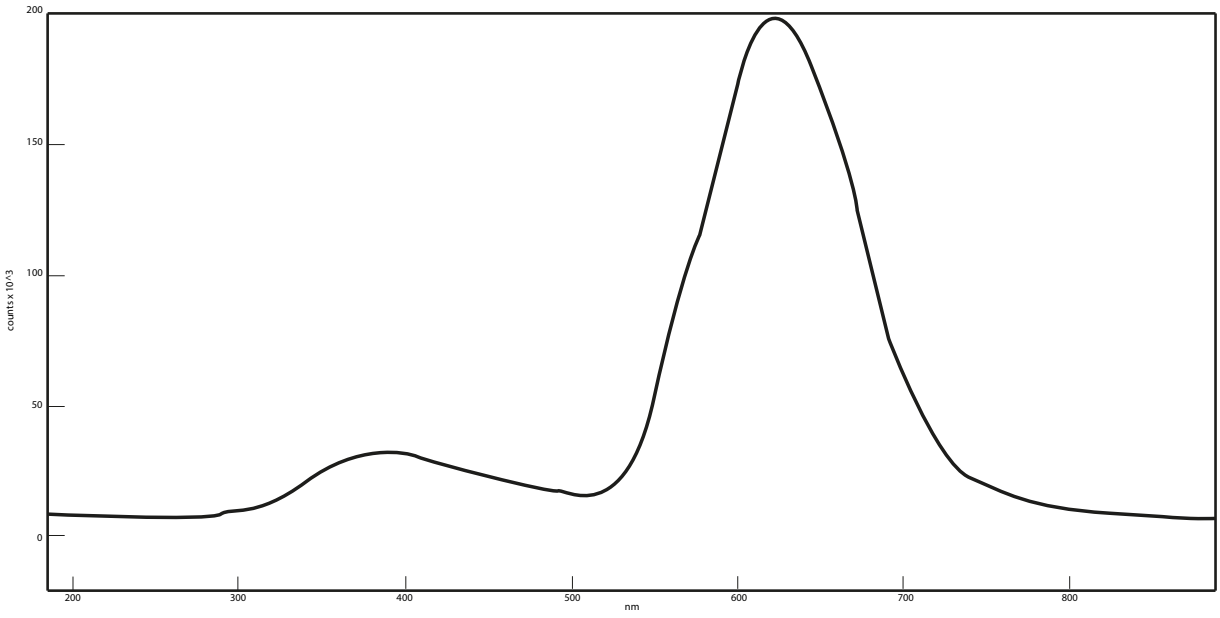

**Figure 2.6: CL-SEM spectrum of quartz; emission band of this silica lies between 540 – 740 nm.**

## 2.5 Conclusion

Silicified fossils are common in the upper Oligocene limestones of Antigua. These rocks overlie and are regionally interbedded with a range of volcanic and volcaniclastic rocks, providing an obvious source of silica. The proximity of these extrusive igneous rocks to the fossils provides a key test of the efficacy of some of techniques available to identify the source of silica in diagenetically altered shells. In particular, those molluscs with low magnesium shells, oysters and scallops, seem particularly prone to silicification. The technique of studying patterns of variable-intensity mono CL in quartz grains has been applied to many provenance studies (Seyedolali et al., 1997; Boggs et al., 2002), but in this case we have focused on the conditions of formation of the silica. We infer that silica replacement in these fossils was a multi-stage process, indicated by the variety of textures and crystal sizes visible under CL. The minerals from both localities show a characteristic mottled texture with irregular zoning and fractures throughout (Fig. 2.5). The emission band of this silica lies between 540 – 740 nm (Fig. 2.6), suggestive of a possible hydrothermal source (Götze et al., 2001; Götze, 2012). This evidence is not incompatible with silicification driven by the hydrothermal products of a volcanic arc, much of which forms the basement of the Limestone Caribees.

## 2.6 References


Aparicio, A., and Bustillo, A., 2012, Cathodoluminescence spectral characteristics of quartz and feldspars in unaltered and hydrothermally altered volcanic rocks (Almeria, Spain): Spectroscopy Letters, v. 45, p. 104-108.

Barbin, V., and Gaspard, D., 1995, Cathodoluminescence of Recent articulate brachiopod shells: implications for growth stages and diagenesis evaluation: Geobios, v. 28, p. 39- 45.

Bernet, M., and Bassett, K., 2005, Provenance analysis by single-quartz-grain SEM- CL/optical microscopy: Journal of Sedimentary Research, v. 75, p. 492-500.

Boggs, S., Kwon, Y.I., Goles, G.G., Rusk, B.G., Krinsley, D., and Seyedolali, A., 2002, Is quartz cathodoluminescence color a reliable provenance tool? A quantitative examination: Journal of Sedimentary Research, v. 72, p. 408-415.

Brown, A.P., 1913, Notes on the geology of the island of Antigua: Proceedings of the Academy of Natural Sciences of Philadelphia, v. 65, p. 584-616.

Butts, S., 2014, Silicification. In: M. Laflamme, J. D., Schiffbauer and S. A. Darroch (Eds), Reading and Writing of the Fossil Record: Preservational Pathways to Exceptional Fossilization: Paleontological Society Papers, v. 20, p. 15-34.

Collins, J.S.H., and Donovan, S. K., 1995, A new species of Necronectes (Decapoda) from the Upper Oligocene of Antigua: Caribbean Journal of Science, v. 31, p. 122-127.

Donovan, S.K., 2010, Jamaican rock stars. In: Donovan, S. K. (Ed.), Jamaican Rock Stars, 1823-1971: The Geologists Who Explored Jamaica: Geological Society of America Memoir, v. 205, p. 1-8.

Donovan, S.K., Harper, D.A.T. and Portell, R.W., 2015, In deep water: a crinoid–brachiopod association in the Upper Oligocene of Antigua, West Indies: Lethaia, v. 48, p. 291-298.

Donovan, S.K., Harper, D.A.T., Portell, R.W. and Renema, W., 2014a, Neoichnology and implications for stratigraphy of reworked Upper Oligocene oysters, Antigua, West Indies: Proceedings of the Geologists' Association, v. 125, p. 99-106.

Donovan, S.K., Jackson, T.A., Harper, D.A.T., Portell, R.W. and Renema, W, 2014b, Classic localities explained 16. The Upper Oligocene of Antigua: the volcanic to limestone transition in a limestone Caribbee: Geology Today, v. 30, p. 151– 158.

England, J., Cusack, M., Paterson, N.W., Edwards, P., Lee, M.R., and Martin, R., 2006, Hyperspectral cathodoluminescence imaging of modern and fossil carbonate shells: Journal of Geophysical Research, v. 111, p. G03001

Frelinger, S.N., Ledvina, M.D., Kyle, J.R., and Zhao, D., 2015, Scanning electron microscopy cathodoluminescence of quartz: Principles, techniques and applications in ore geology: Ore Geology Reviews, v. 65, p. 840-852.

Götze, J., 2012, Application of Cathodoluminescence Microscopy and Spectroscopy in Geosciences: Microscope and Microscopy, v. 18, p. 1270-1284.

Götze, J., Plötze, M., and Habermann, D., 2001, Origin, spectral characteristics and practical applications of the cathodoluminescence (CL) of quartz–a review: Mineralogy and Petrology, v. 71, p. 225-250.

Maliva, R.G., and Siever, R., 1988, Mechanism and controls of silicification of fossils in limestones: Journal of Geology, v. 96, p. 387-398.

Matter, A., and Ramseyer, K., 1985, Cathodoluminescence microscopy as a tool for provenance studies of sandstones. In: Zuffa, G. G. (Ed.), Provenance of Arenites, 191-211. Springer, Dordrecht.

Schieber, J., Krinsley, D., and Riciputi, L., 2000, Diagenetic origin of quartz silt in mudstones and implications for silica cycling: Nature, v. 406, p. 981-985.

Ségalen, L., de Rafélis, M., Lee-Thorp, J.A., Maurer, A.-F., and Renard, M., 2008, Cathodoluminescence tools provide clues to depositional history in Miocene and Pliocene mammalian teeth: Palaeogeography, Palaeoclimatology, Palaeoecology, v. 266, p. 246-253.

Seyedolali, A., Krinsley, D., and Boggs, S., 1997, Provenance interpretation of quartz by scanning electron microscope–cathodoluminescence fabric analysis: Geology, v. 25, no. 9, p. 787–790.

Upchurch, S.B., Strom, R.N., and Nuckels, M.G., 1980, Silicification of Miocene rocks from central Florida. In: Scott, T.M. and Upchurch, S.B. (Eds.), Miocene of the Southeastern United States, 251-284. Florida Department of Natural Resources, Division of Resource Management, Bureau of Geology, Special Publication, 25.

Wadge, G., 1994, The Lesser Antilles. In: Donovan, S. K. and Jackson, T. A. (Eds.), Caribbean Geology: An Introduction, 167–177. University of the West Indies Publishers' Association, Mona.

Weiss, M.P., 1994, Oligocene limestones of Antigua, West Indies: Neptune succeeds Vulcan. Caribbean Journal of Science, v. 30, p. 1–29.

# Chapter 3. The Sirius Passet Lagerstätte: Silica death masking opens the window on the earliest matground community of the Cambrian Explosion – A detailed study on the taphonomy of trilobite *Buenellus higginsi*.

## 3.1 Abstract

In this chapter we address aspects of the exceptionally preserved Sirius Passet Lagerstätte, one of the earliest examples of soft-bodied preservation from the lower Cambrian. A version of this chapter is published in the journal *Lethaia* (Appendix II). The Sirius Passet Lagerstätte (SP), Peary Land, North Greenland, occurs in black slates deposited at or just below storm wave base. It represents the earliest Cambrian microbial mat community with exceptional preservation, predating the Burgess Shale by 10 million years. The Cambrian Explosion is one of the most important events in the history of life, recording the diversification of many bilaterian animal body plans and the expansion of marine ecosystems. Research on exceptionally preserved Lagerstätten is extremely important in helping us understand this early evolution of life. We use a combination of analytical techniques, such as petrography and SEM analyses with detailed methodology outlined in chapter 1, section 1.6. Here we demonstrate the sequence of events leading to the preservation of concave hyporelief external moulds and convex epirelief casts of *Buenellus higginsi*, the most common element of the Sirius Passet. There are three main types of preservation in the SP – moulds, films and guts. *Buenellus* was chosen due to its abundance and availability of specimens, and it being a good representative of the typical mouldic preservation throughout this Lagerstätte. In this chapter we also present a detailed description of the sedimentary petrology, revealing two end-member lithofacies, a 'spotted' and a silt-rich facies. The main element of our proposed trilobite taphonomy is the sealing of the specimens and early silicification, within the microbial mats on which they lived. This taphonomy, generating death masks, is relatively common in the Ediacaran, however it is unique to the Cambrian and may only have existed for a short time due the absence of the mat grazing organisms that appeared later during the Cambrian Explosion. Trilobites from the SP are preserved as complete, three-dimensional, concave hyporelief external moulds and convex epirelief casts. External moulds are shown to consist of a thin veneer of authigenic silica. The casts are formed from silicified cyanobacterial mat material. Silicification in both cases occurred

shortly after death within benthic cyanobacterial mats. Pore waters were alkali, silica saturated, high in ferric iron but low in oxygen and sulphate. Excess silica was likely derived from remobilized biogenic silica. The remarkable siliceous death mask preservation opens a new window on the environment and location of the Cambrian Explosion. This window closed with the appearance of abundant mat grazers later as the Cambrian Explosion intensified.

## 3.2 Introduction

The Cambrian Explosion records the diversification of complex, mainly bilaterian, animal body plans and the expansion of animal-based marine ecosystems (Butterfield, 2003). Much of what we know about this event is recorded in a succession of black shale conservation Lagerstätten. The Sirius Passet (SP) is the oldest of these and is located in J.P. Koch Fjord, N. Greenland, at 82°47.6'N, 42°13.7'W (Fig. 3.1A) and during the Cambrian lay at approximately 10ºS (Fig. 1B; Peel and Ineson, 2011). The black slates have been mapped as the "Transitional" Buen, previously interpreted as fine-grained turbidites (Peel and Ineson, 2011). *Buenellus higginsi* is the most common macrofossil, indicative of the *Nevadella* Biozone in Laurentia, equivalent to the middle part of Stage 3 (lowest stage of Series 2; 520 to 535 Ma; see Babcock, 2005).

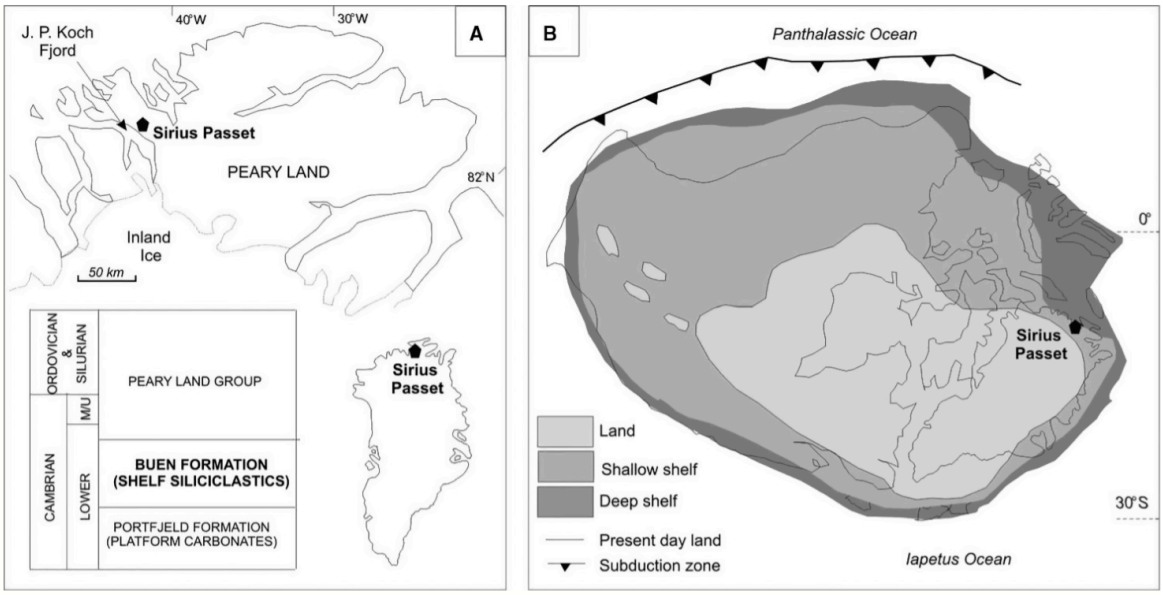


**Figure 3.1: Figure 3.1: A. Sirius Passet locality map, lithostratigraphy. B, Cambrian palaeogeography. Fig. 1B redrawn after Cocks and Torsvik (2011).**

The SP fauna is similar to that of the Burgess Shale, comprising ca. 50 species including trilobites, sponges, worms, halkieriids, lobopods, and non-trilobite bivalved arthropods. The SP Lagerstätte pre-dates the Burgess Shale (510 Ma) and Chengjiang biotas (520 Ma) and is therefore the earliest example of high-fidelity, soft-tissue preservation in the Cambrian. As recognised from studies of

other Lagerstätten, an understanding of taphonomy is crucial in aiding anatomical interpretations of the SP fauna and provides for a better understanding of the palaeoenvironment, community reconstruction and early diagenesis (e.g. Gaines & Droser, 2005; Zhu et al., 2006).

Similarities have been drawn between the depositional setting of the Burgess Shale and SP, for example proximity to a submarine cliff line and supposed basinal, turbiditic sedimentation (Ineson & Peel, 2011). These similarities have led to the untested inference that SP fossils show Burgess Shale type preservation (Gaines et al., 2008; Ineson & Peel, 2011). Burgess Shale type preservation is defined as "exceptionally preserved fossils whose primary taphonomic mode is one of non-mineralising organisms preserved as carbonaceous compressions in fully marine sediments" (Butterfield, 1995). In the Burgess Shale the soft-bodied fossils are preserved as thin, multi-layered silvery films (Whittington, 1980). Significant discussion has focussed on the composition of the films. Are they predominantly organic and result from coalification during metamorphism (Butterfield, 1990, 1995; Page et al., 1998) or predominantly composed of aligned clay minerals (Towe, 1996; Orr et al., 1998)? Disagreement regarding the composition of the fossils has led to a lack of consensus regarding the mode of fossilization. Butterfield (1990, 1995) proposed that the clay which surrounded the fossils during burial acted as a catalyst that inhibited microbial decomposition of the labile tissues, leaving the organic material to be "tanned" (Butterfield, 1990) and produce a kerogen film during diagenesis. In comparison, Orr et al., (1998) concluded that fossilization occurred during decomposition as a consequence of chemical interactions between the tissues and the surrounding clays. In this model, variations in composition and reactivity of the different tissues during decomposition resulted in varying accumulations of clays on the carcass either by accumulation or direct precipitation from the pore water. The enhanced preservation of non-mineralized tissues may have also resulted from a combination of environmental factors. Near bottom anoxia, would have prevented sediment irrigation by bioturbators. Reduced permeability of the seafloor and exclusion of oxygen may have also resulted from an absence of coarse grains such as silt, faecal pellets or bioclasts and the presence of reduced bottom waters that may have acted to

deflocculate clay mineral aggregations and facilitated the precipitation of early diagenetic pore occluding carbonate cements (Gaines et al., 2005).

Some of the controversy surrounding the mechanisms of Burgess Shale type preservation is in part due to the loss of primary features during post-depositional diagenesis and metamorphism. As a consequence of low greenschist facies metamorphism and cleavage formation, the phyllosilicates of the Burgess Shale currently associated with the fossils are not the same as the minerals that initially buried the fossils (Powell, 2003). A detailed understanding of the metamorphic history and reconstruction of the primary bulk mineralogy of the Burgess Shale precludes the presence of highly reactive clay species necessary for the Butterfield model involving organic preservation due to clay-related suppression of decomposition-related reactions (Powell, 2003). Instead it indicates there was nothing unusual about the initial mud sediment and lends support to the Orr hypothesis of clay templating during decomposition (Powell, 2003). This re-evaluation challenges the nature of Burgess Shale type preservation, and shows the importance of determining the mineralogical changes in Cambrian black shale Lagerstätten during metamorphism. This is critical to understanding the taphonomy which in previous discussions of the SP, metamorphism has been largely ignored.

In this contribution we use a combination of observations, petrography and SEM analyses to demonstrate the sequence of events leading to an early “death mask” preservation of the trilobites within the SP and discount the influence of metamorphic processes. The trilobite *Buenellus* is the most abundant element of the SP and therefore critical to the overall understanding of the taphonomic history. A key element of our proposed trilobite taphonomy is the sealing of the specimens and early silicification, within the microbial mats on which they lived. This taphonomy though common in the Ediacaran is unique to the Cambrian and may only have existed for a short time due the absence of the mat grazing guild that appeared later in the Cambrian Explosion.

## 3.3 Results

**3.3.1 Specimens.** *Buenellus* specimens are preserved complete, in life position and in 3D. Two types of preservation are shown: 1) concave external moulds comprise thin (<1 mm) veneers of silica (Fig. 3.2A) and, 2) convex epirelief casts composed predominantly of silicified microbial mat material (Fig. 3.2B-C). The microbial mat occurs as aggregates of hollow, cell-like structures with only the cell wall mineralized. Two microbial textures are preserved: (1) the sheath, which consists of small (<5 μm) equidimensional cells and spherical vesicles up to 2μm in diameter (Fig. 3.2D-E), and (2) tubular or dendritically branching microbial filaments (Fig. 3.2F), observed only on the surface of the fossils.

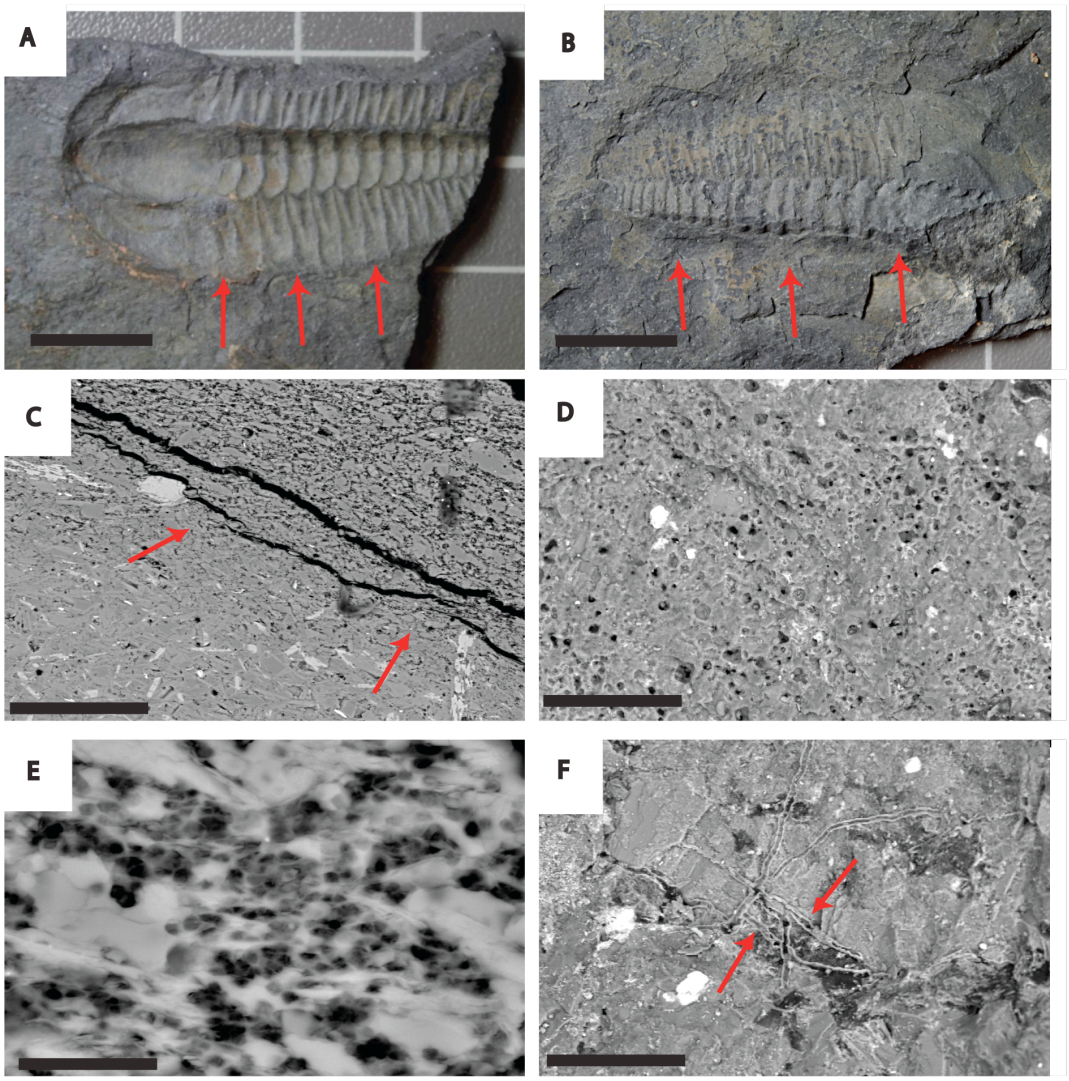

**Figure 3.2: High resolution photographs and SEM images. A, Image showing convex external mould of *Buenellus*; arrows indicate where thin sections were cut. Scale bar 1 cm. B, Convex epirelief cast of *Buenellus*; arrows indicate where thin sections were cut. Scale bar 1 cm. C, BSE SEM image showing matrix and microbial material; arrows indicate where mat material begins. Scale bar 1 cm. D, SE SEM image showing microbial mat material as aggregates of hollow, cell-like structures with only the cell wall mineralized, scale bar 1 cm. E, High magnification SEM BSE image showing 'webbed' silicified microbial mat structures. F, SEM SE image showing branching microbial filaments growing on the surface of the fossil. Scale bar 100 mm.**

**3.3.2 Sedimentary petrography.** The cleavage parallels sedimentary bedding and primary sedimentary textures are preserved. Two end-member lithofacies are recognised, a "spotted" and a silt-rich facies (Fig. 3.5). The "spotted" facies consists of structureless to discontinuously laminated phyllosilicates containing Al-rich chlorite-mica aggregates that are 10–20 mm in diameter (Fig 3.5A-B). Significantly, outsized clasts of silicified microbial mat occur infrequently in both the "spotted" facies and the silt-rich facies (Fig. 3.5C). The silt-rich facies consists of clay to very fine silt particles composed predominantly of phyllosilicates with minor detrital quartz grains in the silt fraction (Fig. 3.5D-E). Outsized, lenticular mud clasts are present in a few beds (Fig. 3.5F). Bedsets are planar and cross-laminated (Fig. 3.5G), with sharp to gradational boundaries between coarser and finer layers (Fig. 3.5H).

**3.3.3 X-Ray Diffraction.** XRD was carried out on both the "spotted" (Fig. 3.3) and the silt-rich facies (Fig. 3.4). Results show that the overall mineralogy was similar with both facies composed of biotite, illite, quartz and chlorite. Although broadly similar, the intensities of each mineral varied between facies, likely as an artefact of the differing compositions prior to metamorphism.

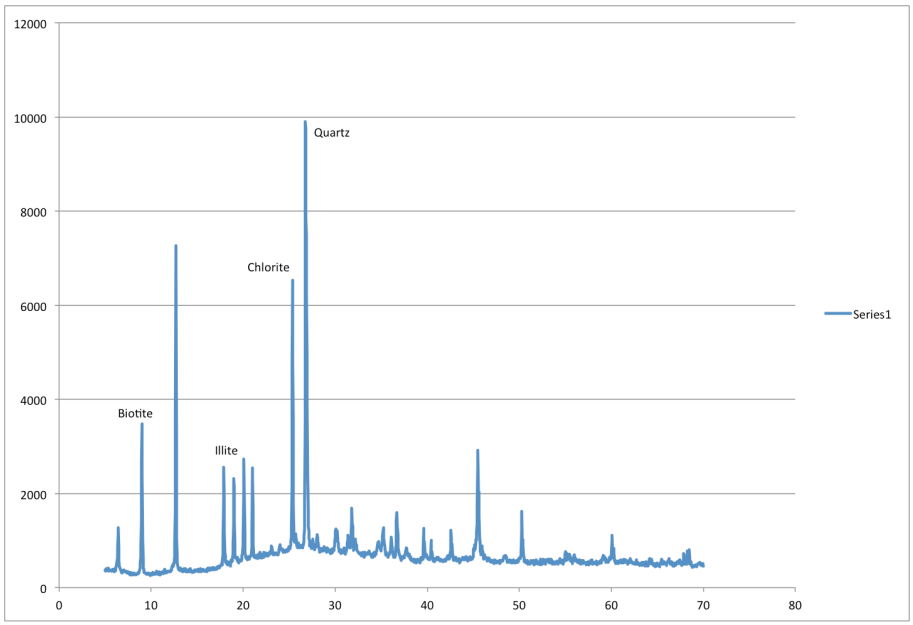


**Figure 3.3: XRD plot of 2θ against intensity with labels showing normalized peaks for each main clay mineral, interpreted using Moore and Reynolds (1997). These data are from sample 0.06 which is the 'spotted' facies.**

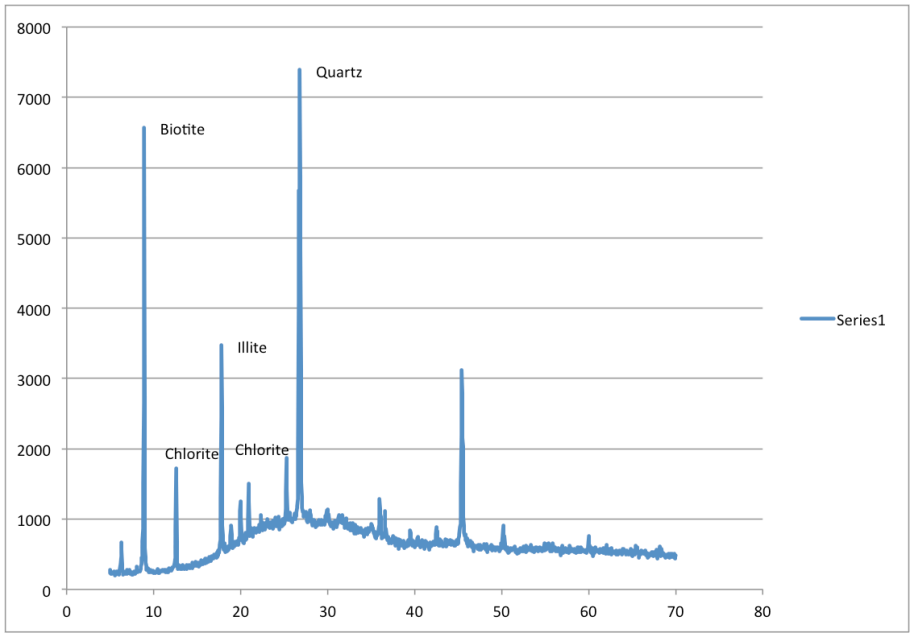


**Figure 3.4: XRD plot of 2θ against intensity with labels showing normalized peaks for each main clay mineral, interpreted using Moore and Reynolds (1997). These data are for sample 4.56, the silt-rich facies.**

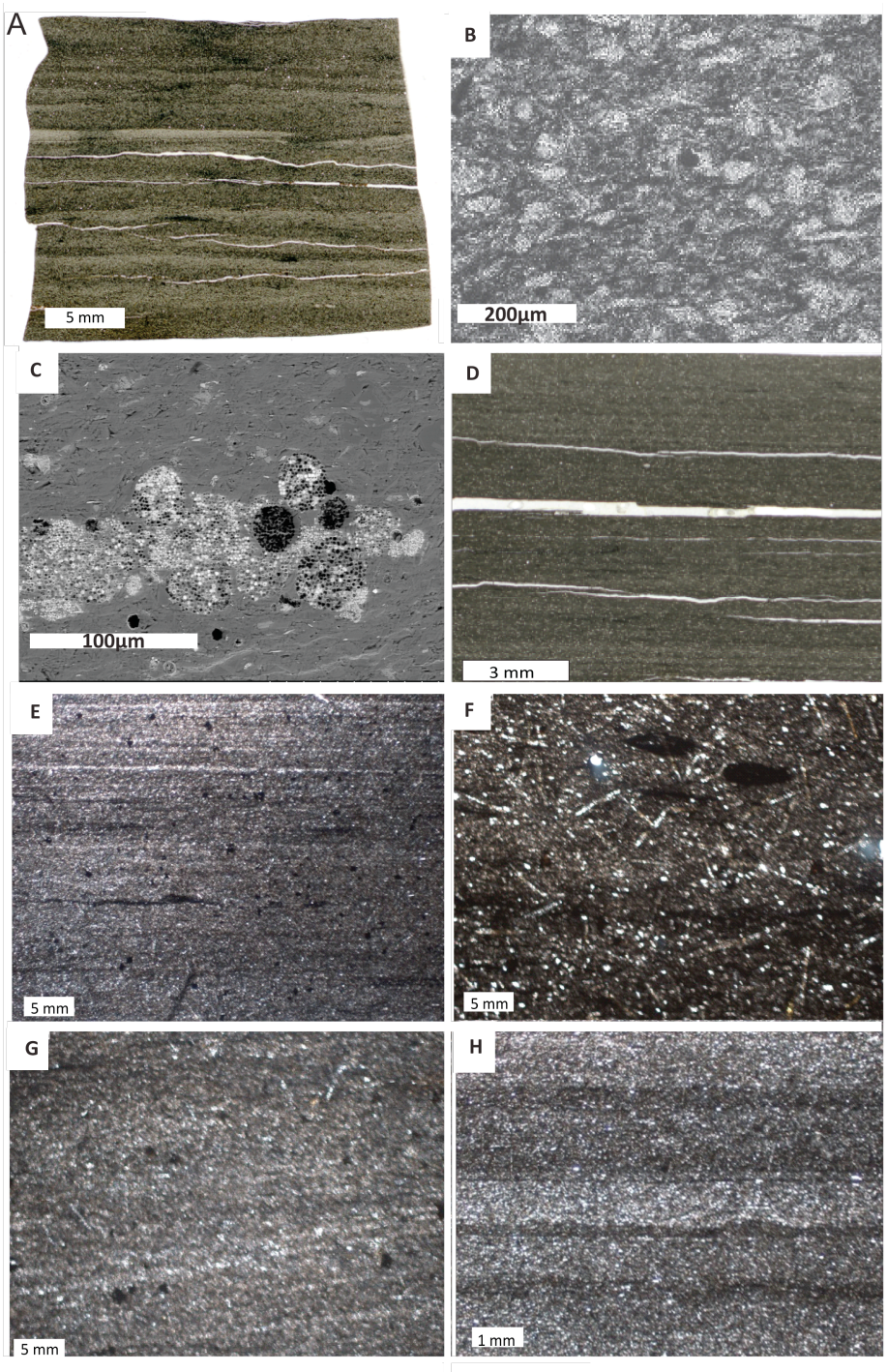


**Figure 3.5: Thin section photomicrographs; SEM and BSE images showing the different facies types. A, High-resolution photomicrograph of a thin section showing the concentration of chlorite-mica aggregates into discontinuous wavy beds (3.4 m from base of log). B, Photomicrograph in plane polarized light showing chlorite-mica aggregates of varying sizes (1.12 m above base of log). C, BSE photomicrograph of silicified microbial mat fragment in the silt rich facies (5.5 m above base of log). D, Photomicrograph of a thin section showing laminated fabric and continuous and discontinuous silt layers (2.62 m from base of log). E, Photomicrograph in plane polarized light showing lamination picked out by single grain thickness layers of detrital quartz (4.56 m up from base of log). F,**

**Photomicrograph in plane-polarized light showing elliptical outsized floating grains of dark mudstone within a matrix of phyllosilicates, quartz, and chloritoid porphyroblasts (3.31 m above the base of log). G, Photomicrograph showing planar cross laminated bedsets. H, Photomicrograph of the silt rich facies showing sharp to gradational boundaries between course and fine layers.**

**3.3.4 Bulk mineralogy.** Bulk rock composition is similar to that of average shale (Post Archean Australian Shale (PAAS), but differs from the Burgess Shale or PAAS in higher detrital quartz, lower K/Al (0.165, see Supplementary information) and an absence of calcite (Table 3.1). The mineral assemblage of chlorite-mica-quartz and minor/trace of carbon, albite and illite and absence of sulphates is that found to be stable from upper subgreenschist to middle greenschist facies (Powell, 2003). The absence of carbonate is a consequence of the sediment having passed through the smectite – illite transition (S-I; below). Abundant chloritoid porphyroblasts are indicative of low greenschist facies metamorphism (Higgins et al., 2001; equivalent to ~10km burial) and their random orientation relative to bedding indicates relatively low-pressure conditions or possible formation during retrogressive regional metamorphism. Chloritoid is represented by the general formula $(Fe,Mg,Mn)Al_2SiO_5(OH)_2$ and occurs in high Al, low temperature metapelites (Halferdahl, 1961). It is normally formed through the reaction of pyrophyllite, a phyllosilicate clay, and chlorite forming chloritoid, quartz and water. During this reaction, any excess silica can be precipitated as inclusions within the chloritoid. Quartz inclusions are common in the chloritoid needles, and appear as irregular shaped grains within the needle.

Total organic carbon ranges from 0.5 to 1%. However, Raiswell & Berner (1987) documented an exponential loss of organic carbon relative to vitrinite reflectance in shales. Lower greenschist facies metamorphism would correspond to a minimum vitrinite reflectance of 5% (Kish, 1987). Projecting the Raiswell & Berner curve to a greenschist facies equivalent yields an estimated organic carbon preservation of 15%. The initial organic carbon content of the SP would therefore have been >3%; a value typical for many oil source rocks.

**Table 3.**1: Bulk-rock chemistry (in wt. %) of the low-carbonate Burgess Shale metamudstones (Walcott Quarry, Raymond Quarry and Tuzoia Beds extracted from Powell 2003) compared with the bulk-rock chemistry of SP.

| Wt. % | Walcott 1 | Walcott 2 | Raymond | Tuzoia | PAAS | Sirius Passet |
|---|---|---|---|---|---|---|
| $SiO_2$ | 53.71 | 50.34 | 50.10 | 50.63 | 62.8 | 63.46 |
| $Al_2O_3$ | 24.11 | 23.32 | 21.25 | 24.54 | 18.90 | 26.61 |
| $K_2O$ | 6.75 | 7.07 | 4.15 | 6.15 | 3.70 | 4.39 |
| K/Al | 0.280 | 0.303 | 0.195 | 0.250 | 0.196 | 0.165 |

**3.3.5 SEM-EDAX.** Quantitative elemental mapping across a convex epirelief cast of *Buenellus* (Fig. 3.5A) shows typical values for Si (84%), Al (11%), and Fe (5%) compared with the matrix (Tables 3.2-3.4). There is evidence of small framboidal pyrite associated with the mat material, which is absent from the matrix (Fig. 3.5B).

Table 3.2: Results from EDAX (sample 4.56) silt-rich facies converted to oxides using INCA processing software

| Spectrum 4.56 | $Na_2O$ | MgO | $Al_20_3$ | $Si0_2$ | $K_20$ | Fe0 | Total |
|---|---|---|---|---|---|---|---|
| 1 | 0.00 | 1.39 | 44.64 | 30.04 | 0.34 | 23.59 | 100.00 |
| 2 | 0.00 | 0.00 | 0.49 | 98.11 | 0.00 | 1.40 | 100.00 |
| 3 | 0.81 | 0.73 | 33.01 | 56.62 | 7.88 | 0.95 | 100.00 |
| 4 | 0.00 | 0.00 | 9.52 | 86.65 | 0.51 | 3.32 | 100.00 |
| 5 | 0.67 | 1.15 | 34.65 | 54.60 | 7.48 | 1.44 | 100.00 |
| 6 | 0.63 | 0.46 | 34.98 | 54.90 | 8.41 | 0.61 | 100.00 |
| 7 | 1.01 | 0.79 | 29.00 | 61.87 | 6.45 | 0.88 | 100.00 |

Table 3.3: EDAX spectra from sample 1.12 m from the spotted facies converted to oxides using INCA processing software.

| Spectrum 1.12 | MgO | $Al_2O_3$ | $SiO_2$ | $K_2O$ | FeO | Total |
|---|---|---|---|---|---|---|
| Spectrum 1 | 12.79 | 29.10 | 30.90 | 0.26 | 26.95 | 100.00 |
| Spectrum 2 | 12.53 | 27.01 | 30.85 | 1.03 | 28.58 | 100.00 |
| Spectrum 3 | 14.03 | 27.93 | 31.86 | 0.57 | 26.05 | 100.00 |
| Spectrum 4 | 0.00 | 0.56 | 97.85 | 1.16 | 0.43 | 100.00 |
| Spectrum 5 | 1.19 | 37.61 | 50.86 | 8.74 | 1.59 | 100.00 |
| Spectrum 6 | 0.69 | 31.82 | 58.75 | 7.46 | 1.29 | 100.00 |
| Spectrum 7 | 0.00 | 1.47 | 97.56 | 0.42 | 0.54 | 100.00 |

Table 3.4: EDAX spectra data from the mat material (taken from a cross section through an epirelief cast of Buenellus) from sample 340.103a. Converted to oxides using INCA processing software

| Spectrum<br><br>Sample 340.103.a | $Na_2O$ | MgO | $Al_20_3$ | $Si0_2$ | $K_20$ | Fe0 | Total |
|---|---|---|---|---|---|---|---|
| 1 | 0.00 | 0.00 | 11.29 | 82.96 | 0.78 | 4.97 | 100.00 |
| 2 | 0.00 | 0.63 | 10.67 | 82.67 | 1.69 | 4.34 | 100.00 |
| 3 | 0.00 | 0.00 | 12.34 | 80.01 | 1.88 | 5.68 | 100.00 |
| 4 | 0.00 | 0.00 | 11.78 | 82.12 | 2.41 | 3.69 | 100.00 |
| 5 | 0.00 | 0.00 | 12.96 | 84.67 | 0.93 | 1.44 | 100.00 |
| 6 | 0.00 | 0.00 | 14.95 | 83.70 | 1.21 | 0.14 | 100.00 |
| 7 | 0.00 | 0.00 | 12.45 | 82.90 | 0.98 | 3.67 | 100.00 |
| 8. | 0.00 | 0.00 | 0.67 | 97.34 | 1.36 | 0.63 | 100.00 |

**3.3.6 SEM-CL.** Panchromatic cathodoluminescence analysis shows the presence of two quartz phases. Detrital quartz grains in the matrix exhibit true colour RGB-CL brown shade of luminescence at around 540–550 nm (Fig. 3.6C). Silica in the mineralised mat and concave external moulds exhibits almost no

luminescence (Figs 3.6D). Mono-CL of metamorphic quartz grains found as inclusions within the chloritoid needle show medium grey luminosity and a mottled texture (Fig. 3.6E). These were compared with individual grains of silica associated with the fossils, which exhibit no luminosity under mono-CL and appear black and textureless (Fig. 3.6D).

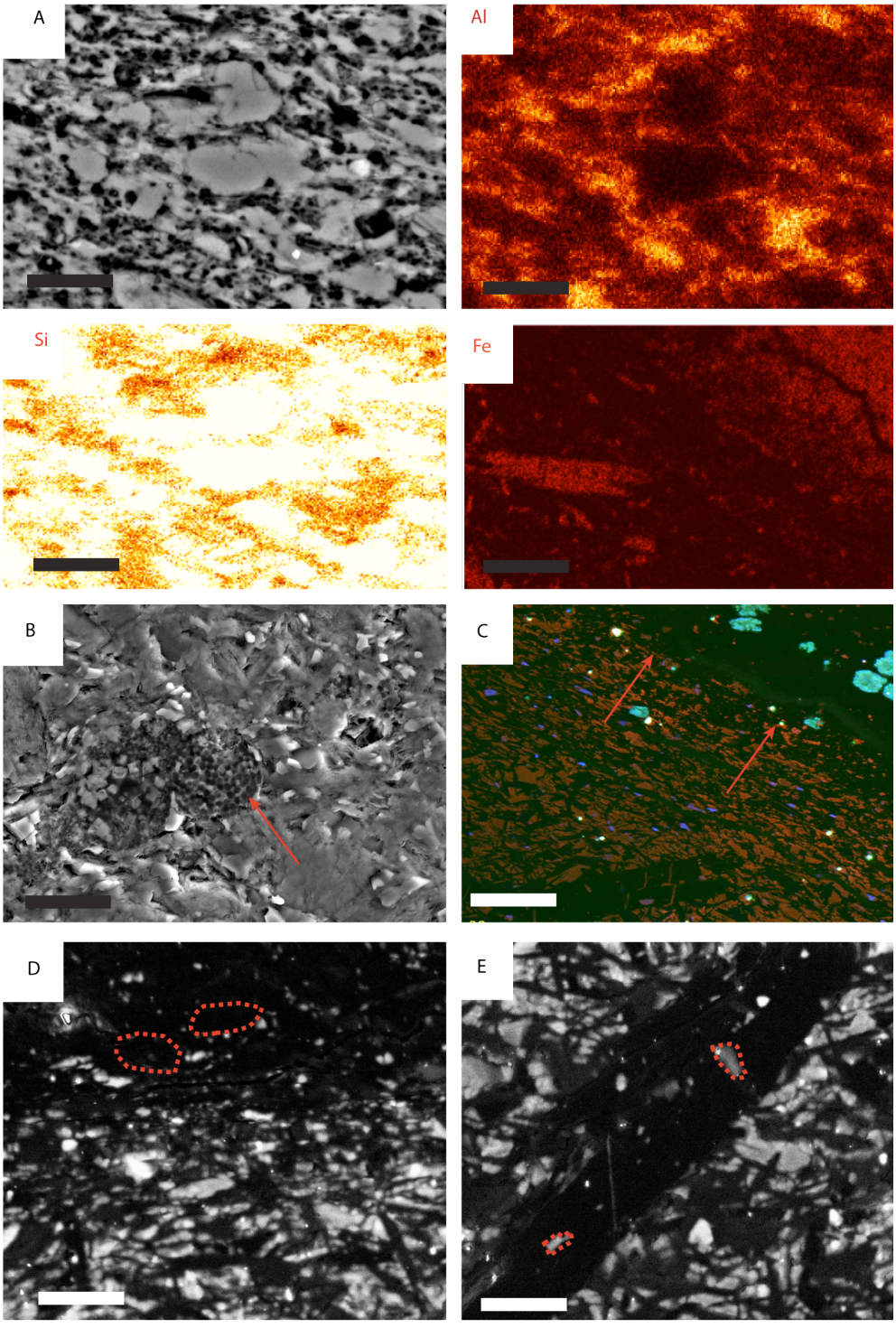


**Figure 3.6: A, elemental maps (top left SEM image to show locality of maps) taken across the mat material. Al, Si and Fe maps shown, notice the abundance of silica. Scale bar – 20µm. B, BSE SEM image showing framboidal pyrite associated with the mat material. Scale bar 30µm. C, RGB true colour CL showing brown shades of luminescence in the matrix, above arrows indicate area of mat material which has a distinctly different luminosity. D, mono-CL image, bottom half of image is matrix, whereas the top shows microbial material. Grains of non-luminescing silica associated with the fossils have been outlined (dashed line). Scale bar 20µm. E,**

**mono-CL image of chloritoid needle. Inclusions of metamorphic silica showing medium grey luminosity are outlined (dashed line). Scale bar 10μm.**

## 3.4 Discussion

Marine carbonaceous shales in the Cambrian were limited to shallow-water regions with turbulent circulation (Raiswell & Berner, 1986). The presence in the SP of normal and reverse grading, scouring, and cross lamination indicates deposition from low-density sediment gravity flows at or just below storm wave base. Cross-lamination suggests sediment transport by ripple migration. Compacted mud ripples have been observed as extremely low-angle cross-lamination in ancient mudstones (Komárek and Anagnostidis, 1986) and are consistent with sediment transport by mud-laden sediment gravity flows (Kremer and Kazmierczak, 2005). The presence of oversized clasts in the normally graded sediment suggests flows had sufficient competence to transport larger clasts, such as a denser, mud-rich 'slurry-flow', transitional between a turbidity current and a debris flow (Komarek and Anagnostidis, 1986).

The chlorite-mica aggregates in the spotted facies could have originated as primary detrital grains modified during weathering and transport or, formed as the result of diagenetic or metamorphic minerals mimicking existing sedimentary textures (see Craig et al., 2009). Aggregates are concentrated into discontinuous beds. These beds are sharp-based, normally graded with scour fills and faint cross lamination. The aggregates were probably transported and size sorted at the seafloor. Normal grading suggests deposition was from sediment gravity flows producing successive beds of rapidly accumulated sediment (Best, 2005). The fabric is primary and the texture produced by metamorphism is inherited from a pre-existing sedimentary texture. Today, aggregates are produced largely by the activities of organisms living in the water column (e.g. through filter feeding, faecal pellet production, test building) or random collisions between grains in the water column (McCave, 1985). The dense accumulations of pellets suggest these were originally hemipelagites deposited during quiescent periods.

If an average uncompacted thickness of 50 m (10 m compacted) for the SP and an age span of ca. 3 myr for the interval are taken, then a minimum average, long-term sedimentation rate of about 15 mm/kyr is realistic. We infer that this high sedimentation rate improved the chance of the fossils being buried, isolating them from the oxidizing environment at the seafloor. Given the lack of penetrative burrowing, it is likely that pore waters were already anoxic a few millimeters below the seafloor.

In modern pericontinental shelves, distance from shore is a good proxy for water depth. The SP pericontinental shelf was much wider than modern analogues (Fig. 3.7). Due to their distance from shore, distal, yet shallow-water deposits on wide shelves may have biological and geochemical characteristics indicative of deeper-water facies. On very wide shelves, with sufficiently low seafloor gradients, incoming waves dissipate their energy well before reaching the shore (Keulegan and Krumbein, 1949). This may explain why, despite the large fetch expected from the palaeogeographical setting of SP, the shallow seafloor would be little subjected to swell, thereby allowing mud deposition. The seafloor was also consolidated by mat-forming cyanobacteria shortly after deposition.

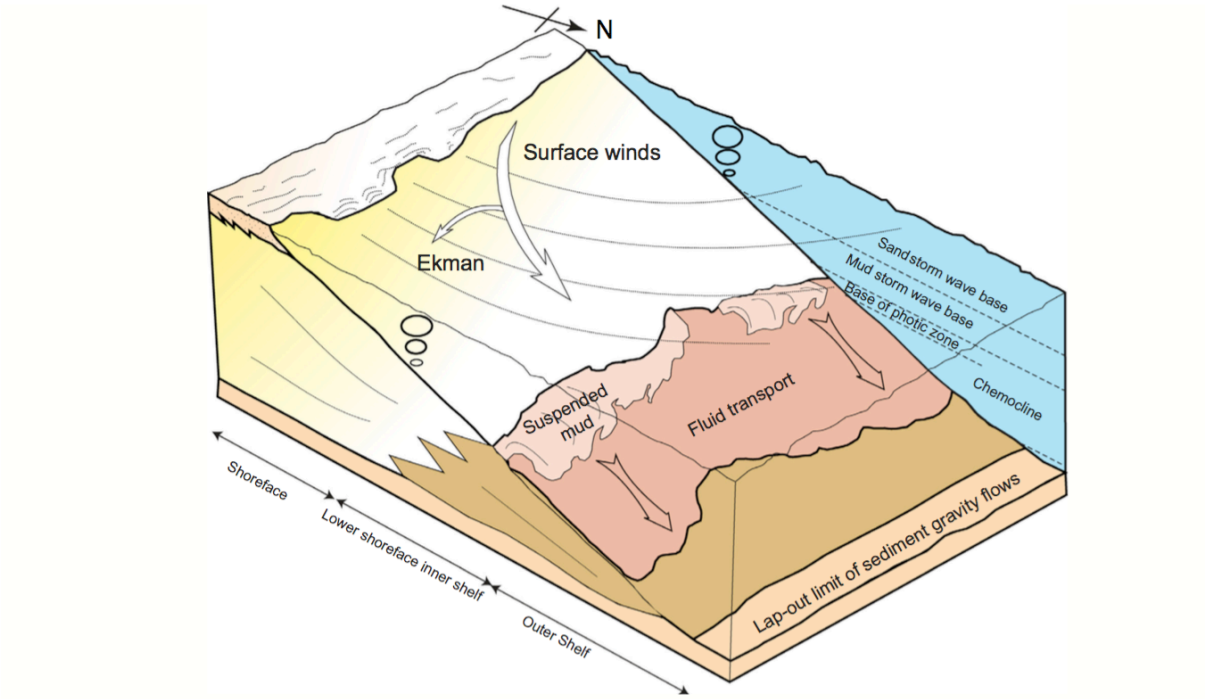


**Figure 3.7: Block diagram illustrating the depositional environment at Sirius Passet during the Early Cambrian (modified after Plint 2014).**

Similar storm influenced environments are proposed for the dark grey to black laminated mudstones of the Emu Bay Shale (Jago et al., 2012), the Alum (Thickpenny and Leggett, 1987), and Burgess Shales (Gabbott et al., 2008). In common with the SP these deposits also lack penetrative bioturbation suggesting anoxic conditions immediately below the seafloor. The presence of a diverse invertebrate benthos in the SP and an absence of pyrite framboids in the matrix indicate the lower water column was oxic with a sharp redox boundary at the sediment-water interface. Bioturbation is surficial and typically only occurs in association with generally large arthropod carcasses (Mangano et al., 2012). Benthic cyanobacteria were the dominant photoautotrophic and oxygenic microorganisms in the SP and could have produced or enhanced the oxygenated conditions at the seafloor. However, in extant cyanobacterial mats, sulphate reduction of the biomass can produce periodic hydrogen sulfide ($H_2S$) emissions above the mat surface, particularly at night (Jørgensen, 1979). This could have been a major factor impeding the settlement of benthic organisms on the seafloor. Either, the mat dwelling fauna was ephemeral and able to escape $H_2S$ emissions or had adapted a resistance to short-lived $H_2S$ toxicity. Occasional

massive $H_2S$ expulsion from the decaying mats might have led to mass mortalities of the mat dwelling community (see also Weeks et al., 2002).

Microbial mat textures observed on the concave external moulds, epirelief convex casts and evidence of microbial mat growing over trilobites (see Mangano et al., 2012, fig. 1) indicate that the fauna was an autochthonous matground community previously only known from trace fossil evidence (Buatois et al., 2014).

The dense cellular aggregates comprising the microbial textures are compared with colonies of modern coccoid cyanobacteria, particularly with the exclusively benthic *Entophysalis* or *Chlorogloea* (e.g. Kremer and Kazmierczak, 2005). The globular structures (Fig. 3.2E and Fig 3.5C) resemble the encapsulated aggregates of extant benthic coccoid cyanobacteria Pleurocapsales, particularly *Chroococcidiopsis* and *Stanieria* (Kremer and Kazmierczak, 2005; Komarek and Anagnostidis, 1986; Silva and Pienaar, 2000). Similar structures have been documented from the Athel Silicyte in the South Oman Salt Basin, Sultanate of Oman by Rajaibi et al., (2014) and provide evidence of microbially mediated syndepositional precipitation of silica. These genera are known from freshwater and marine environments, and some pleurocapsaleans are adapted to low light levels within the photic zone (Stal and Walsby, 2000). Similar material has been described from the Proterozoic (Gehling, 1999) and Silurian (Kremer and Kazmierczak, 2005). As cyanobacteria are a morphologically conservative group, SP specimens are probably part of the same groups.

We propose that the arthropod-lobopodian fauna that characterizes the Sirius Passet inhabited a warm, muddy, matground habitat close to or just below storm wave base, but within the photic zone. We have found no evidence for aeolian deposition of clay or silt in the field or in our thin sections, in contrast to the study by Boudec et al., (2014). Primary productivity was principally by benthic cyanobacteria. Contemporary shallow subtidal to intertidal carbonate environments had a distinct shelly fauna including archaeocyathans, halkieriids, tommotiids, hyoliths, molluscs, rare trilobites, and a variety of other small shelly

fossils of unknown affinity (examples cited in Mount and Signer, 1985). The rapid appearance in the geological record and ecological stability of the "Burgess Shale-type assemblages," over some 10 million years, suggest that rather than being long-lived holdovers, successively displaced from the shallow water (Mount and Signer, 1985; Morris, 2009), these animals were members of new Bambachian megaguilds (groups of organisms with mutually similar adaptive strategies), highly specialized and adapted to the dynamic and unstable nature of the tropical, muddy lower shoreface and shelf (Fig. 3.7).

The three dimensional preservation of cyanobacterial structure, the hyporelief external moulds and particularly the epirelief casts indicate the trilobite carapace remained intact long enough for the internal labile tissues to decompose and the body cavity to be injected with mat material. Dewatering and compaction occurs during early burial. Experimental and core studies indicate porosity in muds is reduced to 33-36% by 175m depth. Effective porosity (~70%) is lost by 1 km depth of burial (Hedberg, 1936). At the inferred sedimentation rates specimens that had not been permineralised would have been flattened to one third the original volume after 100 kyr-1myr. Thus providing sufficient time for early silicification and critically before the S-I transition between 1.8 to 3.7 km depth of burial. Major mineralogical changes with depth take place over the S-I transition (Hower, 1976). The most abundant mineral, illite/smectite, undergoes a conversion from less than 20% to about 80% percent illite layers over this interval, after which the proportion of illite layers remains constant. As the transition proceeds, illite packets grow within a shrinking matrix of smectite, dislocations decrease, and pathways for ion transport are restricted, this causes a loss of local permeability and a rise in the fluid pressure gradient. Consequent loss of hydraulic continuity with the surface and a more efficient geopressure, seals the clay to fluid flow (Freed and Peacor, 1989). In the S-I transition calcite decreases from about 20% percent of the rock to almost zero, disappearing from progressively larger size fractions with increasing depth; potassium feldspar (but not albite) decreases to zero; and chlorite appears to increase in amount. At these depths smectite reacts with $Al^{3+}$ and $K^{+}$ from the decomposition of potassium feldspar to form illite with the

release of $Si^{4+}$. Magnesium and iron lost from the smectite form chlorite and ultimately chloritoid. The stable clay mineral assemblage following the S-I transition is thus illite, quartz and chlorite. All the major mineralogical and chemical changes, as the response to burial and metamorphism, occurred in a closed system for all components except $H_2O$, CaO, $Na_2O$, and $CO_2$ (Hower et al., 1976). Reactions during the S-I transition therefore explain the absence of calcite in the SP. The remaining reactions into lower greenschist facies metamorphism include conversion of remaining smectite to illite (up to ~175°C) and the recrystallization of illite to micas (200-300°C: Totten and Blatt, 1993).

The timing of silicification is critical to understanding the taphonomic pathway. Silica supersaturation of pore fluids occurred due to the syn-sedimentary remobilisation of biogenic silica; from silica released during the S-I transition or during greenschist facies metamorphism. Our key evidence for silicification being early, shortly after death includes:

1. The 3D preservation of moulds and casts and cellular textures in the microbial mat material indicate silicification occurred before compaction and dewatering of the muds. The observation that 3D cells are filled with monocrystalline quartz preserved within the cyanobacterial mat material indicates that silica deposition prior to dewatering and compaction. Because the mat material is porous and the decay of labile cell contents occurred soon after death it is unlikely that internal cell fluid pressure would have supported the primary structures on burial. Alternately, decay gasses from decomposition may have formed cavities (Reineck and Singh, 1980) that prevented the collapse of the cells prior to silicification. A similar mechanism of mineral deposition in gas has been proposed for the formation of pyrite framboids in muds (e.g. Rickard, 1970) and silica infilling of *Tasmanite* cysts (Schieber, 1996). That and the fact that spherical gas bubbles are found close to the sediment surface has been documented by Forstner et al., (1968). Silica deposition is therefore most likely to have occurred very early in diagenesis and within centimeters to decimeters of the sediment-water interface. At the

proposed sedimentation rates for the SP this would have been equivalent to a few thousand years of deposition.

2) The presence of syn-sedimentary rip-up clasts.

3) Microbial mat and convex external moulds are formed of non-luminescent, textureless silica. Non-luminescing authigenic quartz lacks crystal lattice defects generated during metamorphism or volcanism (Seyedolali et al., 1997; Augustsson and Bahlburg, 2003; Frelinger et al., 2014).

4) Metamorphic quartz inclusions in the chloritoid needles exhibit strong luminosity with a smooth to mottled texture. This is distinctly different from the silica associated with the fossils.

5) The fact that chloritoid needles cross cut all other textures indicates metamorphism occurred after silicification.

The presence of very early diagenetic silica deposition, excludes a silica source during the S-I transition and during diagenetic to low-grade metamorphic recrystallization of illite to muscovite mica. Further, the early and largely biogenic porosity within the SP muds was filled by silica and not calcium carbonate (compare data from the Wheeler Formation: Gaines et al., 2005). That chalcedony appears to have been the initial silica phase deposited in the voids is not unusual, first documented by Folk and Weaver (1952) and subsequently in numerous other studies (e.g. Heath and Moberly, 1971; Meyers, 1977; Frondel, 1978; Milikem, 1979; Noble and Van Stempvoort, 1989). The presence of pyrite framboids in the mat material indicates sulphate reduction and that pyrite remained a stable phase through to greenschist facies metamorphism.

Decay experiments show that silica precipitates from low pH pore waters in extracellular and intracellular environments within a mat (Krauskopf, 1959), particularly when the pore fluids have reduced dissolved sulphate (Birnbaum and Wireman, 1985; Schultze-Lam et al., 1995). Soluble silica, in the form of monosilicic acid, $H_4SiO_4$, dissociates to $H_3SiO_4^-$ at pH values above ca. 9.7 (Birnbaum and Wireman, 1985; Arp et al., 2003). $H_3SiO_4^-$ is a highly soluble form of silicic acid, and it reacts with hydrogen ions to form $SiO_2$ (Rickert et al., 2002,

fig. 3). Silica nucleation and precipitation is sensitive to iron content of bottom/pore water and, in early Cambrian seawater, $Fe^{2+}$ appears to have been high relative to FeOOH (Muscente et al., 2014). We hypothesize that sediment water was saturated in silica, high in $Fe^{2+}$, and low in oxygen and sulphate. Localised pH reduction was associated with the decay-initiated silica nucleation and precipitation within the mat. Silica saturated pore waters could have been derived from the siliciclastic mud, by remobilisation of biogenic silica (e.g. sponge spicules), or from the overlying seawater.

Early silicification as a mechanism of exceptional preservation is rare outside volcanic hot springs and a number of hypotheses for silicification have been proposed: 1) direct precipitation into void spaces; 2) microbial mediated silica precipitation (Schultze-Lam et al., 1995; Yee et al., 2003) and, 3) chemically mediated silica precipitation (Patwardhan et al., 2011). It has been shown that microbial surfaces do not directly nucleate silica mineral formation however they play an important role in the aggregation of polymeric silica and the deposition of silica colloids on microbial surfaces (Patwardhan et al., 2011). For example in in modern hot spring environments, silica sinters actively form in close spatial relation to microorganisms (Yee et al., 2003 and references within). Decay compounds, proteins and amino acids are all known to affect the kinetics, surface area of material, pore structure and particle size and are therefore implicated in silicification (Perry and Keeling-Tucker, 2003). At present we cannot distinguish between the different mechanisms proposed for silicification and all may have been important.

Figure 3.8 shows our preferred taphonomic pathway. We propose that *Buenellus* was the dominant member of the matground community preserved in the SP. After death, the carapace was sealed by the growth of the microbial mat. During early burial internal labile tissues decayed, mat material was injected into the carcass to produce epirelief casts. The subsequent decay of the trilobite cuticle produced external moulds. All voids spaces were progressively infilled by silica as a consequence of localised pH reduction, associated with decay, occurred in the pore waters. Specimens were clearly permineralised, preserved in 3D,

before significant dewatering of the muds had taken place. Subsequent chemical reactions associated with the S-I transition and low greenschist facies metamorphism did not materially affect the preservation of the specimens.

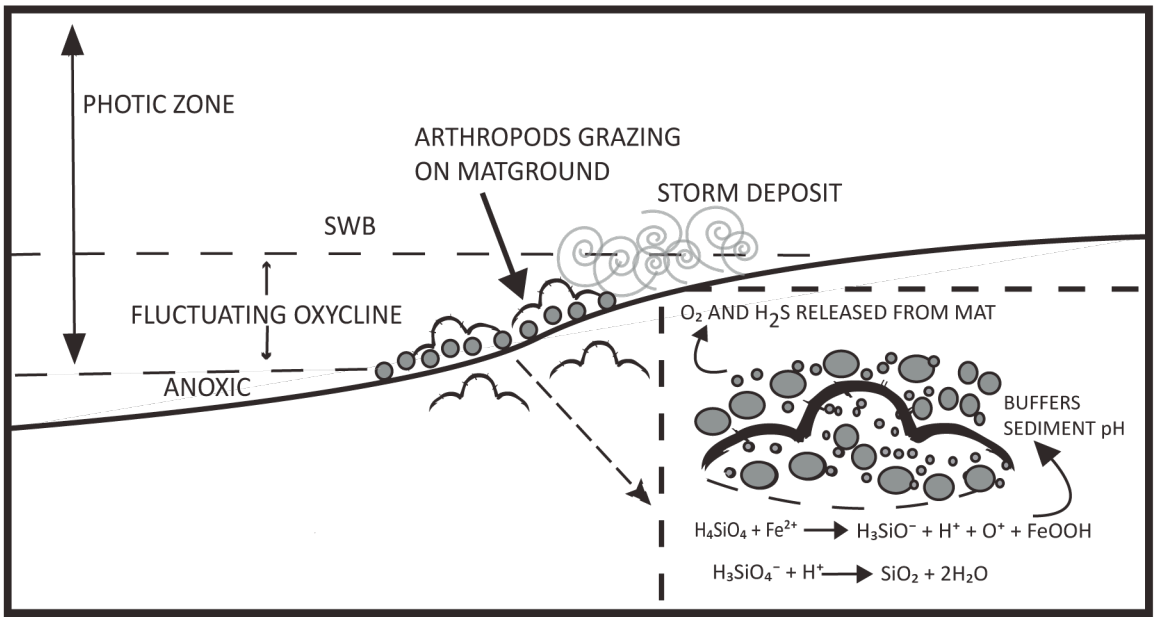


**Figure 3.8: Chemical pathways leading to the precipitation of silica and the reconstructed taphonomy of Buenellus.**

Similar "death mask" preservation has been described for the external moulds of soft-bodied Ediacaran biotas from the uppermost Proterozoic Rawnsley Quartzite, South Australia. Though, in this example the sole veneer resulted from bacterial precipitation of iron minerals (Gehling, 1999). A number of Cambrian Lagerstätten are characterized by pyritization of soft-bodied fossils, for example Chengjiang and Guanshan (Gabbott et al., 2004; Forchielli et al., 2014)), secondary coating by iron (e.g. Emu Bay: Brett et al., 2009), or phosphatisation (Zhu et al., 2014). Silica death mask preservation thus appears to be unique to the SP.

## 3.5 Conclusions

The arthropod-lobopdian fauna that characterizes the Sirius Passet inhabited a warm, muddy, matground habitat close to or just below storm wave base, but within the photic zone. Primary productivity was principally by benthic cyanobacteria. Trilobites from the SP are preserved as complete, concave hyporelief external moulds and convex epirelief casts. External moulds are shown to consist of a thin veneer of authigenic silica. The casts are silicified cyanobacterial mat material. Early silicification is supported by the presence of syn-sedimentary mat rip-up clasts, 3D preservation which indicates silicification prior to sediment compaction and textural and mono-CL evidence. The growth of metamorphic chloritoid needles, which cross cut the silica in the matrix, indicates metamorphism occurred much later. It is hypothesised that silicification was initiated by falling pH in the decaying mat. Pore waters are interpreted to have been initially alkali, silica saturated, high in ferric iron but low in oxygen and sulphate. Excess silica was likely derived from remobilised biogenic silica, probably sponge spicules in the muddy sediment. Decay resulted in a lowering of pore water pH and the conditions necessary for silicification. It is not clear whether silicification was microbially- or chemically mediated.

The remarkable preservation during very early silica mineralisation provides a new window on the environment and location of the Cambrian Explosion. The iconic organisms of the Cambrian Explosion formed the first mat ground communities. At least in the case of the SP the presence of cyanobacterial mats, sealing both the sediments and fossils was fundamental to the preservation of this community. With the rise of mat grazing organisms during the later Cambrian this taphonomic window disappeared.

## 3.6 References


Arp, G., Reimer, A., and Reitner, J., 2003, Microbialite formation in seawater of increased alkalinity, Satonda Crater Lake, Indonesia: Journal of Sedimentary Research, v. 73, p. 105–127.

Augustsson, C., and Bahlburg, H., 2003, Cathodoluminescence spectra of detrital quartz as provenance indicators for Paleozoic metasediments in southern Andean Patagonia: Journal of South American Earth Sciences, v. 16, p. 15–26.

Babcock, L.E., 2005, Interpretation of biological and environmental changes across the Neoproterozoic–Cambrian boundary: developing a refined understanding of the radiation and preservational record of early multicellular organisms: Palaeogeography, Palaeoclimatology, Palaeoecology, v. 220, p. 1–5.

Best, J., 2005, The fluid dynamics of river dunes: A review and some future research directions: Journal of Geophysical Research, v. 110, p. F04S02.

Birnbaum, S.J., and Wireman, J.W., 1985, Sulfate-reducing bacteria and silica solubility: a possible mechanism for evaporite diagenesis and silica precipitation in banded iron formations: Canadian Journal of Earth Sciences, v. 22, p. 1904–1909.

Boudec, A.L., Ineson, J., Rosing, M., Døssing, L., Martineau, F., Lécuyer, C., and Albarède, F., 2014, Geochemistry of the Cambrian Sirius Passet Lagerstätte, Northern Greenland: Geochemistry, Geophysics, Geosystems, v. 15, p. 886-904.

Brett, C.E., Allison, P.A., DeSantis, M.K., Liddell, W.D., and Kramer, A., 2009, Sequence stratigraphy, cyclic facies, and Lagerstätten in the Middle Cambrian Wheeler and Marjum Formations, Great Basin, Utah: Palaeogeography, Palaeoclimatology, Palaeoecology, v. 277, p. 9–33.

Buatois, L.A., Narbonne, G.M., Mángano, M.G., Carmona, N.B., and Myrow, P., 2014, Ediacaran matground ecology persisted into the earliest Cambrian: Nature communications, v.5, p. 3544-3549.

Butterfield, N.J., 1995, Secular distribution of Burgess-Shale-type preservation: Lethaia, v. 28, p. 1–13.

Butterfield, N.J., 1990, Organic preservation of non-mineralizing organisms and the taphonomy of the burgess Shale: Paleobiology, v. 16, p. 272-286.

Butterfield, N.J., 2003, Exceptional fossil preservation and the Cambrian explosion: Integrative and Comparative Biology, v. 43, p. 166–177.

Cocks, L.R.M., and Torsvik, T.H., 2011, The Palaeozoic geography of Laurentia and western Laurussia: a stable craton with mobile margins: Earth-Science Reviews, v. 106, p. 1-51.

Conway Morris, S., 2009, A Redescription of a Rare Chordate, Metaspriggina walcotti Simonetta and Insom, from the Burgess Shale (Middle Cambrian), British Columbia, Canada: Journal of Paleontology, v. 82, p. 424-430.

Craig, J., Fitches, W.R., and Maltman, A.J., 2009, Chlorite-mica stacks in low-strain rocks from central Wales: Geological Magazine, v. 119, p. 243-256.

Folk, R.L., and Weaver, C.E., 1952, A study of the texture and composition of chert: American Journal of Science, v. 250, p. 498-510.

Forchielli, A., Steiner, M., Kasbohm, J., Hu, S., and Keupp, H., 2014, Taphonomic traits of clay-hosted early Cambrian Burgess Shale-type fossil Lagerstätten

in South China: Palaeogeography, Palaeoclimatology, Palaeoecology, v. 398, p. 59–85.
Freed, R.L., and Peacor, D.R. 1989, Geopressured shale and sealing effect of smectite to illite transition: AAPG Bulletin, v. 73, p. 1223-1232.
Frelinger, S.N., Ledvina, M.D., Kyle, J.R., and Zhao, D., 2014, Scanning electron microscopy cathodoluminescence of quartz: Principles, techniques and applications in ore geology: Ore Geology Reviews, v. 65, p. 840–852.
Frondel, C., 1978, Characters of quartz fibers: American Mineralogist, v. 63, p. 17-27.
Gaines, R.R., and Droser, M.L., 2005, New approaches to understanding the mechanics of Burgess Shale-type deposits: From the micron scale to the global picture: The Sedimentary Record, v. 3, p. 4-8.
Gaines, R.R., Briggs, D.E.G., and Yuanlong, Z., 2008, Cambrian Burgess Shale–type deposits share a common mode of fossilization: Geology, v. 36, p. 755-758.
Gaines, R.R., Kennedy, M.J., and Droser, M.L., 2005, A new hypothesis for organic preservation of Burgess Shale taxa in the middle Cambrian Wheeler Formation, House Range, Utah: Palaeogeography, Palaeoclimatology, Palaeoecology, v. 220, p. 193-205.
Gabbott, S.E., Xian-Guang, H., Norry, M.J., and Siveter, D. J., 2004, Preservation of Early Cambrian animals of the Chengjiang biota: Geology, v. 32, p. 901-904.
Gabbott, S.E., Zalasiewicz, J., and Collins, D., 2008, Sedimentation of the Phyllopod Bed within the Cambrian Burgess Shale Formation of British Columbia: Journal of the Geological Society, v. 165, p. 307–318.
Gehling, J.G., 1999, Microbial Mats in Terminal Proterozoic Siliciclastics: Ediacaran Death Masks: PALAIOS, v. 14, p. 40-57.
Halferdahl, L.B., 1961, Chloritoid: its composition, X-ray and optical properties, stability, and occurance: Journal of Petrology, v. 2, p. 49-135.
Higgins, A.K., Leslie, A.G., and Smith, M.P., 2001, Neoproterozoic–Lower Palaeozoic stratigraphical relationships in the marginal thin-skinned thrust belt of the East Greenland Caledonides: comparisons with the foreland in Scotland: Geological Magazine, v. 138, p. 143–160.
Hower, J., Eslinger, E.V., Hower, M.E., and Perry, E. A., 1976, Mechanism of burial metamorphism of argillaceous sediment: 1. Mineralogical and chemical evidence: Geological Society of America Bulletin, v. 87, p. 725-737
Jago, J.B., Gehling, J.G., Paterson, J.R., and Brock, G.A., 2012, Cambrian stratigraphy and biostratigraphy of the Flinders Ranges and the north coast of Kangaroo Island, South Australia: Episodes Newsmagazine of the International Union of Geological Sciences, v. 35, p. 247–255.
Jørgensen, B., 1979, Diurnal cycle of oxygen and sulfide microgradients and microbial photosynthesis in a cyanobacterial mat sediment: Applied and Environmental Microbiology, v. 38, p. 46-58.
Keulegan, G.H., and Krumbein, W.C., 1949, Stable configuration of bottom slope in a shallow sea and its bearing on geological processes: Transactions, American Geophysical Union, v. 30, p. 855-861.
Komárek, J., and Anagnostidis, K., 1986, Modern approach to the classification system of cyanophytes. 2-Chroococcales: Archiv für Hydrobiologie Supplement, v. 73, p. 157–226.
Krauskopf, K.B., 1959, The Geochemistry of Silica in Sedimentary Environments: Special Publications of SEPM, v. 7, p. 4–12.

Kremer, B., and Kazmierczak, J., 2005, Cyanobacterial Mats from Silurian Black Radiolarian Cherts: Phototrophic Life at the Edge of Darkness?: Journal of Sedimentary Research, v. 75, p. 897–906.

Mángano, M.G., Bromley, R.G., Harper, D.A.T., Nielsen, A.T., Smith, M.P., and Vinther, J., 2012, Nonbiomineralized carapaces in Cambrian seafloor landscapes (Sirius Passet, Greenland): Opening a new window into early Phanerozoic benthic ecology: Geology, v. 40, no. 6, p. 519–522.

McCave, I.N., 1985, Recent shelf clastic sediments: Geological Society, London, Special Publications, v. 18, p. 49–65.

Meyers W.J., 1977, Chertification in the Mississippian Lake Valley Formation, Sacramento Mountains, New Mexico: Sedimentology, v. 24, p. 75-105.

Milliken K.L., 1979, The silicified evaporite syndrome--two aspects of silicification history of former evaporite nodules from southern Kentucky and northern Tennessee: Journal of Sedimentary Research, v. 49, p. 245-256

Mount, J.F., and Signer, P.W., 1985, Early Cambrian innovation in shallow subtidal environments: Paleoenvironments of Early Cambrian shelly fossils: Geology, v. 13, p. 730–733.

Muscente, A.D., Hawkins, A.D. and Xiao, S., 2014, Fossil preservation through phosphatization and silicification in the Ediacaran Doushantuo Formation (South China): a comparative synthesis: Palaeogeography, Palaeoclimatology, Palaeoecology, v. 434, p. 46-62.

Noble J.P.A., and Van Stempvoort, D.R., 1989, Early burial quartz authigenesis in Silurian platform carbonates, New Brunswick, Canada: Journal of Sedimentary Research, v. 59, p. 65-76

Orr, P.J., Briggs, D.E., and Kearns, S.L., 1998, Cambrian Burgess Shale animals replicated in clay minerals: Science, v. 281, p. 1173-1175.

Page, A., Gabbott, S.E., Wilby, P., and Zalasiewicz, J., 2008, Ubiquitous Burgess Shale-style “clay templates” in low-grade metamorphic mudrocks: Geology, v. 36, p. 855-858

Patwardhan, S.V., Tilburey, G.E., and Perry, C.C., 2011, Interactions of amines with silicon species in undersaturated solutions leads to dissolution and/or precipitation of silica: Langmuir, v. 27, p. 15135-15145

Perry C.C., and Keeling-Tucker, T., 2003, Model studies of colloidal silica precipitation using biosilica extracts from Equisetum telmateia: Colloid & Polymer Science, v. 281, p. 652-664

Plint, A., 2014, Mud dispersal across a Cretaceous prodelta: Storm-generated, wave-enhanced sediment gravity flows inferred from mudstone microtexture and microfacies: Sedimentology, v. 61, no. 3, p. 609–647.

Peel, J.S., and Ineson, J.R., 2011, The extent of the Sirius Passet Lagerstätte (early Cambrian) of North Greenland: Bulletin of Geosciences, p. 535–543.

Powell, W., 2003, Greenschist-facies metamorphism of the Burgess Shale and its implications for models of fossil: Canadian Journal of Earth Sciences, v. 40, p. 13–25.

Raiswell, R., and Berner, R.A., 1986, Pyrite and organic matter in Phanerozoic normal marine shales: Geochimica et Cosmochimica Acta, v. 50, p. 1967–1976.

Rajaibi, I.M., Hollis, C., and Macquaker, J.H., 2015, Origin and variability of a terminal Proterozoic primary silica precipitate, Athel Silicilyte, South Oman Salt Basin, Sultanate of Oman: Sedimentology, v. 62, p. 793–825.

Reineck, H.E., and Singh, I.B., 1980, Tidal flats: Depositional Sedimentary Environments, p. 430-456.
Rickard, D.T., 1970, The origin of framboids: Lithos, v. 3, p. 269-293.
Rickert, D., Schlüter, M., and Wallmann, K., 2002, Dissolution kinetics of biogenic silica from the water column to the sediments: Geochimica et Cosmochimica Acta, v. 66, p. 439–455.
Schieber, J., 1996, Early diagenetic silica deposition in algal cysts and spores: a source of sand in black shales?: Journal of Sedimentary Research, v. 66, p. 175-183.
Schieber, J., Krinsley, D., and Riciputi, L., 2000, Diagenetic origin of quartz silt in mudstones and implications for silica cycling: Nature, v. 406, p. 981-985.
Schultze-Lam, S., Ferris, F.G., Konhauser, K.O., and Wiese, R.G., 1995, In situ silicification of an Icelandic hot spring microbial mat: implications for microfossil formation: Canadian Journal of Earth Sciences, v. 32, p. 2021–2026.
Seyedolali, A., Krinsley, D., and Boggs, S., 1997, Provenance interpretation of quartz by scanning electron microscope–cathodoluminescence fabric analysis: Geology, v. 25, p. 787–790.
Silva. S.M., and Pienaar, R.N., 2000, Benthic marine Cyanophyceae from Kwa-Zula Natal, South Africa: Gebruder Borntraeger Verlagsbuchland Lung, p. 456.
Stal, L.J., and Walsby, A.E., 2000, Photosyenthesis and nitrogen fixation in a cyanobacterial bloom in the Baltic Sea: European Journal of Phycology, v. 35, p. 97-108.
Thickpenny, A., and Leggett, J.K., 1987, Stratigraphic distribution and palaeo-oceanographic significance of European early Palaeozoic organic-rich sediments: Geological Society, London, Special Publications, v. 26, p. 231–247.
Totten M.W., and Blatt, H., 1993, Alterations in the non-clay-mineral fraction of pelitic rocks across the diagenetic to low-grade metamorphic transition, Ouachita Mountains, Oklahoma and Arkansas: Journal of Sedimentary Research, v. 63, p. 899-908
Towe, K.M., 1996, Fossil preservation in the Burgess Shale: Lethaia, v. 29, p. 107-108.
Weeks, S.J., Currie, B., and Bakun, A., 2002, Massive emissions of toxic gas in the Atlantic: Nature, v. 415, p. 493–494.
Whittington, H.B., 1980, The significance of the fauna of the Burgess Shale, Middle Cambrian, British Columbia: Proceedings of the Geologists' Association, v. 91, p. 127-148.
Yee N., Phoenix, V.R., Konhauser, K.O., Benning, L.G.. and Ferris, F.G., 2003, The effect of cyanobacteria on silica precipitation at neutral pH: implications for bacterial silicification in geothermal hot springs: Chemical Geology, v. 199, p. 83-90.
Zhu, M., Babcock, L., and Peng, S., 2006, Advances in Cambrian stratigraphy and paleontology: integrating correlation techniques, paleobiology, taphonomy and paleoenvironmental reconstruction: Paleoworld, v. 15, p. 217-222.
Zhu, X., Lerosey-Aubril, R., and Esteve, J., 2014, Gut content fossilization and evidence for detritus feeding habits in an enrolled trilobite from the Cambrian of China: Lethaia, v. 47, p. 66–76.

# Chapter 4. Minerals in the gut: Scoping a Cambrian digestive system – A detailed study on the three-dimensionally preserved guts of *Campanamuta mantonae*

## 4.1 Abstract

In this chapter we look at another common mode of preservation present in the Sirius Passet Lagerstätte, the presence of three-dimensional axial traces, including gut tracts, diverticulae and muscle tissue. A version of this chapter is published in *Royal Society Open Science* (Appendix III). Three-dimensionally preserved gut tracts are a key preservation style which typifies the SP, therefore critical to our understanding of the overall taphonomy of the Lagerstätte. We use SEM, SEM-CL and optical microscopy to look at the non-mineralized arthropod *Campanamuta mantonae,* which exhibits exceptional preservation of gut tracts and muscle tissue. The detailed methodology is outlined in chapter 1, section 1.6. The Sirius Passet Lagerstätte of North Greenland contains the first exceptionally preserved mat-ground community of the Cambrian, dominated, in terms of abundance, by trilobites but particularly characterized by iconic arthropods and lobopods, some also occurring in the Burgess shale. High-resolution photography, scanning electron imaging and elemental mapping have been carried out on a variety of specimens of the non-mineralized arthropod *Campanamuta mantonae* (Budd, 2011) which has three-dimensional gut and muscle preservation. Results show that the guts contain a high concentration of calcium phosphate (approximating to the mineral francolite), whereas the adjacent muscles are silicified. This indicates a unique, tissue-specific taphonomy for this Cambrian taxon. We hypothesize that the precipitation of calcium phosphate in the guts occurs rapidly after death by 'crystal seed' processes in suboxic, slightly acidic conditions; critically, the gut wall remained intact during precipitation. We postulate that the calcium phosphate was derived from ingested cellular material. Silicification of the muscles followed as the localized water chemistry became saturated in silica, high in $Fe^{2+}$, and low in oxygen and sulfate. We document here the unique occurrence of two distinct but mechanistically similar taphonomic pathways within a diverse suite of possibilities in an Early Cambrian Lagerstätte.

## 4.2 Introduction

The fossil record offers us invaluable insights into important intervals in the history of life. The record is however generally biased by poor preservation, and even in exceptionally preserved specimens from fossil Lagerstätten, there is potential for key traits to be removed by decay. Sites that can be demonstrated to have very early, soft tissue preservation not only provide insights into taphonomic processes, but are also critical for reconstructing ancient communities and phylogenies (Sansom et al., 2010). This becomes particularly important when considering the very earliest radiations of bilaterian animals during the Cambrian explosion and hypotheses of likely ancestors in the Ediacara biota. A list of elements of the Sirius Passet (SP) fauna is provided by Peel & Ineson (2011).

The Lower Cambrian black shales of SP, North Greenland preserve the oldest known examples of soft-bodied fossils from the Cambrian explosion together with more typical Cambrian skeletal animals. These include trilobites, other arthropods, lobopods, halkieriids and sponges (Conway Morris and Peel, 2008). The fauna is broadly similar to that found in the younger Burgess shale (Smith and Harper, 2013). The SP is located in J. P. Koch Fjord, N. Greenland, at 82°47.6′ N, 42°13.7′ W and during the Cambrian lay at approximately 10° S (Peel and Ineson, 2011). The locality was included in the 'transitional' Buen, and the fauna represents the earliest Cambrian community with exceptional preservation together with evidence for microbial mats, predating the Burgess shale by 10 Myr (Peel and Ineson, 2011). *Buenellus higginsi* is the most common macrofossil, indicative of the Laurentian Atdabanian/Botomian boundary, at the top of stage 3 to the base of stage 4, occurring between 511 and 521 Myr. However, precise correlation of the unit remains a subject of debate. The detailed petrography, mineralogy and metamorphic history were described by Strang et al. (2016) and these properties are only outlined here. The shales are a poorly sorted mix largely consisting of quartz (60–65%), clay minerals, chloritoid porphyroblasts (indicating low P/T greenschist facies metamorphism) and silicified microbial

mat material. A detailed description of the depositional environment, dating and metamorphic history has recently been presented (Strang et al., 2016).

The SP exhibits a diversity of taphonomic pathways; for example, the trilobites from the SP are preserved as complete, concave hyporelief external moulds and convex epirelief casts. External moulds are shown to consist of a thin veneer of authigenic silica. The casts are composed of silicified cyanobacterial mat material. Early silicification is supported by the presence of synsedimentary mat rip-up clasts, three-dimensional preservation, which indicates silicification prior to sediment compaction and textural and mono-CL evidence. The growth of metamorphic chloritoid needles, which crosscut the silica in the matrix, indicates that metamorphism occurred much later. Silicification was initiated by falling pH in the decaying mat. Pore waters are interpreted to have been initially alkali, silica-saturated, high in ferric iron but low in oxygen and sulfate. Excess silica was likely derived from remobilized biogenic silica, probably sponge spicules in the muddy sediment. It is not clear whether silicification was microbially or chemically mediated. The presence of cyanobacterial mats, sealing both the sediments and fossils was however fundamental to the preservation of this community.

*Campanamuta mantonae* (Budd, 2011) is also a common arthropod in the SP fauna and is non-mineralized. Approximately 1700 specimens have been reported to date (Budd, 2011). Specimens are flattened but preserve three-dimensional axial traces, including gut tracts, diverticulae and muscle tissue (Budd, 2011). The parts and counterparts often show different anatomical details in the axial region and sometimes exhibit cavities (Budd, 2011). Distinguishing whether these cavities are the original anatomical features of the organism or are voids left by the later decay of soft parts or minerals is hard to determine. Budd (2011) argued that the fossils are mostly (or completely) replacements of the original tissues, rather than preserved as moulds (Budd, 2011). In this chapter, we describe the taphonomy of these specimens and propose a taphonomic model for elements of the SP that enhances in some respects closer comparison with Lagerstätten from the Neoproterozoic than

those from the Late Cambrian. The preservation of gut contents also allows for an interpretation of the mode of life of *C. mantonae*.

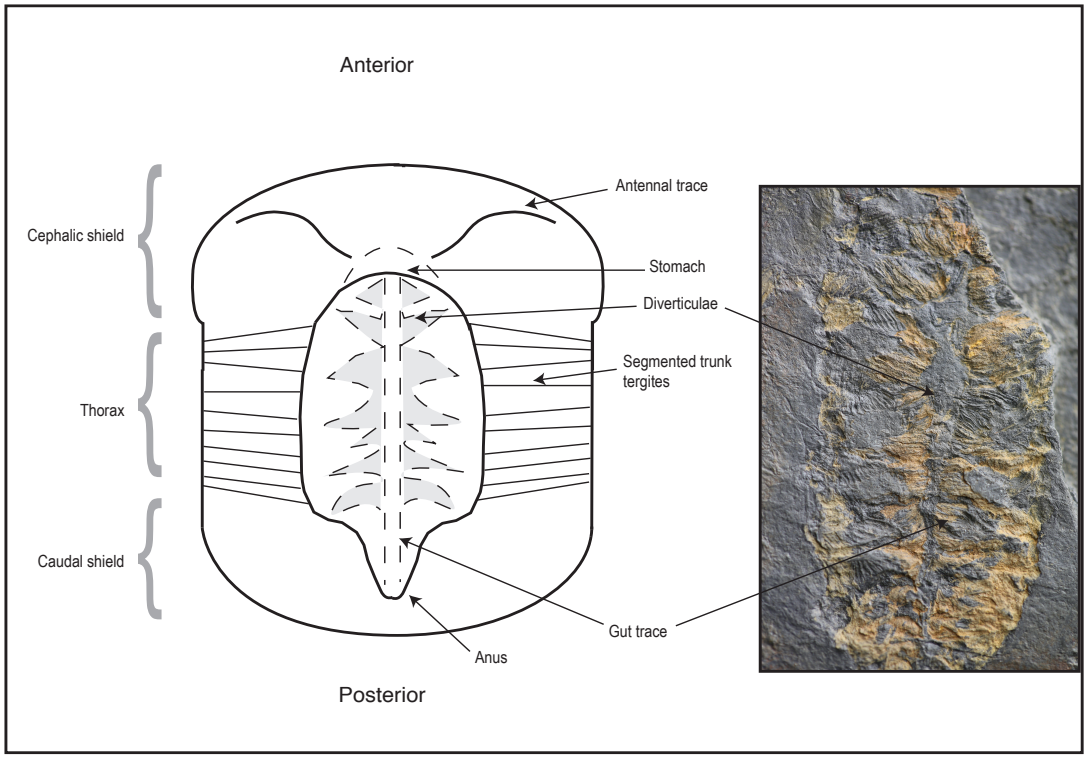


**Figure 4.1: Diagram shows the main features, appendages and internal anatomy of *Campanamuta mantonae.* Photo inlay is a specimen of *C. mantonae* (MGUH 31567) that shows the gut tract and diverticulae which are most readily preserved. Specimen is 2 cm wide.**

## 4.3 Specimens

The numbered specimens (MGUH 31567–31572) including thin sections are reposited in the Natural History Museum of Denmark (Geological Museum), University of Copenhagen. Budd (2011) described the anatomy of *C. mantonae* in considerable detail. It is a relatively large arthropod (mean length approx. 65 mm and width 35 mm) comprising three segments, with a smooth exoskeleton and a semicircular cephalic shield. The main morphological features are illustrated in figure 4.1. The external morphology is not well preserved. The only preserved internal anatomy is situated in the axial region and consists of the main digestive structures (Fig. 4.1). In rare specimens, the outline of the stomach

can be identified, situated anteriorly in the cephalon. The gut tract extends posteriorly where it terminates at the anus. The triangular diverticulae are paired not only on either side of the gut, but also extend down towards the anus (Fig. 4.1).

## 4.4 Results

In specimens with digestive structures preserved, usually there is only limited preservation of the outer appendages. The area of the specimens outside the axial region is visible as a thin, dark film of silica. When preserved, bundles of muscle fibres adjacent to the digestive tract are yellow in colour and have three-dimensional relief. The muscle fibres track transversely and outwards from beside the diverticulae towards the thoracic tergites (Fig. 4.1) and exhibit well-preserved, oblique, micrometre-scale striations (figure 4.3A). The gut of *C. mantonae* is a broad tube-like structure, which runs down the central axis, terminating at the anus (see also [Budd, 2011 fig. 1]). In the cephalic region (Fig. 4.1), the digestive tract consists of a sclerotized oesophagus which leads into the stomach, situated behind the head. The diverticulae are segmented and paired and open out from the gut (Budd, 2011: fig. 1). The anus is clearly defined by a ring of plates (Budd, 2011: fig. 5*a*,*b*).

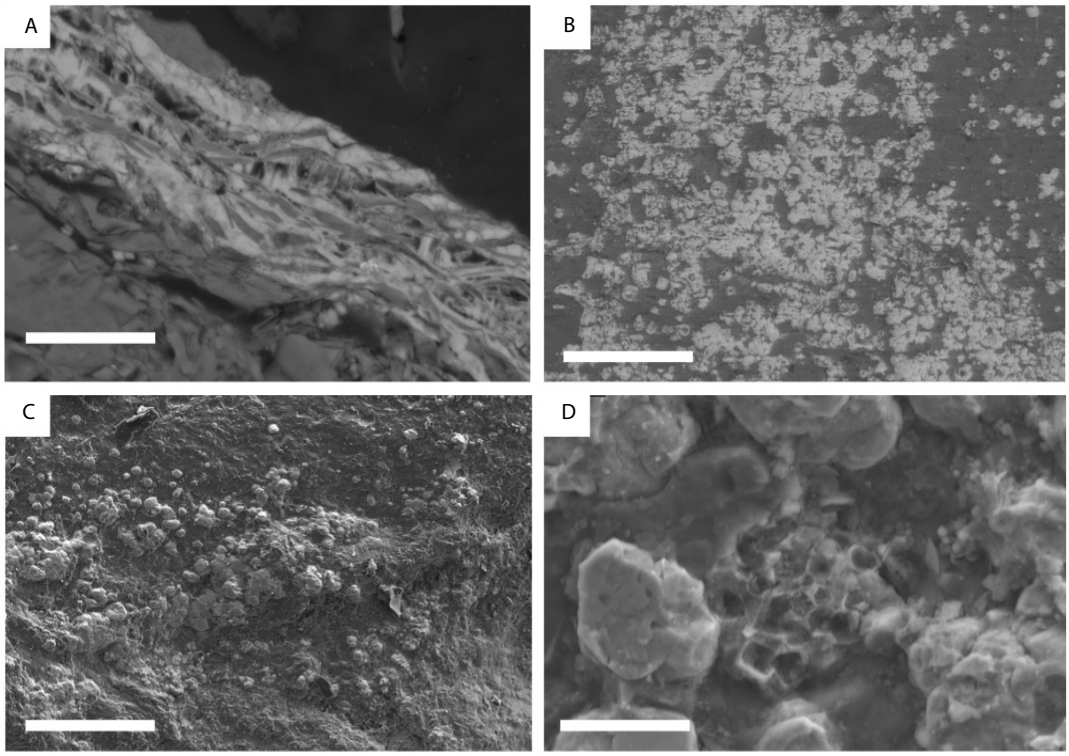


**Figure 4.2: SEM and BSE images of the phosphate contained in the gut of *C. mantonae.* A. SEM image of a cross section taken through a sample of *C. mantonae* (MGUH 31568), light grey material is phosphatised. Small pyrite framboids can be seen. Scale bar, 50 µm. B. BSE image showing spherical texture of phosphate nodules in sample MGUH 31569. Scale bar, 100 µm. C. Higher magnification SEM image shows spherical phosphate interpreted as possible microbial moulds. Scale**

**bar, 20 µm (MGUH 31569). D. High-resolution SEM image showing a pyrite framboid within the phosphate clusters. Scale bar, 10 µm (MGUH 31569).**

Three-dimensional gut traces contain high concentrations of calcium phosphate ($Ca_3(PO_4)_2$; table 4.1) approximating to the mineral francolite. There are some traces of Si, Al and Fe but these are very minor and probably derived from the matrix. Phosphatization extends along the entire gut tract to the anus. The phosphatized areas have a sponge-like texture composed of small (less than 5 µm in diameter) spheres (Fig. 4.2B-C) organized into layers (Fig. 4.2A). The layers commonly contain small (less than 10 µm) pyrite framboids. There is no visible evidence for preserved biological material or sediment grains. In thin section, the boundary between the gut trace and the sediment below is sharp; there is no evidence in either hand specimen or thin section of preserved cuticle.

Table 4.1: EDAX data for phosphatized regions in sample SP0511. Data given in %.

| Spectrum | Al | Si | P | K | Ca | Fe | O | Total |
|---|---|---|---|---|---|---|---|---|
| Spectrum 1 | 0.44 | 0.69 | 18.36 | 0.00 | 38.53 | 1.34 | 40.65 | 100.00 |
| Spectrum 2 | 2.68 | 4.89 | 11.00 | 0.00 | 37.65 | 5.13 | 38.65 | 100.00 |
| Spectrum 3 | 0.00 | 0.00 | 18.60 | 0.00 | 41.01 | 0.00 | 40.39 | 100.00 |
| Spectrum 4 | 0.67 | 1.42 | 19.67 | 0.00 | 36.18 | 0.00 | 42.06 | 100.00 |
| Spectrum 5 | 0.56 | 0.59 | 19.05 | 0.50 | 36.26 | 2.19 | 40.94 | 100.00 |

EDAX data confirm that muscle fibres are composed of finely microcrystalline silica (table 4.2) with very minute traces of Mg, possibly derived from the surrounding matrix. The preservation of these is relatively unvaried and forms distinct aligned blocks of muscle fibres, arranged *in situ*. The outer surfaces have a spherulitic texture at the micrometre scale (Fig. 4.3A). An approximately 5µm thick layer of silica occurs at the edges of the phosphatized region (Fig. 4.2A). SEM-CL indicates the silica has very low luminosity with no distinct colour under both monochromatic filter and RGB filters (Fig. 4.3D).

Table 4.2: EDAX data for silicified regions in sample SP0511. Data given in %.

| Spectrum | Al | Si | P | K | Ca | Fe | O | Total |
|---|---|---|---|---|---|---|---|---|
| Spectrum 1 | 0.32 | 45.80 | 0.00 | 0.00 | 0.00 | 1.11 | 52.78 | 100.00 |
| Spectrum 2 | 0.00 | 46.74 | 0.00 | 0.00 | 0.00 | 1.00 | 52.86 | 100.00 |
| Spectrum 3 | 0.00 | 46.74 | 0.00 | 0.00 | 0.00 | 0.00 | 53.26 | 100.00 |
| Spectrum 4 | 0.00 | 45.76 | 0.00 | 0.00 | 0.00 | 0.00 | 52.68 | 100.00 |
| Spectrum 5 | 2.80 | 43.12 | 0.00 | 0.64 | 0.00 | 1.32 | 52.12 | 100.00 |

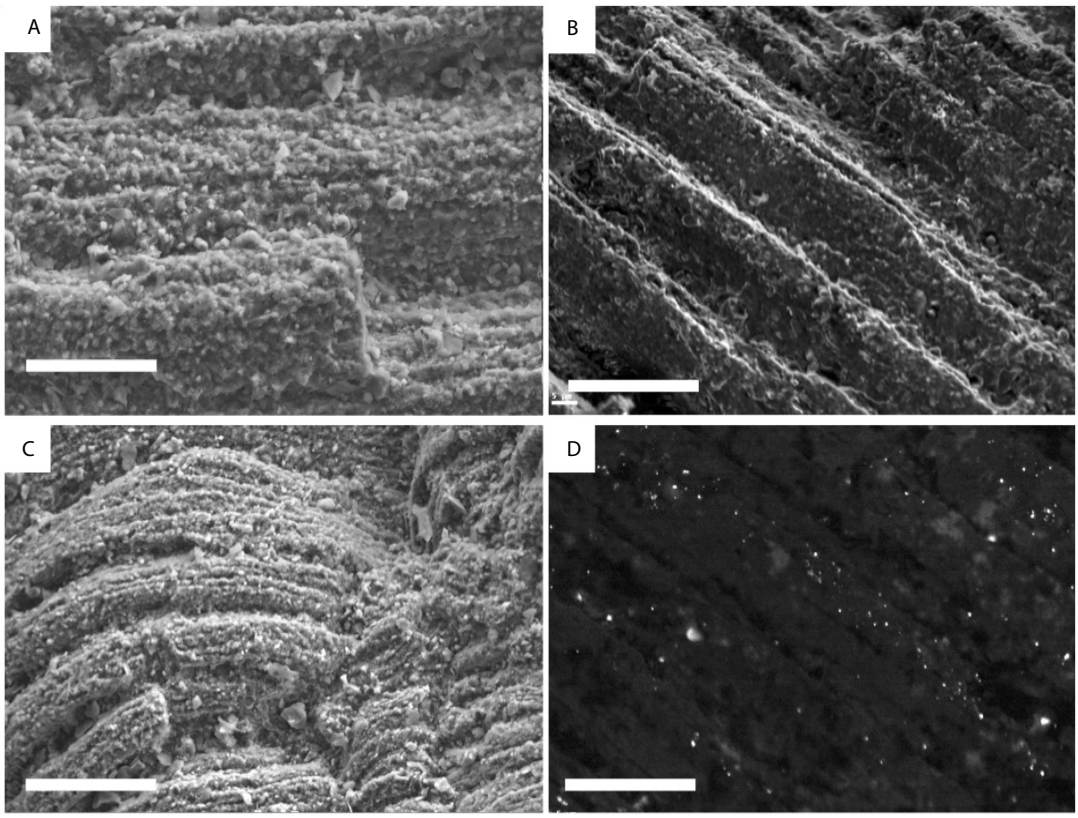


**Figure 4.3: SEM, BSE and SEM-CL images of the silicified muscle tissue. A. BSE image shows silicified muscle tissue. Scale bar, 20 µm (MGUH 31568). B. SEM image of muscle tissue shows fibrous nature and small spherical nodules of silica. Scale bar, 20 µm (MGUH 31570). C. BSE image showing truncated silicified muscle tissue. Scale bar, 20 µm (MGUH 31571). D. SEM-CL image showing low monotone grey luminosity of the silica in the muscles, indicating similar formation conditions as that found in *Buenellus* (Strang et al., 2016) (MGUH 31572).**

## 4.5 Discussion

The key drivers of decay are autolysis and microbial activity, and the latter is a key mediator in autogenic mineralization of soft tissues (Butler et al., 2015). Microbial communities have the highest surface area to volume ratio of any group of living organisms and this combined with the abundance of charged chemicals and molecules on their surface makes them ideal environments for mineral nucleation and precipitation (Douglas and Beveridge, 1998). The gut traces in *C. mantonae* are preserved almost exclusively as francolite. The preservation of the three-dimensional structure indicates early mineralization prior to the compaction/collapse of the gut. Three-dimensional preservation of the gut is also commonly observed in a variety of taxa from Cambrian (and younger) Lagerstätten, indicating the gut is the most readily preserved internal structure. Examples include the Burgess shale arthropod *Leanchoilia, Odaria, Canadaspis, Perspicaris, Sidneyia, Anomalocaris* and *Opabinia* which all possess phosphatized midgut structures in their axial region (Butterfield, 2002; Lin and Briggs, 2010) *Myoscolex*, an Early Cambrian arthropod from the Emu Bay shale, is described as having only its trunk muscles phosphatized, which is in stark contrast to the preservation in the SP (Briggs and Nedin, 1997). Phosphatized muscles are also found associated with hard parts in the Mesozoic, such as the muscle tissue in the horseshoe crab *Mesolimulus* (Briggs et al., 2005) and preservation of muscles in phosphate from the Konservat-Lagerstätten in Lebanon (Wilson et al., 2016).

The close proximity of distinct tissues with distinct taphonomies is extremely unusual. Experimental decay studies of modern brine shrimp *Artemia* indicate chemistry of the gut contents and the presence of endogenous bacteria are the key factors in creating a unique microenvironment in which the gut is preserved (Butler et al., 2015). The nature of the preservation of the surrounding tissues is dependent on whether the gut wall remains intact. If the gut ruptures, the endogenous microbes leak into the body cavity where they control the tissue preservation through mineral templating (Butler et al., 2015). In the *C. mantonae* specimens from the SP, only the gut is phosphatized, and the remaining axial tissues and structures are preserved as silica replacement. This would indicate

the gut wall remained intact and that endogenous bacteria remained within the gut and were responsible for the preservation of the gut.

Phosphatization and silicification occur under markedly different environmental and chemical conditions (Muscente et al., 2014). Phosphatization is widely recognized in the preservation of soft tissues (Douglas and Beveridge, 1998; Wilby et al., 1996). There are two sources of phosphate: (i) from the breakdown of organic matter during bacterial sulfate reduction and (ii) phosphate can also be released from absorption sites on ferric oxyhydroxide, during reduction of the iron ($Fe^{3+}$ > $Fe^{2+}$ (Krom and Berner, 1980). Phosphatization occurs predominantly in a suboxic environment within the upper few centimetres of the sediment (Jahnke et al., 1983), at lowered pH induced by decaying organic matter and with sufficient time under these conditions, free from scavengers (Wilby et al., 1996; Lerosey-Aubril et al., 2012).

Decay experiments have shown that the digestive and other internal organs of marine arthropods are particularly prone to rapid decay (2–3 days) and liquidation under open, aerobic conditions at room temperature (Butler et al., 2015; Hof and Briggs, 1997). Butler et al., (2015) also showed that the carcass of the brine shrimp was rapidly consumed (2–3 days) by endogeneous, gut-derived microbes and pervasive phosphatization of the internal tissues occurred following the rupture of the gut wall. Decay rarely lasts longer than one month (Fatka et al., 2015). By inference, the three-dimensional preservation of the guts in the *C. mantonae* specimens must have started very early after the death of the organism when the gut wall remained. The precipitation of calcium phosphate is favoured over calcium carbonate under slightly acidic marine conditions (Lerosey-Aubril et al., 2012).

Both sulfide-oxidizing bacteria (SOB) and sulfate-reducing bacteria (SRB) have been implicated in the precipitation of phosphate in the marine environment (Briggs and Nedin, 1997; Briggs et al., 2005; Briggs, 2003, Wilby and Briggs, 1997). SOB are able to store polyphosphate under oxic conditions, this polyphosphate being used as an additional energy source (Schulz and Schulz et al., 2005). Examples of SOB include *Thioploca, Beggiatoa* and *Thiomargarita,* and

these taxa are major components in the benthic sulfur cycle, where they reoxidize sulfide (Arning et al., (2009) and references therein). SRB facilitate phosphate precipitation by increasing the phosphate concentrations in pore waters through the decay of organic matter. Degradation of organic matter by SRB is a predominantly anaerobic process, where supersaturation with respect to phosphate is commonly reached (Arning et al., 2009). The presence of pyrite framboids within the phosphate supports the role of SRB in the release of $PO_4^-$ from the organic gut contents, from either ingested seawater or iron- rich sediment (see also Butterfield, (2002)). We have no evidence from imaging for the presence of sediment particles within the gut material and conclude the phosphate was derived from ingested organic material. Furthermore, the absence of phosphate in the rock matrix also suggests it came from an internal source.

The molecular initiation and aggregation of silica plays a major role in biosilicification and the presence of proteinaceous material resulting from decay (Belton et al., 2004). In microbially mediated silica precipitation, it has been shown that microbial surfaces do not directly nucleate silica mineral formation; however, they play an important role in the aggregation of polymeric silica and the deposition of silica colloids on microbial surfaces, for example in modern hot spring environments, silica sinters actively form in close spatial relation to microorganisms (Yee et al., (2003) and references within). In the former, direct precipitation of silica into void spaces is the likely scenario in the SP (Strang et al., 2016). Sedimentary factors that control silicification are the permeability of sediment, silica availability (both in the pore waters and sediment) and the concentration of organic matter (Butts, 2014 and references therein; Akahane et al., 2004). Silica-rich pore waters were likely derived from remobilization of biogenic silica from sponge spicules (Strang et al., 2016). Soluble silica, in the form of monosilicic acid, $H_4SiO_4$, dissociates to $H_3SiO_4^-$ at pH values above *ca* 9.7 (Birnbaum and Wireman, 1985; Arp et al., 2003). $H_3SiO^-$ is a highly soluble form of silicic acid, and it reacts with hydrogen ions to form $SiO_2$ (Rickert et al., 2002: fig. 3).

Silica precipitation is sensitive to the iron content of bottom/pore waters and in Early Cambrian seawater and $Fe^{2+}$ appears to be high relative to FeOOH (Muscente et al., 2014). Unlike the trilobite specimens, silicification in the non-mineralized *C. mantonae* is restricted to the muscles. Muscle tissue in modern arthropods is composed of actin and myosin (Neville, 2012) and it is likely that muscle tissue in extinct arthropods had a similar composition. While the involvement of microbes in silica precipitation cannot be directly excluded, more extensive mineralization of all the tissues might be expected. Alternatively, the arrangement of muscles into micrometre-scale fibres provides an excellent substrate for silica precipitation, as it creates a large surface area comprising the reactive proteinaceous and amino acids necessary for initial silica aggregation (Butts, 2014). Three-dimensionally preserved internal organs have also been documented from the Burgess shale in the Stephen formation (Cambrian) (Butterfield, 2002) annelids from the Cretaceous Konservat- Lagerstätten of Hakel and Hjoula, Lebanon (Wilson et al., 2016), the Guizhou Province in South China (see (Lin and Briggs, 2010; Lin, 2006)) and are also associated with flattened hard parts, interpreted as a result of syndiagenetic microbial decay.

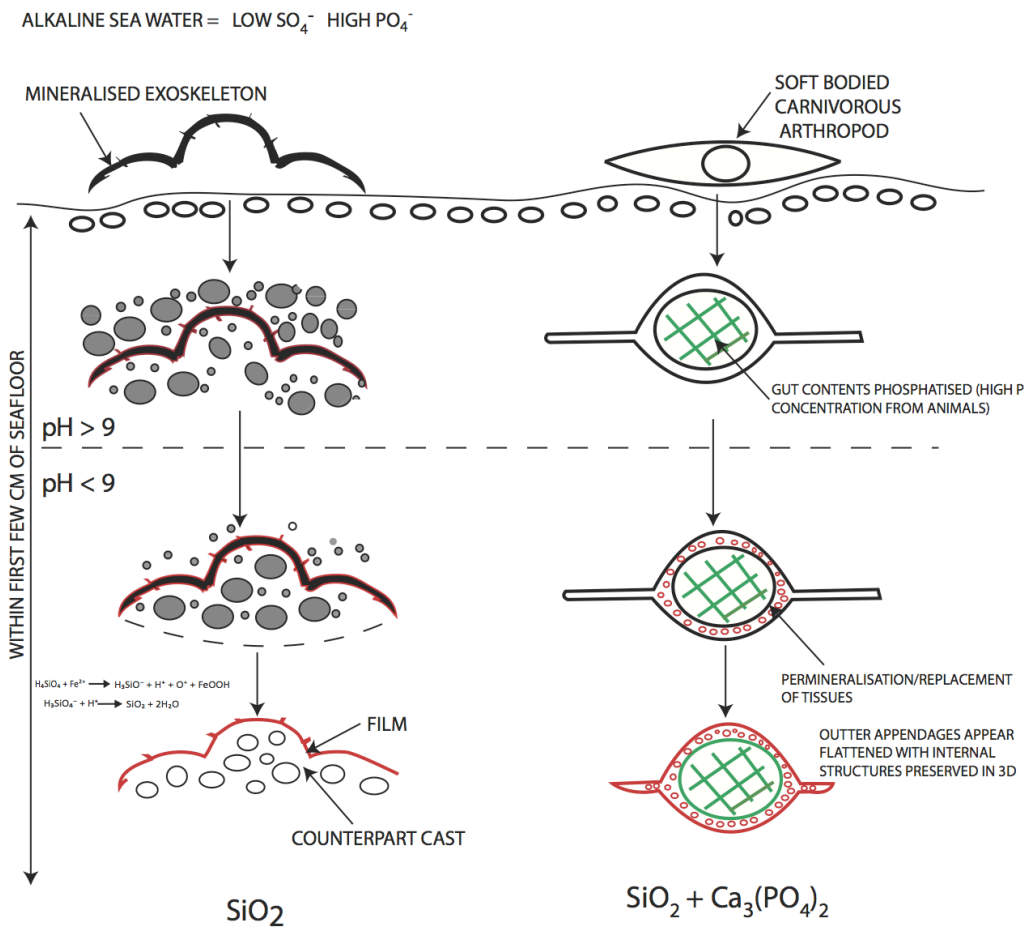


**Figure 4.4: Schematic model shows the preferred taphonomic pathway of non-mineralizing *C. mantonae* (right) compared with that of mineralizing *Buenellus* (left).**

## 4.6 Taphonomic pathway

Figure 4.4 shows the proposed taphonomic pathway and compares this to that proposed for the mineralized trilobite *Buenellus*. The precipitation of two distinct mineral phases in the gut and axial muscle fibres of *C. mantonae* indicates the formation in different and isolated microenvironments along a redox gradient. Phosphatization of the gut contents occurred in slightly acidic, suboxic conditions, under the control of endogenous SRB, within days of death and therefore at the seafloor. The three-dimensional preservation indicates of the gut trace was fully permineralized before specimen collapse during decay, burial and

sedimentary compaction. Silicification of the adjacent muscle fibres occurred in the presence of silica-saturated pore waters with a pH around 9.7 within the microbial mat.

The relative timing of these two processes is not easily constrained. That both tissues are preserved in three dimensions suggests both were mineralized early during decay. Postmortem sealing of the specimens by cyanobacterial mats has been hypothesized as a mechanism for rapid sealing of the specimens from decay and predation, resulting in a localized pH environment suitable for controlling the silicification of the mineralized trilobites in the SP (Strang et al., 2016). It is possible that silicification was initiated once the specimens became entombed in the decaying microbial mat and this would have provided the necessary conditions for decay-related reduction in pH > 7 (Brinbaum and Wireman, 1985; Strang et al., 2016).

### 4.7 Gut morphology and ecological implications

Well-preserved digestive systems in Cambrian arthropods display a variety of biserial midgut glands, from simple bunch-like or lobe-like digestive glands to complex branching features (Vannier et al., 2014). This suggests that, like their modern relatives, these arthropods ingested phosphate from their food sources (Vannier et al., 2014). *C. mantonae* possessed a relatively complex gut consisting of a tube-like structure which runs down the central axis of the animal (Fig. 4.1) (Budd, 2011, fig. 5*a,b*). Paired leaf-like diverticulae are attached to the midgut and provide evidence that *C. mantonae* would have been able to process and digest more complex food sources, such as smaller arthropods. In living branchiurans, the diverticulae are used to store food prior to enzymatic breakdown and the absorption of nutrients in a rich but infrequent diet (Butterfield, 2002; Vannier, 2014). The evolution of more complex guts with digestive glands work by allowing the animal to increase the efficiency of food processing by increasing the surface area between nutrients and epithelial tissues, thus allowing larger particles to be consumed which, in turn, would have enabled them to uphold the energy demands of a more active and predatory

lifestyle (Vannier et al., 2014). The ability to process larger food particles would have been clearly advantageous for active Cambrian arthropods. Unlike their modern counterparts, early Cambrian arthropods do not possess a large array of differentiated appendages used for capturing and breaking up prey (Vannier et al., 2014). *C. mantonae* only appears to have possessed long, slender antennae (Budd, 2011) (Fig. 4.1) which would have acquired a sensory function. The antennae only protruded a short distance from the anterior shield margin, as most of their length is hidden under the shield (Budd, 2011). Protection by the shield may be the reason for antennae being the most readily preserved appendage of this animal. Evidence that other trilobites grazed the microbial mat (Strang et al., 2016) and the lack of sediment particles in the gut suggest that *C. mantonae* may have been consuming other smaller arthropods, which would have provided a rich source of phosphate. It would appear predators, in significant numbers, occupied both the benthos and nekton in the Early Cambrian.

## 4.8 Conclusions

Detailed micrometre-scale analysis of the distribution of phosphate and silica in relation to the internal morphological structure of the soft-bodied arthropod *C. mantonae* from SP indicates a complex tissue- specific preservation of internal structures. The guts contain a high concentration of calcium phosphate (approximating to francolite), whereas the adjacent muscles are silicified. We hypothesize that the precipitation of calcium phosphate in the guts occurs rapidly after death by 'crystal seed' processes in suboxic, slightly acidic conditions; critically, the gut wall remained intact during precipitation. We postulate the calcium phosphate was derived from ingested organic material. Silicification of the muscles followed as the localized water chemistry became saturated in silica, high in $Fe^{2+}$, and low in oxygen and sulfate. These modes of preservation indicate a diversity of taphonomic pathways in faunas, chronostratigraphically intermediate between the Neoproterozoic Ediacara biota and the Middle Cambrian Burgess shale. The absence of sediment particles in the gut suggests that *C. mantonae* was either a scavenger or predating smaller arthropods.

## 4.9 References


Akahane, H., Furuno, T., Miyajima, H., Yoshikawa, T., and Yamamoto, S., 2004, Rapid wood silicification in hot spring water: an explanation of silicification of wood during the Earth's history: Sedimentary Geology, v. 169, no. 3–4, p. 219–228.

Arning, E.T., Birgel, D., Brunner, B., and Peckmann, J., 2009, Bacterial formation of phosphatic laminites off Peru.: Geobiology, v. 7, no. 3, p. 295–307.

Arp, G., Reimer, A., and Reitner, J., 2003, Microbialite Formation in Seawater of Increased Alkalinity, Satonda Crater Lake, Indonesia: Journal of Sedimentary Research, v. 73, no. 1, p. 105–127.

Belton, D., Paine, G., Patwardhan, S. V., and Perry, C.C., 2004, Towards an understanding of (bio)silicification: the role of amino acids and lysine oligomers in silicification: Journal of Materials Chemistry, v. 14, no. 14, p. 2231-2241.

Birnbaum, S.J., and Wireman, J.W., 1985, Sulfate-reducing bacteria and silica solubility: a possible mechanism for evaporite diagenesis and silica precipitation in banded iron formations: Canadian Journal of Earth Sciences, v. 22, no. 12, p. 1904–1909.

Briggs, D.E.G., 2003, The role of decay and mineralization in the preservation of soft-bodied fossils: Annual Review of Earth and Planetary Sciences, v. 31, no. 1, p. 275–301.

Briggs, D.E.., Moore, R.A., Shultz, J.W., and Schweigert, G., 2005, Mineralization of soft-part anatomy and invading microbes in the horseshoe crab Mesolimulus from the Upper Jurassic Lagerstätte of Nusplingen, Germany: Proceedings of the Royal Society of London B: Biological Sciences, v. 272, no. 1563, p. 627-632.

Briggs, D.E.G., and Nedin, C., 1997, The Taphonomy and Affinities of the Problematic Fossil Myoscolex from the Lower Cambrian Emu Bay Shale of South Australia: v. 71, no. 1, p. 22–32.

Budd, G.E., 2011, Campanamuta mantonae gen. et. sp. nov., an exceptionally preserved arthropod from the Sirius Passet Fauna (Buen Formation, lower Cambrian, North Greenland): Journal of Systematic Palaeontology, v. 9, no. 2, p. 217–260.

Butler, A.D., Cunningham, J.A., Budd, G.E., and Donoghue, P.C.J., 2015, Experimental taphonomy of Artemia reveals the role of endogenous microbes in mediating decay and fossilization.: Proceedings of the Royal Society B, Biological sciences, v. 282, no. 1808, p. 20150476.

Butterfield, N.J., 2002, Leanchoilia guts and the interpretation of three-dimensional structures in Burgess Shale-type fossils: Paleobiology, v. 28, no. 1, p. 155–171.

Butts, S.H., 2014, Silicification: In Reading and writing of the fossil record: preservational pathways to exceptional fossilization (eds M Laflamme, JD Schiffbauer, SAF Darroch): The Paleontological Society Papers, v. 20, p. 15–33.

Douglas, S., and Beveridge, T.J., 1998, Mineral formation by bacteria in natural microbial communities: FEMS Microbiology Ecology, v. 26, no. 2, p. 79–88.

Fatka, O., Budil, P., and David, M., 2015, Digestive structures in Ordovician trilobites Colpocoryphe and Flexicalymene from the Barrandian area of Czech Republic: Estonian Journal of Earth Sciences, v. 64, p. 255–266.

Frelinger, S.N., Ledvina, M.D., Kyle, J.R., and Zhao, D., 2015, Scanning electron microscopy cathodoluminescence of quartz: Principles, techniques and applications in ore geology: Ore Geology Reviews, v. 65, no. P4, p. 840–852.

Hof, C.H.J., and Briggs, D.E.G., 1997, Decay and mineralization of mantis shrimps (Stomatopoda; Crustacea); a key to their fossil record: PALAIOS, v. 12, no. 5, p. 420–438.

Jahnke, R.A., Emerson, S.R., Roe, K.K., and Burnett, W.C., 1983, The present day formation of apatite in Mexican continental margin sediments: Geochimica et Cosmochimica Acta, v. 47, no. 2, p. 259–266.

Krom, M.D., and Berner, R.A., 1980, Adsorption of phosphate in anoxic marine sediments: Limnology and Oceanography, v. 25, no. 5, p. 797–806.

Lerosey-Aubril, R., Hegna, T.A, Kier, C., Bonino, E., Habersetzer, J., and Carré, M., 2012, Controls on gut phosphatisation: the trilobites from the Weeks Formation Lagerstätte (Cambrian; Utah).: PloS one, v. 7, no. 3, p. e32934.

Lin, J.-P., 2006, Taphonomy of Naraoiids (Arthropoda) from the Middle Cambrian Kaili Biota, Guizhou Province, South China: PALAIOS, v. 21, no. 1, p. 15–25.

Lin, J.-P., and Briggs, D.E.G., 2010, Burgess Shale-Type Preservation: a Comparison of Naraoiids (Arthropoda) From Three Cambrian Localities: PALIOS, v. 25, no. 7, p. 463–467.

Morris, S.C., and Peel, J.S., 2008, The Earliest Annelids: Lower Cambrian Polychaetes from the Sirius Passet Lagerstätte, Peary Land, North Greenland: Acta Palaeontologica Polonica, v. 53, no. 1, p. 137–148.

Muscente, A. D., Hawkins, A.D. and Xiao, S., 2014, Fossil preservation through phosphatization and silicification in the Ediacaran Doushantuo Formation (South China): a comparative synthesis: Palaeogeography, Palaeoclimatology, Palaeoecology, v. 434, p. 46-62.

Neville, A.C., 2012, Biology of the Arthropod Cuticle: Springer Science & Business Media.

Peel, J.S., and Ineson, J.R., 2011, The extent of the Sirius Passet Lagerstätte (early Cambrian) of North Greenland: Bulletin of Geosciences, p. 535–543.

Rickert, D., Schlüter, M., and Wallmann, K., 2002, Dissolution kinetics of biogenic silica from the water column to the sediments: Geochimica et Cosmochimica Acta, v. 66, no. 3, p. 439–455.

Sansom, R.S., Gabbott, S.E., and Purnell, M. a, 2010, Non-random decay of chordate characters causes bias in fossil interpretation.: Nature, v. 463, no. 7282, p. 797–800.

Schulz, H.N., and Schulz, H.D., 2005, Large sulfur bacteria and the formation of phosphorite.: Science, v. 307, no. 5708, p. 416–418.

Seyedolali, A., Krinsley, D.H., Boggs, S., Hara, P.F.O., Dypvik, H., Gordon, G., Exploration, K., and Drive, R., 1997, Provenance interpretation of quartz by scanning electron microscope – cathodoluminescence fabric analysis: Geology, v. 25, p. 787-790.

Smith, M.P., and Harper, D.A.T., 2013, Causes of the Cambrian explosion.: Science, v. 341, no. 6152, p. 1355–1356.

Strang, K.M., Armstrong, H.A., Harper, D.A.T., and Trabucho-Alexandre, J.P., 2016, The Sirius Passet Lagerstatte: Silica death masking opens the window on the

earliest matground community of the Cambrian explosion: Lethaia, v. 49, p. 631-643.
Vannier, J., Liu, J., Lerosey-Aubril, R., Vinther, J., and Daley, A.C., 2014, Sophisticated digestive systems in early arthropods.: Nature communications, v. 5, p. 3641.
Wilby, P.R., and Briggs, D.E.G., 1997, Taxonomic trends in the resolution of detail preserved in fossil phosphatized soft tissues: Geobios, v. 30, p. 493–502.
Wilby, Philip R., Briggs, D.E.G., Bernier, P., and Gaillard, C., 1996, Role of microbial mats in the fossilization of soft tissues: Geology, v. 24, no. 9, p. 787-790.
Wilson, P., Parry, L.A., Vinther, J., and Edgecombe, G.D., 2016, Unveiling biases in soft-tissue phosphatization: extensive preservation of musculature in the Cretaceous (Cenomanian) polychaete Rollinschaeta myoplena (Annelida: Amphinomidae): Palaeontology, v. 59, no. 3, p. 463-479.
Yee, N., Phoenix, V.R., Konhauser, K.O., Benning, L.G., and Ferris, F.G., 2003, The effect of cyanobacteria on silica precipitation at neutral pH: implications for bacterial silicification in geothermal hot springs: Chemical Geology, v. 199, no. 1–2, p. 83–90.

# Chapter 5. Conclusions

## 5.1 Summary

The chapters, and associated papers, presented in this thesis examine aspects of the taphonomy of the Sirius Passet Lagerstätten, with particular focus on two of the most common elements, trilobite *Buenellus* and non-trilobite arthropod *Campanamuta mantonae*. In addition, Chapter 2 provides a methodological case study using Energy dispersive spectroscopy (EDS) and cathodoluminescence (CL) that previously, as far as we are aware, has mainly been used to look at shells of calcitic composition. SEM-CL was applied to characterise the silicification and its conditions of formation from a geological setting that is considerably less complex than that of the SP.

Burgess Shale-type preservation represents a unique and non-analogous taphonomic window that was widespread during the Cambrian (Allison and Briggs, 1993; Butterfield, 1995) and these BST Lagerstätten have been the subject of much scientific investigation, and the importance of these sites is widely recognised. The Early Cambrian radiation was a period of significant morphologic and taxonomic diversification (Wills et al., 1994) and fossils from these sites are the primary basis for understanding patterns of morphological diversity and disparity of the Cambrian fauna (Conway Morris, 1989; Wills et al., 1994; Budd and Jensen, 2000; Briggs and Fortey, 2005; Marshall, 2006; Erwin et al., 2011) as well as understanding phylogenetic patterns of the Cambrian explosion (Gaines, 2014). Without these Lagerstätten, our only window into the origin of animal phyla would be the fossil record of mineralised parts and because biomineralisation has developed numerous times across different animal lineages (Murdock and Donoghue, 2011), most of their early history would be missing from the fossil record. Therefore, this soft-bodied fossil record provides us with a window into early evolution of the major animal groups.

The analyses conducted in Chapter 3 provide the first detailed study focused primarily on the taphonomy of the Sirius Passet with relation to 'matground' habitats. Using petrography and SEM analysis we demonstrate the sequence of events leading to the preservation of concave hyporelief external moulds and

convex epirelief casts of *Buenellus higginsi* and its association with preserved microbial mat material. A detailed description and interpretation of the depositional environment was also undertaken, revealing two end-member lithofacies, a 'spotted' and a silt-rich facies. Findings suggest a 'death mask' taphonomy, unique to the Cambrian, where casts of *Buenellus* are formed from silicified cyanobacterial mat material. This siliceous death mask preservation is relatively common in the Ediacaran (e.g. Gehling, 1999), however it is unique to the Cambrian and may only have existed for a short time due the absence of the mat grazing organisms that appeared later as the Cambrian Explosion intensified.

Another important taphonomic pathway of selective soft tissue mineralisation in BST type biotas are replacement by calcium phosphate (Butterfield, 2002; Gaines, 2014; Schiffbauer et al., 2014). Phosphatisation is largely restricted to the guts of arthropods, where digestive tracts are sometimes preserved (Butterfield, 2002). Phosphatisation as a mode of preservation is challenging because although gut tracts of certain animals would have provided chemical microenvironments which favoured precipitation of phosphate (Butterfield, 2002; Lerosey-Aubril et al., 2012), it is argued that mass-balance considerations would require an additional source outwith the gut (Gaines, 2014). The detailed account of the SP sediments in Chapter 3 and the characteristically organic-poor sediments of other BST localities (Gaines et al., 2012) would suggest that these sediments would not account for an additional source of phosphate. However in Chapter 4 we find evidence for silicification in close proximity surrounding the phosphatised gut tracts, implying that the source of phosphate is likely internal and the high phosphate concentrations were a result of the animals diet, this has also been cited as a hypothesis in other Cambrian localities (Butterfield, 2002; Lerosey-Aubril et al., 2012).

The results presented in this thesis suggest that the iconic arthropod-lobopodian fauna that characterizes the Sirius Passet Lagerstätte inhabited a warm, muddy, habitat close to storm wave base. Seasonal salinity stratification of the bottom waters would have resulted in warm saline brines at the seafloor and extensive

growth of sulphate-reducing bacteria (which are documented in Chapter 2 and 3) resulting in euxinia. Mixing during tropical storms would have introduced oxygenic waters and allowed for the colonisation of the seafloor by invertebrates, providing the perfect habitat for them to thrive. Primary productivity would have been by benthic cyanobacteria, evidenced by their presence in thin sections (Strang et al., 2016a). Periodic storm events resulted in mixing of sediment and thus aided the preservation of organic matter in the sediment. Taphonomic processes (biological, chemical and physical factors) intrinsic to these mat ground habitats provide the "rare" preservational window through which we view the record of the Cambrian Explosion in the Sirius Passet. Taphonomy therefore brings together aspects of environment and ecology of this "special place" and is critical in our understanding of where and when (but not how) the Cambrian Explosion originated.

## 5.2 Overview of key findings addressing the research questions

The Sirius Passet fauna displays a diversity of taphonomic pathways. Although typical Burgess Shale Type preservation may indeed be represented in some of the taphonomic styles (e.g. vetulicolians; see Vinther et al., 2011), a key taphonomic pathway, involving silicified death mask preservation, is more likely a holdover from the Late Proterozoic mat-ground communities. Three-dimensional preservation of gut tracts by phosphatisation is another key process. These occur in addition to mouldic preservation (see e.g. Mángano et al., 2012). Here we outline the key findings addressing the research questions outlined in Chapter 1, section 1.5.

Cathodoluminescence (CL) is a tool for determining the nature and distribution of luminescence in quartz. These data may reflect specific conditions during the formation of quartz. CL is the result of photon emission in the visible range resulting from excitation of high-energy electrons (Ségalen et al., 2008). The intensity of CL is dependent on the density of intrinsic and extrinsic defects within the band gap of the mineral and these defects are usually structural imperfections in the quartz crystal due to vacancies within the crystal lattice. By studying these defects in Chapter 2 we infer that silica replacement in these Antiguan fossils was a multi-stage process, indicated by the variety of textures and crystal sizes visible under CL. This CL methodology was then applied in the studies undertaken in both Chapter 3 and 4. In Chapter 3, the detailed study of *Buenellus*, the presence of two quartz phases, one associated with the quartz of the sedimentary matrix and one associated with the silica in the mineralised mat and concave external moulds, which exhibits almost no luminescence, lead us to conclude, along with other evidence, that silicification of the trilobites occurred early, shortly after death. In the case of Chapter 4 we highlight the CL data, in which the silicified muscles of *Campanamuta mantonae* show a low monotone grey luminosity, which is indicative of similar formation conditions as that found in *Buenellus* (Strang et al., 2016a; 2016b).

Based on the evidence from Chapter 3 and Chapter 4, a detailed timeline of the taphonomic history of the Sirius Passet Lagerstätte is provided, from the death of

organisms to diagenesis and finally to metamorphism. This section addresses the research questions pertaining to the association of common SP arthropods with 'matground' communities, and their role in taphonomy. It also explores the preservation of three-dimensionally preserved gut tracts and looks to explain the presence of both phosphate and silica in such close proximity within the guts.

As previously discussed, the Sirius Passet fauna is characterized by abundant microbial mats (Mángano et al., 2012; Strang et al., 2016a; Strang et al., 2016b) and an iconic Burgess Shale Type fauna, mainly dominated by arthropods and lobopods. There is also evidence of annulated burrows and interconnected burrow systems (Mángano et al., 2012) and other ichnotraces which infer re-use of burrowing systems by organisms, as they burrowed to graze on the nutrient rich microbial mats.

Mass fatalities were likely caused by storm events that resulted in an influx of sediment burying the organisms, more or less instantaneously. However, another possible cause of community wide mortality is the release of $H_2S$ from the microbial mats, effectively poisoning the surrounding fauna. After death, organisms were rapidly covered with microbial mats, as they grow upwards to reach the sediment-water interface. This sealing by the mat results in the creation of a unique microenvironment and distinct chemical conditions. At this point the taphonomic pathway is determined by the composition and degree of mineralogy of the particular taxa. The chapters of this thesis describe the detailed taphonomic pathways of some of the most common elements of the Sirius Passet fauna across the widest range of body types. Mineralizing organisms such as *Buenellus* were able to withstand compaction, allowing for infilling with microbial material, leaving behind a counterpart cast and mould. However, non-mineralized faunas such as *C. mantonae* possessed no tough exoskeleton, thus after death the animal's appendages would rapidly become flattened, but rapid mineralization due to unique endogenous bacteria in the animals gut allowed certain internal features such as the gut to be preserved, commonly in 3D.

It is proposed that the earliest stage of permineralisation seen in the SP Lagerstätte is phosphatisation in the guts of the non-mineralised arthropod *C. mantonae.* The sealed environments of the gut and the gut wall remaining intact are key to maintaining the integrity of the tube-like gut to allow for the precipitation of phosphate under slightly alkaline conditions (< Ph 7). The phosphatisation of the gut occurred in sub-oxic conditions under the control of endogenous sulphate reducing bacteria, and occurred within days of death and therefore at the sediment surface. Although there is no direct evidence for microbes in the guts, the spherical, spongy texture of the phosphate infers their original presence and likely represents possible microbial moulds (Similar to those documented in Lerosey-Aubril et al., 2012).

Silicification would have been initiated after phosphatisation as the carcass became engulfed in the growing mat, as it acted as a seal from the surrounding water chemistry, creating unique micro environmental conditions necessary for tissue specific silicification of the fibrous muscle bands. It is also hypothesised that sediment-laden water was saturated in silica, high in $Fe^{2+}$, and low in oxygen and sulphate. It is inferred that *C. mantonae* was sealed in the mat but the lack of a mineralized carapace meant less resistance to compaction by surrounding sediment, this is hypothesised by comparing to the biomineralising trilobite *Buenellus*, which are preserved as complete concave hyporelief external moulds and convex counterpart casts. However, external features of *C. montanae* are poorly preserved and only the tubular gut is preserved in 3D; suggesting the lack of a mineralized exoskeleton resulted in the poor preservation of surrounding appendages.

Silicification and phosphatisation occur very close together in *C. montanae* and are separated only by the gut wall remaining intact after death. As discussed there are differing preferences for both mechanisms. This suggests that these elements of the SP biota were initially phosphatised due to endogenous bacteria present in the gut, and then silicification was initiated as biofilm of exogenous bacteria sealed the organism creating the required conditions for silicification. However, direct evidence of the timing of events is not present.

The significance between the silicification and the phosphatisation is down to the timing of events and original composition of the tissues and changing localized environments created by microbial activity. The contrast of the high phosphate concentrations in the guts is due to the higher organic content and digestive enzyme being present at the time of death. It is thought that, due to the lack of sediment present in the gut, *Campanamuta mantonae* was carnivorous rather than a deposit feeder. Although these two taphonomic pathways are usually thought to occur independently, the robustness of the gut remaining intact during phosphatisation and the presence of dense microbial mat material has allowed optimal micro conditions for these pathways to occur alongside each other. We can hypothesis that the phosphatisation occurs first due to the presence of endogenous bacteria within the gut, which creates a microenvironment favouring the precipitation of phosphate. As the animal decays and phosphate precipitates, silicification is then initiated as the chemistry of the closed environment changed to become saturated relative to FeOOH and exogenous bacteria colonise the body cavity, replicating soft tissues such as muscle. Therefore, the presence of both these pathways in a localized environment suggests microbial sealing has an influence on sediment-water chemistry interactions and may be the fundamental driver of the SP taphonomic history.

After the death and rapid burial of the organisms, the first few hours and days are critical to whether or not the organism survives in the fossil record. At around 400 million years ago the rocks of the Buen Formation underwent intense regional metamorphism, significantly after diagenesis. The shales of the Sirius Passet underwent greenschist facies metamorphism, evidenced by the presence of chloritoid needles. Despite this deformation event, primary sedimentary fabric is still preserved (Strang et al., 2016a).

We therefore propose that the taphonomy of the Sirius Passet is tissue specific, and the chemistry takes two distinct pathways depending on the degree of mineralization of the dead organism. Thus the taphonomy is variable across tissue types as well as taxa. Furthermore, These ecosystems were mat-grazer dominated, evidenced by the presence of preserved microbial mats and thus mark a transitional state between the Ediacaran Biota and the Cambrian Evolutionary Fauna.

## 5.3 Summary of palaeobiological implications

The occurrence of a near identical arthropod-lobopod fauna in a muddy habitat at or about storm-wave base over some 10 million years suggests remarkably ecological stability. The Cambrian is characterised by many "mass extinction events" resulting in major faunal turnovers; nevertheless the arthropod-lobopod assemblage represents a fauna which is resilient in these muddy, mat dominated environments. Rapid ecological differentiation of a relatively species-rich offshore siliciclastic microbial mat community occurred in the early Cambrian. What was the origin of this fauna? This differentiation may have reflected nutrient levels in the two habitats. Oligotrophic carbonates versus mesotrophic mat communities. Were these higher nutrient systems related to ITCZ runoff related or upwelling? Was it nutrient availability that enabled the first complex communities to evolve?

Along marine coasts, mud particles are introduced by rivers. These particles are commonly amalgamated into larger aggregates composed of both organic and mineral matter as a result of electrochemical, biological, and biochemically mediated processes; the resulting aggregates settle to the sea floor, typically within a few tens of kilometers of river mouths (e.g., McCave, 1985; Alldredge and Silver, 1988). In view of this rapid settling, the presence of siliciclastic mud in shelf sediments at distances of up to hundreds of kilometers from shore would require additional mechanisms such as storms events. Such events were responsible for remobilizing and transporting mud farther seaward. On storm influenced shelves, combined flows are capable of re-suspending bottom sediment to depths of well over 100 m (Snedden and Nummedal, 1991) Wave energy can maintain a dense suspension of sediment near the seabed. The key to the exceptional preservation within these deposits was rapid burial by microbial mats, essentially resulting in an anoxic substrate. The sea floor of the Sirius Passet was rapidly sealed by microbial mats and permineralised during bacterially mediated sulphate reduction. An absence of bioturbation restricted the ingress of oxygen and allowed mats to flourish. Evidence suggests the Sirius Passet community was intact, thriving at the base of the euphotic zone, just

below storm wave base, dominated by mat grazers such as *Buenellus*, the most common element. Carnivores like *Campanamuta mantonae* fed on taxa such as these trilobites, due to their rich nutrient intake from the mats.

Taking into account the "facies area hypothesis" i.e. the expansion and spread of the key facies on the continental shelves, as a cause of the Cambrian Explosion we can query whether this was responsible for triggering an adaptive radiation in the fossil record? It could also be argued that particular habitats in the Cambrian provided "ocean islands," where particular variants could live, under low selection pressure, with an increase in abundance (in terms of biomass) and abundance over time, thus enough to leave behind a fossil record through not one but a variety of taphonomic pathways. At present these are intractable questions, but nonetheless highly important to ponder.

## 5.4 Future work

There is still much to be learnt from the SP and, indeed, other Cambrian BST deposits and thus the potential for future work is enormous. Further work on the SP involving systematic investigation of the detailed taphonomy of other organisms, particularly of non-arthropod taxa, would help to elucidate and constrain the whole story of the taphonomic history. Future research would benefit from an interdisciplinary approach involving (but not limited to) experimental taphonomy, geology, geochemistry, genetics and cladistics to allow insight into the 'bigger picture' of the SP and it's position in space and time with relation to the other exceptionally preserved BST biotas. Furthermore, the SP would benefit from broad assemblage comparison analysis (similar studies have been undertaken for the Burgess Shale and Chengjiang biotas), particularly from an ecological perspective, using abundance data for individual localities, which would ultimately lead to a greater understanding of the relationships between sites, especially from an environmental perspective.

## 5.5 References


Alldredge, A.L., and Silver, M.W., 1988, Characteristics, dynamics and significance of marine snow: Progress in Oceanography, v. 20, no. 1, p. 41–82.

Allison, P.A., and Briggs, D.E.G., 1993, Exceptional fossil record: distribution of soft-tissue preservation through the Phanerozoic: Geology, v. 21, no. 6, p. 527–530.

Briggs, D.E.G., and Fortey, R.A., 2005, Wonderful strife: systematics, stem groups, and the phylogenetic signal of the Cambrian radiation: Paleobiology, v. 31, no. 2, p. 94–112.

Budd, G.E., and Jensen, S., 2000, A critical reappraisal of the fossil record of bilaterian phyla: Biological Reviews, v. 75, no. 2, p. 253–295.

Butterfield, N.J., 2002, Leanchoilia guts and the interpretation of three-dimensional structures in Burgess Shale-type fossils: Paleobiology, v. 28, no. 1, p. 155–171.

Butterfield, N.J., 1995, Secular distribution of Burgess-Shale-type preservation: Lethaia, v. 28, no. 1, p. 1–13.

Conway Morris, S., 1989, The persistence of Burgess Shale-type faunas: implications for the evolution of deeper-water faunas: Transactions of the Royal Society of Edinburgh: Earth Sciences, v. 80, no. 3–4, p. 271–283.

Erwin, D.H., Laflamme, M., Tweedt, S.M., Sperling, E.A., Pisani, D., and Peterson, K.J., 2011, The Cambrian conundrum: early divergence and later ecological success in the early history of animals.: Science, v. 334, no. 6059, p. 1091–1097.

Gaines, R.R., 2014, Burgess shale-type preservation and its distribution in space and time: Palaeontological Society Papers, v. 20, p. 123–146.

Gaines, R.R., Hammarlund, E.U., Hou, X., Qi, C., Gabbott, S.E., Zhao, Y., Peng, J., and Canfield, D.E., 2012, Mechanism for Burgess Shale-type preservation: Proceedings of the National Academy of Sciences of the United States of America, v. 109, no. 14, p. 5180–5184.

Gehling, J.G., 1999, Microbial Mats in Terminal Proterozoic Siliciclastics: Ediacaran Death Masks: PALAIOS, v. 14, no. 1, p. 40-47.

Lerosey-Aubril, R., Hegna, T.A, Kier, C., Bonino, E., Habersetzer, J., and Carré, M., 2012, Controls on gut phosphatisation: the trilobites from the Weeks Formation Lagerstätte (Cambrian; Utah): PloS one, v. 7, no. 3, p. e32934.

Marshall, C.R., 2006, Explaining the Cambrian "Explosion" of animals: Annual Review of Earth and Planetary Sciences, v. 34, no. 1, p. 355–384.

Mángano, M.G., Bromley, R.G., Harper, D.A.T., Nielsen, A.T., Smith, M.P., and Vinther, J., 2012, Nonbiomineralized carapaces in Cambrian seafloor landscapes (Sirius Passet, Greenland): Opening a new window into early Phanerozoic benthic ecology: Geology, v. 40, no. 6, p. 519–522.

McCave, I.N., 1985, Recent shelf clastic sediments: Geological Society, London, Special Publications, v. 18, no. 1, p. 49–65.

Murdock, D.J.E., and Donoghue, P.C.J., 2011, Evolutionary origins of animal skeletal biomineralization: Cells Tissues Organs, v. 194, no. 2-4, p. 98–102.

Schiffbauer, J.D., Wallace, A.F., Broce, J., and Xiao, S., 2014, Exceptional fossil conservation through phosphatization: Paleontological Society Papers, v. 20, p. 59–82.

Ségalen, L., de Rafélis, M., Lee-Thorp, J.A., Maurer, A.-F., and Renard, M., 2008, Cathodoluminescence tools provide clues to depositional history in Miocene and Pliocene mammalian teeth: Palaeogeography, Palaeoclimatology, Palaeoecology, v. 266, p. 246-253.

Snedden, J.W., and Nummedal, D., 1991, Origin and geometry of storm-deposited sand beds in modern sediments of the Texas continental shelf, *in* Shelf Sand and Sandstone Bodies, Blackwell Publishing Ltd., Oxford, UK, p. 283–308

Strang, K.M., Armstrong, H.A., Harper, D.A.T., and Trabucho-Alexandre, J.P., 2016a, The Sirius Passet Lagerstätte: silica death masking opens the window on the earliest matground community of the Cambrian explosion: Lethaia, v. 49, no. 4, p. 631–643.

Strang, K.M., Armstrong, H.A., and Harper, D.A.T., 2016b, Minerals in the gut: scoping a Cambrian digestive system: Royal Society Open Science, v. 3, no. 11.

Vinther, J., Smith, M.P., and Harper, D.A.T., 2011, Vetulicolians from the Lower Cambrian Sirius Passet Lagerstätte, North Greenland, and the polarity of morphological characters in basal deuterostomes: Palaeontology, v. 54, no. 3, p. 711–719.

Wills, M.A., Briggs, D.E.G., and Fortey, R.A., 1994, Disparity as an Evolutionary Index: A Comparison of Cambrian and Recent Arthropods: Paleobiology, v. 20, no. 2, p. 93–130.

# Appendix I: Silicification of low-magnesium mollusc shells from the Upper Oligocene of Antigua, Lesser Antilles

Strang, K.M., Harper, D.A.T., Donovan, S.K., and Portell, R.W., in press, Silicification of low-magnesium mollusc shells from the Upper Oligocene of Antigua, Lesser Antilles: Caribbean Journal of Earth Sciences.

# Silicification of low-magnesium mollusc shells from the Upper Oligocene of Antigua, Lesser Antilles

KATIE M. STRANG[1], DAVID A.T. HARPER[1], STEPHEN K. DONOVAN[2] AND ROGER W. PORTELL[3]

[1] *Palaeoecosystems Group, Department of Earth Sciences, Durham University, Durham, DH1 3LE, UK. E-mail: david.harper@durham.ac.uk*

[2] *Taxonomy and Systematics Group, Naturalis Biodiversity Center, Postbus 9517, 2300 RA Leiden, the Netherlands. E-mail: steve.donovan@naturalis.nl*

[3] *Florida Museum of Natural History, University of Florida, Gainesville, 32611 Florida, USA. E-mail: portell@flmnh.ufl.edu*

**ABSTRACT. Silicified molluscs, namely the oyster *Hyotissa* and the scallop *Aequipecten*?, are commonly preserved as silica in the carbonate successions on the island of Antigua. These fossil assemblages are located within the Antigua Formation, above and adjacent to a variety of volcanic and volcaniclastic rocks, suggesting, on geological grounds, an igneous source for the silica. Energy dispersive spectroscopy (EDS) and cathodoluminescence (CL) have been applied to characterise the silcification and its conditions of formation which may have been associated with hydrothermal activity.**

**Key words: Antigua Formation, limestone, EDS, cathodoluminescence, *Aequipecten*?, *Hyotissa*.**

## 1. INTRODUCTION

Silicification is a relatively common mode of preservation in the fossil record. It generally occurs along thin zones within the fossil as the original calcium carbonate is dissolved and replaced by silica. The process of silicification (see Butts, 2014, for a comprehensive review) can occur through permineralization (precipitation of silica into voids), entombment (precipitation on external surfaces) and replacement (or silicification *sensu stricto*), that is, dissolution of skeletal material virtually concurrent with the precipitation of silica. The process is controlled by shell mineralogy, including the amount and location of organic matter, and the availability of silica. Thus, silicification of fossils in limestones can be considered an indication of early diagenetic conditions whereby there is a source of excess dissolved silica and the replacement mechanism is the likely one where monomers bond directly with organic material (Butts, 2014) rather than by force of crystallization (Maliva and Siever, 1998). The sources of silica can be many and various (e.g., Upchurch et al., 1980).

Cathodoluminescence (CL) is a tool for determining the nature and distribution of luminescence in quartz. These data may reflect specific conditions during the formation of quartz. Cathodoluminescence is the result of photon emission in the visible range resulting from excitation of high-energy electrons (Ségalen et al., 2008). The intensity of CL is dependent on the density of intrinsic and extrinsic defects within the band gap of the mineral. These defects are usually structural imperfections in the quartz crystal due to vacancies within the crystal lattice, and include point and planar lattice defects, radiation damage, shock damage, melt inclusions and fluid inclusions (Frelinger et al., 2015). These defects can provide information on the conditions during mineralization, and subsequent post-mineralization events such as deformation and metamorphism. The combination of scanning electron microscope (SEM) and CL data highlighting textural features allows distinction of

different quartz types more easily than with conventional microscopy or colour CL analysis (Bernet and Bassett, 2005). Studies have shown that CL textures such as zoning, microcracks and deformation fractures can remain preserved in sedimentary rocks, withstanding processes such as uplift, sediment deposition and diagenesis (Seyedolali et al., 1997; Bernet and Bassett, 2005; Götze, 2012). This has made the textures a useful tool, because comparison with published CL data of specimens from well-typified settings enables the identification of the provenance of minerals and their conditions of formation. To the best of our knowledge, previous CL studies on Recent and fossil shells have focussed only on those with a carbonate composition, to determine, for example, growth trajectories, and the luminosity of calcite has been used to decide whether a shell is modern or ancient (see, for example, Barbin and Gaspard, 1995; England et al., 2006; and references therein). The application of using CL to determine information from silicified shells is therefore a new approach.

Herein, we characterise the silica prevalent in bioclasts of the Antigua Formation (upper Oligocene) of Antigua using a number of spectroscopy techniques. The island of Antigua (Figure 1) is characterised by an abundant and diverse Oligocene fossil fauna. Locally, these fossils are beautifully preserved, albeit silicified.

## 2. GEOLOGICAL SETTING

The Caribbean island of Antigua lies towards the northern end of the Lesser Antilles volcanic arc. It is a Limestone Caribee, an island of volcanic origin capped by carbonates (Wadge, 1994; Donovan et al., 2014a, b). As such, it is a perfect field laboratory to investigate the relationships between a volcanic arc and the evolution of its carbonate cover succession. The

rock record of the entire island is late Oligocene in age (Weiss, 1994), with the exception of some minor upper Quaternary sediments. The regional dip of the strata is towards the northeast, with the oldest rocks, the Basal Volcanic Suite, cropping out and exposed in the western and southern regions of the island. The stratigraphical succession can be defined in terms of three conformable units, in ascending order: the Basal Volcanic Suite; the Central Plain Group; and the Antigua Formation. The Antigua Formation is a succession of diverse limestones with minor siliciclastic and volcaniclastic, commonly tuffaceous, horizons that are exposed in the north and east of the island (Figure 1).

## 3. LOCALITIES

The specimens analysed herein were collected from two localities in the Antigua Formation.

### 3.1. Locality 1. Hughes Point

Oysters were collected from float and *in situ* from limestone beds in the Hughes Point area on the south coast of Nonsuch Bay, parish of St. Philip, eastern Antigua (Locality 1). Large gryphaeid oysters assigned to *Hyotissa antiguensis* (Brown, 1913) are locally common both *in situ* in an extensive coastal exposure, and reworked as float in adjacent shallow water, the latter associated with common bored clasts of limestone (Donovan et al., 2014a). A measured section of part of the coastal exposure appeared in Collins and Donovan (1995, fig. 2; Figure 2 herein). Oysters are common and were noted in all beds identified in this illustration.

### 3.2. Locality 2. Half Moon Bay

Scallops, including *Aequipecten*? sp., were collected from the northeast point of Half Moon Bay, parish of Saint Philip, southeast Antigua (Locality 2). Here the section exposes over 8 m of the Antigua Formation. These limestones have yielded a diverse fauna (Donovan et al., 2015), including calcareous algae, articulated sponges, brachiopods, crinoid columnals, asteroid marginal ossicles, echinoids, rare oysters and other benthic molluscs, including scallops. Foraminiferans from these beds include flat *Lepidocyclina canellei* Lemoine and Douville and inflated *Eulepidina* sp. cf. *E. undosa* (Cushman). A measured section was published in Donovan *et al*. (2015, fig. 3; Figure 3 herein).

## 4. MATERIALS AND METHODS

Samples were studied for texture and composition using the SEM. Thin sections were cut at regular 10 mm transverse intervals perpendicular to the direction of growth through the samples to create cross sectional views. Thin sections were coated in Epo Tek 301 two-part epoxy resin and polished with diamond. Samples were then coated with *c*. 20 nm carbon to avoid charging during analysis. Imaging and analysis by SEM was carried out using the Hitachi SU-70 FEG SEM in Durham University using secondary electron and backscattered electron detectors at 12 kV. Both primary and secondary backscatter techniques were used to produce general images prior to SEM-EDS and SEM-CL analysis. Energy dispersive X-ray analysis was carried out using the backscatter detector and the same voltage settings were used for imaging. Results were processed using the QUANT software and running the standard several times to ensure maximum accuracy (100 ± 5%).

A mirror-type detector (Gatan Mono-CL) was used for SEM-CL analysis. The machine was set to low magnification with a 10 kV voltage to allow the site of interest to be determined. The working distance was set to 20 mm and then adjusted as necessary to allow

focusing of the sample. Results were obtained using the panchromatic mode (clear filter) with both mirrors adjusted to panchromatic mono-CL settings. Working distance was set to 16.2–16.7 mm and CL luminosities collected. Grey-scale pictures were produced using mono-CL, due to the increased speed and smaller scale resolution achievable from grey scale CL imaging. Various studies have been carried out which show that quartz grains display a variety of luminosity intensities dependent on their provenance. The characterization of the distinctive CL fabrics and methods were adapted from Seyedolali et al. (1997). A more recent study suggests that textural features can provide additional support to investigations of colour and CL wavelength in determining provenance of quartz (Schieber et al., 2000).

## 5. RESULTS

### 5.1. Locality 1: Hughes Point

Data using EDS show that the gryphaeid oysters are composed predominantly of silica (>80 %) intermixed with calcite (Table 1), lacking any correspondence to the original growth lamellae or shell ultrastructure (Figure 4A). Under the backscatter detector (BSE), the silica grains in the samples appear relatively uniform with no visible distinguishing features (Figure 5A). The silica studied by SEM-CL shows a range of grey scale luminosities ranging from dark grey to white (white being the strongest luminescence) with the majority of grains appearing mottled in texture (Figure 5B). These varying intensities highlight features in the silica such as zoning. This distinct zoning appears as varying shades of grey, with the outer rim showing almost no luminescence; however, zonation is not uniform. An emission spectrum was produced using the intensity of counts against wavelength. The

emission band of this silica lies between 540 – 740 nm (Figure 6), indicated neoformed silica (e.g., Aparicio and Bustillo 2012), which correlates with a possible hydrothermal source (Götze et al., 2001).

### 5.2. Locality 2: Half Moon Bay

Scallops (pectinid bivalves) from Half Moon Bay share the same composition as the oysters (Table 2) from Locality 1, composed of silica and calcite; this pattern, similar to that of the oysters from Hughes Point, does not conform to the original growth lines or shell ultrastructure (Figure 4B). The optical BSE textures are homogenous, and there are no clear defects visible under normal SEM imaging (Figure 5C). However, SEM-CL again shows a distinct mottled texture and similar irregular distribution of luminosity intensities, as at Locality 1. This irregular distribution (Figure 5D) of luminosity helps distinguish neoformed silica from that of metamorphic origin (Matter and Ramseyer, 1985). There is also evidence of zoning present, with the overall texture similar to that found at Hughes Point.

## 6. DISCUSSION

Silicified fossils are common in the upper Oligocene limestones of Antigua. These rocks overlie and are regionally interbedded with a range of volcanic and volcaniclastic rocks, providing an obvious source of silica. The proximity of these extrusive igneous rocks to the fossils provides a key test of the efficacy of some of techniques available to identify the source of silica in diagenetically altered shells. In particular, those molluscs with low magnesium shells, oysters and scallops, seem particularly prone to silicification. The technique of studying patterns of variable-intensity mono CL in quartz grains has been

applied to many provenance studies (Seyedolali et al., 1997; Boggs et al., 2002), but in this case we have focused on the conditions of formation of the silica. We infer that silica replacement in these fossils was a multi-stage process, indicated by the variety of textures and crystal sizes visible under CL. The minerals from both localities show a characteristic mottled texture with irregular zoning and fractures throughout (Figure 5). The emission band of this silica lies between 540 – 740 nm (Figure 6), suggestive of a possible hydrothermal source (Götze et al., 2001; Götze, 2012). This evidence is not incompatible with silicification driven by the hydrothermal products of a volcanic arc, much of which forms the basement of the Limestone Caribees.

***Acknowledgements.*** Fieldwork in Antigua by D.A.T.H., S.K.D., R.W.P. and the late Trevor A. Jackson was supported by National Geographic Society grant #GEFNE55-12. This paper was in the early stages of writing when Trevor died; otherwise, he would have been a collaborator on this rather different approach to the volcanic geology of Antigua. K.M.S. acknowledges receipt of a NERC CASE Studentship (RF050232) and D.A.T.H. thanks for the support provided by a Leverhulme Research Fellowship. We thank Susan Butts (Yale University) and a second, anonymous reviewer for their wise comments which helped change the focus of the paper, and tightened up its content and significance.

## REFERENCES

**Aparicio, A. and Bustillo, A. 2012.** Cathodoluminescence spectral characteristics of quartz and feldspars in unaltered and hydrothermally altered volcanic rocks (Almeria, Spain). *Spectroscopy Letters*, **45**, 104-108.

**Barbin, V. and Gaspard, D. 1995.** Cathodoluminescence of Recent articulate brachiopod shells: implications for growth stages and diagenesis evaluation. *Geobios*, **28**, 39-45.

**Bernet, M. and Bassett, K. 2005.** Provenance analysis by single-quartz-grain SEM-CL/optical microscopy. *Journal of Sedimentary Research*, **75**, 492-500.

**Boggs, S., Kwon, Y. I., Goles, G. G., Rusk, B. G., Krinsley, D. and Seyedolali, A. 2002.** Is quartz cathodoluminescence color a reliable provenance tool? A quantitative examination. *Journal of Sedimentary Research*, **72**, 408-415.

**Brown, A.P. 1913.** Notes on the geology of the island of Antigua. *Proceedings of the Academy of Natural Sciences of Philadelphia*, **65**, 584-616.

**Butts, S. 2014.** Silicification. *In*: **M. Laflamme, J. D., Schiffbauer and S. A. Darroch (Eds),** *Reading and Writing of the Fossil Record: Preservational Pathways to Exceptional Fossilization.* Paleontological Society Papers, **20**, 15-34.

**Collins, J. S. H. and Donovan, S. K. 1995.** A new species of *Necronectes* (Decapoda) from the Upper Oligocene of Antigua. *Caribbean Journal of Science*, **31**, 122-127.

**Donovan, S. K. 2010.** Jamaican rock stars. *In*: **Donovan, S. K. (Ed.),** *Jamaican Rock Stars, 1823-1971: The Geologists Who Explored Jamaica*. Geological Society of America Memoir, **205**, 1-8.

**Donovan, S. K., Harper, D. A. T. and Portell, R. W. 2015.** In deep water: a crinoid–brachiopod association in the Upper Oligocene of Antigua, West Indies. *Lethaia*, **48**, 291-298.

**Donovan, S. K., Harper, D. A. T., Portell, R. W. and Renema, W. 2014a.** Neoichnology and implications for stratigraphy of reworked Upper Oligocene oysters, Antigua, West Indies. *Proceedings of the Geologists' Association*, **125**, 99-106.

**Donovan, S. K., Jackson, T. A., Harper, D. A. T., Portell, R. W. and Renema, W. 2014b.** Classic localities explained 16. The Upper Oligocene of Antigua: the volcanic to limestone transition in a limestone Caribbee. *Geology Today*, **30**, 151–158.

**England, J., Cusack, M., Paterson, N. W., Edwards, P., Lee, M. R. and Martin, R. 2006**. Hyperspectral cathodoluminescence imaging of modern and fossil carbonate shells. *Journal of Geophysical Research*, **111**, G03001 [8 pages], doi: 10.1029/2005JG000144.

**Frelinger, S. N., Ledvina, M. D., Kyle, J. R. and Zhao, D. 2015.** Scanning electron microscopy cathodoluminescence of quartz: Principles, techniques and applications in ore geology. *Ore Geology Reviews*, **65**, 840-852.

**Götze, J. 2012.** Application of Cathodoluminescence Microscopy and Spectroscopy in Geosciences. *Microscope and Microscopy*, **18**, 1270-1284.

**Götze, J., Plötze, M. and Habermann, D. 2001.** Origin, spectral characteristics and practical applications of the cathodoluminescence (CL) of quartz–a review. *Mineralogy and Petrology*, **71**, 225-250.

**Maliva, R. G. and Siever, R. 1988.** Mechanism and controls of silicification of fossils in limestones. *Journal of Geology*, **96**, 387-398.

**Matter, A. and Ramseyer, K. 1985.** Cathodoluminescence microscopy as a tool for provenance studies of sandstones. *In*: **Zuffa, G. G. (Ed.),** *Provenance of Arenites*, 191-211. Springer, Dordrecht.

**Schieber, J., Krinsley, D. and Riciputi, L. 2000.** Diagenetic origin of quartz silt in mudstones and implications for silica cycling. *Nature*, **406**, 981-985.

**Ségalen, L., de Rafélis, M., Lee-Thorp, J. A., Maurer, A.-F. and Renard, M. 2008.** Cathodoluminescence tools provide clues to depositional history in Miocene and

Pliocene mammalian teeth. *Palaeogeography, Palaeoclimatology, Palaeoecology*, **266**, 246-253.

**Seyedolali, A., Krinsley, D., Boggs, S., O'Hara, P. F., Dypvik, H. and Goles, G. G. 1997.** Provenance interpretation of quartz by scanning electron microscope–cathodoluminescence fabric analysis. *Geology*, **25**, 787–790.

**Upchurch, S.B., Strom, R.N. and Nuckels, M.G. 1980.** Silicification of Miocene rocks from central Florida**.** *In*: **Scott, T.M. and Upchurch, S.B. (Eds.)**, *Miocene of the Southeastern United States*, 251-284. Florida Department of Natural Resources, Division of Resource Management, Bureau of Geology, Special Publication, **25**.

**Wadge, G. 1994.** The Lesser Antilles. *In*: **Donovan, S. K. and Jackson, T. A. (Eds.),** *Caribbean Geology: An Introduction*, 167–177. University of the West Indies Publishers' Association, Mona.

**Weiss, M.P. 1994.** Oligocene limestones of Antigua, West Indies: Neptune succeeds Vulcan. *Caribbean Journal of Science*, **30**, 1–29.

## FIGURE CAPTIONS

**Figure 1. Outline map of Antigua (redrawn and modified after Weiss, 1994, fig. 3), showing the principal geological subdivisions and the city of Saint John's. The regional dip is towards the northeast. Localities 1 (Hughes Point) and 2 (Half Moon Bay) are marked. Inset map (modified after Donovan, 2010, fig. 2) shows the position of Antigua in the Caribbean. Key (clockwise from Jamaica): J=Jamaica; C=Cuba; H=Hispaniola (Haiti+Dominican Republic); PR=Puerto Rico; A = Antigua (arrowed); LA=Lesser Antilles; T=Trinidad; V=Venezuela; Co=Colombia.**

**Figure 2. Measured section in the lower part of the cliff at Hughes Point (Locality 1), Nonsuch Bay, Antigua Formation (modified after Collins and Donovan, 1995, fig. 2). Key: F, M, C = fine-, medium- and coarse-grained sandstone, respectively; P = pebble conglomerate; K = cobble conglomerate; all rocks are limestone.**

**Figure 3. A measured section of the northeast point of Half Moon Bay (Locality 2), parish of Saint Philip, south-east Antigua; Antigua Formation (Upper Oligocene) (after Donovan *et al*., 2015, fig. 3). Note the section is entirely in limestone; terms such as sandstone and mudrock refer to grain size. Crinoid columnals and a brachiopod were collected from bed 4; crinoid columnals are present, but rare, higher in the section.**

**Figure 4. Elemental maps of specimens from both localities. A. Elemental maps showing the distribution of Si, Ca and O of a sample from Hughes Point of the oyster *Hyotissa antiguensis*. B. Elemental maps showing the distribution of Si, Ca and O of the Half Moon Bay sample of *Aequipecten*? sp. Scale bars represent 100µm.**

**Figure 5. SEM and CL images of specimens from Hughes Point and Half Moon Bay. A. SE image showing the relationship of calcite to silica zones in the oyster *Hyotissa antiguensis*. B.**

**SEM-CL of same area and specimen as (A), showing distinct mottled texture (red arrow). C. SE image of *Aequipecten*? sp. from Half Moon Bay, showing the distribution of calcite and silica zones. D. SEM-CL of same area and specimen as (C), showing differing luminosity in silica and mottled textures (red arrows). Scale bars represent 20 µm (above) and 10 µm (below). Abbreviations: Cc – calcite; Qz – quartz.**

**Figure 6. CL-SEM spectrum of quartz; emission band of this silica lies between 540 – 740 nm.**

| Spot | CaO | MgO | SiO | Total |
|---|---|---|---|---|
| 1 | 0 | 0 | 100.00 | 100.00 |
| 2 | 0 | 0 | 100.00 | 100.00 |
| 3 | 98.61 | 1.39 | 0 | 100.00 |
| 4 | 100.00 | 0.00 | 0 | 100.00 |

**Table 1. EDS data for specimen from Hughes Point (Locality 1). These data (wt.100%) are normalised to 100 and are calculated using the oxide option in QUANT software.**

| Spot | CaO | MgO | SiO | Total |
|---|---|---|---|---|
| 1 | 0 | 0.11 | 99.89 | 100.00 |
| 2 | 0 | 3.17 | 96.83 | 100.00 |
| 3 | 97.24 | 2.76 | 0 | 100.00 |
| 4 | 100.00 | 0 | 0 | 100.00 |

**Table 2. EDS data for specimen from Half Moon Bay (Locality 2). These data (wt.100%) are normalised to 100 and are calculated using the oxide option in QUANT software. Note – the value for MgO of 3.17 is probably an artefact.**

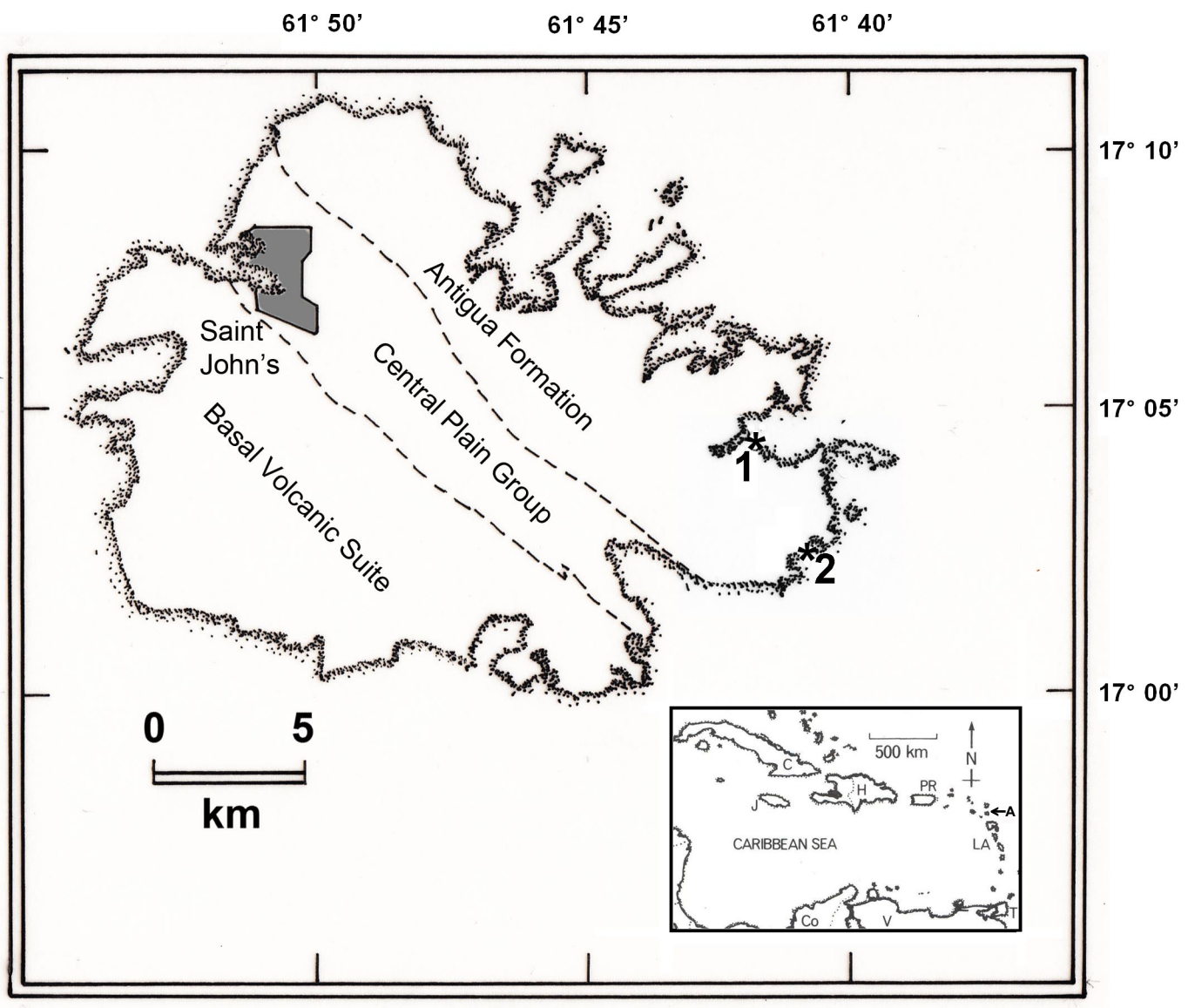
61° 50'
61° 45'
61° 40'
17° 10'
17° 05'
17° 00'
Saint John's
Antigua Formation
Central Plain Group
Basal Volcanic Suite
1
2
0
5
km
500 km
N
C
H
PR
J
A
CARIBBEAN SEA
LA
Co
V
T

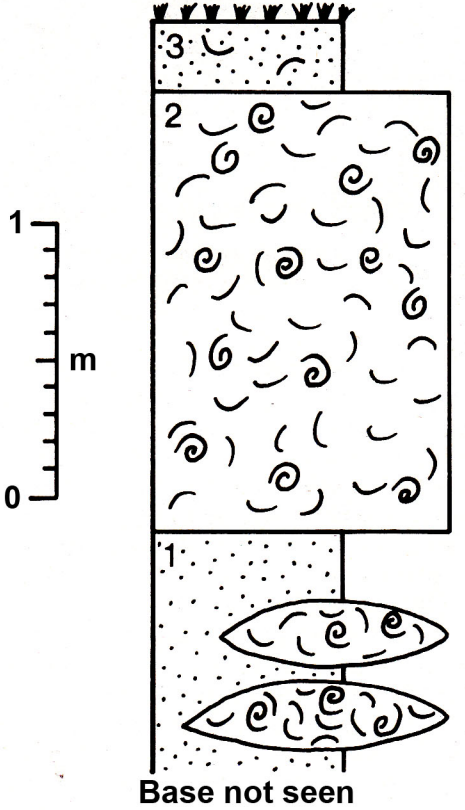


Similar to bed 1. Bioclasts include oysters and *Clypeaster.*

Conglomeratic bioclastic layer with bedding discontinuous and weakly developed on 10 cm scale. Clasts include oysters, scallop valves, *Clypeaster,* gastropods and coral debris; *Spondylus* and *Echinolampas* are rare. Matrix sandy and orange-brown in colour.

Fine-grained sandstones with conglomeratic lenses including large bioclasts (oysters, scallops, gastropods, *Clypeaster*). Fauna includes chelae of crab *Necronectes summus* Collins & Donovan.

F M C P K

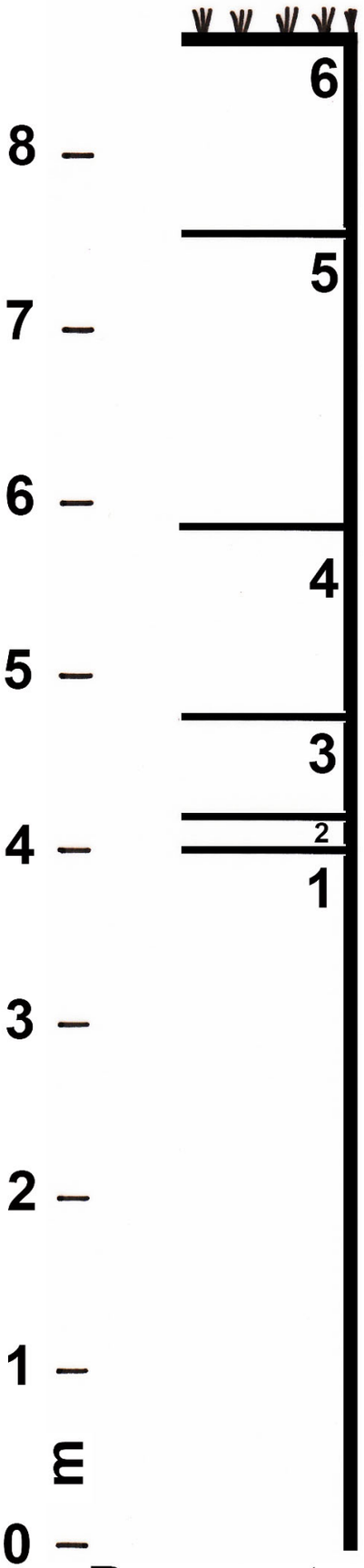


Base not seen

Medium-grained sandstone. Orange-brown colour. Large benthic foraminiferans, calcareous algae and shelly debris.

Silty mudrock. Pale grey (bottom) to orange brown. Poorly fossiliferous.

Fine- to medium-grained sandstone. *Thalassinoides* towards top. Crinoid columnals and brachiopods.

(2-3) Well-lithified fine-grained sandstone. Straw-brown colour. Abundant larger benthic foraminiferans, common echinoids, especially spatangoids. Calcareous algae.

Well-lithified fine-grained sandstone. Straw-coloured, but weathered brick red. Forms low sea cliff. Apparently unfossiliferous, but probably weathering effect.

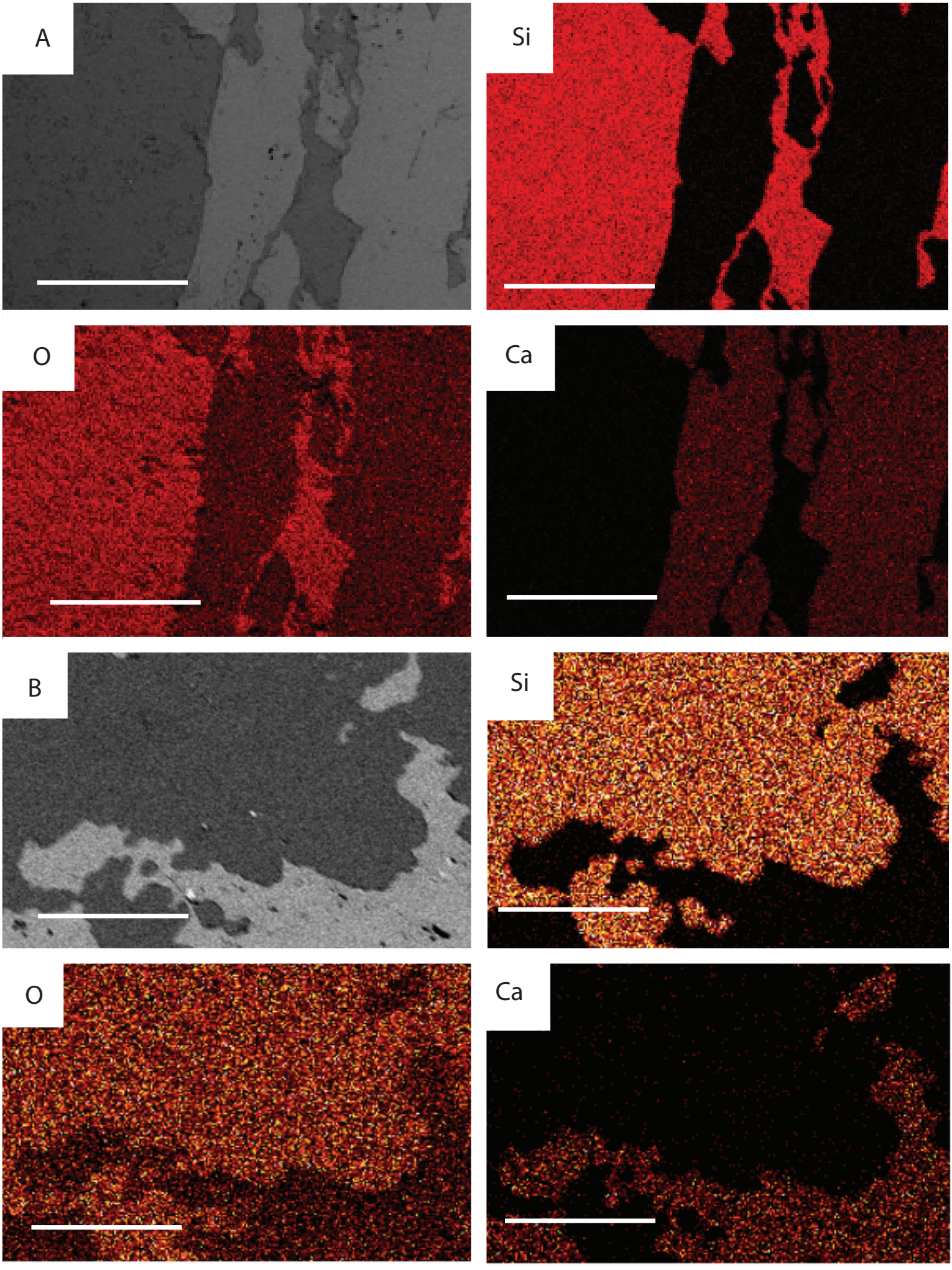
A
Si
O
Ca
B
Si
O
Ca

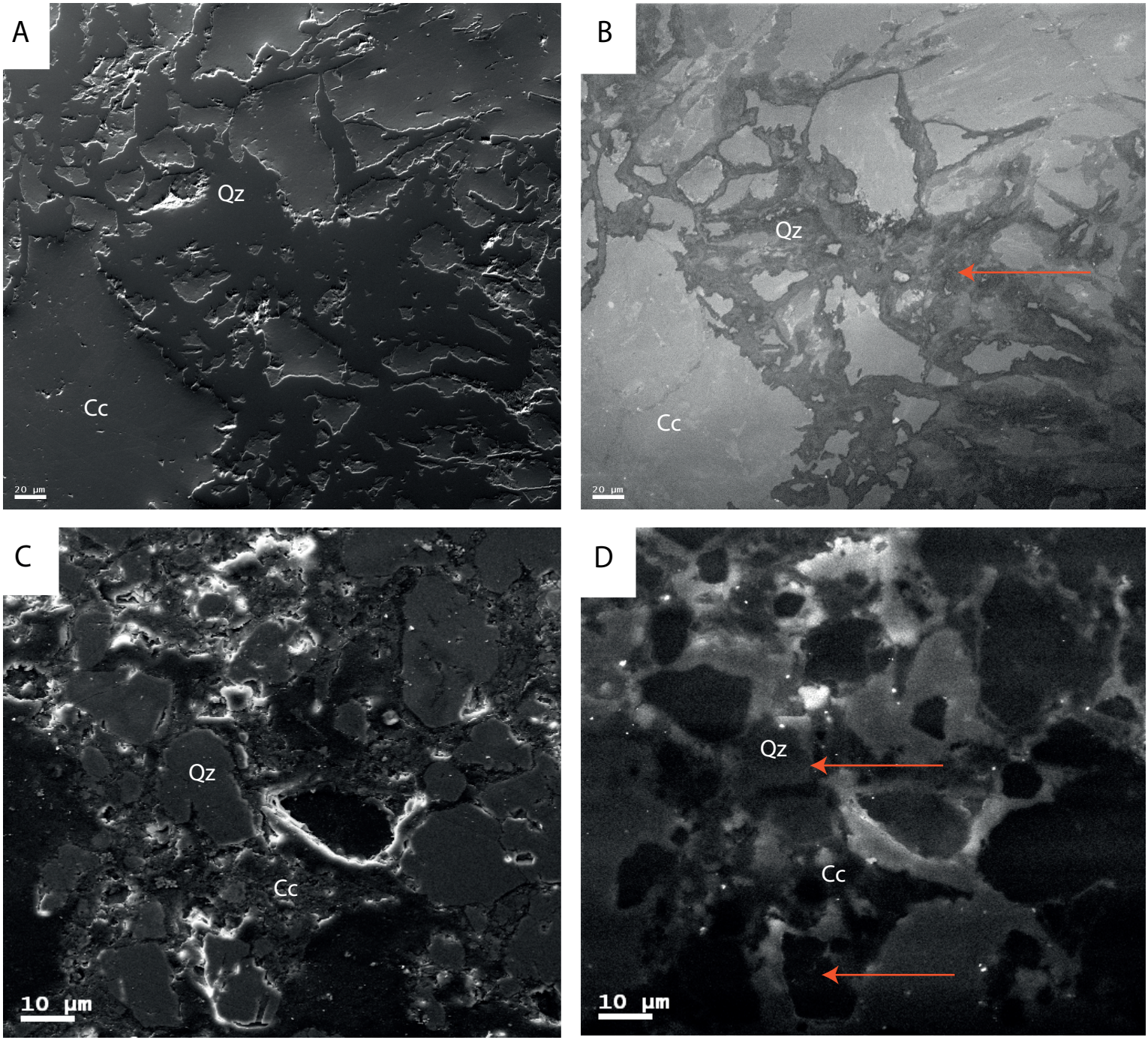
A
Qz
Cc
20 µm
B
Qz
Cc
20 µm
C
Qz
Cc
10 µm
D
Qz
Cc
10 µm

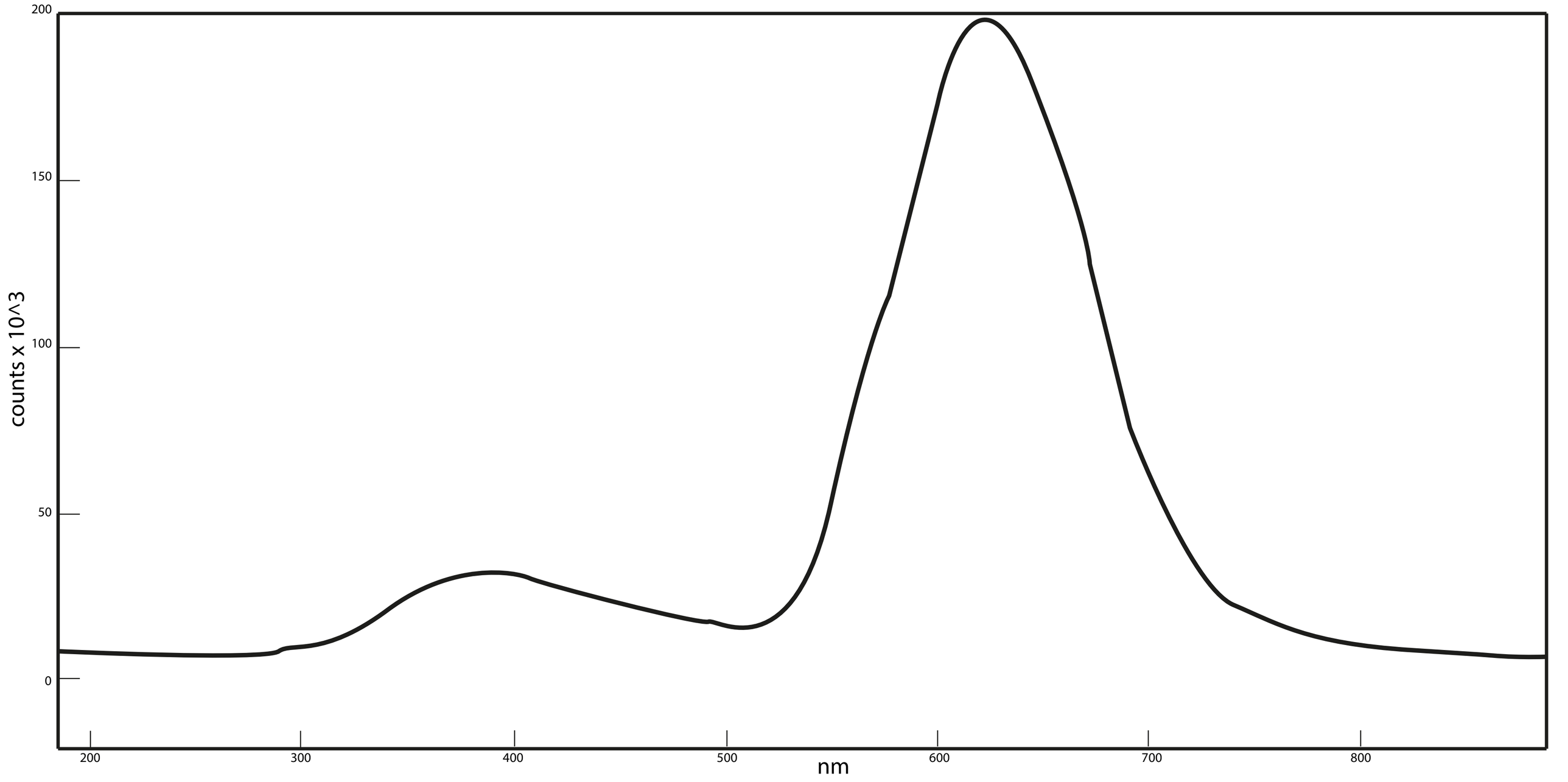
200
150
100
50
0
counts x 10^3
200
300
400
500
600
700
800
nm

# Appendix II. The Sirius Passet Lagerstatte: Silica death masking opens the window on the earliest matground community of the Cambrian explosion

Strang, K.M., Armstrong, H.A.A., Harper, D.A.T., Trabucho-Alexandre, J.P., 2016, The Sirius Passet Lagerstätte: silica death masking opens the window on the earliest matground community of the Cambrian explosion: Lethaia, v. 49, no. 4, p. 631–643.

Lethaia
AN INTERNATIONAL JOURNAL OF PALAEONTOLOGY AND STRATIGRAPHY

# The Sirius Passet Lagerstätte: silica death masking opens the window on the earliest matground community of the Cambrian explosion

KATIE M. STRANG, HOWARD A. ARMSTRONG, DAVID A. T. HARPER AND JOÃO P. TRABUCHO-ALEXANDRE

LETHAIA

Strang, K.M., Armstrong, H.A., Harper, D.A.T. & Trabucho-Alexandre, J.P. 2016: The Sirius Passet Lagerstätte: silica death masking opens the window on the earliest matground community of the Cambrian explosion. *Lethaia*, DOI: 10.1111/let.12174.

The Sirius Passet Lagerstätte (SP), Peary Land, North Greenland, occurs in black slates deposited at or just below storm wave base. It represents the earliest Cambrian microbial mat community with exceptional preservation, predating the Burgess Shale by 10 million years. Trilobites from the SP are preserved as complete, three-dimensional, concave hyporelief external moulds and convex epirelief casts. External moulds are shown to consist of a thin veneer of authigenic silica. The casts are formed from silicified cyanobacterial mat material. Silicification in both cases occurred shortly after death within benthic cyanobacterial mats. Pore waters were alkali, silica-saturated, high in ferric iron but low in oxygen and sulphate. Excess silica was likely derived from remobilized biogenic silica. The remarkable siliceous death mask preservation opens a new window on the environment and location of the Cambrian Explosion. This window closed with the appearance of abundant mat grazers later as the Cambrian Explosion intensified. ☐ *Cyanobacteria, depositional environment, silicification, Sirius Passet Lagerstätte, trilobite taphonomy.*

*Katie M. Strang [k.m.strang@durham.ac.uk], Howard A. Armstrong [h.a.armstrong@durham.ac.uk], and David A. T. Harper [david.harper@durham.ac.uk], Department of Earth Sciences, Palaeoecosystems Group, Durham DH1 1LE, UK; João P. Trabucho-Alexandre [j.trabucho@uu.nl], Institute of Earth Sciences Utrecht, Utrecht University, Budapestlaan 4 3584 CD Utrecht, The Netherlands;* *manuscript received on 20/04/2015; manuscript accepted on 11/12/2015.*

The Cambrian Explosion records the diversification of complex, mainly bilaterian, animal body plans and the expansion of animal-based marine ecosystems (Butterfield 2003). Much of what we know about this event is recorded in a succession of black shale conservation Lagerstätten. The Sirius Passet (SP) is the oldest of these and is located in J.P. Koch Fjord, N. Greenland, at 82°47.6′N, 42°13.7′W (Fig. 1A) and during the Cambrian lay at approximately 10°S (Fig. 1B; Peel & Ineson 2011). The black slates have been mapped as the 'Transitional' Buen, previously interpreted as fine-grained turbidites (Peel & Ineson 2011). *Buenellus higginsi* is the most common macrofossil, indicative of the *Nevadella* Biozone in Laurentia, equivalent to the middle part of Stage 3 (lowest stage of Series 2; 520–535 Ma; see Babcock 2005).

The SP fauna is similar to that of the Burgess Shale, comprising ca. 50 species including trilobites, sponges, worms, halkieriids, lobopods and non-trilobite bivalved arthropods. The SP Lagerstätte predates the Burgess Shale (510 Ma) and Chengjiang biotas (520 Ma) and is therefore possibly the earliest example of high-fidelity, soft-tissue preservation in the Cambrian. As recognized from studies of other Lagerstätten, an understanding of taphonomy is crucial in aiding anatomical interpretations of the SP fauna and provides for a better understanding of the palaeoenvironment, community reconstruction and early diagenesis (e.g. Gaines & Droser 2005; Zhu *et al.* 2006).

Similarities have been drawn between the depositional setting of the Burgess Shale and SP, for example proximity to a submarine cliff line and supposed basinal, turbiditic sedimentation (Peel & Ineson 2011). These similarities have led to the untested inference that SP fossils show Burgess Shale-type preservation (Gaines *et al.* 2008; Peel & Ineson 2011). Burgess Shale-type preservation is defined as 'exceptionally preserved fossils whose primary taphonomic mode is one of non-mineralizing organisms preserved as carbonaceous compressions in fully marine sediments' (Butterfield 1995). In the Burgess Shale, the soft-bodied fossils are preserved as thin, multi-layered silvery films (Whittington 1980). Significant discussion has focused on the composition of the films. Are they predomi-

[The copyright line for this article was changed on April 28 after original online publication]

DOI 10.1111/let.12174 

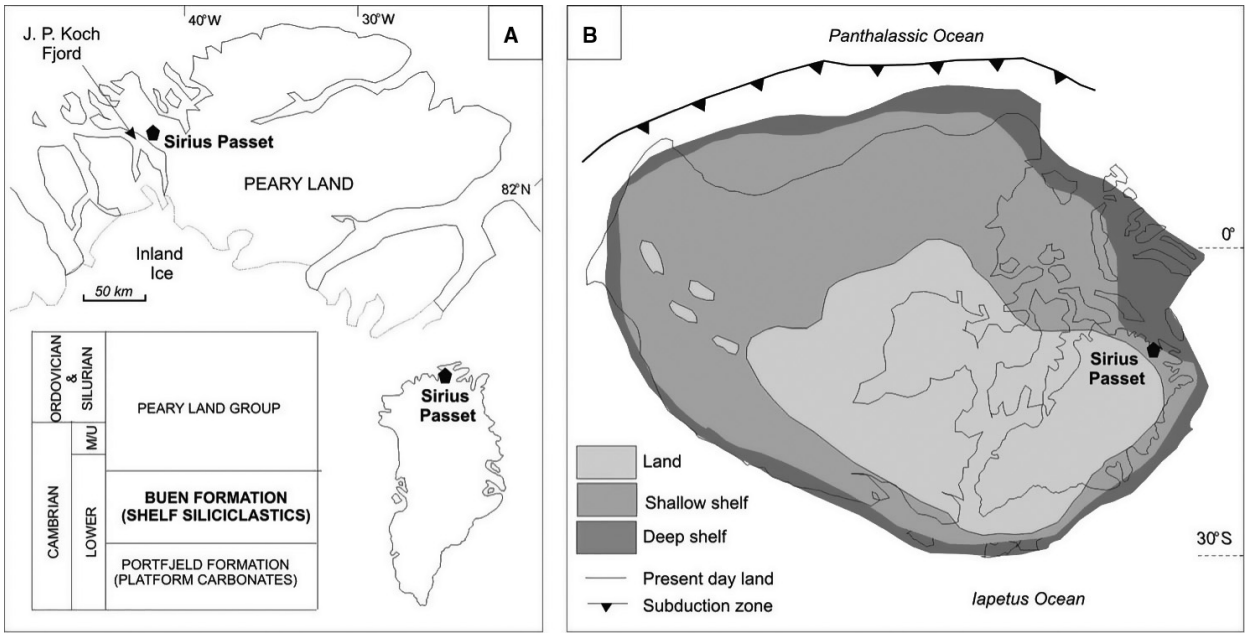


*Fig. 1.* A, Sirius Passet locality map, lithostratigraphy. B, Cambrian palaeogeography. Fig. 1B redrawn after Cocks and Torsvik (2011).

nantly organic and result from coalification during metamorphism (Butterfield 1990, 1995; Page *et al.* 2008) or predominantly composed of aligned clay minerals (Towe 1996; Orr *et al.* 1998)? Disagreement regarding the composition of the fossils has led to a lack of consensus regarding the mode of fossilization. Butterfield (1990, 1995) proposed that the clay which surrounded the fossils during burial acted as a catalyst that inhibited microbial decomposition of the labile tissues, leaving the organic material to be 'tanned' (Butterfield 1990) and producing a kerogen film during diagenesis. In comparison, Orr *et al.* (1998) concluded that fossilization occurred during decomposition as a consequence of chemical interactions between the tissues and the surrounding clays. In this model, variations in composition and reactivity of the different tissues during decomposition resulted in varying accumulations of clays on the carcass either by accumulation or direct precipitation from the pore water. The enhanced preservation of non-mineralized tissues may have also resulted from a combination of environmental factors. Near bottom anoxia would have prevented sediment irrigation by bioturbators. Reduced permeability of the seafloor and exclusion of oxygen may have also resulted from an absence of coarse grains such as silt, faecal pellets or bioclasts and the presence of reduced bottom waters that may have acted to deflocculate clay mineral aggregations and facilitated the precipitation of early diagenetic pore occluding carbonate cements (Gaines *et al.* 2005).

Some of the controversy surrounding the mechanisms of Burgess Shale-type preservation is in part due to the loss of primary features during post-depositional diagenesis and metamorphism. As a consequence of low greenschist facies metamorphism and cleavage formation, the phyllosilicates of the Burgess Shale currently associated with the fossils are not the same as the minerals that initially buried the fossils (Powell 2003). A detailed understanding of the metamorphic history and reconstruction of the primary bulk mineralogy of the Burgess Shale precludes the presence of highly reactive clay species necessary for the Butterfield model involving organic preservation due to clay-related suppression of decomposition-related reactions (Powell 2003). Instead, it indicates there was nothing unusual about the initial mud sediment and lends support to the Orr hypothesis of clay templating during decomposition (Powell 2003). This re-evaluation challenges the nature of Burgess Shale-type preservation and shows the importance of determining the mineralogical changes in Cambrian black shale Lagerstätten during metamorphism. This is critical for understanding the taphonomy, in which previous discussions of the SP, metamorphism has been largely ignored.

In this contribution, we use a combination of observations, petrography and SEM analyses to demonstrate the sequence of events leading to an early 'death mask' preservation of the trilobites within the SP and discount the influence of metamorphic processes. A key element of our proposed

trilobite taphonomy is the sealing of the specimens and early silicification, within the microbial mats on which they lived. This taphonomy though common in the Ediacaran is unique to the Cambrian and may only have existed for a short time due the absence of the mat grazing guild that appeared later in the Cambrian Explosion.

## Methods

Samples were collected during expeditions to SP led by Harper in 2009 and 2011. Thin (25 $\mu$m) double-polished thin sections, cut perpendicular to bedding, provided petrographic and textural data. Samples were studied for texture and composition using optical microscopy and scanning electron microscopy. Prior to SEM imaging, all samples were coated with a ca. 20 nm layer of carbon.

SEM imaging and analysis were carried out using the Hitachi SU-70 FEG SEM in Durham University using secondary electron and backscattered electron detectors at 15 kV. Both primary and secondary backscatter techniques were used to produce general images prior to elemental mapping (SEM-EDAX) and SEM-CL analysis. EDAX was carried out using the backscatter detector and the same voltage settings used for imaging. For point analysis, a cobalt standard was run before analysis to confirm quantitative results, and Tables 1 and S2 (See supplementary information) provide detailed mineralogical data. This was performed using the QUANT software and running the standard several times to ensure maximum accuracy (100 $\pm$ 5%).

SEM-CL (cathodoluminescence) was carried out using a mirror-type detector (Gatan Mono-CL) based in Durham University (Department of Physics). The machine was set to low magnification with a 10 kV voltage to allow the site of interest to be determined. The working distance was set to 20 mm and then adjusted as necessary to allow focusing of the sample. Working distance is then set to 16.2–16.7 mm and CL luminosities collected. Results were obtained using both the panchromatic mode (mono-CL) with both mirrors adjusted to panchromatic settings and then each colour filter was inserted one by one (red >600 nm, green >480–580 nm, and blue <480 nm). For individual grain studies, mono-CL was used to produce grey-scale pictures rather than true colour RGB CL. The former is faster at producing images with textural details, especially at high magnification (Schieber *et al.* 2000). Various studies have been carried out which show that quartz grains display a variety of luminescence intensities dependent on their provenance. The standards used were adapted from Seyedolali *et al.* (1997) and Schieber *et al.* (2000). CL intensity is dependent on the density of intrinsic and extrinsic defects within the band gap of the mineral. These defects are usually structural imperfections in the quartz crystal due to vacancies within the crystal lattice. These include point defects, translations, radiation damage, shock damage, melt inclusions and fluid inclusions. These types of defects can provide information on the conditions during mineralization and subsequent post-mineralization events such as deformation and metamorphism (Frelinger *et al.* 2014). The results were compared to other quartz CL provenance data in the literature to identify the luminosities.

Bulk mineralogy was checked using XRD of the <2$\mu$ clay fraction following the standard procedures outlined by Moore & Reynolds (1997). Rock samples were gently disaggregated in an agate mortar and pestle to avoid shearing the clays. Organic matter was removed by leaving the sample in a solution of 5% hydrogen peroxide until reaction ceased. The sample was then centrifuged at 2000 rpm, before decanting the supernatant liquid. Distilled water was then added and the sample was stirred. This was repeated until the supernatant liquid was neutral and the clay no longer fluctuated. Separation of clay fraction and saturation for XRD analysis was carried out using the following procedure. About 5 ml of dispersion agent was added and the sample was stirred well before centrifuging for 84 seconds at 800 rpm. The supernatant liquid was decanted into another tube. These steps were repeated until the sample was clean. Separated clays were then air-dried and samples placed on coverslips. Samples were analysed in a Bruker D8 Advance Diffractometer. CuK$\alpha$ radiation counting ranged from 2 to 60°

*Table 1.* Bulk-rock chemistry (in wt. %) of the low-carbonate Burgess Shale metamudstones (Walcott Quarry, Raymond Quarry and Tuzoia Beds extracted from Powell 2003) compared with the bulk-rock chemistry of SP.

| Wt. % | Walcott 1 | Walcott 2 | Raymond | Tuzoia | PAAS | Sirius Passet |
|---|---|---|---|---|---|---|
| $SiO_2$ | 53.71 | 50.34 | 50.10 | 50.63 | 62.8 | 63.46 |
| $Al_2O_3$ | 24.11 | 23.32 | 21.25 | 24.54 | 18.90 | 26.61 |
| $K_2O$ | 6.75 | 7.07 | 4.15 | 6.15 | 3.70 | 4.39 |
| K/Al | 0.280 | 0.303 | 0.195 | 0.250 | 0.196 | 0.165 |

$2\theta$ with a 0.02° $2\theta$ steps at 0.85 seconds per step. Lower angles were run than in bulk analysis in order to see low-angle clay peaks. Standard d spacing was calculated following Moore & Reynolds (1997).

# Results

## *Specimens*

*Buenellus* specimens are preserved complete, in life position and in 3-D. Two types of preservation are shown: (1) concave external moulds comprise thin (<1 mm) veneers of silica (Fig. 2A); and (2) convex epirelief casts composed predominantly of silicified microbial mat material (Fig. 2B, C). The microbial mat occurs as aggregates of hollow, cell-like structures with only the cell wall mineralized. Two microbial textures are preserved: (1) the sheath, which consists of small (<5 $\mu$m) equidimensional cells and spherical vesicles up to 2 $\mu$m in diameter (Fig. 2D, E); and (2) tubular or dendritically branching microbial filaments (Fig. 2F), observed only on the surface of the fossils.

## *Sedimentary petrography*

The cleavage parallels sedimentary bedding and primary sedimentary textures are preserved. Two end-member lithofacies are recognized, a 'spotted' and a silt-rich facies (Fig. 3). The 'spotted' facies consists of structureless to discontinuously laminated phyllosilicates containing Al-rich chlorite-mica aggregates that are 10–20 $\mu$m in diameter (Fig. 3A, B). Significantly, outsized clasts of silicified microbial mat occur infrequently in both the 'spotted' facies and the silt-rich facies (Fig. 3C). The silt-rich facies consists of clay to very fine silt particles composed predominantly of phyllosilicates with minor detrital quartz grains in the silt fraction (Fig. 3D, E). Outsized, lenticular mud clasts are present in a few beds (Fig. 3F). Bedsets are planar and cross-laminated

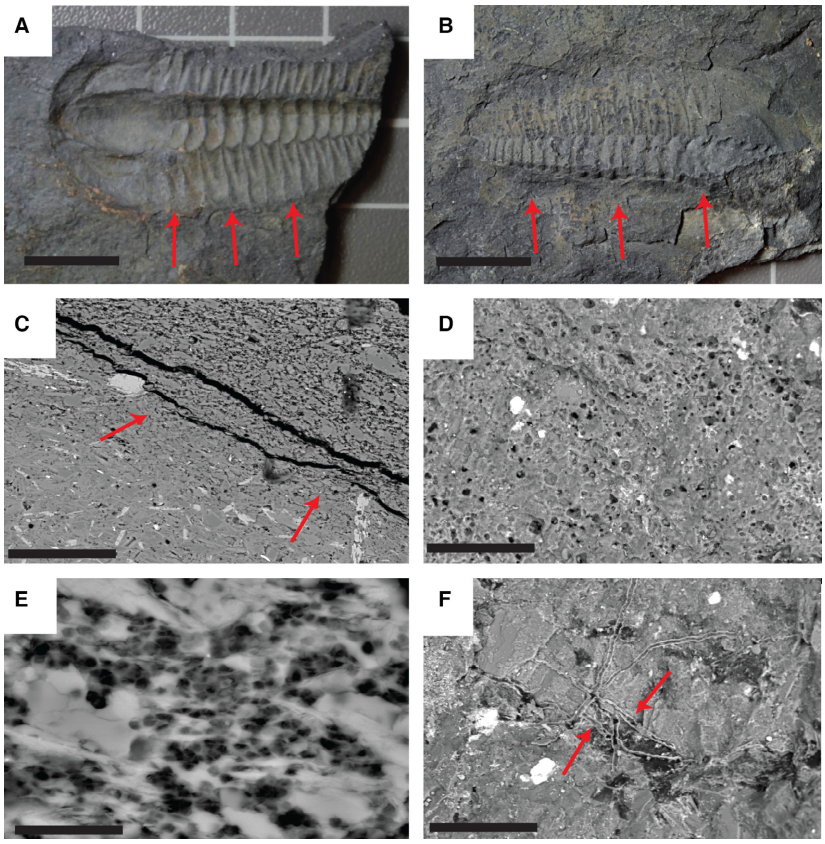


*Fig. 2.* High resolution photographs and SEM images. A, Image showing convex external mould of *Buenellus*; arrows indicate where thin sections were cut. Scale bar 1 cm. B, Convex epirelief cast of *Buenellus*; arrows indicate where thin sections were cut. Scale bar 1 cm. C, BSE SEM image showing matrix and microbial material; arrows indicate where mat material begins. Scale bar 1 cm. D, SE SEM image showing microbial mat material as aggregates of hollow, cell-like structures with only the cell wall mineralized, scale bar 1 cm. E, High magnification SEM BSE image showing 'webbed' silicified microbial mat structures. F, SEM SE image showing branching microbial filaments growing on the surface of the fossil. Scale bar 100 mm.

(Fig. 3G), with sharp to gradational boundaries between coarser and finer layers (Fig. 3H).

## *Bulk mineralogy*

Bulk-rock composition is similar to that of average shale (Post-Archean Australian Shale (PAAS), but differs from the Burgess Shale or PAAS in higher detrital quartz, lower K/Al (0.165, see Supporting information) and an absence of calcite (Table 1). The mineral assemblage of chlorite–mica–quartz and minor/trace of carbon, albite and illite and the absence of sulphates is found to be stable from upper sub-greenschist to middle greenschist facies (Powell

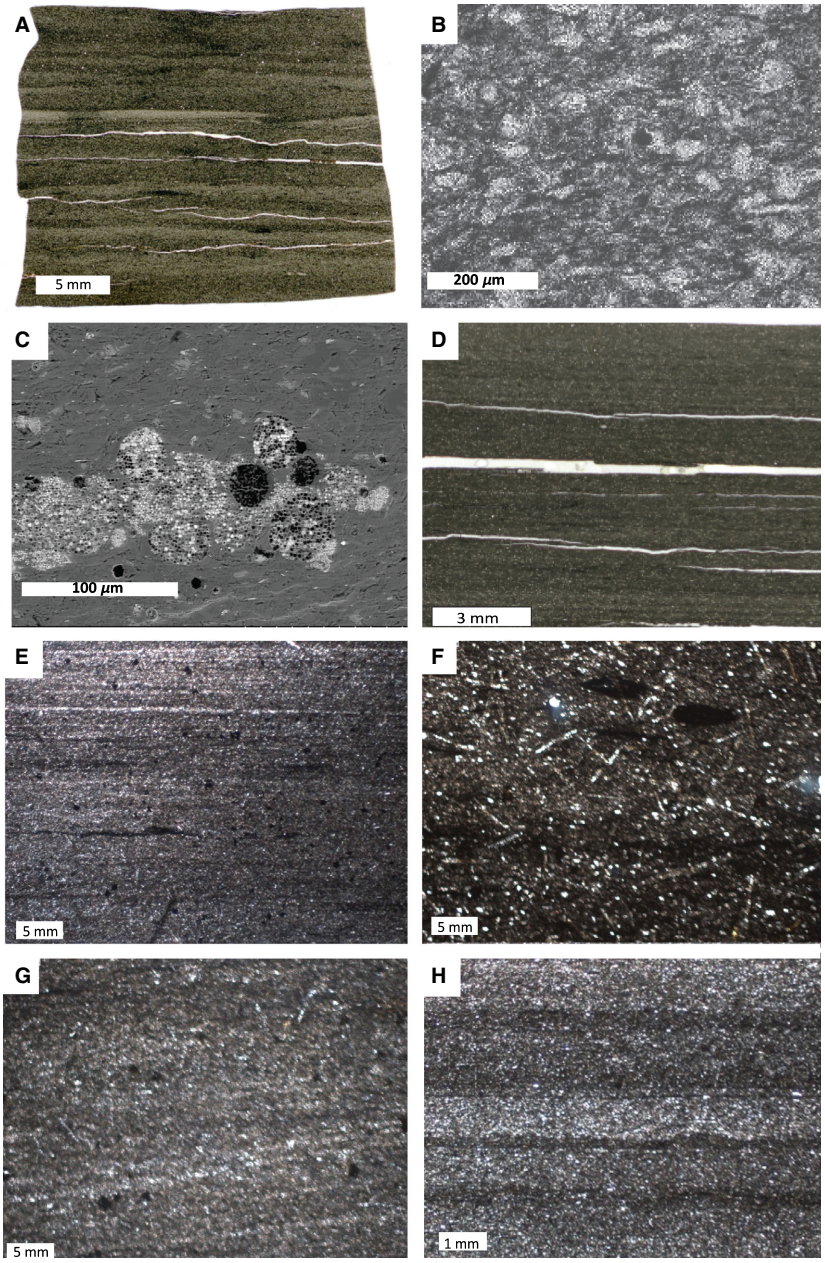


*Fig. 3.* Thin section photomicrographs; SEM and BSE images showing the different facies types. A, High resolution photomicrograph of a thin section showing the concentration of chlorite-mica aggregates into discontinuous wavy beds (3.4 m from base of log). B, Photomicrograph in plane polarized light showing chlorite-mica aggregates of varying sizes (1.12 m above base of log). C, BSE photomicrograph of silicified microbial mat fragment in the silt rich facies (5.5 m above base of log). D, Photomicrograph of a thin section showing laminated fabric and continuous and discontinuous silt layers (2.62 m from base of log). E, Photomicrograph in plane polarized light showing lamination picked out by single grain thickness layers of detrital quartz (4.56 m up from base of log). F, Photomicrograph in plane polarized light showing elliptical outsized floating grains of dark mudstone within a matrix of phyllosilicates, quartz, and chloritoid porphyroblasts (3.31 m above the base of log). G, Photomicrograph showing planar cross laminated bedsets. H, Photomicrograph of the silt rich facies showing sharp to gradational boundaries between course and fine layers.

2003). The absence of carbonate is a consequence of the sediment having passed through the smectite–illite transition (S-I; below). Abundant chloritoid porphyroblasts are indicative of low greenschist facies metamorphism (Higgins *et al.* 2001; equivalent to ~10 km burial) and their random orientation relative to bedding indicates relatively low-pressure conditions or possible formation during retrogressive regional metamorphism. Chloritoid is represented by the general formula $(Fe,Mg,Mn)Al_2SiO_5(OH)_2$ and occurs in high-Al, low-temperature metapelites (Halferdahl 1961). It is normally formed through the reaction of pyrophyllite, a phyllosilicate clay and chlorite-forming chloritoid, quartz and water. During this reaction, any excess silica can be precipitated as inclusions within the chloritoid. Quartz inclusions are common in the chloritoid needles and appear as irregular shaped grains within the needle.

Total organic carbon ranges from 0.5 to 1%. However, Raiswell & Berner (1986) documented an exponential loss of organic carbon relative to vitrinite reflectance in shales. Lower greenschist facies metamorphism would correspond to a minimum vitrinite reflectance of 5% (Kisch 1987). Projecting the Raiswell & Berner curve to a greenschist facies equivalent yields an estimated organic carbon preservation of 15%. The initial organic carbon content of the SP would therefore have been >3%, a value typical for many oil source rocks.

### *SEM-EDAX*

Quantitative elemental mapping across a convex epirelief cast of *Buenellus* (Fig. 4A) shows typical values for Si (84%), Al (11%) and Fe (5%) compared with the matrix (Supporting Information Tables S1–S3). There is evidence of small framboidal pyrite associated with the mat material, which is absent from the matrix (Fig. 4B).

### *SEM-CL*

Panchromatic cathodoluminescence analysis shows the presence of two quartz phases. Detrital quartz grains in the matrix exhibit true colour RGB-CL brown shade of luminescence at around 540–550 nm (Fig. 4C). Silica in the mineralized mat and concave external moulds exhibits almost no luminescence (Fig. 4D). Mono-CL of metamorphic quartz grains found as inclusions within the chloritoid needle shows medium grey luminosity and a mottled texture (Fig. 4E). These were compared with individual grains of silica associated with the fossils, which exhibit no luminosity under mono-CL and appear black and textureless (Fig. 4D).

## Discussion

Marine carbonaceous shales in the Cambrian were limited to shallow-water regions with turbulent circulation (Raiswell & Berner 1986). The presence in the SP of normal and reverse grading, scouring and cross-lamination indicates deposition from low-density sediment gravity flows at or just below storm wave base. Cross-lamination suggests sediment transport by ripple migration. Compacted mud ripples have been observed as extremely low-angle cross-lamination in ancient mudstones (Komárek & Anagnostidis 1986) and are consistent with sediment transport by mud-laden sediment gravity flows (Kremer & Kazmierczak 2005). The presence of oversized clasts in the normally graded sediment suggests flows had sufficient competence to transport larger clasts, such as a denser, mud-rich 'slurry-flow', transitional between a turbidity current and a debris flow (Komárek & Anagnostidis 1986).

The chlorite–mica aggregates in the spotted facies could have originated as primary detrital grains modified during weathering and transport or, formed as the result of diagenetic or metamorphic minerals mimicking existing sedimentary textures (see Craig *et al.* 2009). Aggregates are concentrated into discontinuous beds. These beds are sharp-based, normally graded with scour fills and faint cross-lamination. The aggregates were probably transported and size-sorted at the seafloor. Normal grading suggests deposition was from sediment gravity flows producing successive beds of rapidly accumulated sediment (Best 2005). The fabric is primary and the texture produced by metamorphism is inherited from a pre-existing sedimentary texture. Today, aggregates are produced largely by the activities of organisms living in the water column (e.g. through filter feeding, faecal pellet production, test building) or random collisions between grains in the water column (McCave 1985). The dense accumulations of pellets suggest these were originally hemipelagites deposited during quiescent periods.

If an average uncompacted thickness of 50 m (10 m compacted) for the SP and an age span of ca. 3 myr for the interval are taken, then a minimum average, long-term sedimentation rate of about 15 mm/kyr is realistic. We infer that this high sedimentation rate improved the chance of the fossils being buried, isolating them from the oxidizing environment at the seafloor. Given the lack of penetrative burrowing, it is likely that pore waters were already anoxic a few millimetres below the seafloor.

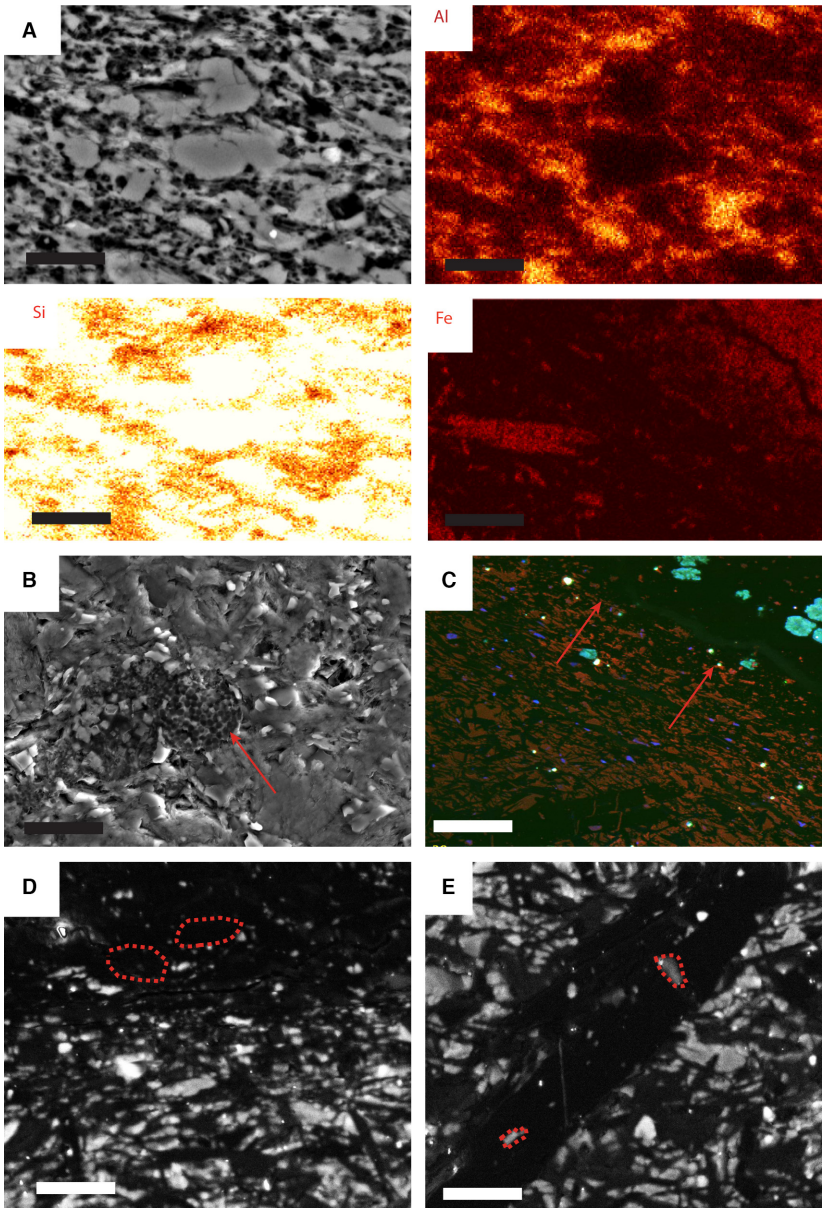


*Fig. 4.* A, elemental maps (top left SEM image to show locality of maps) taken across the mat material. Al, Si and Fe maps shown, notice the abundance of silica. Scale bar – 20 $\mu$m. B, BSE SEM image showing framboidal pyrite associated with the mat material. Scale bar 30 $\mu$m. C, RGB true colour CL showing brown shades of luminescence in the matrix, above arrows indicate area of mat material which has a distinctly different luminosity. D, mono-CL image, bottom half of image is matrix, whereas the top shows microbial material. Grains of non-luminescing silica associated with the fossils have been outlined (dashed line). Scale bar 20 $\mu$m. E, mono-CL image of chloritoid needle. Inclusions of metamorphic silica showing medium grey luminosity are outlined (dashed line). Scale bar 10 $\mu$m.

In modern pericontinental shelves, distance from shore is a good proxy for water depth. The SP pericontinental shelf was much wider than modern analogues (Fig. 5). Due to their distance from shore, distal, yet shallow-water deposits on wide shelves may have biological and geochemical characteristics indicative of deeper-water facies. On very wide shelves, with sufficiently low seafloor gradients, incoming waves dissipate their energy well before reaching the shore (Keulegan & Krumbein 1949). This may explain why, despite the large fetch expected from the palaeogeographical setting of SP, the shallow seafloor would be little subjected to swell, thereby allowing mud deposition. The seafloor was also consolidated by mat-forming cyanobacteria shortly after deposition.

Similar storm-influenced environments are proposed for the dark grey to black laminated mudstones of the Emu Bay Shale (Jago *et al.* 2012), the Alum (Thickpenny & Leggett 1987) and Burgess

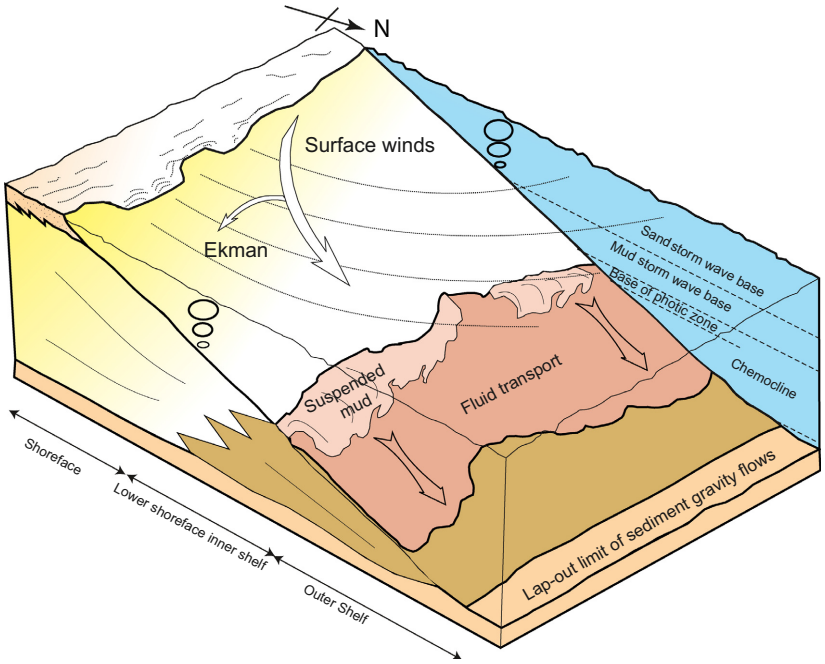


*Fig. 5.* Block diagram illustrating the depositional environment at Sirius Passet during the Early Cambrian (modified after Plint 2014).

Shales (Gabbott *et al.* 2008). In common with the SP, these deposits also lack penetrative bioturbation, suggesting anoxic conditions immediately below the seafloor. The presence of a diverse invertebrate benthos in the SP and an absence of pyrite framboids in the matrix indicate the lower water column was oxic with a sharp redox boundary at the sediment–water interface. Bioturbation is surficial and typically only occurs in association with generally large arthropod carcasses (Mangano *et al.* 2012). Benthic cyanobacteria were the dominant photoautotrophic and oxygenic microorganisms in the SP and could have produced or enhanced the oxygenated conditions at the seafloor. However, in extant cyanobacterial mats, sulphate reduction in the biomass can produce periodic hydrogen sulphide ($H_2S$) emissions above the mat surface, particularly at night (Jørgensen 1979). This could have been a major factor impeding the settlement of benthic organisms on the seafloor. The mat-dwelling fauna was ephemeral and either able to escape $H_2S$ emissions or had adapted a resistance to short-lived $H_2S$ toxicity. Occasional massive $H_2S$ expulsion from the decaying mats might have led to mass mortalities of the mat-dwelling community (see also Weeks *et al.* 2002).

Microbial mat textures observed on the concave external moulds, epirelief convex casts and evidence of microbial mat growing over trilobites (see Mangano *et al.* 2012; fig. 1) indicate that the fauna was an autochthonous matground community previously only known from trace fossil evidence (Buatois *et al.* 2014).

The dense cellular aggregates comprising the microbial textures are compared with colonies of modern coccoid cyanobacteria, particularly with the exclusively benthic *Entophysalis* or *Chlorogloea* (e.g. Kremer & Kazmierczak 2005). The globular structures (Figs 2E, 3C) resemble the encapsulated aggregates of extant benthic coccoid cyanobacteria Pleurocapsales, particularly *Chroococcidiopsis* and *Stanieria* (Komárek & Anagnostidis 1986; Silva & Pienaar 2000; Kremer & Kazmierczak 2005). Similar structures have been documented from the Athel Silicyte in the South Oman Salt Basin, Sultanate of Oman by Rajaibi *et al.* (2015), and provide evidence of microbially mediated syndepositional precipitation of silica. These genera are known from freshwater and marine environments, and some pleurocapsaleans are adapted to low light levels within the photic zone (Stal & Walsby 2000). Similar material has been described from the Proterozoic (Gehling 1999) and Silurian (Kremer & Kazmierczak 2005). As cyanobacteria are a morphologically conservative group, SP specimens are probably part of the same groups.

We propose the arthropod-lobopodian fauna that characterizes the Sirius Passet inhabited a warm, muddy, matground habitat close to or just below storm wave base, but within the photic zone. We have found no evidence for aeolian deposition of clay or silt in the field or in our thin sections, in contrast to the study by Boudec *et al.* (2014). Primary productivity was principally by benthic cyanobacteria. Contemporary shallow subtidal to intertidal car-

bonate environments had a distinct shelly fauna including archaeocyathans, halkieriids, tommotiids, hyoliths, molluscs, rare trilobites, and a variety of other small shelly fossils of unknown affinity (examples cited in Mount & Signer 1985). The rapid appearance in the geological record and ecological stability of the 'Burgess Shale-type assemblages,' over some 10 million years, suggests that rather than being long-lived holdovers, successively displaced from the shallow water (Mount & Signer 1985; Morris 2009), these animals were members of new Bambachian megaguilds (groups of organisms with mutually similar adaptive strategies), highly specialized and adapted to the dynamic and unstable nature of the tropical, muddy lower shoreface and shelf (Fig. 5).

The three-dimensional preservation of cyanobacterial structure, the hyporelief external moulds and particularly the epirelief casts indicate the trilobite carapace remained intact long enough for the internal labile tissues to decompose and the body cavity to be injected with mat material. Dewatering and compaction occurs during early burial. Experimental and core studies indicate porosity in muds is reduced to 33–36% by 175 m depth. Effective porosity (~70%) is lost by 1 km depth of burial (Hedberg 1936). At the inferred sedimentation rates, specimens that had not been permineralized would have been flattened to one-third the original volume after 100 kyr–1 myr, thus providing sufficient time for early silicification and critically before the S-I transition between 1.8 and 3.7 km depth of burial. Major mineralogical changes with depth take place over the S-I transition (Hower *et al.* 1976). The most abundant mineral, illite/smectite, undergoes a conversion from less than 20% to about 80% illite layers over this interval, after which the proportion of illite layers remains constant. As the transition proceeds, illite packets grow within a shrinking matrix of smectite, dislocations decrease and pathways for ion transport are restricted, this causes a loss of local permeability and a rise in the fluid pressure gradient. Consequent loss of hydraulic continuity with the surface and a more efficient geopressure seals the clay to fluid flow (Freed & Peacor 1989). In the S-I transition, calcite decreases from about 20 percent of the rock to almost zero, disappearing from progressively larger size fractions with increasing depth; potassium feldspar (but not albite) decreases to zero; and chlorite appears to increase in amount. At these depths, smectite reacts with $Al^{3+}$ and $K^{+}$ from the decomposition of potassium feldspar to form illite with the release of $Si^{4+}$. Magnesium and iron lost from the smectite form chlorite and ultimately chloritoid. The stable clay mineral assemblage following the S-I transition is thus illite, quartz and chlorite. All the major mineralogical and chemical changes, as the response to burial and metamorphism, occurred in a closed system for all components except $H_2O$, CaO, $Na_2O$ and $CO_2$ (Hower *et al.* 1976). Reactions during the S-I transition therefore explain the absence of calcite in the SP. The remaining reactions into lower greenschist facies metamorphism include conversion of remaining smectite to illite (up to ~175 °C) and the recrystallization of illite to micas (200–300 °C: Totten & Blatt 1993).

The timing of silicification is critical to understanding the taphonomic pathway. Silica supersaturation of pore fluids occurred due to the synsedimentary remobilization of biogenic silica; from silica released during the S-I transition or during greenschist facies metamorphism. Our key evidence for silicification being early, shortly after death includes the following:

1 The 3-D preservation of moulds and casts and cellular textures in the microbial mat material indicate silicification occurred before compaction and dewatering of the muds. The observation that 3-D cells are filled with monocrystalline quartz preserved within the cyanobacterial mat material indicates silica deposition prior to dewatering and compaction. Because the mat material is porous and the decay of labile cell contents occurred soon after death, it is unlikely that internal cell fluid pressure would have supported the primary structures on burial. Alternately, decay gasses from decomposition may have formed cavities (Reineck & Singh 1980) that prevented the collapse of the cells prior to silicification. A similar mechanism of mineral deposition in gas has been proposed for the formation of pyrite framboids in muds (e.g. Rickard 1970) and silica infilling of *Tasmanite* cysts (Schieber 1996). And the fact that spherical gas bubbles are found close to the sediment surface has been documented by Forstner *et al.* (1968). Silica deposition is therefore most likely to have occurred very early in diagenesis and within centimetres to decimetres of the sediment–water interface. At the proposed sedimentation rates for the SP, this would have been equivalent to a few thousand years of deposition;
2 The presence of synsedimentary rip-up clasts;
3 Microbial mat and convex external moulds are formed of non-luminescent, textureless silica.

Non-luminescing authigenic quartz lacks crystal lattice defects generated during metamorphism or volcanism (Seyedolali *et al.* 1997; Augustsson & Bahlburg 2003; Frelinger *et al.* 2014);

4 Metamorphic quartz inclusions in the chloritoid needles exhibit strong luminosity with a smooth to mottled texture. This is distinctly different from the silica associated with the fossils; and

5 The fact that chloritoid needles cross-cut all other textures indicates metamorphism occurred after silicification.

The presence of very early diagenetic silica deposition excludes a silica source during the S-I transition and during diagenetic to low-grade metamorphic recrystallization of illite to muscovite mica. Further, the early and largely biogenic porosity within the SP muds was filled by silica and not calcium carbonate (compare data from the Wheeler Formation: Gaines *et al.* 2005). That chalcedony appears to have been the initial silica phase deposited in the voids is not unusual, first documented by Folk & Weaver (1952) and subsequently in numerous other studies (e.g. Heath & Moberly 1971; Meyers 1977; Frondel 1978; Milliken 1979; Noble & Van Stempvoort 1989). The presence of pyrite framboids in the mat material indicates sulphate reduction and that pyrite remained a stable phase through to greenschist facies metamorphism.

Decay experiments show that silica precipitates from low-pH pore waters in extracellular and intracellular environments within a mat (Krauskopf 1959), particularly when the pore fluids have reduced dissolved sulphate (Birnbaum & Wireman 1985; Schultze-Lam *et al.* 1995). Soluble silica, in the form of monosilicic acid, $H_4SiO_4$, dissociates to $H_3SiO_4^-$ at pH values above ca. 9.7 (Birnbaum & Wireman 1985; Arp *et al.* 2003). $H_3SiO_4^-$ is a highly soluble form of silicic acid, and it reacts with hydrogen ions to form $SiO_2$ (Rickert *et al.* 2002; fig. 3). Silica nucleation and precipitation is sensitive to iron content of bottom/pore water and, in early Cambrian seawater, $Fe^{2+}$ appears to have been high relative to FeOOH (Muscente *et al.* 2014). We hypothesize that sediment–water was saturated in silica, high in $Fe^{2+}$ and low in oxygen and sulphate. Localized pH reduction was associated with the decay-initiated silica nucleation and precipitation within the mat. Silica-saturated pore waters could have been derived from the siliciclastic mud, by remobilization of biogenic silica (e.g. sponge spicules), or from the overlying seawater.

Early silicification as a mechanism of exceptional preservation is rare outside volcanic hot springs and a number of hypotheses for silicification have been proposed: (1) direct precipitation into void spaces; (2) microbial mediated silica precipitation (Schultze-Lam *et al.* 1995; Yee *et al.* 2003); and (3) chemically mediated silica precipitation (Patwardhan *et al.* 2011). It has been shown that microbial surfaces do not directly nucleate silica mineral formation; however, they play an important role in the aggregation of polymeric silica and the deposition of silica colloids on microbial surfaces (Patwardhan *et al.* 2011). For example, in modern hot spring environments, silica sinters actively form in close spatial relation to microorganisms (Yee *et al.* 2003 and references therein). Decay compounds, proteins and amino acids are all known to affect the kinetics, surface area of material, pore structure and particle size and are therefore implicated in silicification (Perry & Keeling-Tucker 2003). At present, we cannot distinguish between the different mechanisms proposed for silicification and all may have been important.

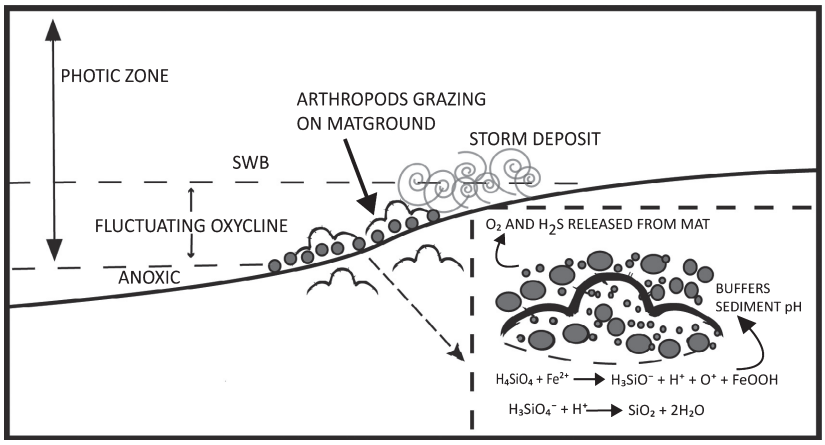


*Fig. 6.* Chemical pathways leading to the precipitation of silica and the reconstructed taphonomy of *Buenellus*.

Figure 6 shows our preferred taphonomic pathway. We propose that *Buenellus* was the dominant member of the matground community preserved in the SP. After death, the carapace was sealed by the growth of the microbial mat. During early burial, internal labile tissues decayed, and mat material was injected into the carcass to produce epirelief casts. The subsequent decay of the trilobite cuticle produced external moulds. All voids spaces were progressively infilled by silica as a consequence of localized pH reduction, associated with decay, occurring in the pore waters. Specimens were clearly permineralized, preserved in 3-D, before significant dewatering of the muds had taken place. Subsequent chemical reactions associated with the S-I transition and low greenschist facies metamorphism did not materially affect the preservation of the specimens.

Similar 'death mask' preservation has been described for the external moulds of soft-bodied Ediacaran biotas from the uppermost Proterozoic Rawnsley Quartzite, South Australia. However, in this example the sole veneer resulted from bacterial precipitation of iron minerals (Gehling 1999). A number of Cambrian Lagerstätten are characterized by pyritization of soft-bodied fossils, for example Chengjiang and Guanshan (Gabbott *et al.* 2004; Forchielli *et al.* 2014), secondary coating by iron (e.g. Emu Bay: Brett *et al.* 2009), or phosphatization (Zhu *et al.* 2014). Silica death mask preservation thus appears to be currently unique to the SP.

## Conclusions

The arthropod-lobopodian fauna that characterizes the Sirius Passet inhabited a warm, muddy, matground habitat close to or just below storm wave base, but within the photic zone. Primary productivity was principally by benthic cyanobacteria. Trilobites from the SP are preserved as complete, concave hyporelief external moulds and convex epirelief casts. External moulds are shown to consist of a thin veneer of authigenic silica. The casts are silicified cyanobacterial mat material. Early silicification is supported by the presence of synsedimentary mat rip-up clasts, 3-D preservation, which indicates silicification prior to sediment compaction and textural and mono-CL evidence. The growth of metamorphic chloritoid needles, which cross-cut the silica in the matrix, indicates that metamorphism occurred much later. It is hypothesized that silicification was initiated by falling pH in the decaying mat. Pore waters are interpreted to have been initially alkali, silica-saturated, high in ferric iron but low in oxygen and sulphate. Excess silica was likely derived from remobilized biogenic silica, probably sponge spicules in the muddy sediment. Decay resulted in a lowering of pore water pH and the conditions necessary for silicification. It is not clear whether silicification was microbially or chemically mediated.

The remarkable preservation during very early silica mineralization provides a new window on the environment and location of the Cambrian Explosion. The iconic organisms of the Cambrian Explosion formed the first mat ground communities. At least in the case of the SP the presence of cyanobacterial mats, sealing both the sediments and fossils, was fundamental to the preservation of this community. With the rise of mat grazing organisms during the later Cambrian, this taphonomic window disappeared.

*Acknowledgments.* – Leon Bowen, Ian Chaplin, Chris Greenwell and Manohara Gv gave technical assistance. GEUS (Geological Survey of Denmark and Greenland), The Danish Council for Independent Research, Agouron Institute and the Carlsberg Foundation provided funding. Strang is in receipt of a NERC CASE Studentship (RF050232). The manuscript benefitted from the recommendations of two referees and careful editing by Dr A. W. Owen.

## References

Arp, G., Reimer, A. & Reitner, J. 2003: Microbialite formation in seawater of increased alkalinity, Satonda Crater Lake, Indonesia. *Journal of Sedimentary Research 73*, 105–127.

Augustsson, C. & Bahlburg, H. 2003: Cathodoluminescence spectra of detrital quartz as provenance indicators for Paleozoic metasediments in southern Andean Patagonia. *Journal of South American Earth Sciences 16*, 15–26.

Babcock, L.E. 2005: Interpretation of biological and environmental changes across the Neoproterozoic-Cambrian boundary: developing a refined understanding of the radiation and preservational record of early multicellular organisms. *Palaeogeography, Palaeoclimatology, Palaeoecology 220*, 1–5.

Best, J. 2005: The fluid dynamics of river dunes: a review and some future research directions. *Journal of Geophysical Research 110*, F04S02.

Birnbaum, S.J. & Wireman, J.W. 1985: Sulfate-reducing bacteria and silica solubility: a possible mechanism for evaporite diagenesis and silica precipitation in banded iron formations. *Canadian Journal of Earth Sciences 22*, 1904–1909.

Boudec, A.L., Ineson, J., Rosing, M., Døssing, L., Martineau, F., Lécuyer, C. & Albarède, F. 2014: Geochemistry of the Cambrian Sirius Passet Lagerstätte, Northern Greenland. *Geochemistry, Geophysics, Geosystems 15*, 886–904.

Brett, C.E., Allison, P.A., DeSantis, M.K., Liddell, W.D. & Kramer, A. 2009: Sequence stratigraphy, cyclic facies, and Lagerstätten in the Middle Cambrian wheeler and Marjum formations, Great Basin, Utah. *Palaeogeography, Palaeoclimatology, Palaeoecology 277*, 9–33.

Buatois, L.A., Narbonne, G.M., Mángano, M.G., Carmona, N.B. & Myrow, P. 2014: Ediacaran matground ecology persisted into the earliest Cambrian. *Nature Communications 5*, 3544–3549.

Butterfield, N.J. 1990: Organic preservation of non-mineralizing organisms and the taphonomy of the burgess Shale. *Paleobiology 16*, 272–286.

Butterfield, N.J. 1995: Secular distribution of Burgess-Shale-type preservation. *Lethaia 28*, 1–13.
Butterfield, N.J. 2003: Exceptional fossil preservation and the Cambrian explosion. *Integrative and Comparative Biology 43*, 166–177.
Cocks, L.R.M. & Torsvik, T.H. 2011: The Palaeozoic geography of Laurentia and western Laurussia: a stable craton with mobile margins. *Earth-Science Reviews 106*, 1–51.
Craig, J., Fitches, W.R. & Maltman, A.J. 2009: Chlorite-mica stacks in low-strain rocks from central Wales. *Geological Magazine 119*, 243–256.
Folk, R.L. & Weaver, C.E. 1952: A study of the texture and composition of chert. *American Journal of Science 250*, 498–510.
Förstner, U., Müller, G. & Reineck, H. 1968: Sedimente und Sedimentgefüge des Rheindeltas im Bodensee. *Neues Jahrbuch für Mineraralogie Abh. 109*, 33–62.
Forchielli, A., Steiner, M., Kasbohm, J., Hu, S. & Keupp, H. 2014: Taphonomic traits of clay-hosted early Cambrian Burgess Shale-type fossil Lagerstätten in South China. *Palaeogeography, Palaeoclimatology, Palaeoecology 398*, 59–85.
Freed, R.L. & Peacor, D.R. 1989: Geopressured shale and sealing effect of smectite to illite transition. *AAPG Bulletin 73*, 1223–1232.
Frelinger, S.N., Ledvina, M.D., Kyle, J.R. & Zhao, D. 2014: Scanning electron microscopy cathodoluminescence of quartz: principles, techniques and applications in ore geology. *Ore Geology Reviews 65*, 840–852.
Frondel, C. 1978: Characters of quartz fibers. *American Mineralogist 63*, 17–27.
Gabbott, S.E., Xian-Guang, H., Norry, M.J. & Siveter, D.J. 2004: Preservation of Early Cambrian animals of the Chengjiang biota. *Geology 32*, 901–904.
Gabbott, S.E., Zalasiewicz, J. & Collins, D. 2008: Sedimentation of the phyllopod bed within the Cambrian Burgess Shale Formation of British Columbia. *Journal of the Geological Society 165*, 307–318.
Gaines, R.R. & Droser, M.L. 2005: New approaches to understanding the mechanics of Burgess Shale-type deposits: from the micron scale to the global picture. *The Sedimentary Record 3*, 4–8.
Gaines, R.R., Kennedy, M.J. & Droser, M.L. 2005: A new hypothesis for organic preservation of Burgess Shale taxa in the middle Cambrian Wheeler formation, House Range, Utah. *Palaeogeography, Palaeoclimatology, Palaeoecology 220*, 193–205.
Gaines, R.R., Briggs, D.E.G. & Yuanlong, Z. 2008: Cambrian Burgess Shale–type deposits share a common mode of fossilization. *Geology 36*, 755–758.
Gehling, J.G. 1999: Microbial mats in terminal Proterozoic siliciclastics: ediacaran death masks. *Palaios 14*, 40–57.
Halferdahl, L.B. 1961: Chloritoid: its composition, X-ray and optical properties, stability, and occurence. *Journal of Petrology 2*, 49–135.
Heath, G.R. & Moberly, R. Jr., 1971: Cherts from the western Pacific, Leg 7, Deep Sea Drilling Project. *In* Winterer E.L. & Riedel W.R., et al. (eds): *Initial Reports of the Deep Sea Drilling project*, *Volume 7*, U.S. Government Printing Office, Washington.
Hedberg, H.D. 1936: Gravitational compaction of clays and shales. *American Journal of Science 31*, 241–287.
Higgins, A.K., Leslie, A.G. & Smith, M.P. 2001: Neoproterozoic-Lower Palaeozoic stratigraphical relationships in the marginal thin-skinned thrust belt of the East Greenland Caledonides: comparisons with the foreland in Scotland. *Geological Magazine 138*, 143–160.
Hower, J., Eslinger, E.V., Hower, M.E. & Perry, E.A. 1976: Mechanism of burial metamorphism of argillaceous sediment: 1. Mineralogical and chemical evidence. *Geological Society of America Bulletin 87*, 725–737.
Jago, J.B., Gehling, J.G., Paterson, J.R. & Brock, G.A. 2012: Cambrian stratigraphy and biostratigraphy of the flinders ranges and the north coast of Kangaroo Island, South Australia. *Episodes 35*, 247–255.
Jørgensen, B. 1979: Diurnal cycle of oxygen and sulfide microgradients and microbial photosynthesis in a cyanobacterial mat sediment. *Applied and Environmental Microbiology 38*, 46–58.
Keulegan, G.H. & Krumbein, W.C. 1949: Stable configuration of bottom slope in a shallow sea and its bearing on geological processes. *Transactions, American Geophysical Union 30*, 855–861.
Kisch, H.J. 1987: Correlation between indicators of very low-grade metamorphism. *In* Frey M. (ed.): *Low Temperature Metamorphism*, 227–300. Blackie, Edinburgh.
Komárek, J. & Anagnostidis, K. 1986: Modern approach to the classification system of cyanophytes. 2-Chroococcales. *Archiv für Hydrobiologie Supplement 73*, 157–226.
Krauskopf, K.B. 1959: The geochemistry of silica in sedimentary environments. *Special Publications of SEPM 7*, 4–12.
Kremer, B. & Kazmierczak, J. 2005: Cyanobacterial mats from Silurian black radiolarian cherts: phototrophic life at the edge of darkness? *Journal of Sedimentary Research 75*, 897–906.
Mangano, M.G., Bromley, R.G., Harper, D.A.T., Nielsen, A.T., Smith, M.P. & Vinther, J. 2012: Nonbiomineralized carapaces in Cambrian seafloor landscapes (Sirius Passet, Greenland): opening a new window into early Phanerozoic benthic ecology. *Geology 40*, 519–522.
McCave, I.N. 1985: Recent shelf clastic sediments. *Geological Society, London, Special Publications 18*, 49–65.
Meyers, W.J. 1977: Chertification in the Mississippian Lake valley formation, Sacramento Mountains, New Mexico. *Sedimentology 24*, 75–105.
Milliken, K.L. 1979: The silicified evaporite syndrome–two aspects of silicification history of former evaporite nodules from southern Kentucky and northern Tennessee. *Journal of Sedimentary Research 49*, 245–256.
Moore, D.M. & Reynolds, R.C. Jr., 1997. *X-Ray Diffraction and the Identification and Analysis of Clay Minerals*, 2nd edn, xviii + 378 pp. Oxford, New York: Oxford University Press.
Morris, S.C. 2009: A redescription of a rare chordate, Metaspriggina walcotti Simonetta and Insom, from the Burgess Shale (Middle Cambrian), British Columbia, Canada. *Journal of Paleontology 82*, 424–430.
Mount, J.F. & Signer, P.W. 1985: Early Cambrian innovation in shallow subtidal environments: paleoenvironments of early Cambrian shelly fossils. *Geology 13*, 730–733.
Muscente, A.D., Hawkins, A.D. & Xiao, S. 2014: Fossil preservation through phosphatization and silicification in the Ediacaran Doushantuo Formation (South China): a comparative synthesis. *Palaeogeography, Palaeoclimatology, Palaeoecology 434*, 46–62.
Noble, J.P.A. & Van Stempvoort, D.R. 1989: Early burial quartz authigenesis in Silurian platform carbonates, New Brunswick, Canada. *Journal of Sedimentary Research 59*, 65–76.
Orr, P.J., Briggs, D.E. & Kearns, S.L. 1998: Cambrian Burgess Shale animals replicated in clay minerals. *Science 281*, 1173–1175.
Page, A., Gabbott, S., Wilby, P. & Zalasiewicz, J. 2008: Ubiquitous Burgess Shale-style 'clay templates' in low-grade metamorphic mudrocks. *Geology 36*, 855–858.
Patwardhan, S.V., Tilburey, G.E. & Perry, C.C. 2011: Interactions of amines with silicon species in undersaturated solutions leads to dissolution and/or precipitation of silica. *Langmuir 27*, 15135–15145.
Peel, J.S. & Ineson, J.R. 2011: The extent of the Sirius Passet Lagerstätte (early Cambrian) of North Greenland. *Bulletin of Geosciences 86*, 535–543.
Perry, C.C. & Keeling-Tucker, T. 2003: Model studies of colloidal silica precipitation using biosilica extracts from *Equisetum telmateia*. *Colloid & Polymer Science 281*, 652–664.
Plint, A.G. 2014: Mud dispersal across a Cretaceous prodelta: storm-generated, wave-enhanced sediment gravity flows inferred from mudstone microtexture and microfacies. *Sedimentology 61*, 609–647.
Powell, W. 2003: Greenschist-facies metamorphism of the Burgess Shale and its implications for models of fossil. *Canadian Journal of Earth Sciences 40*, 13–25.

Raiswell, R. & Berner, R.A. 1986: Pyrite and organic matter in phanerozoic normal marine shales. *Geochimica et Cosmochimica Acta 50*, 1967–1976.
Rajaibi, I.M., Hollis, C. & Macquaker, J.H. 2015: Origin and variability of a terminal proterozoic primary silica precipitate, athel silicilyte, South Oman Salt Basin, Sultanate of Oman. *Sedimentology 62*, 793–825.
Reineck, H.E. & Singh, I.B. 1980: *Tidal Flats. I Depositional Sedimentary Environments*, pp. 430–456. Springer, Berlin, Heidelberg.
Rickard, D.T. 1970: The origin of framboids. *Lithos 3*, 269–293.
Rickert, D., Schlüter, M. & Wallmann, K. 2002: Dissolution kinetics of biogenic silica from the water column to the sediments. *Geochimica et Cosmochimica Acta 66*, 439–455.
Schieber, J. 1996: Early diagenetic silica deposition in algal cysts and spores: a source of sand in black shales? *Journal of Sedimentary Research 66*, 175–183.
Schieber, J., Krinsley, D. & Riciputi, L. 2000: Diagenetic origin of quartz silt in mudstones and implications for silica cycling. *Nature 406*, 981–985.
Schultze-Lam, S., Ferris, F.G., Konhauser, K.O. & Wiese, R.G. 1995: In situ silicification of an Icelandic hot spring microbial mat: implications for microfossil formation. *Canadian Journal of Earth Sciences 32*, 2021–2026.
Seyedolali, A., Krinsley, D. & Boggs, S. 1997: Provenance interpretation of quartz by scanning electron microscope–cathodoluminescence fabric analysis. *Geology 25*, 787–790.
Silva, S.M. & Pienaar, R.N. 2000: *Benthic Marine Cyanophyceae from Kwa-Zula Natal, South Africa*. Gebruder Borntraeger Verlagsbuchland Lung, Berlin, 456 pp.
Stal, L.J. & Walsby, A.E. 2000: Photosynthesis and nitrogen fixation in a cyanobacterial bloom in the Baltic Sea. *European Journal of Phycology 35*, 97–108.
Thickpenny, A. & Leggett, J.K. 1987: Stratigraphic distribution and palaeo-oceanographic significance of European early Palaeozoic organic-rich sediments. *Geological Society, London, Special Publications 26*, 231–247.
Totten, M.W. & Blatt, H. 1993: Alterations in the non-clay-mineral fraction of pelitic rocks across the diagenetic to low-grade metamorphic transition, Ouachita Mountains, Oklahoma and Arkansas. *Journal of Sedimentary Research 63*, 899–908.
Towe, K.M. 1996: Fossil preservation in the Burgess Shale. *Lethaia 29*, 107–108.
Weeks, S.J., Currie, B. & Bakun, A. 2002: Massive emissions of toxic gas in the Atlantic. *Nature 415*, 493–494.
Whittington, H.B. 1980: The significance of the fauna of the Burgess Shale, Middle Cambrian, British Columbia. *Proceedings of the Geologists' Association 91*, 127–148.
Yee, N., Phoenix, V.R., Konhauser, K.O., Benning, L.G. & Ferris, F.G. 2003: The effect of cyanobacteria on silica precipitation at neutral pH: implications for bacterial silicification in geothermal hot springs. *Chemical Geology 199*, 83–90.
Zhu, M., Babcock, L. & Peng, S. 2006: Advances in Cambrian stratigraphy and paleontology: integrating correlation techniques, paleobiology, taphonomy and paleoenvironmental reconstruction. *Paleoworld 15*, 217–222.
Zhu, X., Lerosey-Aubril, R. & Esteve, J. 2014: Gut content fossilization and evidence for detritus feeding habits in an enrolled trilobite from the Cambrian of China. *Lethaia 47*, 66–76.

# Supporting Information

Additional Supporting Information may be found in the online version of this article:

**Table S1.** Results from EDAX (sample 4.56) silt-rich facies converted to oxides using INCA processing software.

**Table S2.** EDAX spectra from sample 1.12 m from the spotted facies converted to oxides using INCA processing software.

**Table S3.** EDAX spectra data from the mat material (taken from a cross section through an epirelief cast of *Buenellu*) from sample 340.103a.

**Fig. S1.** Graphic log of the Buen Formation at Sirius Passet.

**Fig. S2.** XRD plot of 2θ against intensity with labels showing normalized peaks for each main clay mineral, interpreted using Moore and Reynolds (1997). These data are from sample 0.06 which is the 'lozenge rich' facies.

**Fig. S3.** XRD plot of 2θ against intensity with labels showing normalized peaks for each main clay mineral, interpreted using Moore and Reynolds (1997). These data are for sample 4.56, the 'mud-rich' facies.

Supplementary information for

# The Sirius Passet Lagerstätte: Silica death masking opens the window on the earliest matground community of the Cambrian Explosion

KATIE M. STRANG, HOWARD A. ARMSTRONG, DAVID A.T. HARPER AND JOÃO P. TRABUCHO-ALEXANDRE

[1] Durham University, Department of Earth Sciences, Durham, DH1 1LE, UK
[2] Institute of Earth Sciences Utrecht, Utrecht University, Budapestlaan 4, 3583 CD Utrecht, the Netherlands

## Contents

1. **SEM and SEM-CL**
    a. **Geochemical data for the two facies types in SP (matrix)**
    b. **Geochemical data through convex epirelief cast of *Buenellus***
    c. **XRD results**
2. **Fieldwork, biostratigraphy, and depositional environment**
    a. **Biostratigraphical framework**
    b. **Depositional environment**

## 1. SEM and SEM-CL

### a. Geochemical data for the two facies types in SP

**See Figure S1 for a graphic log showing distribution of these two facies types.**

| Spectrum 4.56 | $Na_2O$ | MgO | $Al_20_3$ | $Si0_2$ | $K_20$ | Fe0 | Total |
|---|---|---|---|---|---|---|---|
| 1 | 0.00 | 1.39 | 44.64 | 30.04 | 0.34 | 23.59 | 100.00 |
| 2 | 0.00 | 0.00 | 0.49 | 98.11 | 0.00 | 1.40 | 100.00 |
| 3 | 0.81 | 0.73 | 33.01 | 56.62 | 7.88 | 0.95 | 100.00 |
| 4 | 0.00 | 0.00 | 9.52 | 86.65 | 0.51 | 3.32 | 100.00 |
| 5 | 0.67 | 1.15 | 34.65 | 54.60 | 7.48 | 1.44 | 100.00 |
| 6 | 0.63 | 0.46 | 34.98 | 54.90 | 8.41 | 0.61 | 100.00 |
| 7 | 1.01 | 0.79 | 29.00 | 61.87 | 6.45 | 0.88 | 100.00 |

Supplementary Table S1. Results from EDAX (sample 4.56) silt-rich facies converted to oxides using INCA processing software

| Spectrum 1.12 | MgO | $Al_2O_3$ | $SiO_2$ | $K_2O$ | FeO | Total |
|---|---|---|---|---|---|---|
| Spectrum 1 | 12.79 | 29.10 | 30.90 | 0.26 | 26.95 | 100.00 |
| Spectrum 2 | 12.53 | 27.01 | 30.85 | 1.03 | 28.58 | 100.00 |
| Spectrum 3 | 14.03 | 27.93 | 31.86 | 0.57 | 26.05 | 100.00 |
| Spectrum 4 | 0.00 | 0.56 | 97.85 | 1.16 | 0.43 | 100.00 |
| Spectrum 5 | 1.19 | 37.61 | 50.86 | 8.74 | 1.59 | 100.00 |
| Spectrum 6 | 0.69 | 31.82 | 58.75 | 7.46 | 1.29 | 100.00 |
| Spectrum 7 | 0.00 | 1.47 | 97.56 | 0.42 | 0.54 | 100.00 |

Supplementary Table S2. EDAX spectra from sample 1.12 m from the spotted facies converted to oxides using INCA processing software.

### b. Geochemical data for convex epirelief cast of *Buenellus*

| Spectrum Sample 340.103.a | $Na_2O$ | MgO | $Al_20_3$ | $Si0_2$ | $K_20$ | Fe0 | Total |
|---|---|---|---|---|---|---|---|
| 1 | 0.00 | 0.00 | 11.29 | 82.96 | 0.78 | 4.97 | 100.00 |
| 2 | 0.00 | 0.63 | 10.67 | 82.67 | 1.69 | 4.34 | 100.00 |
| 3 | 0.00 | 0.00 | 12.34 | 80.01 | 1.88 | 5.68 | 100.00 |
| 4 | 0.00 | 0.00 | 11.78 | 82.12 | 2.41 | 3.69 | 100.00 |
| 5 | 0.00 | 0.00 | 12.96 | 84.67 | 0.93 | 1.44 | 100.00 |
| 6 | 0.00 | 0.00 | 14.95 | 83.70 | 1.21 | 0.14 | 100.00 |
| 7 | 0.00 | 0.00 | 12.45 | 82.90 | 0.98 | 3.67 | 100.00 |
| 8. | 0.00 | 0.00 | 0.67 | 97.34 | 1.36 | 0.63 | 100.00 |

Supplementary table S3. EDAX spectra data from the mat material (taken from a cross section through an epirelief cast of *Buenellu* ) from sample 340.103a. Converted to oxides using INCA processing software.

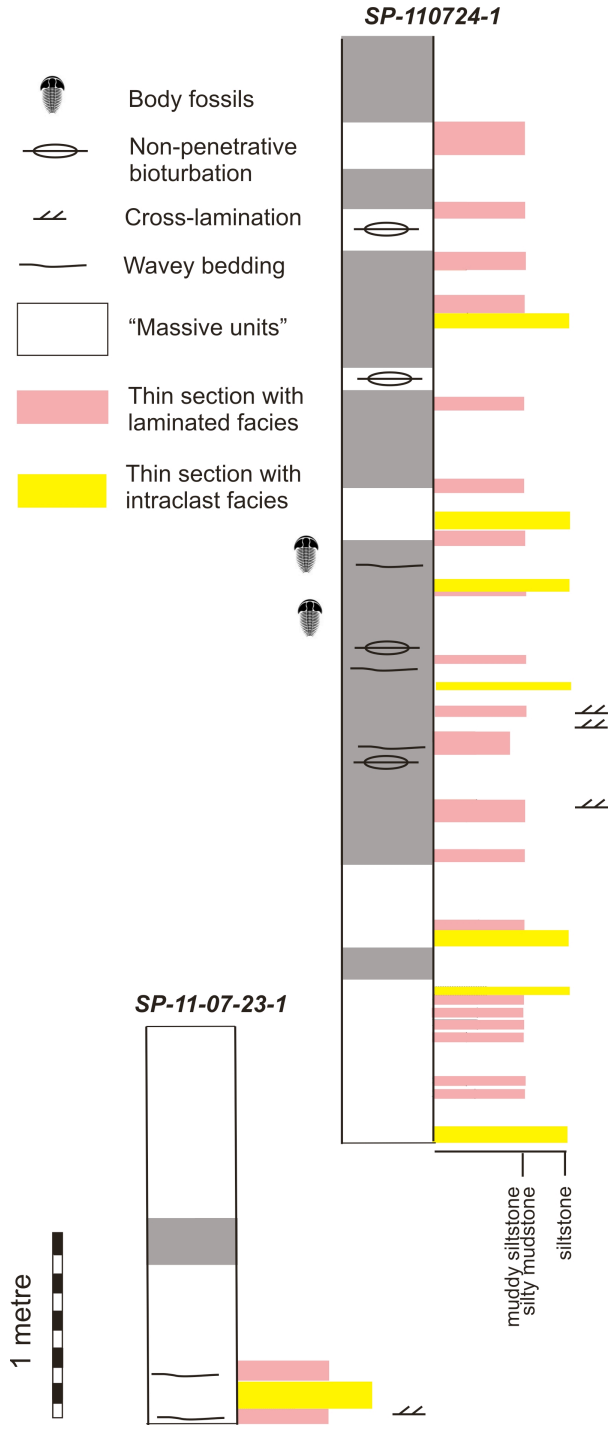


**Figure S1**. Graphic log of the Buen Formation at Sirius Passet. Pink bars indicate thin sections showing laminated facies. Yellow bars are thin sections with “spotted” facies.

## c. XRD

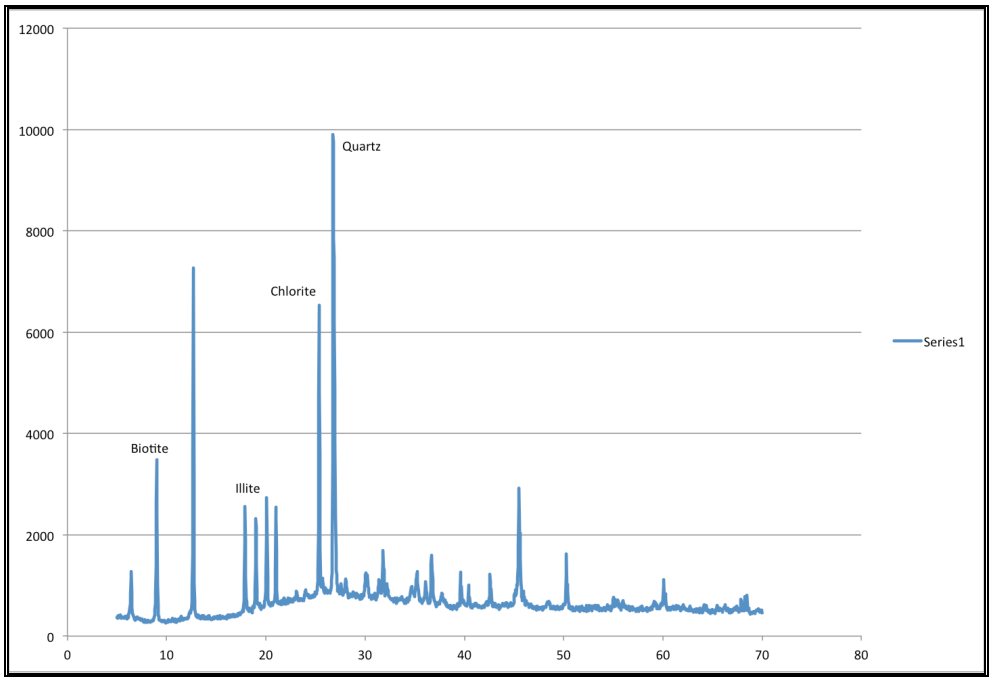


Figure S2. XRD plot of 2θ against intensity with labels showing normalized peaks for each main clay mineral, interpreted using Moore and Reynolds (1997). These data are from sample 0.06 which is the 'lozenge rich' facies.

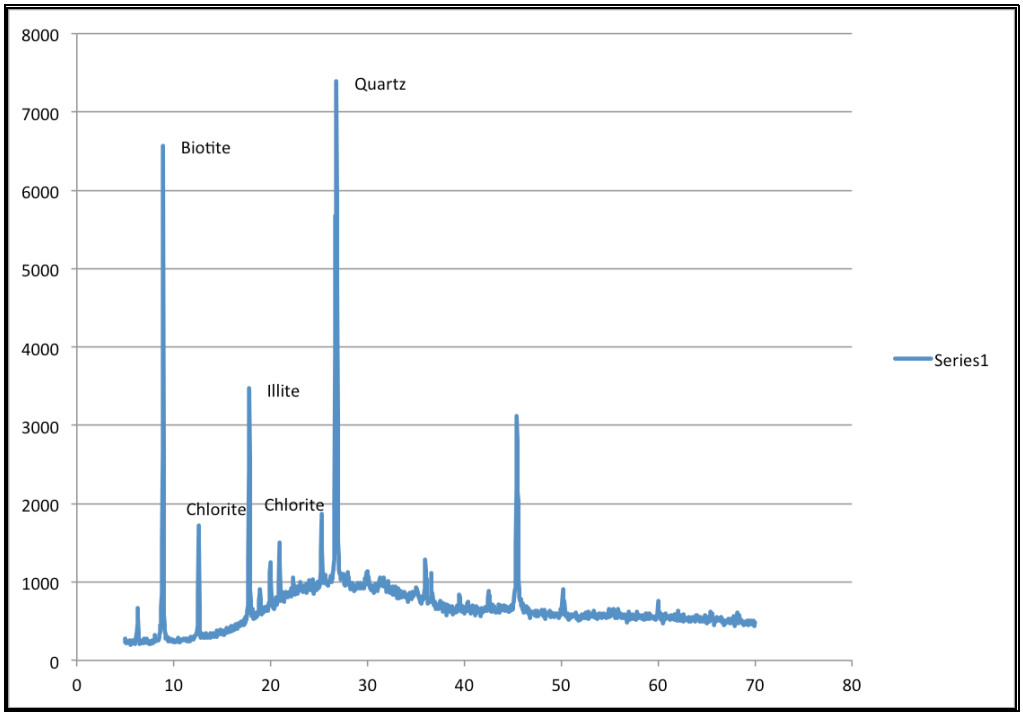


Figure S3. XRD plot of 2θ against intensity with labels showing normalized peaks for each main clay mineral, interpreted using Moore and Reynolds (1997). These data are for sample 4.56, the 'mud-rich' facies. It shows differing intensities for the minerals suggesting the composition, although broadly similar, is different due to the initial composition of the rock before metamorphism.

## 2. Biostratigraphy, and depositional environment

### a. Biostratigraphical framework

Acritarchs and olenelloid trilobites have been recovered from the informal member of the Buen Formation, the "Transitional" Buen, in Peary Land, and they broadly constrain the stratigraphical position of the lower Buen Formation to Cambrian Stage 3 (Babcock and Peel, 2007). Acritarchs are indicative of the *Heliosphaeridium dissimilare–Skiagia ciliosa* Biozone and perhaps the *Volkovia dentifera–Liepaina plana* Biozone as used in the Eastern European Platform and Baltoscandinavia (Moczydłowska and Vidal, 1986; Vidal and Peel, 1993). The biozones correlate approximately with the *Holmia* and *Protolenus* trilobite biozones [*sensu* (Geyer and Shergold, 2000)] indicative of Cambrian Series 2 (Babcock, 2005). The *Holmia* Biozone correlates to the upper part of Cambrian Stage 3 and the lower part of Stage 4 and the *Protolenus* Biozone correlates to Stage 4 as presently conceived (Babcock and Peel, 2007). The occurrence of the olenelloid trilobites *Olenellus hyperboreus* and *O. svalbardensis* in the upper Buen Formation indicates the *Olenellus* Biozone of Laurentian usage (Blaker and Peel, 1997) The *Olenellus* Biozone belongs to the provisional Stage 4 of the Cambrian (Babcock, 2005). Its base is historically regarded as the base of the Dyeran Stage of Laurentian usage (Palmer, 2011) and correlates approximately with the onset of the Mingxinsi Carbon Isotope Excursion [MICE:(Zhu et al., 2006)].

*Buenellus higginsi* is the most common macrofossil in the "Transitional" Buen at Sirius Passet and provides a biostratigraphical age. This species is included within the family Nevadiidae and its presence is indicative of the *Nevadella* Biozone as used in Laurentia (Blaker and Peel, 1997; Blaker, 1988). This biozone correlates to the middle part of provisional Stage 3 (the lowest stage of the provisional Series 2) (Babcock et al., 2005). Historically, the *Nevadella* Biozone has been assigned to the upper part of the Montezuman Stage as used in Laurentia (Palmer, 2011). Sirius Passet has been correlated with the Chengjiang and Guanshan Lagerstätten from South China which are temporally related to the Cambrian Arthropod Radiation (CARE) isotopic excursion (Zhu et al., 2006). Within biostratigraphical uncertainty the "Transitional" Buen is older than the Buen Formation *s.s.* in southern Peary Land.

### b. Depositional environment

The presence of a diverse invertebrate benthos in Cambrian Konservat-Lagerstätten indicates the overlying water column was oxic with a sharp redox boundary at the sediment-water interface. Bioturbation is surficial and typically only occurs in association with generally large arthropod carcasses (Mangano et al., 2012).

Cyanobacteria are photoautotrophic and oxygenic microorganisms and could have produced the oxygenated conditions at the seafloor. However, in extant cyanobacterial mats, sulfate reduction of the biomass can produce hydrogen sulfide ($H_2S$) emissions above the mat surface, particularly at night (Jørgensen, 1979). Periodic high levels of $H_2S$ could have been a major factor impeding the settlement of benthonic organisms on the seafloor. Either the mat dwelling fauna was ephemeral and able to escape $H_2S$ emissions or had adapted a resistance to $H_2S$ toxicity. Occasional massive sulfide expulsion from the decaying mats might have led to mass mortalities of the mat dwelling community [cf. (Weeks et al., 2002)].

It appears that normal marine carbonaceous shales in the Cambrian were limited to shallow-water regions with turbulent circulation (Raiswell and Berner 1986). Negative $\delta^{13}C$ values commonly associated with Cambrian black shale deposition indicate either: (1) export production was low due to the removal of phosphorous into deep-water brines and nitrate by expansion of nitrate-reducing bacteria in association with an expanded oxygen minimum zone (Brasier, 1992), or (2) extensive fractionation by sulphate reducing or methanogenic bacteria (Codispoti 1989) The latter is supported by widespread positive $\delta^{34}S$ during black shale deposition and relatively low C/S, which are both indicative of a major expansion of the sulphate-reducing biotope (Raiswell and Berner 1986).

We propose the arthropod-lobopdian fauna that characterizes the Sirius Passet inhabited a warm, muddy, matground habitat close to or just below storm wave base, but within the photic zone. Primary productivity was primarily by benthonic cyanobacteria. Contemporary shallow subtidal to intertidal carbonate environments had a distinct shelly fauna including archaeocyathans, halkieriids, tommotiids, hyoliths, molluscs, rare trilobites, and a variety of other small shelly fossils of unknown affinity [examples cited in (Mount and Signer, 1985)]. The rapid appearance in the geological record and ecological stability of the "Burgess Shale-type assemblages," over some 10 million years, suggest that rather than being long-lived holdovers, successively displaced from the shallow water (Mount and Signer, 1985; Morris, 2009), these animals were members of new Bambachian megaguilds (groups of organisms with mutually similar adaptive strategies), highly specialized and adapted to the dynamic and unstable nature of the tropical, muddy lower shoreface and shelf.

# REFERENCES


Babcock, L.E., 2005: Interpretation of biological and environmental changes across the Neoproterozoic–Cambrian boundary: developing a refined understanding of the radiation and preservational record of early multicellular organisms: *Palaeogeography, Palaeoclimatology, Palaeoecology 220*, 1–5.

Babcock, L.E., and Peel, J.S., 2007: Palaeobiology, Taphonomy and Stratigraphic Significance of the Trilobite Buenellus from the Sirius Passet Biota, Cambrian of North Greenland. *Memoirs of the Association of Australasian Palaeontologists 34*, 401-418.

Babcock, L., Peng, S., Geyef, G., and Shergold, J., 2005: Changing perspectives on Cambrian chronostratigraphy and progress toward subdivision of the Cambrian System: *Geosciences Journal 9*, 101-106.

Blaker, M., 1988: A new genus of nevadiid trilobite from the Buen Formation (Early Cambrian) of Peary Land, central North Greenland: *Grønlands Geologiske Undersøgelse Rapport 137*, 33-41.

Blaker, M., and Peel, J., 1997: Lower Cambrian trilobites from North Greenland: *Meddr Grønland Geoscience 35*.

Brasier, M. D.,1992: Global ocean—atmosphere change across the Precambrian—Cambrian transition: *Geological Magazine 129*, 161-168.

Codispoti, L. A., 1989: in *Productivity of the Oceans* Vol. Dahlem Workshop Report (eds W.H. Berger, V.S. Smetacek, & W. Wefer); *Wiley*, 377-384.

Geyer, G., and Shergold, J., 2000: The quest for internationally recognized divisions of Cambrian time: *Episodes 23,* 188-195.

Jørgensen, B., 1979: Diurnal cycle of oxygen and sulfide microgradients and microbial photosynthesis in a cyanobacterial mat sediment: *Applied and Environmental Microbiology 38*, 46-58.*

Mangano, M.G., Bromley, R.G., Harper, D. a. T., Nielsen, a. T., Smith, M.P., and Vinther, J., 2012: Nonbiomineralized carapaces in Cambrian seafloor landscapes (Sirius Passet, Greenland): Opening a new window into early Phanerozoic benthic ecology: *Geology 40*, 519–522.

Moczydłowska, M., and Vidal, G., 1986: Lower Cambrian acritarch zonation in southern Scandinavia and southeastern Poland: *Geologiska Foereningan i Stockholm. Foerhandlingar 108*, 201–223. *

Morris, S.C., 2009: A Redescription of a Rare Chordate, Metaspriggina walcotti Simonetta and Insom, from the Burgess Shale (Middle Cambrian), British Columbia, Canada: *Journal of Paleontology 82,* 424-430.

Mount, J.F., and Signer, P.W., 1985: Early Cambrian innovation in shallow subtidal environments: Paleoenvironments of Early Cambrian shelly fossils: *Geology 13*, 730–733.

Palmer, A.R., 2011: A proposed nomenclature for stages and series for the Cambrian of Laurentia: *Canadian Journal of Earth Sciences 35*, 323–328.

Raiswell, R., and Berner, R.A., 1986: Pyrite and organic matter in Phanerozoic normal marine shales: *Geochimica et Cosmochimica Acta 50*, 1967–1976.

Vidal, G., and Peel, J., 1993: Acritarchs from the Lower Cambrian Buen Formation in North Greenland: *Bull./Gronlands geol. undersogelse*.

Weeks, S.J., Currie, B., and Bakun, A., 2002: Massive emissions of toxic gas in the Atlantic.: *Nature 415*, 493–494.

Zhu, M., Babcock, L., and Peng, S., 2006: Advances in Cambrian stratigraphy and paleontology: integrating correlation techniques, paleobiology, taphonomy and paleoenvironmental reconstruction: *Palaeoworld 15*, 217-222.

# Appendix III. Minerals in the gut: scoping a Cambrian digestive system

Strang, K.M., Armstrong, H.A., and Harper, D.A.T., 2016, Minerals in the gut: scoping a Cambrian digestive system: Royal Society Open Science, v. 3, no. 11.

ROYAL SOCIETY OPEN SCIENCE

rsos.royalsocietypublishing.org

Research

**Cite this article:** Strang KM, Armstrong HA, Harper DAT. 2016 Minerals in the gut: scoping a Cambrian digestive system. *R. Soc. open sci.* **3**: 160420.
http://dx.doi.org/10.1098/rsos.160420

Received: 18 July 2016
Accepted: 18 October 2016

**Subject Category:**
Earth science

**Subject Areas:**
palaeontology

**Keywords:**
arthropod digestive system, taphonomy, Cambrian Lagerstätten

**Author for correspondence:**
K. M. Strang
e-mail: k.m.strang@durham.ac.uk

# Minerals in the gut: scoping a Cambrian digestive system

K. M. Strang, H. A. Armstrong and D. A. T. Harper

Palaeoecosystems Group, Department of Earth Sciences, Durham University, Durham DH1 1LE, UK

KMS, 0000-0002-2739-3102

The Sirius Passet Lagerstätte of North Greenland contains the first exceptionally preserved mat-ground community of the Cambrian, dominated, in terms of abundance, by trilobites but particularly characterized by iconic arthropods and lobopods, some also occurring in the Burgess shale. High-resolution photography, scanning electron imaging and elemental mapping have been carried out on a variety of specimens of the non-mineralized arthropod *Campanamuta mantonae* (Budd 2011 *J. Syst. Palaeontol.* **9**, 217–260 (doi:10.1080/14772019.2010.492644)) which has three-dimensional gut and muscle preservation. Results show that the guts contain a high concentration of calcium phosphate (approximating to the mineral francolite), whereas the adjacent muscles are silicified. This indicates a unique, tissue-specific taphonomy for this Cambrian taxon. We hypothesize that the precipitation of calcium phosphate in the guts occurs rapidly after death by 'crystal seed' processes in suboxic, slightly acidic conditions; critically, the gut wall remained intact during precipitation. We postulate that the calcium phosphate was derived from ingested cellular material. Silicification of the muscles followed as the localized water chemistry became saturated in silica, high in $Fe^{2+}$, and low in oxygen and sulfate. We document here the unique occurrence of two distinct but mechanistically similar taphonomic pathways within a diverse suite of possibilities in an Early Cambrian Lagerstätte.

## 1. Introduction

The fossil record offers us invaluable insights into important intervals in the history of life. The record is however generally biased by poor preservation, and even in exceptionally preserved specimens from fossil Lagerstätten, there is potential for key traits to be removed by decay. Sites that can be demonstrated to have very early, soft tissue preservation not only provide insights into taphonomic processes, but are also critical for reconstructing ancient communities and phylogenies [1].

THE ROYAL SOCIETY PUBLISHING

This becomes particularly important when considering the very earliest radiations of bilaterian animals during the Cambrian explosion and hypotheses of likely ancestors in the Ediacara biota. A list of elements of the Sirius Passet (SP) fauna is provided by Peel & Ineson [2].

The Lower Cambrian black shales of SP, North Greenland preserve the oldest known examples of soft-bodied fossils from the Cambrian explosion together with more typical Cambrian skeletal animals. These include trilobites, other arthropods, lobopods, halkieriids and sponges [3]. The fauna is broadly similar to that found in the younger Burgess shale [4]. SP is located in J. P. Koch Fjord, N. Greenland, at 82°47.6′ N, 42°13.7′ W and during the Cambrian lay at approximately 10° S [2]. The locality was included in the 'transitional' Buen, and the fauna represents the earliest Cambrian community with exceptional preservation together with evidence for microbial mats, predating the Burgess shale by 10 Myr [2]. *Buenellus higginsi* is the most common macrofossil, indicative of the Laurentian Atdabanian/Botomian boundary, at the top of stage 3 to the base of stage 4, occurring between 511 and 521 Myr. However, precise correlation of the unit remains a subject of debate. The detailed petrography, mineralogy and metamorphic history were described by Strang *et al.* [5], and these properties are only outlined here. The shales are a poorly sorted mix largely consisting of quartz (60–65%), clay minerals, chloritoid porphyroblasts (indicating low P/T greenschist facies metamorphism) and silicified microbial mat material. A detailed description of the depositional environment, dating and metamorphic history has recently been presented [5].

The SP exhibits a diversity of taphonomic pathways; for example, the trilobites from the SP are preserved as complete, concave hyporelief external moulds and convex epirelief casts. External moulds are shown to consist of a thin veneer of authigenic silica. The casts are composed of silicified cyanobacterial mat material. Early silicification is supported by the presence of synsedimentary mat rip-up clasts, three-dimensional preservation, which indicates silicification prior to sediment compaction and textural and mono-CL evidence. The growth of metamorphic chloritoid needles, which crosscut the silica in the matrix, indicates that metamorphism occurred much later. Silicification was initiated by falling pH in the decaying mat. Pore waters are interpreted to have been initially alkali, silica-saturated, high in ferric iron but low in oxygen and sulfate. Excess silica was likely derived from remobilized biogenic silica, probably sponge spicules in the muddy sediment. It is not clear whether silicification was microbially or chemically mediated. The presence of cyanobacterial mats, sealing both the sediments and fossils was however fundamental to the preservation of this community.

*Campanamuta mantonae* [6] is also a common arthropod in the SP fauna and is non-mineralized. Approximately 1700 specimens have been reported to date [6]. Specimens are flattened but preserve three-dimensional axial traces, including gut tracts, diverticulae and muscle tissue [6]. The parts and counterparts often show different anatomical details in the axial region and sometimes exhibit cavities [6]. Distinguishing whether these cavities are the original anatomical features of the organism or are voids left by the later decay of soft parts or minerals is hard to determine. Budd [6] argued that the fossils are mostly (or completely) replacements of the original tissues, rather than preserved as moulds [6]. In this paper, we describe the taphonomy of these specimens and propose a taphonomic model for elements of the SP that enhances in some respects closer comparison with Lagerstätten from the Neoproterozoic than those from the Late Cambrian. The preservation of gut contents also allows for an interpretation of the mode of life of *C. mantonae*.

# 2. Material and methods

## 2.1. Specimens

The numbered specimens (MGUH 31567–31572) including thin sections are reposited in the Natural History Museum of Denmark (Geological Museum), University of Copenhagen. Budd [6] described the anatomy of *C. mantonae* in considerable detail. It is a relatively large arthropod (mean length approx. 65 mm and width 35 mm) comprising three segments, with a smooth exoskeleton and a semicircular cephalic shield. The main morphological features are illustrated in figure 1. The external morphology is not well preserved. The only preserved internal anatomy is situated in the axial region and consists of the main digestive structures (figure 1). In rare specimens, the outline of the stomach can be identified, situated anteriorly in the cephalon. The gut tract extends posteriorly where it terminates at the anus. The triangular diverticulae are paired not only on either side of the gut, but also extend down towards the anus (figure 1).

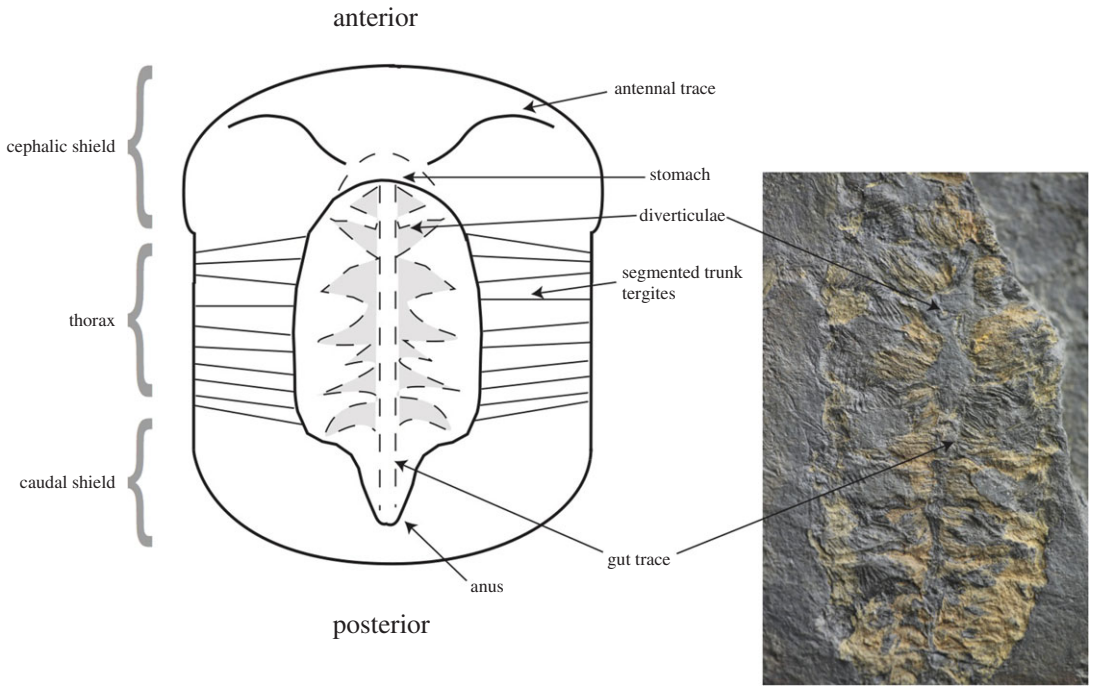


**Figure 1.** Diagram shows the main features, appendages and internal anatomy of *Campanamuta mantonae*. Photo inlay is a specimen of *C. mantonae* (MGUH 31567) that shows the gut tract and diverticulae which are most readily preserved. Specimen is 2 cm wide.

## 2.2. Analysis

High-resolution photography was carried out on four samples of *C. mantonae* using a digital Cannon 5D mark III. Specimens were photographed, using low incidence lighting (directed from the NW). Contrast and saturation of the images were then then edited using Adobe PHOTOSHOP and Adobe ILLUSTRATOR CS3 to reveal the best outlines of the preserved anatomy. Line drawings were constructed from photographs and camera lucida images. Specimens were carbon coated prior to scanning (approx. 20 µm thickness). This was undertaken, using the Hitachi SU-70 FEG SEM Facility (Department of Physics, Durham University). The machine was operated at 12 kV and with a current density of 46 µA. SEM-EDAX analysis was carried out using the backscatter detector and the same voltage settings used for imaging. For point analysis, a cobalt standard was run before analysis to provide quantitative results, analysed using QUANT software and running the standard several times to ensure maximum accuracy ($100 \pm 5\%$). SEM-cathodoluminescence (CL) was carried out using a mirror-type detector (Gatan Mono-CL). The machine was set to low magnification with a 10 kV and CL luminosities collected, using each colour filter (red > 600 nm, green > 480–580 nm and blue < 480 nm) and a panchromatic lens. Quartz grains display a variety of luminescence intensity dependent on their provenance. The standards used were adapted from Seyedolali *et al*. [7]. CL intensity is dependent on the density of intrinsic and extrinsic defects within the band gap of the mineral. These defects are usually structural imperfections in the quartz crystal owing to vacancies within the crystal lattice and can provide information on the conditions during mineralization and subsequent post-mineralization events such as deformation and metamorphism [8].

# 3. Results

In specimens with digestive structures preserved, usually there is only limited preservation of the outer appendages. The area of the specimens outside the axial region is visible as a thin, dark film of silica. When preserved, bundles of muscle fibres adjacent to the digestive tract are yellow in colour and have three-dimensional relief. The muscle fibres track transversely and outwards from beside the diverticulae towards the thoracic tergites (figure 1) and exhibit well-preserved, oblique, micrometre-scale striations (figure 3*a*).

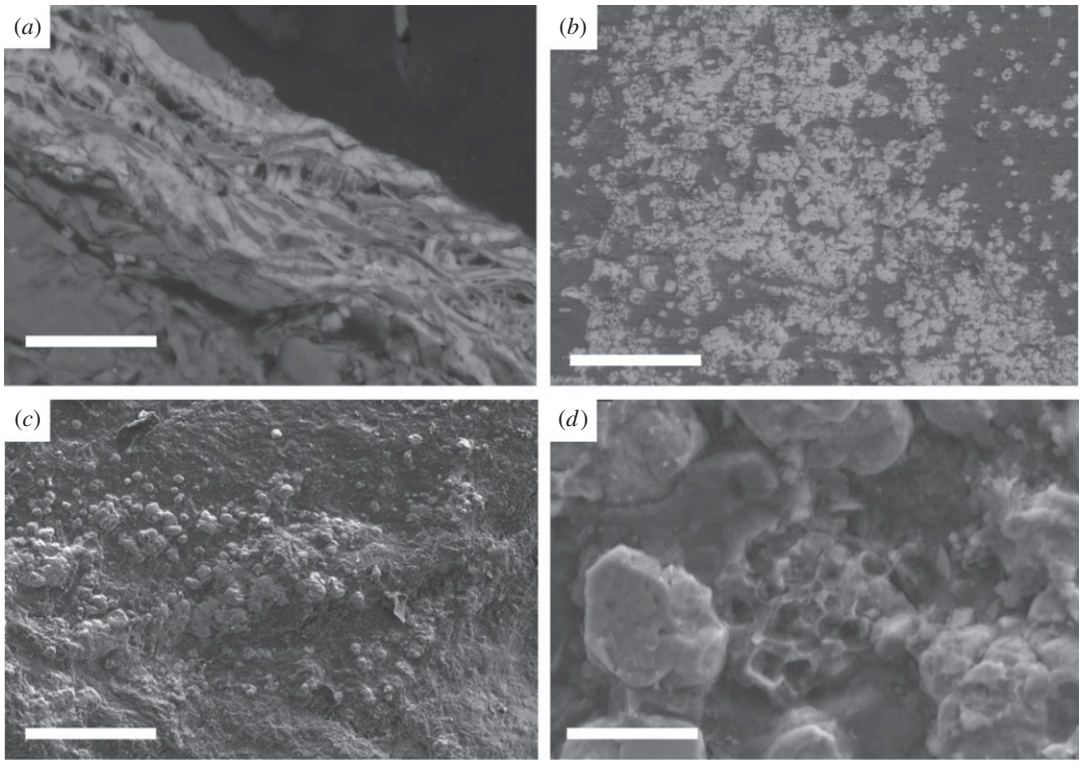


**Figure 2.** SEM and BSE images of the phosphate contained in the gut of *C. mantonae*. (*a*) SEM image of a cross section taken through a sample of *C. mantonae* (MGUH 31568), light grey material is phosphatized. Small pyrite framboids can be seen. Scale bar, 50 µm. (*b*) BSE image showing spherical texture of phosphate nodules in sample MGUH 31569. Scale bar, 100 µm. (*c*) Higher magnification SEM image shows spherical phosphate interpreted as possible microbial moulds. Scale bar, 20 µm (MGUH 31569). (*d*) High-resolution SEM image showing a pyrite framboid within the phosphate clusters. Scale bar, 10 µm (MGUH 31569).

**Table 1.** EDAX data for phosphatized regions in sample SP0511. Data given in %.

| spectrum | Al | Si | P | Ca | Fe | O |
|---|---|---|---|---|---|---|
| spectrum 1 | 1.90 | 0.00 | 21.34 | 20.04 | 0.00 | 56.36 |
| spectrum 2 | 0.00 | 5.96 | 23.09 | 16.91 | 1.30 | 52.74 |
| spectrum 3 | 0.67 | 1.42 | 19.67 | 36.18 | 0.00 | 42.06 |
| spectrum 4 | 1.74 | 3.94 | 31.17 | 17.19 | 5.28 | 40.67 |

The gut of *C. mantonae* is a broad tube-like structure, which runs down the central axis, terminating at the anus (see also [6, fig. 1]). In the cephalic region (figure 1), the digestive tract consists of a sclerotized oesophagus which leads into the stomach, situated behind the head. The diverticulae are segmented and paired and open out from the gut [6, fig. 1]. The anus is clearly defined by a ring of plates [6, fig. 5*a*,*b*].

Three-dimensional gut traces contain high concentrations of calcium phosphate ($Ca_3(PO_4)_2$; table 1) approximating to the mineral francolite. There are some traces of Si, Al and Fe but these are very minor and probably derived from the matrix. Phosphatization extends along the entire gut tract to the anus. The phosphatized areas have a sponge-like texture composed of small (less than 5 µm in diameter) spheres (figure 2*b*,*c*) organized into layers (figure 2*a*). The layers commonly contain small (less than 10 µm) pyrite framboids. There is no visible evidence for preserved biological material or sediment grains. In thin section, the boundary between the gut trace and the sediment below is sharp; there is no evidence in either hand specimen or thin section of preserved cuticle.

EDAX data confirm that muscle fibres are composed of finely microcrystalline silica (table 2) with very minute traces of Mg, possibly derived from the surrounding matrix. The preservation of these is relatively unvaried and forms distinct aligned blocks of muscle fibres, arranged *in situ*. The outer surfaces have a spherulitic texture at the micrometre scale (figure 3*a*). An approximately 5 µm thick layer of silica

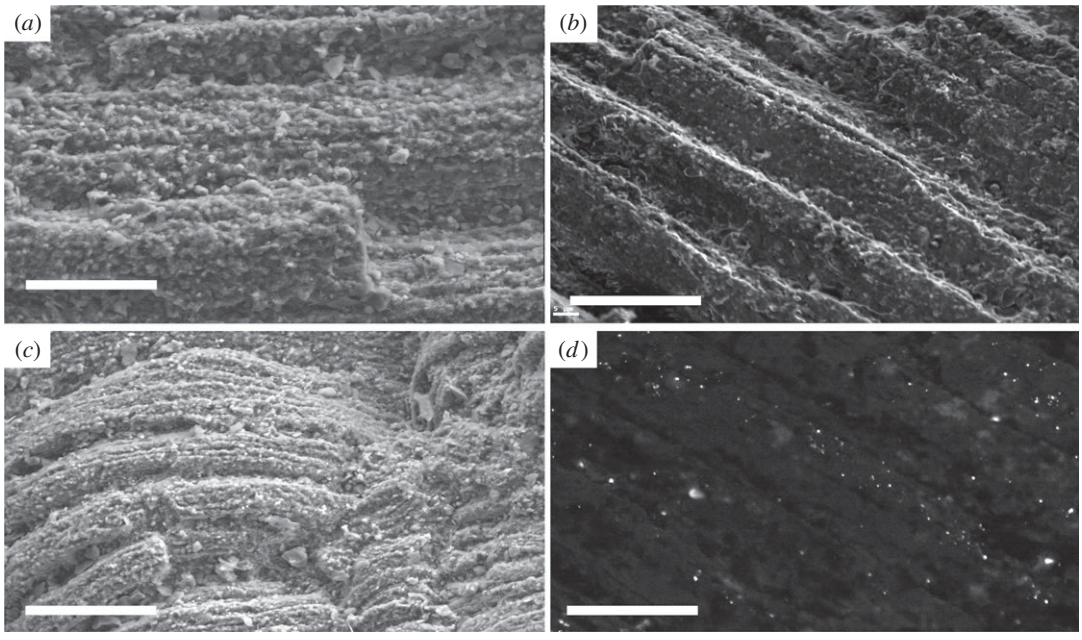


**Figure 3.** SEM, BSE and SEM-CL images of the silicified muscle tissue. (*a*) BSE image shows silicified muscle tissue. Scale bar, 20 µm (MGUH 31568). (*b*) SEM image of muscle tissue shows fibrous nature and small spherical nodules of silica. Scale bar, 20 µm (MGUH 31570). (*c*) BSE image showing truncated silicified muscle tissue. Scale bar, 20 µm (MGUH 31571). (*d*) SEM-CL image showing low monotone grey luminosity of the silica in the muscles, indicating similar formation conditions as that found in *Buenellus* [5] (MGUH 31572).

**Table 2.** EDAX data for silicified regions in sample SP0511. Data given in %.

| spectrum | Mg | Si | O |
|---|---|---|---|
| spectrum 1 | 3.09 | 43.65 | 53.26 |
| spectrum 2 | 2.30 | 46.74 | 53.26 |
| spectrum 3 | 2.28 | 44.98 | 52.74 |
| spectrum 4 | 1.37 | 45.68 | 52.95 |

occurs at the edges of the phosphatized region (figure 2*a*). SEM-CL indicates the silica has very low luminosity with no distinct colour under both monochromatic filter and RGB filters (figure 3*d*).

# 4. Discussion

The key drivers of decay are autolysis and microbial activity, and the latter is a key mediator in autogenic mineralization of soft tissues [9]. Microbial communities have the highest surface area to volume ratio of any group of living organisms and this combined with the abundance of charged chemicals and molecules on their surface makes them ideal environments for mineral nucleation and precipitation [10]. The gut traces in *C. mantonae* are preserved almost exclusively as francolite. The preservation of the three-dimensional structure indicates early mineralization prior to the compaction/collapse of the gut. Three-dimensional preservation of the gut is also commonly observed in a variety of taxa from Cambrian (and younger) Lagerstätten, indicating the gut is the most readily preserved internal structure. Examples include the Burgess shale arthropod *Leanchoilia*, *Odaria*, *Canadaspis*, *Perspicaris*, *Sidneyia*, *Anomalocaris* and *Opabinia* which all possess phosphatized midgut structures in their axial region [11,12]. *Myoscolex*, an Early Cambrian arthropod from the Emu Bay shale, is described as having only its trunk muscles phosphatized, which is in stark contrast to the preservation in the SP [13]. Phosphatized muscles are also found associated with hard parts in the Mesozoic, such as the muscle tissue in the horseshoe crab *Mesolimulus* [14] and preservation of muscles in phosphate from the Konservat-Lagerstätten in Lebanon [15].

The close proximity of distinct tissues with distinct taphonomies is extremely unusual. Experimental decay studies of modern brine shrimp *Artemia* indicate chemistry of the gut contents and the presence of endogenous bacteria are the key factors in creating a unique microenvironment in which the gut is preserved [9]. The nature of the preservation of the surrounding tissues is dependent on whether the gut wall remains intact. If the gut ruptures, the endogenous microbes leak into the body cavity where they control the tissue preservation through mineral templating [9]. In the *C. mantonae* specimens from the SP, only the gut is phosphatized, and the remaining axial tissues and structures are preserved as silica replacement. This would indicate the gut wall remained intact and that endogenous bacteria remained within the gut and were responsible for the preservation of the gut.

Phosphatization and silicification occur under markedly different environmental and chemical conditions [16]. Phosphatization is widely recognized in the preservation of soft tissues [10,17]. There are two sources of phosphate: (i) from the breakdown of organic matter during bacterial sulfate reduction and (ii) phosphate can also be released from absorption sites on ferric oxyhydroxide, during reduction of the iron ($Fe^{3+} > Fe^{2+}$ [18]). Phosphatization occurs predominantly in a suboxic environment within the upper few centimetres of the sediment [19], at lowered pH induced by decaying organic matter and with sufficient time under these conditions, free from scavengers [17,20].

Decay experiments have shown that the digestive and other internal organs of marine arthropods are particularly prone to rapid decay (2–3 days) and liquidation under open, aerobic conditions at room temperature [9,21]. Butler *et al*. [9] also showed that the carcass of the brine shrimp was rapidly consumed (2–3 days) by endogeneous, gut-derived microbes and pervasive phosphatization of the internal tissues occurred following the rupture of the gut wall. Decay rarely lasts longer than one month [22]. By inference, the three-dimensional preservation of the guts in the *C. mantonae* specimens must have started very early after the death of the organism when the gut wall remained. The precipitation of calcium phosphate is favoured over calcium carbonate under slightly acidic marine conditions [20].

Both sulfide-oxidizing bacteria (SOB) and sulfate-reducing bacteria (SRB) have been implicated in the precipitation of phosphate in the marine environment [13,14,23,24]. SOB are able to store polyphosphate under oxic conditions, this polyphosphate being used as an additional energy source [25]. Examples of SOB include *Thioploca, Beggiatoa* and *Thiomargarita,* and these taxa are major components in the benthic sulfur cycle, where they reoxidize sulfide ([26] and references therein). SRB facilitate phosphate precipitation by increasing the phosphate concentrations in pore waters through the decay of organic matter. Degradation of organic matter by SRB is a predominantly anaerobic process, where supersaturation with respect to phosphate is commonly reached [26]. The presence of pyrite framboids within the phosphate supports the role of SRB in the release of $PO_4^-$ from the organic gut contents, from either ingested seawater or iron-rich sediment (see also [11]). We have no evidence from imaging for the presence of sediment particles within the gut material and conclude the phosphate was derived from ingested organic material. Furthermore, the absence of phosphate in the rock matrix also suggests it came from an internal source.

The molecular initiation and aggregation of silica plays a major role in biosilicification and the presence of proteinaceous material resulting from decay [27]. In microbially mediated silica precipitation, it has been shown that microbial surfaces do not directly nucleate silica mineral formation; however, they play an important role in the aggregation of polymeric silica and the deposition of silica colloids on microbial surfaces, for example in modern hot spring environments, silica sinters actively form in close spatial relation to microorganisms ([28] and references within). In the former, direct precipitation of silica into void spaces is the likely scenario in the SP [5]. Sedimentary factors that control silicification are the permeability of sediment, silica availability (both in the pore waters and sediment) and the concentration of organic matter ([29] and references therein; [30]). Silica-rich pore waters were likely derived from remobilization of biogenic silica from sponge spicules [5]. Soluble silica, in the form of monosilicic acid, $H_4SiO_4$, dissociates to $H_3SiO_4^-$ at pH values above *ca* 9.7 [31,32]. $H_3SiO^-$ is a highly soluble form of silicic acid, and it reacts with hydrogen ions to form $SiO_2$ [33, fig. 3].

Silica precipitation is sensitive to the iron content of bottom/pore waters and in Early Cambrian seawater and $Fe^{2+}$ appears to be high relative to FeOOH [16]. Unlike the trilobite specimens, silicification in the non-mineralized *C. mantonae* is restricted to the muscles. Muscle tissue in modern arthropods is composed of actin and myosin [34] and it is likely that muscle tissue in extinct arthropods had a similar composition. While the involvement of microbes in silica precipitation cannot be directly excluded, more extensive mineralization of all the tissues might be expected. Alternatively, the arrangement of muscles into micrometre-scale fibres provides an excellent substrate for silica precipitation, as it

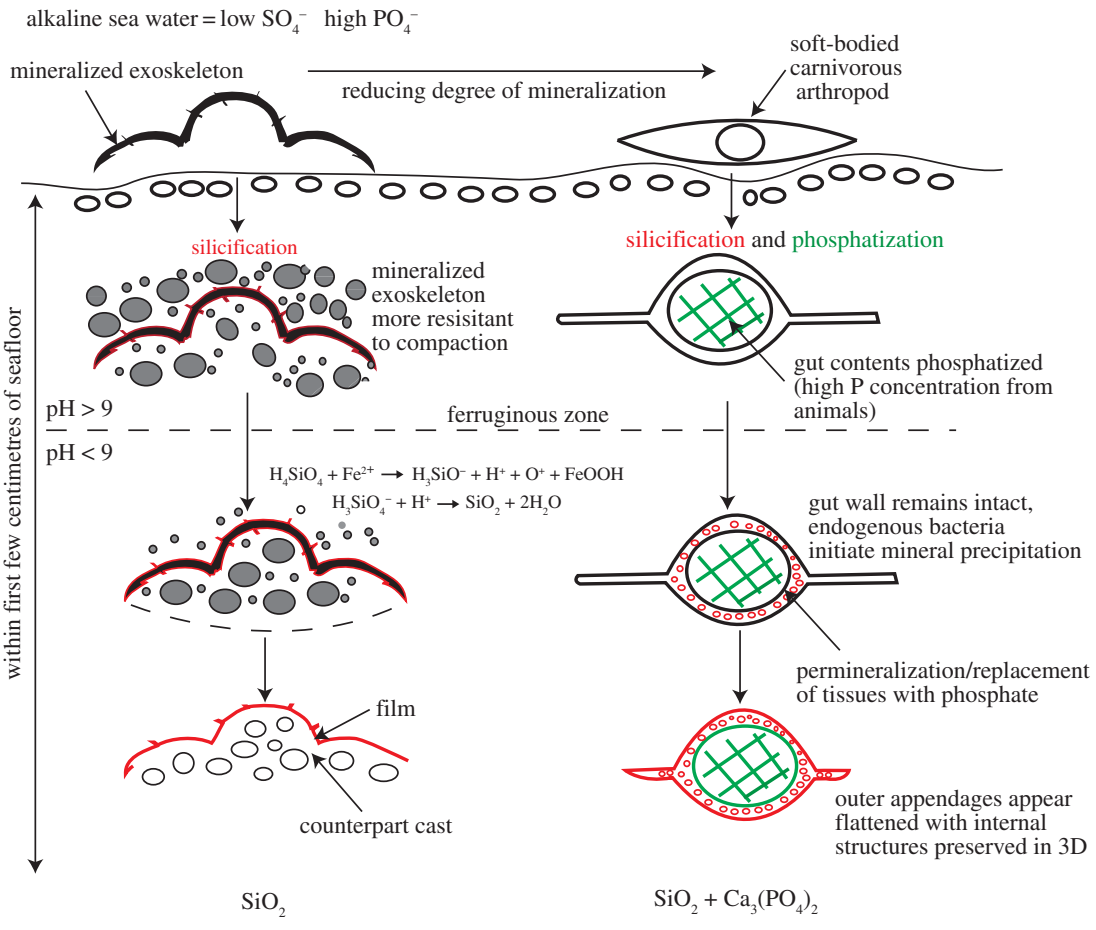


**Figure 4.** Schematic model shows the preferred taphonomic pathway of non-mineralizing *C. mantonae* (right) compared with that of mineralizing *Buenellus* (left).

creates a large surface area comprising the reactive proteinaceous and amino acids necessary for initial silica aggregation [29]. Three-dimensionally preserved internal organs have also been documented from the Burgess shale in the Stephen formation (Cambrian) [11] annelids from the Cretaceous Konservat-Lagerstätten of Hakel and Hjoula, Lebanon [15], the Guizhou Province in South China (see [12,35]) and are also associated with flattened hard parts, interpreted as a result of syndiagenetic microbial decay.

## 5. Taphonomic pathway

Figure 4 shows the proposed taphonomic pathway and compares this to that proposed for the mineralized trilobite *Buenellus*. The precipitation of two distinct mineral phases in the gut and axial muscle fibres of *C. mantonae* indicates the formation in different and isolated microenvironments along a redox gradient. Phosphatization of the gut contents occurred in slightly acidic, suboxic conditions, under the control of endogenous SRB, within days of death and therefore at the seafloor. The three-dimensional preservation indicates of the gut trace was fully permineralized before specimen collapse during decay, burial and sedimentary compaction. Silicification of the adjacent muscle fibres occurred in the presence of silica-saturated pore waters with a pH around 9.7 within the microbial mat.

The relative timing of these two processes is not easily constrained. That both tissues are preserved in three dimensions suggests both were mineralized early during decay. Postmortem sealing of the specimens by cyanobacterial mats has been hypothesized as a mechanism for rapid sealing of the specimens from decay and predation, resulting in a localized pH environment suitable for controlling the silicification of the mineralized trilobites in the SP [5]. It is possible that silicification was initiated once the specimens became entombed in the decaying microbial mat and this would have provided the necessary conditions for decay-related reduction in pH > 7 [5,31].

## 6. Gut morphology and ecological implications

Well-preserved digestive systems in Cambrian arthropods display a variety of biserial midgut glands, from simple bunch-like or lobe-like digestive glands to complex branching features [36]. This suggests that, like their modern relatives, these arthropods ingested phosphate from their food sources [36]. *C. mantonea* possessed a relatively complex gut consisting of a tube-like structure which runs down the central axis of the animal (figure 1) [6, fig. 5*a*,*b*]. Paired leaf-like diverticulae are attached to the midgut and provide evidence that *C. mantonea* would have been able to process and digest more complex food sources, such as smaller arthropods. In living branchiurans, the diverticulae are used to store food prior to enzymatic breakdown and the absorption of nutrients in a rich but infrequent diet [11,36]. The evolution of more complex guts with digestive glands work by allowing the animal to increase the efficiency of food processing by increasing the surface area between nutrients and epithelial tissues, thus allowing larger particles to be consumed which, in turn, would have enabled them to uphold the energy demands of a more active and predatory lifestyle [36]. The ability to process larger food particles would have been clearly advantageous for active Cambrian arthropods. Unlike their modern counterparts, early Cambrian arthropods do not possess a large array of differentiated appendages used for capturing and breaking up prey [36]. *C. mantonae* only appears to have possessed long, slender antennae [6] (figure 1) which would have acquired a sensory function. The antennae only protruded a short distance from the anterior shield margin, as most of their length is hidden under the shield [6]. Protection by the shield may be the reason for antennae being the most readily preserved appendage of this animal. Evidence that other trilobites grazed the microbial mat [5] and the lack of sediment particles in the gut suggest that *C. mantonae* may have been consuming other smaller arthropods, which would have provided a rich source of phosphate. It would appear predators, in significant numbers, occupied both the benthos and nekton in the Early Cambrian.

## 7. Conclusion

Detailed micrometre-scale analysis of the distribution of phosphate and silica in relation to the internal morphological structure of the soft-bodied arthropod *C. mantonae* from SP indicates a complex tissue-specific preservation of internal structures. The guts contain a high concentration of calcium phosphate (approximating to francolite), whereas the adjacent muscles are silicified. We hypothesize that the precipitation of calcium phosphate in the guts occurs rapidly after death by 'crystal seed' processes in suboxic, slightly acidic conditions; critically, the gut wall remained intact during precipitation. We postulate the calcium phosphate was derived from ingested organic material. Silicification of the muscles followed as the localized water chemistry became saturated in silica, high in $Fe^{2+}$, and low in oxygen and sulfate. These modes of preservation indicate a diversity of taphonomic pathways in faunas, chronostratigraphically intermediate between the Neoproterozoic Ediacara biota and the Middle Cambrian Burgess shale. The absence of sediment particles in the gut suggests that *C. mantonae* was either a scavenger or predating smaller arthropods.

Data accessibility. The numbered specimens (MGUH 31567–31572) are reposited in the Natural History Museum of Denmark (Geological Museum), University of Copenhagen.

Authors' contributions. All three authors designed the project. K.S. carried out the SEM work, participated in data analysis and writing of the manuscript. H.A.A. was involved with analysis and revising the article. D.H. assisted with revising and editing the article.

Competing interests. We have no competing interests

Funding. NERC, GEUS (Geological Survey of Denmark and Greenland), the Danish Council for Independent Research, Agouron Institute and the Carlsberg Foundation provided funding. K.M.S. is in receipt of an NERC CASE Studentship (RF050232).

Acknowledgements. Leon Bowen and Ian Chaplin gave technical assistance. Graham Budd is acknowledged for his previous work on *C. mantonae*. Graham Budd and an anonymous reviewer provided some very helpful comments.

## References

1. Sansom RS, Gabbott SE, Purnell MA. 2010 Non-random decay of chordate characters causes bias in fossil interpretation. *Nature* **463**, 797–800. (doi:10.1038/nature08745)
2. Peel JS, Ineson JR. 2011 The extent of the Sirius Passet Lagerstätte (early Cambrian) of North Greenland. *Bull. Geosci.* **86**, 535–543. (doi:10.3140/bull.geosci.1269)
3. Morris SC, Peel JS. 2008 The earliest annelids: lower Cambrian polychaetes from the Sirius Passet Lagerstätte, Peary Land, North Greenland. *Acta Palaeontol. Pol.* **53**, 137–148. (doi:10.4202/app.2008.0110)
4. Smith MP, Harper DAT. 2013 Earth science. Causes of the Cambrian explosion. *Science* **341**, 1355–1356. (doi:10.1126/science.1239450)

5. Strang KM, Armstrong HA, Harper DAT, Trabucho-Alexandre JP. 2016 The Sirius Passet Lagerstätte: silica death masking opens the window on the earliest matground community of the Cambrian explosion. *Lethaia* **49**, 631–643. (doi:10.1111/let.12174)
6. Budd GE. 2011 *Campanamuta mantonae* gen. et. sp. nov., an exceptionally preserved arthropod from the Sirius Passet Fauna (Buen Formation, lower Cambrian, North Greenland). *J. Syst. Palaeontol*. **9**, 217–260. (doi:10.1080/14772019.2010.492644)
7. Seyedolali A, Krinsley DH, Boggs S, O'Hara PF, Dypvik H, Goles GG. 1997 Provenance interpretation of quartz by scanning electron microscope–cathodoluminescence fabric analysis. *Geology* **25**, 787–790. (doi:10.1130/0091-7613(1997)025<0787:PIOQBS>2.3.CO;2)
8. Frelinger SN, Ledvina MD, Kyle JR, Zhao D. 2015 Scanning electron microscopy cathodoluminescence of quartz: principles, techniques and applications in ore geology. *Ore Geol. Rev*. **65**, 840–852. (doi:10.1016/j.oregeorev.2014.10.008)
9. Butler AD, Cunningham JA, Budd GE, Donoghue PCJ. 2015 Experimental taphonomy of Artemia reveals the role of endogenous microbes in mediating decay and fossilization. *Proc. R. Soc. B* **282**, 20150476. (doi:10.1098/rspb.2015.0476)
10. Douglas S, Beveridge TJ. 1998 Mineral formation by bacteria in natural microbial communities. *FEMS Microbiol. Ecol*. **26**, 79–88. (doi:10.1111/j.1574-6941.1998.tb00494.x)
11. Butterfield NJ. 2002 Leanchoilia guts and the interpretation of three-dimensional structures in Burgess Shale-type fossils. *Paleobiology* **28**, 155–171. (doi:10.1666/0094-8373(2002)028<0155:LGATIO>2.0.CO;2)
12. Lin J-P, Briggs DEG. 2010 Burgess shale-type preservation: a comparison of Naraoiids (Arthropoda) from three Cambrian localities. *Palaios* **25**, 463–467. (doi:10.2110/palo.2009.p09-145r)
13. Briggs DEG, Nedin C. 1997 The taphonomy and affinities of the problematic fossil *Myoscolex* from the Lower Cambrian Emu Bay shale of South Australia. *J. Paleontol*. **71**, 22–32. (doi:10.1017/S0022336000038919)
14. Briggs DE, Moore RA, Shultz JW, Schweigert G. 2005 Mineralization of soft-part anatomy and invading microbes in the horseshoe crab *Mesolimulus* from the Upper Jurassic Lagerstätte of Nusplingen, Germany. *Proc. R. Soc. B* **272**, 627–632. (doi:10.1098/rspb.2004.3006)
15. Wilson P, Parry LA, Vinther J, Edgecombe GD. 2016 Unveiling biases in soft-tissue phosphatization: extensive preservation of musculature in the Cretaceous (Cenomanian) polychaete *Rollinschaeta myoplena* (Annelida: Amphinomidae). *Palaeontology* **59**, 463–479. (doi:10.1111/pala.12237)
16. Muscente AD, Hawkins AD, Xiao S. 2014 Fossil preservation through phosphatization and silicification in the Ediacaran Doushantuo formation (South China): a comparative synthesis. *Palaeogeogr. Palaeoclimatol. Palaeoecol*. **434**, 46–62. (doi:10.1016/j.palaeo.2014.10.013)
17. Wilby PR, Briggs DEG, Bernier P, Gaillard C. 1996 Role of microbial mats in the fossilization of soft tissues. *Geology* **24**, 787–790. (doi:10.1130/0091-7613(1996)024<0787:ROMMIT>2.3.CO;2)
18. Krom MD, Berner RA. 1980 Adsorption of phosphate in anoxic marine sediments. *Limnol. Oceanogr*. **25**, 797–806. (doi:10.4319/lo.1980.25.5.0797)
19. Jahnke RA, Emerson SR, Roe KK, Burnett WC. 1983 The present day formation of apatite in Mexican continental margin sediments. *Geochim. Cosmochim. Acta* **47**, 259–266. (doi:10.1016/0016-7037(83)90138-2)
20. Lerosey-Aubril R, Hegna TA, Kier C, Bonino E, Habersetzer J, Carré, M. 2012 Controls on gut phosphatisation: the trilobites from the Weeks Formation Lagerstätte (Cambrian; Utah). *PLoS ONE* **7**, e32934. (doi:10.1371/journal.pone.0032934)
21. Hof CHJ, Briggs DEG. 1997 Decay and mineralization of mantis shrimps (Stomatopoda; Crustacea); a key to their fossil record. *Palaios* **12**, 420–438. (doi:10.1043/0883-1351(1997)012)
22. Fatka O, Budil P, David M. 2015 Digestive structures in Ordovician trilobites *Colpocoryphe* and *Flexicalymene* from the Barrandian area of Czech Republic. *Est. J. Earth Sci*. **64**, 255–266. (doi:10.3176/earth.2015.32)
23. Briggs DEG. 2003 The role of decay and mineralization in the preservation of soft-bodied fossils. *Annu. Rev. Earth Planet. Sci*. **31**, 275–301. (doi:10.1146/annurev.earth.31.100901.144746)
24. Wilby PR, Briggs DEG. 1997 Taxonomic trends in the resolution of detail preserved in fossil phosphatized soft tissues. *Geobios* **30**, 493–502. (doi:10.1016/S0016-6995(97)80056-3)
25. Schulz HN, Schulz HD. 2005 Large sulfur bacteria and the formation of phosphorite. *Science* **307**, 416–418. (doi:10.1126/science.1103096)
26. Arning ET, Birgel D, Brunner B, Peckmann J. 2009 Bacterial formation of phosphatic laminites off Peru. *Geobiology* **7**, 295–307. (doi:10.1111/j.1472-4669.2009.00197.x)
27. Belton D, Paine G, Patwardhan SV, Perry CC. 2004 Towards an understanding of (bio)silicification: the role of amino acids and lysine oligomers in silicification. *J. Mater. Chem*. **14**, 2231–2241. (doi:10.1039/b401882f)
28. Yee N, Phoenix VR, Konhauser KO, Benning LG, Ferris FG. 2003 The effect of cyanobacteria on silica precipitation at neutral pH: implications for bacterial silicification in geothermal hot springs. *Chem. Geol*. **199**, 83–90. (doi:10.1016/S0009-2541(03)00120-7)
29. Butts SH. 2014 Silicification. In *Reading and writing of the fossil record: preservational pathways to exceptional fossilization* (eds M Laflamme, JD Schiffbauer, SAF Darroch). The Paleontological Society Papers, vol. 20, pp. 15–33.
30. Akahane H, Furuno T, Miyajima H, Yoshikawa T, Yamamoto S. 2004 Rapid wood silicification in hot spring water: an explanation of silicification of wood during the Earth's history. *Sediment. Geol*. **169**, 219–228. (doi:10.1016/j.sedgeo.2004.06.003)
31. Birnbaum J, Wireman JW. 1985 Sulfate-reducing bacteria and silica solubility: a possible mechanism for evaporite diagenesis and silica precipitation in banded iron formations. *Can. J. Earth Sci*. **22**, 1904–1909. (doi:10.1139/e85-206)
32. Arp G, Reimer A, Reitner J. 2003 Microbialite formation in seawater of increased alkalinity, Satonda Crater Lake, Indonesia. *J. Sediment. Res*. **73**, 105–127. (doi:10.1306/071002730105)
33. Rickert D, Schlüter M, Wallmann K. 2002 Dissolution kinetics of biogenic silica from the water column to the sediments. *Geochim. Cosmochim. Acta* **66**, 439–455. (doi:10.1016/S0016-7037(01)00757-8)
34. Neville AC. 2012 *Biology of the arthropod cuticle*. Berlin, Germany: Springer Science, Business Media.
35. Lin J-P. 2006 Taphonomy of Naraoiids (Arthropoda) from the Middle Cambrian Kaili Biota, Guizhou Province, South China. *Palaios* **21**, 15–25. (doi:10.2110/palo.2004.p04-83)
36. Vannier J, Liu J, Lerosey-Aubril R, Vinther J, Daley AC. 2014 Sophisticated digestive systems in early arthropods. *Nat. Commun*. **5**, 3641. (doi:10.1038/ncomms4641)